HORIZON NUCLEAR POWER

WYLFA NEWYDD

ENERGY WORKING FOR BRITAIN

Wylfa Newydd Project

6.4.82 ES Volume D - WNDA Development App D12-3 - Wylfa Newydd Main Site Wave Modelling Report

PINS Reference Number: EN010007

Application Reference Number: 6.4.82

June 2018

Revision 1.0

Regulation Number: 5(2)(a)

Planning Act 2008
Infrastructure Planning (Applications: Prescribed Forms and Procedure) Regulations 2009

Horizon Internal DCRM Number: WN0902-JAC-PAC-APP-00163

[This page is intentionally blank]

HR Wallingford
Working with water

Wylfa Newydd

Main site wave modelling

DEM7943-RT004-R04-00 February 2018

Summary

HR Wallingford undertook wave modelling and associated extremes analysis, climate change assessment and estimation of overtopping rates, during the recent Nuclear Safety, Meteorological and Hydrological Hazards Assessment (NSMHHA, Amec, 2015) for Wylfa Newydd. HR Wallingford subsequently undertook detailed wave modelling during the recent Phase 1 study, including calibration of a SWAN wave model against measured wave data. The model and results then served as a baseline starting point, without the presence of Wylfa Newydd structures and without allowances for climate change.

The present study includes the Wylfa Newydd marine structures, future climate change scenarios and new nearshore wave prediction points. It is intended primarily to support environmental impact assessment and environmental permits. However, some parts are relevant to studies related to design of structures, sea defences and the proposed harbour at Wylfa. The scope of work includes wave overtopping rate calculations in addition to wave modelling, analysis, reporting and discussion.

The purpose of the present study is to address the wave modelling, analysis and results required for environmental and permitting issues. These issues include coastal processes, and any impacts caused by the Wylfa Newydd developments, although such impact studies are themselves outside the scope of this report. The permissions comprise the Marine Licence (ML), Development Consent Order (DCO), Habitats Regulations Assessment (HRA), Environment Impact Assessment (EIA) and Flood Consequence Assessment (FCA).

An earlier Phase 1 study produced results designated Offshore, meaning offshore of the proposed Wylfa Newydd structures. The present study, the results of which are designated Nearshore, introduces the Wylfa Newydd structures, the climate change scenarios and extremes analysis for multiple nearshore points.

A SWAN wave transformation model was used to assess wave conditions close to the site. The SWAN model area includes all of the north coast of Anglesey, and was used to transform a 35-year time series of offshore wave data to equivalent information at ten nearshore points. It was run for three layouts (baseline, developed and part-built), and for three future climate changed scenarios in addition to present-day. The wave modelling provides wave climate information. Sensitivity tests including one additional construction layout are also presented.

An ARTEMIS model was used to assess wave disturbance within the harbour area. It was run to transform joint exceedence wave and sea level extremes from its boundary to positions within the harbour at which overtopping rates are estimated.

The main topics of this report are the inclusion of marine structures and climate change scenarios into existing wave models, nearshore wave predictions at points within a finer nearshore grid, summary wave climates and extremes, the joint probability of large waves and high sea levels, and overtopping rate estimation.

Contents

Figures

Tables

1. Introduction

1.1. Background

HR Wallingford undertook wave modelling and associated extremes analysis, climate change assessment and estimation of overtopping rates, during the flood hazard assessment (NSMHHA, Amec, 2015) for Wylfa Newydd. HR Wallingford subsequently undertook further wave modelling during the Phase 1 study, including calibration of a SWAN wave transformation model against measured wave data. The model and results then served as a baseline starting point, without Wylfa Newydd structures and without allowances for climate change and uncertainty, for any subsequent wave modelling studies for Wylfa Newydd. This study therefore produced results designated "Offshore", meaning offshore of the proposed Wylfa Newydd structures.

Amec Foster Wheeler Environment & Infrastructure UK Limited requested the present update of the earlier wave modelling and analysis, based on the latest harbour layout plans and focusing on results specifically required for use in other studies. This includes model outputs to support the Marine Licence (ML), Development Consent Order (DCO), Habitats Regulations Assessment (HRA), Environment Impact Assessment (EIA) and Flood Consequence Assessment (FCA).

The SWAN model area includes all of the north coast of Anglesey, and was used to transform the 35-year time series of offshore wave data to equivalent information at ten nearshore points. It was run for three layouts (baseline, part-built and fully-built), and for three future climate-changed scenarios in addition to present-day. The wave modelling provides wave climate information to coastal process and environmental impact assessments. In addition, a further construction layout configuration, representing a larger structure footprint from an environmental perspective has been modelled as a sensitivity test.

An ARTEMIS wave model is also used to assess wave disturbance within the harbour area. It was run to transform joint exceedence wave and sea level extremes from its boundary to positions within the harbour at which overtopping rates were estimated.

1.2. Scope of Work

Update earlier wave modelling and analysis to provide results for the baseline, and for the fully-built and part-built harbour layouts. Use a two-stage modelling approach, consisting of:

- A spectral coastal area transformation model (SWAN), to transform offshore waves to nearshore locations around the proposed harbour layout;
- A local phase-resolving wave disturbance model (ARTEMIS), to generate wave conditions inside the harbour.

This combined modelling approach is required to provide nearshore time series, extreme wave conditions, high-water joint probability for waves and sea levels, and wave overtopping rate estimates at nearshore locations around and inside the proposed harbour to support the ML, DCO, HRA/EIA and FCA. Provide results for several combinations of harbour layout and climate-changed conditions, including changes in wave conditions that would be caused by construction of the harbour.

1.3. Coordinate systems

The horizontal coordinate system used in this report is British National Grid. The model vertical datum is Chart Datum (CD) at Cemaes Bay, which is 3.6m below Ordnance Datum (OD).

1.4. Structure of report

Chapters 2 and 3 introduce the revised harbour layouts and climate-changed scenarios, respectively. Chapters 4, 5 and 6 describe the SWAN, ARTEMIS and overtopping rate modelling and results, respectively.

2. Marine structure layouts

The marine harbour design layouts are based on RHDHV's 400m-option Western Breakwater design layouts. The description of the fully-built and part-built layouts is given below.

2.1. Part-built layout

The part-built layout and dredging plan used in the wave model were extracted from the drawing *PB6454-300-007* supplied for the study by RHDHV (Figure 2.1). Features of the layout include:

- Partially-built Western breakwater:
  - The first 300m from the cofferdam built up to create a haul road along the crest. The crest elevation of the structure is +4m AOD with a width of 14m. The side slopes are 1 in 1.33 and will be protected with concrete armour units (Xbloc);
  - The last 100m submerged rubble mound with a crest level of -4.5mAOD.
- Causeway in place joining the Western breakwater to the coast.
- The cofferdam in place with a crest level of +5mAOD.
- The crest length of the Eastern breakwater is approximately 150m long, with shore protection connecting the structure and the shoreline, and side slopes of 1:4/3.
- The design bed level within the harbour is -10mAOD.
- The MOLF consists of two berths, made of a vertical block wall structure fronted by mooring and berthing dolphins.
- The rock revetment along the MOLF quay has a slope of 1 in 1.5, and a crest elevation of +5mAOD.
- The berth pocket along Berths 1 and 2 is dredged to -11.9mAOD.

In addition, a sensitivity test was carried out to represent the effect of a 'worst-case' construction layout in terms of changes to waves. This layout included the full Western Breakwater but with the cofferdam and causeway still in place. Results from this layout are presented in Section 4.5.7.

2.2. Fully-built layout

The fully-built layout and dredging plan used in the wave model were extracted from the drawing *PB6454-300-008* supplied for the study by RHDHV (Figure 2.2). Features of the layout include:

- The Western breakwater is 400m long, comprising a 300m southern element unconnected to the coast and oriented approximately NNE-SSW and a 100m northern element oriented North-South.
- The crest length of the Eastern breakwater is approximately 150m long, with shore protection connecting the structure and the shoreline, and side slopes of 1:4/3.
- The design bed level within the harbour is -10mAOD.
- The MOLF consists of two berths, made of a vertical block wall structure fronted by mooring and berthing dolphins.
- The berth pocket along Berths 1 and 2 is dredged to -11.9mAOD.
- The rock revetment along the MOLF quay has a slope of 1 in 1.5, and a crest elevation of +5mAOD.
- The Eastern and Western breakwaters are fully-built, with:
  - Side slopes of 1:4/3;
  - The crest elevation of the Western breakwater varies between +10.7mAOD and +11.6mAOD;
  - The crest elevation of the Eastern breakwater is +11.1mAOD.

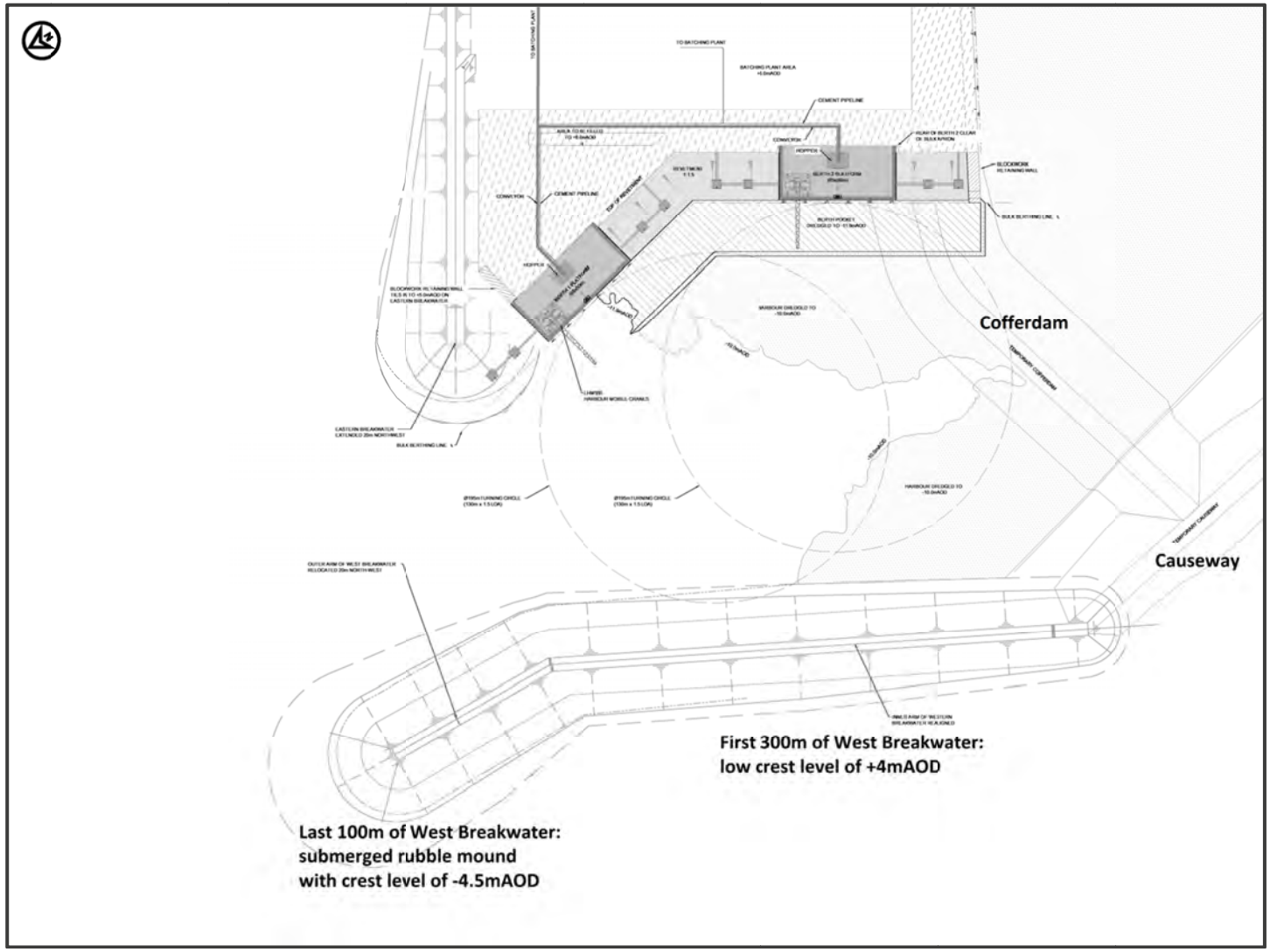

Figure 2.1: Part-built layout, 400m Western breakwater case, based on RHDHV PB6454-300-007 drawing

Source: RHDHV

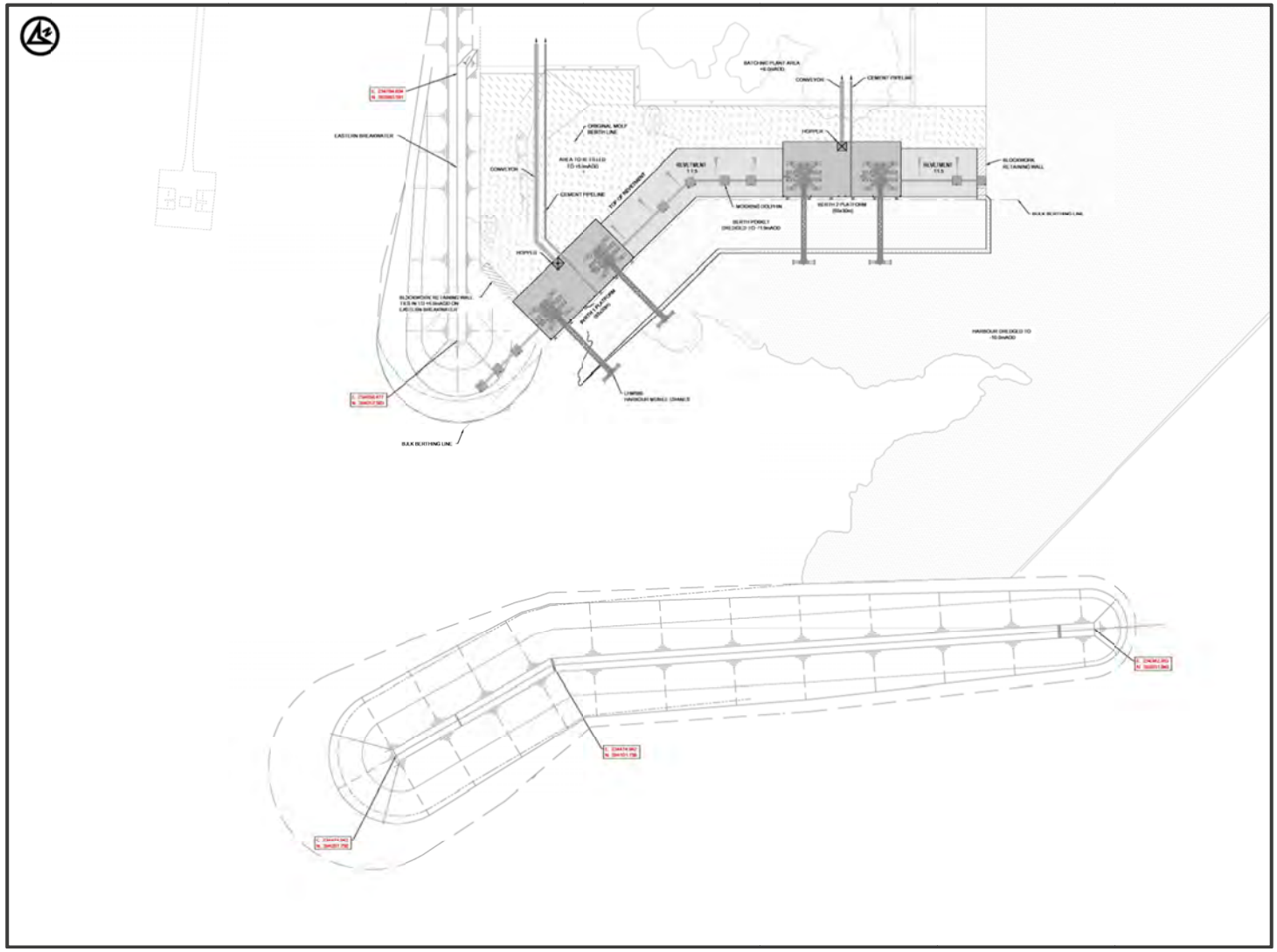

Figure 2.2: Fully-built layout, 400m Western breakwater case, based on RHDHV PB6454-300-008 drawing

Source: RHDHV

3. Climate-changed scenarios

3.1. Introduction

Two future scenarios are considered, representing "reasonably foreseeable" and "credible maximum" conditions. Present-day is taken as 2023. The future date of 2087 is taken to represent the end of power generation and 2187 to represent the end of de-commissioning. Metocean variables relevant to wave, sea level and overtopping prediction, potentially subject to future climate change, are mean sea level, surge, wave height (and period) and wind speed.

In addition to present-day, three of the four combinations of scenario and future date were applied to wave modelling for the baseline and fully-built layouts. Only the present-day scenario is relevant for the part-built layout.

The general approach to representation of climate-changed scenarios was originally developed during the NSMHHA flood hazard study (HR Wallingford, 2013; Amec, 2015). NSMHHA reviews several sources of extreme sea level and climate change information and several regulatory documents. For the purposes of the extreme sea levels derived in NSMHHA, the base date was taken to be 2008. The reasonably foreseeable scenario was based on the 95%ile (upper) projections for the Medium Emissions scenario of UKCP09 (United Kingdom Climate Impacts Program, 2009). The credible maximum scenario was based on the High plus plus approach of UKCP09. The present study bases its reasonably foreseeable case, instead, on more recent Welsh government (2016) advice on future climate change allowances.

3.2. Development of the appropriate allowances

3.2.1. Reasonably foreseeable

Figure 3.1, reproduced from Welsh government (2016), summarises how future sea level rise allowances should be developed. The 3.5mm/year rate of rise 2009-2025 is only fractionally higher than the present globally-averaged measured rate of rise, but the rapid increases from 2026 are fractionally higher than the highest (95%ile High Emissions) projections in UKCIP (2009).

Period	*2009-2025*	*2026-2055*	*2056-2085*	*2086-2116*	*Cumulative rise to 2116*
Annual change (mm/yr)	3.5	8.0	11.5	14.5	
Total increase	59.5 mm	240mm	345mm	449.5mm	1094mm

Figure 3.1: Welsh government (2016) advice on future mean sea level rise allowances

Source: Image from Welsh government (2016); later in the same document it is noted that 14.5mm/year should continue to be used beyond the 2116 end date

As the primary source of the present-day extreme high sea levels used for Wylfa Newydd is the Environment Agency (2011) coastal boundary conditions report, the base year, and hence the start date for climate

change adjustment, is 2008. Based on Figure 3.1, the "reasonably foreseeable" future sea level rise allowances from 2008 to 2023, to 2087 and to 2187 are 0.05m, 0.67m and 2.12m, respectively.

3.2.2. Credible maximum

The "High plus plus" source information (UKCIP, 2009) is summarised as a possible rise in mean sea level of 0.93-1.90m between 1980-1999 and 2095, with the possibility of an additional one metre of surge for extreme conditions. As in NSMHHA, the mean sea level rise amount is doubled for the period 2008 to 2187, and for the new period of 2008 to 2087, both components are factored down by 20% to reflect the end of generation date (from 2103 to 2087). In keeping with the "credible maximum" concept, only the top end of the range of possible mean sea level rise was adopted for the purpose of this assessment. The allowances used the study are summarised in Table 3.1.

3.2.3. Waves and winds

Projections of future wave climate suggest very little change from present-day, but a 10% increase in wave heights is often recommended as a precautionary allowance (for example NSMHHA, Amec, 2015). This 10% increase (and a corresponding 5% increase in wave periods) is applied in all the climate-changed scenarios considered here.

3.3. Appropriate allowances and the resulting sea levels

Table 3.1 summarises the climate change allowances to be used here, between 2008 and 2087, and between 2008 and 2187, appropriate to each scenario to be considered; also, for the reasonably foreseeable scenario only, the adjustment from 2008 to 2023. (Although the 2187 credible maximum scenario is not used within the present report, it is included here for completeness as it has been used in some of the earlier Wylfa Newydd wave modelling reports.) "Commonly occurring" (implying no significant surge component) was taken to refer to sea levels up to Mean High Water Springs, and "extreme" to refer to levels with a return period of 50 years or more. A sliding scale was applied between those two levels, meaning that the 1-year and 10-year levels would take 66% and 87%, respectively, of the extra surge allowance.

Table 3.1: Summary of climate-changed scenarios and allowances considered: between 2008 and 2023 (reasonably foreseeable only); between 2008 and 2087; and between 2008 and 2187

Future scenario	Add (metres) to commonly occurring sea levels			Add (metres) to extreme sea levels			Add (%) to offshore wave heights and wind speeds		
	2008 to 2023	2008 to 2087	2008 to 2187	2008 to 2023	2008 to 2087	2008 to 2187	2008 to 2023	2008 to 2087	2008 to 2187
'reasonably foreseeable'	0.05	0.67	2.12	--	--	--	0	10%	10%
'credible maximum'	--	1.5	3.8	--	2.3	4.8	--	10%	10%

Source: Based on Welsh government (2016) and UKCIP (2009); plus interpretation developed in HR Wallingford (2013) and Amec (2015)

Note: Ranges are given for the credible maximum sea level rise in the source document (UKCIP, 2009, but only the upper limit of the range is used in the wave modelling.

The three climate-changed cases used in this report were taken to have 0.67, 2.12 and 1.5 higher mean sea levels than in 2008 (and the 2187 credible maximum, not used here, would have 3.8m higher mean sea level), each with all offshore wave heights and winds increased by 10% (and wave periods increased by 5%). (The additional surge component of climate-changed sea level was added, where appropriate, during subsequent joint probability analysis.)

Extreme sea levels for a base year of 2008 listed in the top row of Table 3.2 are taken from NSMHHA, which took them from Environment Agency (2011). These are increased by 0.05m, 0.67m, 2.12m, 2.3m and 4.8m, respectively (slightly less for the 1 year level as it does not take the full surge allowance) to represent the five climate-changed cases of interest. Again, these were not used in the SWAN wave climate modelling (which used the MHWS levels also listed in Table 3.2) but were introduced, where appropriate, into the subsequent extremes and joint probability analysis.

Table 3.2: Summary MHWS and extreme sea levels for Wylfa

Scenario	Sea level (m ODN) for given scenario and return period (years)						
	MHWS	1	50	100	200	1000	10000
"EA3" (2008)	N/A	3.81	4.23	4.30	4.36	4.50	4.67
"Present-day" (2023)	3.05	3.86	4.28	4.35	4.41	4.55	4.72
2087, reasonably foreseeable	3.67	4.48	4.90	4.97	5.03	5.17	5.34
2187, reasonably foreseeable	5.12	5.93	6.35	6.42	6.48	6.62	6.79
2087, maximum credible	4.50	5.84	6.53	6.60	6.66	6.80	6.97
2187, maximum credible	6.80	8.27	9.03	9.10	9.16	9.30	9.47

3.4. Combinations of harbour layout and climate-change

The following seven combinations of harbour layout and climate change are considered in this report:

- Baseline, 2023 "present-day" conditions;
- Baseline, 2087 "reasonably foreseeable" conditions;
- Part-built layout, 2023 "present-day" conditions;
- Fully-built layout, 2023 "present-day" conditions;
- Fully-built layout, 2087 "reasonably foreseeable" conditions;
- Fully-built layout, 2087 "credible maximum" conditions;
- Fully-built layout, 2187 "reasonably foreseeable" conditions.

The 'credible maximum' condition was derived to provide a bounding case to support the FCA. The FCA is primarily concerned with conditions within the Harbour, not the wider environment. As such the 'credible maximum' scenario was only run through the ARTEMIS wave disturbance model (the model used for conditions inside the harbour) presented in Section 5.

All other assessments (HRA and EIA) required 'reasonably foreseeable' estimates of climate change to be modelled.

4. Wave conditions outside the harbour

The existing Phase 1 SWAN wave model was taken as the starting point. The model covers the northern half of Anglesey, to about ten kilometres offshore. It includes four nested model grids giving increasing spatial resolution nearer to Wylfa.

The 20m inner model grid was extended both westward and eastward to provide more detail in Cemaes and Cemlyn Bays. As the model changed slightly from the version validated during Phase 1, the wave model validation against wave measurements close to Wylfa was repeated using the refined model. The Wylfa Newydd marine structures and future climate-changed sea conditions were introduced into the model. Nearshore wave conditions are summarised at ten nearshore locations for relevant baseline, part-built and fully-built layouts, and for present-day and for relevant climate-changed conditions.

The purposes of the modelling were to provide wave climates at positions of direct interest in other studies and reports being prepared for regulatory approvals. Results include changes in nearshore wave conditions resulting from the Wylfa Newydd structures, and boundary conditions to a local wave disturbance model of the area immediately around the harbour.

A note on the local wave parameters used in this report

In all cases, significant wave height, mean wave period and mean wave direction are energy-averaged over all frequency and direction components of the wave energy spectrum, at the particular wave prediction point and for the particular layout and climate change scenario which they represent. As waves propagate from offshore to inshore, they can change direction, tending to become more normal to the bed contours. Where a headland or structure either provides an obstacle to wave propagation and/or generates a reflected component of wave energy, mean wave direction can change suddenly. In assessment of changes in wave height caused by introduction of structures, it would be fair to compare individual wave conditions, or to compare the overall distribution of wave height, before and after construction, but not to compare the distribution of wave height within an individual direction bin because individual wave conditions may move between bins.

4.1. The SWAN wave model

As waves propagate towards the site they are modified by the processes of depth refraction and shoaling as they travel through increasingly shallow water. Wave models that simulate the nearshore wave transformation processes are well established and for the present study the SWAN (Simulating WAves Nearshore, Booij et al., 1999) model has been used.

SWAN is a 3rd generation spectral wave model which simulates the transformation of random directional waves considering the following processes:

- Wave shoaling;
- Wave refraction by the bathymetry and by currents;
- Wave blocking by currents;
- Depth-induced breaking, bottom friction and whitecapping;
- Wave growth due to the wind;
- Wave reflections from structures or rocky shorelines;
- Far-field wave diffraction around headlands.

The SWAN model has been extensively validated and is suited to the transformation of wave energy spectra in relatively large coastal areas. This is particularly true where the features of the seabed, such as offshore banks and reefs, result in depth-induced wave breaking and wave-wave interactions. The model also includes wave generation by the wind within the model area. SWAN is, therefore, especially useful in regions such as the shallow area near to the site where wave conditions may comprise a combination of refracted offshore waves and those generated locally by winds. More details of the SWAN model are given in Appendix B.

4.1.1. Application of the SWAN model to Wylfa

The SWAN model was set up to represent wave propagation from offshore. Four nested grids were used:

- The outer grid (Grid 1) covers a wide area approximately 29km x 53km offshore and along the coasts, at a grid resolution of 500m;
- The second grid (Grid 2), further inshore, at a grid resolution of 200m;
- The third grid (Grid 3) covers an area further inshore at a grid resolution of 50m;
- The inner grid (Grid 4) covers the area near the site with a grid resolution of 20m.

The model bathymetry was defined using information obtained from SeaZone TruDepth bathymetry data, supplemented with the local survey data supplied for the study (HR Wallingford, 2013). The data sets were reviewed and corrected to Chart Datum and then merged to provide the model bathymetry used in SWAN. The resulting bathymetry has been incorporated into the model grids.

The extent of the model, arrangement of its four grids, and the positions at which results were summarised in Phase 1, are shown in Figure 4.1.

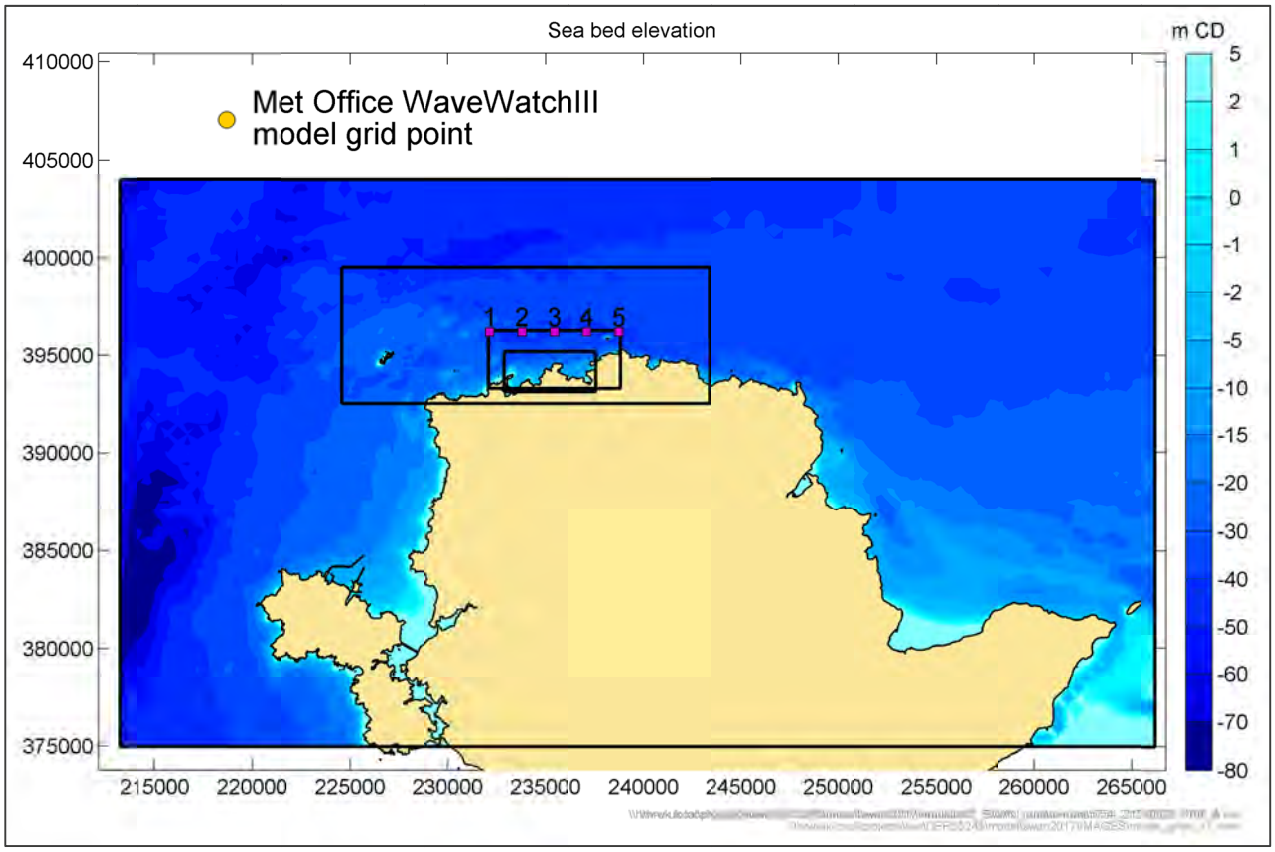

Figure 4.1: Extent of the SWAN wave model outer (500m) grid, also showing its three inner (200, 50 and 20m) grids and Points 1 to 5 at which results were summarised during Phase 1

Source: HR Wallingford

4.1.2. Boundary conditions

The SWAN model was run applying offshore waves, obtained from the 35-year WaveWatchIII Met Office wave and wind model, along the seaward boundary and forced with coincident wind conditions applied spatially uniformly across the whole model domain. The SWAN model was run both for a constant high sea level and for realistically varying tidal sea levels.

4.1.3. Reflection coefficients

The reflection properties of the boundaries were represented in the SWAN model by assigning an appropriate reflection coefficient to each of the boundary types within the model. A reflection coefficient of 1.0 would indicate that all the incident wave energy will be reflected, while a lower reflection coefficient would indicate that some wave energy will be dissipated.

Appropriate wave reflection coefficients were defined for the coastline, breakwaters, quays and other structures depending upon the form of the structures and the wave conditions (Allsop, 1990). The reflection coefficients used for the study are summarised in Table 4.1. Reflections were applied only within the inner model grid.

Table 4.1: Reflection coefficients used in the SWAN model

Boundary types	Reflection coefficient
Rocky coastline	0.4
Beach coastline	0.2
Breakwater (1:4/3 slope)	0.45
Vertical structures along the quays	0.95
Cofferdam (1:1.5 slope)	0.35

4.1.4. Transmission coefficients

In the part-built layout (Figure 2.1), the Western breakwater is partially constructed with a crest elevation of +4mAOD. The difference between the crest level and the present-day MHWS water level is only one metre. Therefore, the breakwater was represented as a partially transmissive structure in the SWAN model.

The wave transmission coefficient was estimated based upon the wave conditions incident on the breakwater and an empirical relationship derived from a physical model database (HR Wallingford, 2009). A transmission coefficient of 1.0 would indicate full transmission. The transmission coefficient used in the model for the partially constructed Western breakwater is 0.35, which is a relatively conservative estimate of transmission for the MHWS present-day conditions.

4.2. Model validation

The model was calibrated and validated against wave measurements at four locations within the two inner model grids during Phase 1 (HR Wallingford, 2015). The approach to wave model validation is that developed, applied and published during a recent National Flood Risk Assessment (NaFRA) State of the Nation in 24 regions covering the whole coast of England (HR Wallingford, 2015b).

The model validation was based upon comparisons between measured and modelled storm peak wave conditions for 18 selected storms for which measured wave conditions are available at some or all of four locations (S2, S4, S9 and S11; see Figure 4.2). The time-varying wind velocity, sea level and spectral representation of the wave conditions were used for each storm. The period of the measurements was generally rather calm (HR Wallingford, 2013; Amec, 2015). The selected storms include a set of winter and summer conditions, covering a range from approximately 1 year return period conditions down to 10 to 20 times a year conditions.

4.2.1. Validation against peak storm events

As the present study is intended primarily to investigate the environmental impact of the schemes, reflection from the coastline is now included in the model. Therefore, the model validation was repeated for the new model (for the baseline case) to ensure its performance was unchanged from Phase 1. The model was run for the selected storms with the same model settings. Table 4.2 to Table 4.5 compare measured (where available) and modelled storm peak wave conditions for each of the eighteen storms. Model validation results are very similar to those of Phase 1 and, if anything, are fractionally improved for S4 and S11.

Comparing with the validation statistics of the NaFRA State of the Nation study for wave height and wave period, the Root Mean Square Error statistics in Table 4.2 to Table 4.5 fall within the range of the best 12 of the equivalent 24 State of the Nation results for wave height, and within the overall range for wave period. In

addition, Section 4.5.3 of Environment Agency (2016) refers to the NaFRA State of the Nation wave models as being of an appropriate standard for use in wave forecasting, and provides criteria against which the accuracy of other models can be judged. The validation results for wave height summarised in Table 4.2 to Table 4.5 meet the criteria of the highest accuracy category for wave height for all four measurement sites, and for wave period for three of four measurement sites (the fourth meeting the criteria of the second accuracy category).

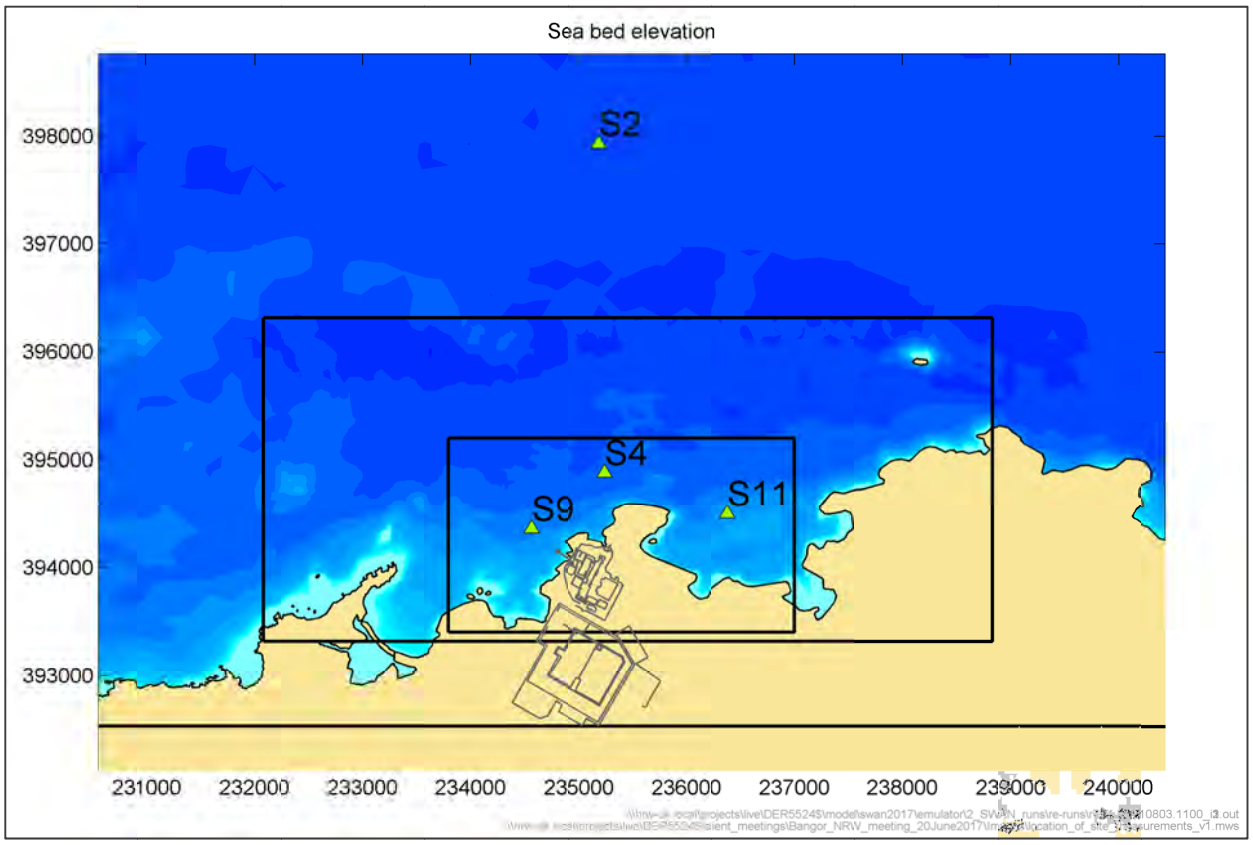

Figure 4.2: Location map for Horizon wave measurements close to Wylfa

Note: The locations of S2, S4, S9 and S11, marked by green triangles on the map, are approximate, as the exact positions varied between successive 3-4 month deployments.

Table 4.2: Validation of the SWAN model for storm peak wave conditions at S2

Storm No.	S2 measured storm peaks			S2 modelled storm peaks			Storm peak summary statistics		
	H_s (m)	T_m (s)	D_m (°N)	H_s (m)	T_m (s)	D_m (°N)			
2	2.59	5.4	331	2.36	5.1	345	H_s (m)	Bias: mean of model error	-0.02
4	3.14	5.8	42	2.82	5.5	14		MAE: mean absolute error	0.28
5	2.45	5.2	1	2.12	4.8	343		RMSE: root mean square model error	0.31
6	2.14	5.3	254	2.47	4.5	206		Std. error: standard deviation model error	0.31
8	2.93	5.8	44	2.51	5.2	14		MAD: median absolute deviation	0.32
9	3.25	5.6	295	3.65	6.1	344	T_m (s)	Bias: mean of model error	-0.32
10	2.46	5.8	271	2.6	4.8	246		MAE: mean absolute error	0.48
11	2.59	5.0	254	3.1	5.3	250		RMSE: root mean square model error	0.56
12	3.33	5.4	243	3.23	5.5	264		Std. error: standard deviation model error	0.46
14	2.99	6.2	268	2.62	5.3	287		MAD: median absolute deviation	0.39
15	3.06	5.9	274	3.16	5.6	270			
16	3.17	5.9	280	3.28	5.7	258			

Source: HR Wallingford

Table 4.3: Validation of the SWAN model for storm peak wave conditions at S4

Storm No.	S4 measured storm peaks			S4 modelled storm peaks			Storm peak summary statistics		
	H_s (m)	T_m (s)	D_m (°N)	H_s (m)	T_m (s)	D_m (°N)			
2	3.05	5.8	308	2.41	5.1	346	H_s (m)	Bias: mean of model error	-0.10
3	2.89	5.8	281	2.78	5.5	284		MAE: mean absolute error	0.35
4	3.09	5.5	28	2.83	5.5	15		RMSE: root mean square model error	0.40
5	2.44	5.1	16	2.18	4.9	343		Std. error: standard deviation model error	0.39
7	4.18	6.2	289	4.73	6.9	285		MAD: median absolute deviation	0.30
8	3.08	5.8	43	2.55	5.2	15	T_m (s)	Bias: mean of model error	-0.61
9	3.02	5.5	326	3.67	6.2	345		MAE: mean absolute error	0.84
10	2.05	6.3	254	2.04	4.0	258		RMSE: root mean square model error	1.04
11	2.21	6.2	250	2.49	4.8	263		Std. error: standard deviation model error	0.84
12	3.39	6.7	269	2.97	5.3	285		MAD: median absolute deviation	0.66
15	2.90	5.7	297	2.59	5.1	289			
16	2.64	6.2	262	2.44	4.9	287			

Source: HR Wallingford

Table 4.4: Validation of the SWAN model for storm peak wave conditions at S9

Storm No.	S9 measured storm peaks			S9 modelled storm peaks		
	H_s (m)	T_m (s)	D_m (°N)	H_s (m)	T_m (s)	D_m (°N)
1	1.76	4.9	360	1.90	4.7	337
2	2.37	5.3	350	2.33	5.1	347
3	1.92	5.1	306	2.18	4.9	302
4	2.54	5.1	18	2.70	5.5	12
5	2.13	5.1	355	2.12	4.9	345
6	1.05	5.6	348	1.10	3.1	299
7	3.10	5.5	294	3.62	6.2	307
8	2.45	5.5	21	2.44	5.2	12
9	2.38	5.3	333	3.48	6.1	347
11	1.40	4.2	292	1.50	3.4	284
12	2.40	5.7	324	2.43	4.7	300
13	1.59	4.3	300	1.71	4.2	297
14	2.08	5.3	305	2.01	4.8	304
16	1.99	5.8	277	2.02	4.4	298
17	2.63	5.5	308	3.17	5.8	308
18	1.95	5.5	293	1.86	4.3	300

Storm peak summary statistics		
H_s (m)	Bias: mean of model error	0.18
	MAE: mean absolute error	0.20
	RMSE: root mean square model error	0.35
	Std. error: standard deviation model error	0.30
	MAD: median absolute deviation	0.09
T_m (s)	Bias: mean of model error	-0.40
	MAE: mean absolute error	0.67
	RMSE: root mean square model error	0.90
	Std. error: standard deviation model error	0.81
	MAD: median absolute deviation	0.45

Source: HR Wallingford

Table 4.5: Validation of the SWAN model for storm peak wave conditions at S11

Storm No.	S11 measured storm peaks			S11 modelled storm peaks			Storm peak summary statistics		
	H_s (m)	T_m (s)	D_m (°N)	H_s (m)	T_m (s)	D_m (°N)			
2	2.27	5.3	349	2.33	5.1	346	H_s (m)	Bias: mean of model error	-0.03
3	2.09	5.8	301	2.25	5.1	302		MAE: mean absolute error	0.24
4	2.46	5.3	9	2.62	5.4	7		RMSE: root mean square model error	0.28
5	2.30	5.1	358	2.12	4.9	343		Std. error: standard deviation model error	0.28
6	1.16	5.2	336	1.10	3.1	299		MAD: median absolute deviation	0.18
7	4.24*	4.8*	318	3.79	6.4	306	T_m (s)	Bias: mean of model error	-0.81
8	2.55	5.3	22	2.36	5.2	8		MAE: mean absolute error	1.06
9	3.19	6.3	295	3.53	6.2	345		RMSE: root mean square model error	1.52
11	1.49	6.6	311	1.17	2.9	296		Std. error: standard deviation model error	1.28
12	2.60	6.7	308	2.15	4.5	309		MAD: median absolute deviation	0.69
13	1.65	6.4	309	1.51	4.0	305			
14	1.80	4.9	339	2.05	4.9	306			
15	2.26	5.7	304	2.21	4.8	301			
16	1.56	5.2	309	2.05	4.6	299			

Source: HR Wallingford

Note: The reported measured H_s and T_m for Storm 7 are incompatible in terms of wave steepness, but the record is retained as it corresponds with the time of maximum wave height at S9 and at the WaveWatchIII point.*

4.2.2. Validation against everyday conditions

Comparison for more frequent,lower wave heights has been carried out at the measurement location S9, nearest to the site which has the best quality in the wave measurement records. A significant number of the wave height records of S2 and S4 had to be filtered out from the measured data following quality control checks and the resulting datasets were therefore not used in the assessment.

Figure 4.3 shows a comparison of the percentage of exceedence of wave heights (H_s) measured and the SWAN wave model predictions for the period of measurements at the S9 location. This indicates that the measurements and model prediction exceedence curves show close agreement for low wave heights (lower than 2m), with a slight over-estimate from the model.

The modelled time-series used for this comparison was generated with the model emulation approach (see details in Section 4.4.1) and does not include the better representation of the peak storm data applying partitioned offshore wave spectra to the boundary of the model, since the comparison focusses on more frequent lower wave heights events. Therefore the comparison for large events (Hs > 2.5m) should not be drawn based on the exceedence curve comparison shown in Figure 4.3 but from the model validation undertaken in Section 4.2.1 which makes use of the more accurate storm data in the model and therefore provides a better comparison between storm peaks and the model.

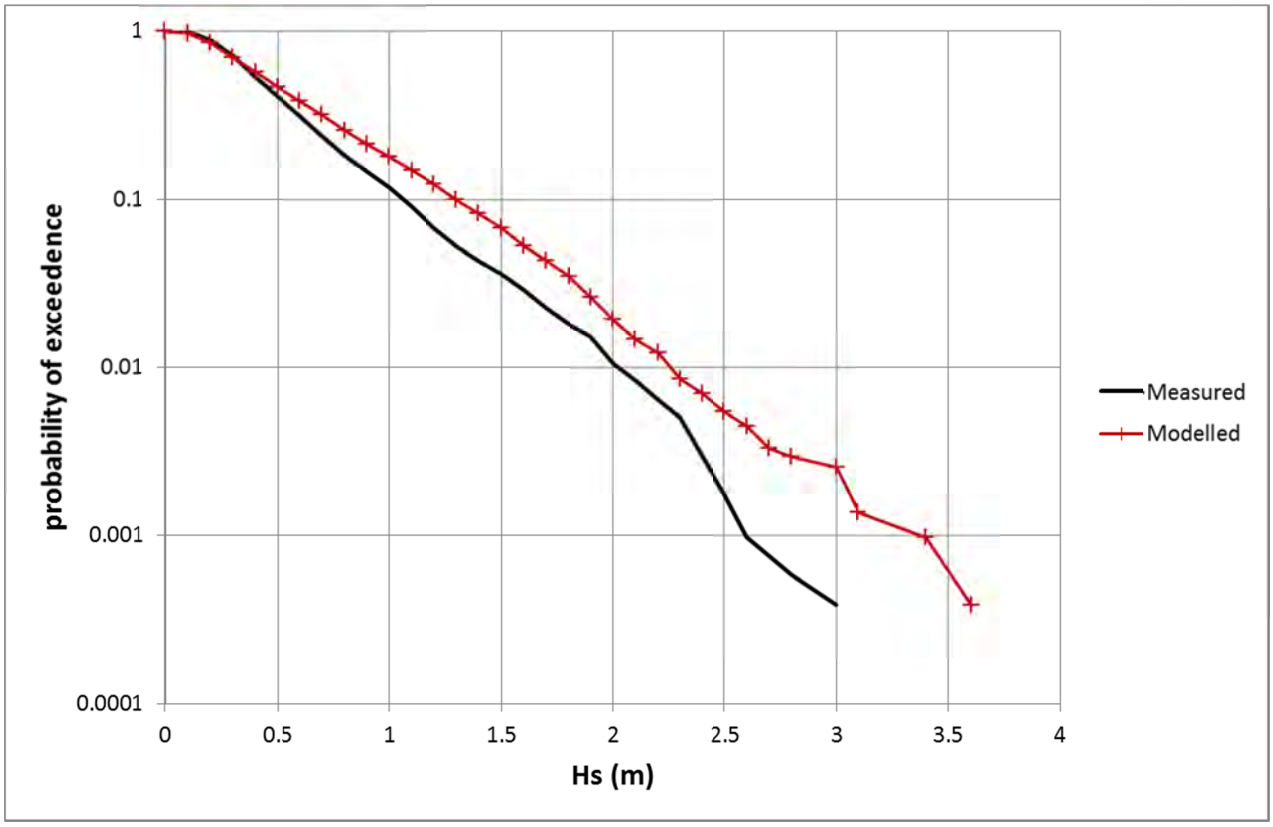

Figure 4.3: Significant wave height exceedence, measured wave data and wave model predictions, S9 location

4.3. Nearshore wave prediction points

Results were collated at ten nearshore wave prediction points shown in Figure 4.4 and defined in Table 4.6.

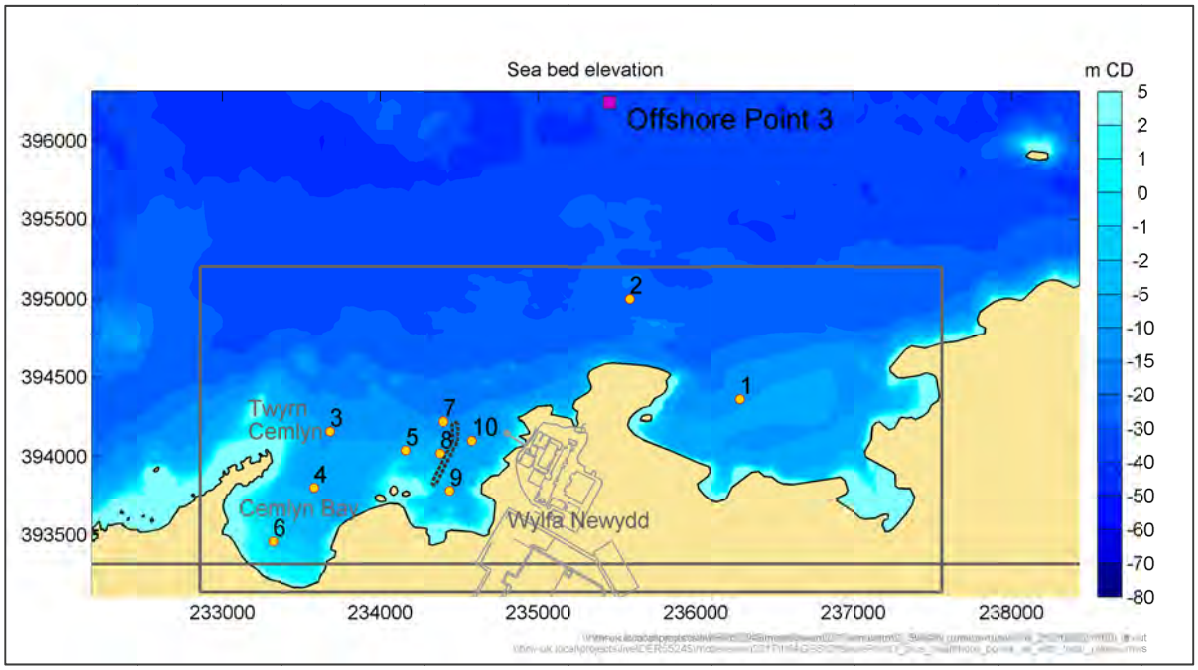

Figure 4.4: Locations of the Offshore Point 3 and the ten nearshore wave prediction points

Note: The grey rectangles indicate the extent of the 50m and the 20m SWAN model grids

Table 4.6: Locations and bed levels of the ten SWAN nearshore wave prediction points (baseline bathymetry)

Point ID	Easting (m)	Northing (m)	Bed level	
1	236280	394360	-11.5mCD	-15.1mOD
2	235580	395000	-21.5mCD	-25.1mOD
3	233680	394160	-11.0mCD	-14.6mOD
4	233580	393800	-5.4mCD	-9.0mOD
5	234160	394040	-4.8mCD	-8.4mOD
6	233320	393460	-1.1mCD	-4.7mOD
7	234400	394220	-13.8mCD	-17.4mOD
8	234380	394020	-6.0mCD	-9.6mOD
9	234440	393780	-5.2mCD	-8.8mOD
10	234580	394100	-10.0mCD	-13.6mOD

4.4. Wave climate results

It is envisaged that the results presented in this chapter will be used for environmental impact assessment. It is understood from Horizon NP, that this type of result should be prepared without deliberate conservatism. Hence, the wave modelling was undertaken at actual sea levels appropriate to each record, with no mark-up of offshore wave and wind conditions beyond that determined during the wave model calibration, and with no allowance for uncertainty.

The results presented in this chapter are intended to be used for environmental impact assessment and not for design.

The modelling reported here responds to a proposed design layout, rather than the model as reported being used to inform or validate the design. The design validation work package is a separate report not forming part of the DCO submission.

4.4.1. Nearshore wave time series

For the wave transformation modelling a model emulation approach was used, whereby the SWAN model is run not for every offshore record, but for a large subset of events. These are then combined with sophisticated interpolation techniques (Camus et al., 2013; Gouldby et al., 2014) to develop a robust simulation that represents the range of multivariate conditions present in the offshore data. The emulator training runs were carefully selected to cover the complete range of offshore boundary conditions (including climate-changed conditions) using six parameters: significant wave height (H_s), mean wave period (T_{m-10}), wave direction, water levels, wind speed and wind direction.

Using the model emulation, 35-year (3-hourly) nearshore time series were generated at varying water levels at the ten nearshore locations for the following layout / scenario conditions:

- baseline, 2023 “present-day” conditions;
- baseline, 2087 “reasonably foreseeable” conditions;
- part-built layout, 2023 “present-day” conditions;
- fully-built layout, 2023 “present-day” conditions;
- fully-built layout, 2087 “reasonably foreseeable” conditions;
- fully-built layout, 2187 “reasonably foreseeable” conditions;
- fully-built layout, 2087 “credible maximum” conditions.

The time series at the temporary cofferdam location (Point 9) was generated for baseline conditions only.

The time series are not presented directly in this report. Instead, they were issued separately in digital editable format for further use in other studies. Note that the date labels for the climate-changed scenario time-series are dummy labels.

4.4.2. Nearshore wave climates

Nearshore wave conditions are summarised at the ten locations along the breakwater structures and along the coastline shown in Figure 4.4 and listed in Table 4.6. For illustration, annual wave roses at Point 5 are shown in Figure 4.5 for the 2023 “present-day” conditions, for the baseline, part-built and fully-built layouts, and in Figure 4.6 for the fully-built layout 2087 “reasonably foreseeable”, 2187 “reasonably foreseeable” and 2087 “credible maximum” conditions. Table 4.7 and Table 4.8 show the distribution of significant wave height against mean wave direction and against mean wave period at Point 5 for 2023 “present-day” baseline conditions.

For all layouts, frequency tables (annual and seasonal) are provided at the nearshore points in digital format. Annual and seasonal wave roses and frequency tables for the nearshore locations are provided in Appendix C.

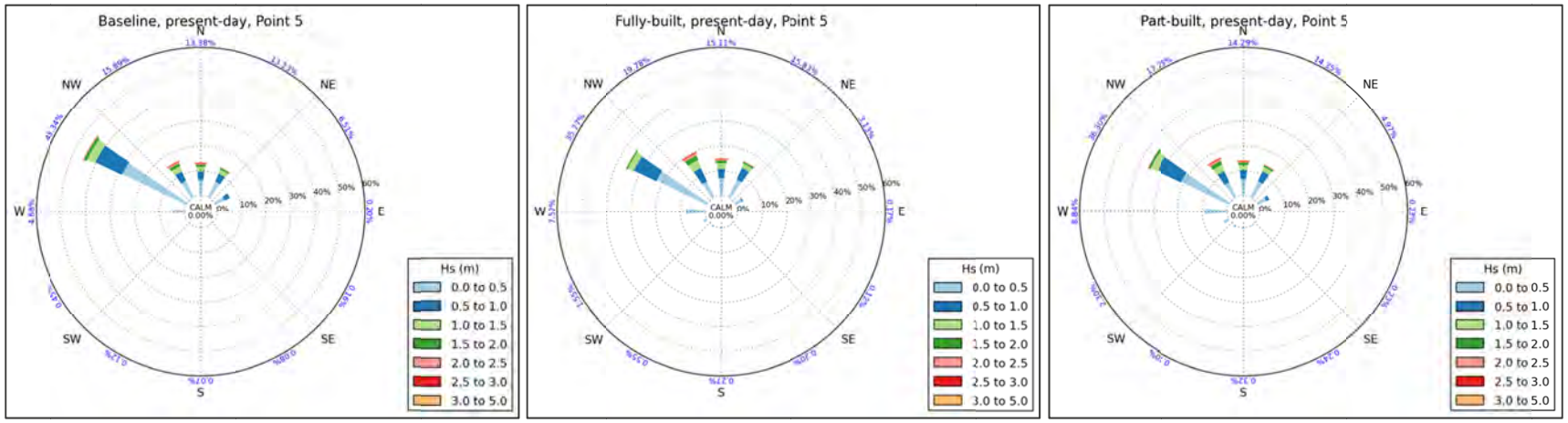

Figure 4.5: Annual wave roses for nearshore prediction Point 5, present-day, baseline, fully-built and part-built layouts

Source: HR Wallingford, SWAN wave transformation and Met Office WW3 offshore data, 1980-2015

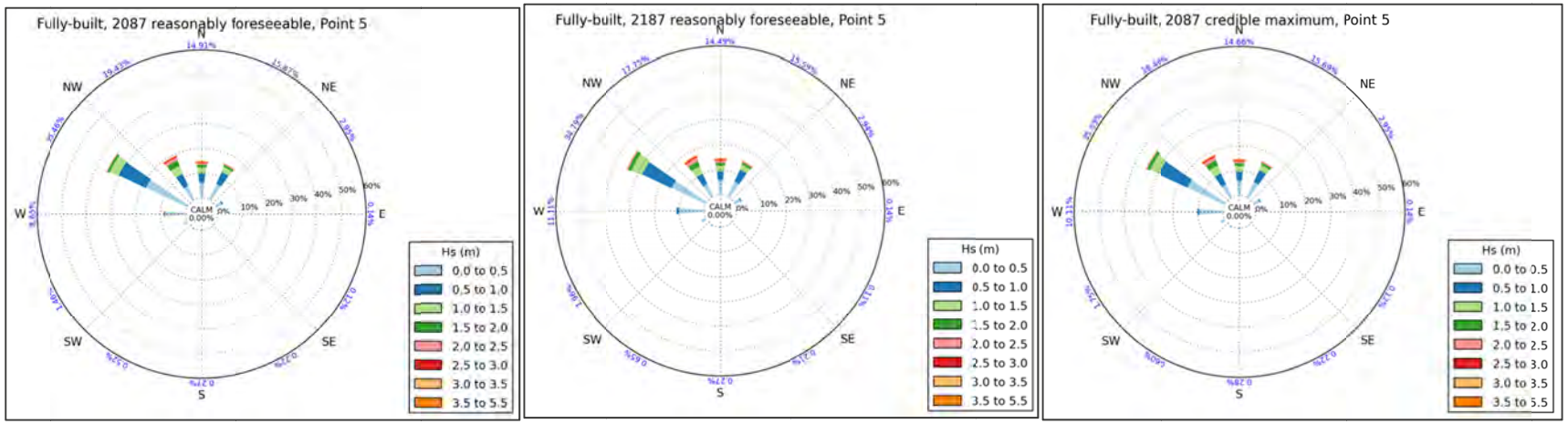

Figure 4.6: Annual wave roses for nearshore prediction Point 5, fully-built layout, future climate-changed scenario conditions

Source: HR Wallingford, SWAN wave transformation and Met Office WW3 offshore data, 1980-2015

Table 4.7: Annual wave climate at Point 5, baseline, 2023 "present-day", significant wave height (H_s) against mean wave direction

			Parts per hundred thousand in the given wave height (m) and wave direction (degrees True North) bin											
			-15	15	45	75	105	135	165	195	225	255	285	315
H_{s1} (m)	H_{s2} (m)	$P(H_s>H_{s1})$	15	45	75	105	135	165	195	225	255	285	315	345
0.0	0.5	100.00%	6326	6922	4032	196	158	80	69	122	449	4648	28498	7248
0.5	1.0	41.25%	3318	3506	2283	-	<1	-	<1	<1	-	34	11874	4111
1.0	1.5	16.13%	1967	1713	185	-	-	-	-	-	-	-	3462	2273
1.5	2.0	6.53%	904	668	8	-	-	-	-	-	-	-	1136	1196
2.0	2.5	2.61%	403	243	-	-	-	-	-	-	-	-	286	641
2.5	3.0	1.04%	243	61	-	-	-	-	-	-	-	-	66	298
3.0	3.5	0.37%	124	13	-	-	-	-	-	-	-	-	14	101
3.5	4.0	0.12%	66	7	-	-	-	-	-	-	-	-	1	15
4.0	4.5	0.03%	21	<1	-	-	-	-	-	-	-	-	-	4
4.5	5.0	0.01%	7	-	-	-	-	-	-	-	-	-	-	-
Percentage occurrence			13.38%	15.77%	13.38%	13.13%	6.51%	0.20%	0.16%	0.08%	0.07%	0.12%	0.45%	4.68%

Source: HR Wallingford, SWAN wave transformation and Met Office WW3 offshore data, 1980-2015; occurrence is in parts per hundred thousand

Table 4.8: Annual wave climate at Point 5, baseline, 2023 “present-day”, significant wave height (H_s) against mean wave period

			Parts per hundred thousand in the given wave height (m) and mean wave period (T_{m-10}, seconds) bin													
			0	1	2	3	4	5	6	7	8	9	10	11	12	13
H_{s1} (m)	H_{s2} (m)	$P(H_s>H_{s1})$	1	2	3	4	5	6	7	8	9	10	11	12	13	14
0.0	0.5	100.00%	8	2173	19091	23865	10464	2464	504	124	33	7	6	5	2	2
0.5	1.0	41.25%	-	3	303	8703	11594	3048	1246	218	10	1	-	-	-	-
1.0	1.5	16.13%	-	-	4	117	5167	3410	493	292	105	12	-	-	-	-
1.5	2.0	6.53%	-	-	-	3	173	2913	708	83	22	10	1	-	-	-
2.0	2.5	2.61%	-	-	-	<1	3	399	1003	151	12	5	-	-	-	-
2.5	3.0	1.04%	-	-	-	-	-	5	365	273	17	4	3	-	-	-
3.0	3.5	0.37%	-	-	-	-	-	-	10	211	23	5	2	-	-	-
3.5	4.0	0.12%	-	-	-	-	-	-	<1	32	54	2	<1	-	-	-
4.0	4.5	0.03%	-	-	-	-	-	-	-	1	21	3	<1	-	-	-
4.5	5.0	0.01%	-	-	-	-	-	-	-	<1	4	3	-	-	-	-
Percentage occurrence			0.01%	2.18%	19.40%	32.69%	27.40%	12.24%	4.33%	1.39%	0.30%	0.05%	0.01%	0.01%	0.00%	0.00%

Source: HR Wallingford, SWAN wave transformation and Met Office WW3 offshore data, 1980-2015; occurrence is in parts per hundred thousand

4.5. Sensitivity of wave height to structures

4.5.1. Representative winter and summer conditions

For the 2023 "present-day" and 2087 "reasonably foreseeable" conditions, and for representative summer and winter conditions, the effects of the structures on wave height are illustrated by comparing the predicted significant wave heights for the part-built and fully-built layouts against those for the baseline conditions.

Typical summer and winter conditions were selected based on the wave climate, for present-day conditions, predicted in HR Wallingford (2015) for Offshore Point 3 (see Figure 4.4). Table 4.11 and Table 4.12 show the summer and winter distribution of significant wave height against mean wave direction at Offshore Point 3 for 2023 "present day" baseline conditions. The summer and winter periods are defined as April to September (inclusive) and October to March (inclusive), respectively.

The representative typical summer wave condition was selected from the wave height and direction bin containing the most records in the Offshore Point 3 summer wave frequency climate tables. For the present-day conditions, this corresponds to a significant wave height of 0.6m from the 225-255°N sector. Winter conditions were defined as selected percentiles, representative of an average winter condition (50%), and more severe winter storm conditions of 90% and 99% within each of the NW, N and NE sectors.

Table 4.9 and Table 4.10 summarise the summer and winter present-day wave conditions used in the model. The "2087 reasonably foreseeable" conditions were obtained from the present-day conditions by applying a 10% increase in wave heights (and corresponding 5% in wave periods) and wind speeds to reflect the future climate change allowances. They were also run in the model, at water levels increased by 0.62m to allow for climate change.

Table 4.9: Representative present-day frequently-occurring Summer wave condition at Offshore Point 3

Condition	H_s (m)	T_{m-10} (s)	Dir (°N)
Summer condition, present-day	0.60	3.3	254

Source: HR Wallingford analysis at Offshore Point 3

Table 4.10: Representative present-day Winter storm wave conditions at Offshore Point 3

Sector	Event	H_s (m)	T_{m-10} (s)	Dir (°N)
N	50th percentile	0.93	4.1	360
	90th percentile	2.49	6.0	343
	99th percentile	4.21	7.8	345
NE	50th percentile	0.89	4.0	57
	90th percentile	2.29	5.9	39
	99th percentile	3.48	6.9	36
NW	50th percentile	1.17	4.4	309
	90th percentile	2.76	6.5	329
	99th percentile	4.03	7.5	303

Source: HR Wallingford analysis at Offshore Point 3

To illustrate the difference in predicted significant wave height between the baseline and the fully-built layout, sample difference plots are shown in Figure 4.7 to Figure 4.10, for the summer present-day conditions, and for the 99th percentile winter “2087 reasonably foreseeable” conditions from the NW, N and NE sectors, respectively. Each figure is in three parts, and represents just one wave condition. The top pane of each figure shows the baseline significant wave height for the area around Wylfa, and the middle pane the corresponding wave heights after introduction of the fully-built layout. The bottom pane shows the difference in significant wave height between the runs with and without structures. Yellow and orange shades show increases in wave height of at least ten centimetres. Blue and green shades show reductions in wave height of at least ten centimetres.

Sample difference plots between the baseline and the part-built layout (as defined in Figure 2.1, including a partially built western breakwater), are shown in Figure 4.11 to Figure 4.14, for the summer present-day conditions, and for the 99th percentile winter “present-day” conditions from the NW, N and NE sectors, respectively.

The extents of the differences in significant wave height (higher than +/- 10cm) due to the structures is localised around the proposed structures. For the largest waves from the NW sector for the fully-built layout “2087 reasonably foreseeable” conditions (see Figure 4.8), the differences extend up to Cemlyn Bay. For this sector, the directions and heights of the reflected waves from the two sections of the Western Breakwater, coupled with refraction and shoaling effects as they approach the coast, appear to be causing a small amount of refocussing of the wave energy in Cemlyn Bay to give a localised area of increase in H_s of just above 10 centimetres. No differences in significant wave height higher than +/- 10cm is predicted in Cemlyn Bay for the “present-day” conditions tested with either the fully-built or part-built layouts.

The additional summer and winter wave conditions cases have been provided in digital format.

The refocussing of the wave energy in Cemlyn Bay is sensitive to the wave direction and further sensitivity tests have been carried out in Section 4.5.2.

Table 4.11: Summer wave climate at Offshore Point 3, baseline, 2023 "present-day", significant wave height (H_s) against mean wave direction

			Wave direction (°N)											
			-15	15	45	75	105	135	165	195	225	255	285	315
H_{s1} (m)	H_{s2} (m)	$P(H_s>H_{s1})$	15	45	75	105	135	165	195	225	255	285	315	345
0.0	0.5	100.00%	4383	2258	4530	3070	995	791	1172	3746	8164	4909	3145	4503
0.5	1.0	58.33%	3038	1552	3238	2354	516	420	560	2089	10495	5794	2880	3688
1.0	1.5	21.71%	1078	706	1330	882	79	42	87	296	3194	2362	1579	2141
1.5	2.0	7.93%	331	271	676	231	-	2	4	19	541	1240	874	984
2.0	2.5	2.76%	177	171	202	4	-	-	-	-	12	347	435	395
2.5	3.0	1.02%	83	100	62	-	-	-	-	-	2	83	175	181
3.0	3.5	0.33%	27	42	46	-	-	-	-	-	-	13	39	81
3.5	4.0	0.09%	2	19	21	-	-	-	-	-	-	-	4	10
4.0	4.5	0.03%	2	12	4	-	-	-	-	-	-	-	-	-
4.5	5.0	0.01%	2	4	2	-	-	-	-	-	-	-	-	-
5.0	5.5	0.01%	4	2	-	-	-	-	-	-	-	-	-	-
5.5	6.0	0.00%	-	-	-	-	-	-	-	-	-	-	-	-
Percentage occurrence			9.13%	5.14%	10.11%	6.54%	1.59%	1.26%	1.82%	6.15%	22.41%	14.75%	9.13%	11.98%

Source: HR Wallingford, SWAN wave transformation (Phase 1) and Met Office WW3 offshore data, 1980-2015; occurrence is in parts per hundred thousand

Table 4.12: Winter wave climate at Offshore Point 3, baseline, 2023 “present day”, significant wave height (Hs) against mean wave direction

			Wave direction (°N)							
			-22.5	22.5	67.5	112.5	157.5	202.5	247.5	292.5
H_{s1} (m)	H_{s2} (m)	$P(H_s>H_{s1})$	22.5	67.5	112.5	157.5	202.5	247.5	292.5	337.5
0	0.5	100.00%	2043	1629	3455	941	1026	2918	3513	2139
0.5	1	82.34%	2238	1975	5513	1335	1395	8160	7963	3098
1	1.5	50.66%	1426	1163	3395	456	464	5878	8197	2278
1.5	2	27.40%	974	752	1704	100	81	1459	7959	1662
2	2.5	12.71%	568	512	500	-	-	48	3588	1310
2.5	3	6.18%	336	305	272	-	-	-	1600	926
3	3.5	2.74%	224	112	62	-	-	-	756	444
3.5	4	1.14%	126	33	12	-	-	-	317	280
4	4.5	0.38%	70	23	4	-	-	-	79	112
4.5	5	0.09%	29	4	4	-	-	-	12	21
5	5.5	0.02%	10	-	2	-	-	-	2	2
5.5	6	0.00%	2	-	-	-	-	-	2	-
	Percentage Occurrence		8.04%	6.51%	14.92%	2.83%	2.97%	18.46%	33.99%	12.27%

Source: HR Wallingford, SWAN wave transformation (Phase 1) and Met Office WW3 offshore data, 1980-2015; occurrence is in parts per hundred thousand

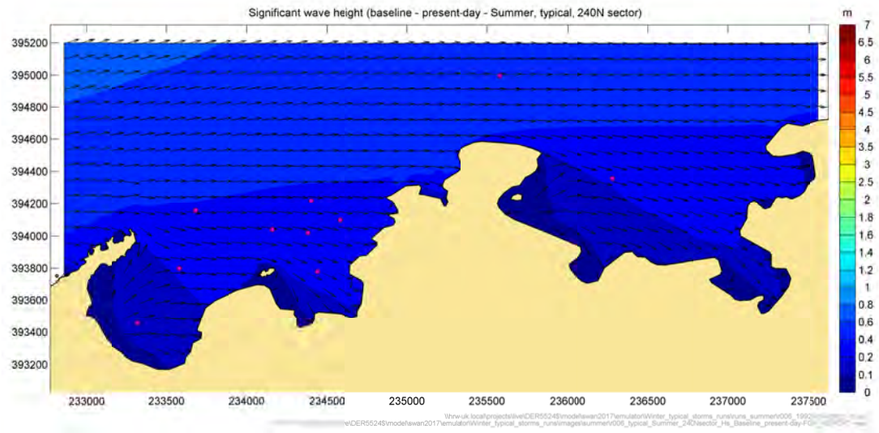

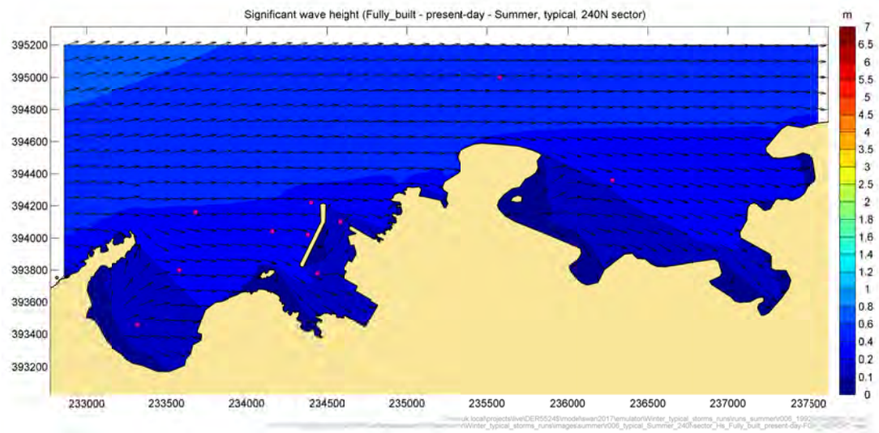

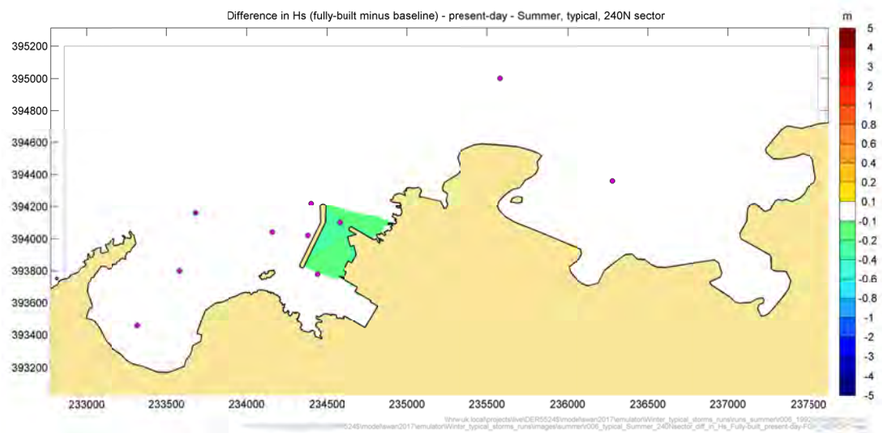

Figure 4.7: Difference in significant wave height, fully-built compared to baseline, typical summer wave condition, 2023 "present-day"

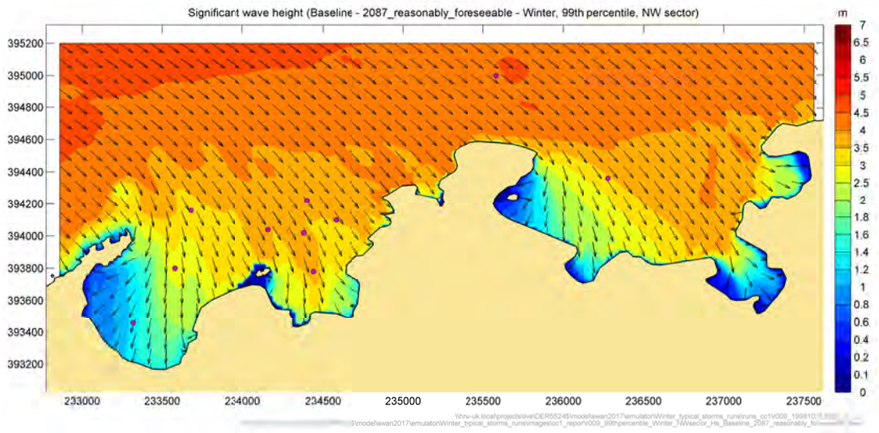

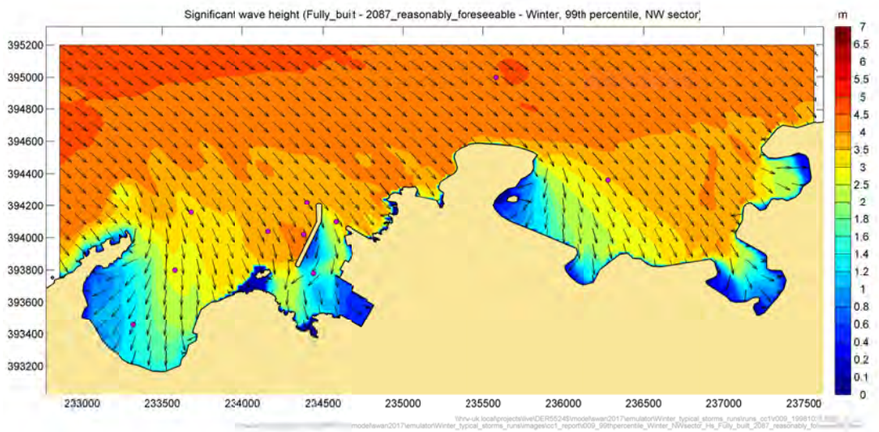

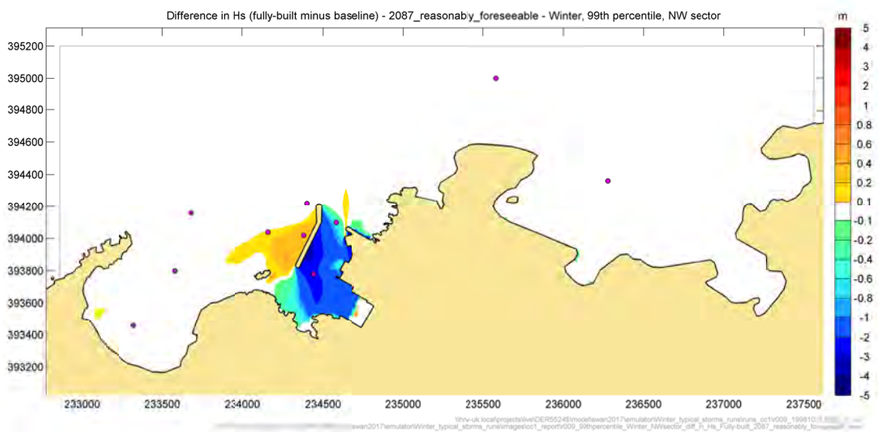

Figure 4.8: Difference in significant wave height, fully-built compared to baseline, 99th percentile winter wave condition, from the NW sector, "2087 reasonably foreseeable"

Source: HR Wallingford SWAN wave model; Wave predictions in the lee of the breakwater are included for illustration only. The HR Wallingford ARTEMIS model is used to provide reliable wave conditions behind the breakwater.

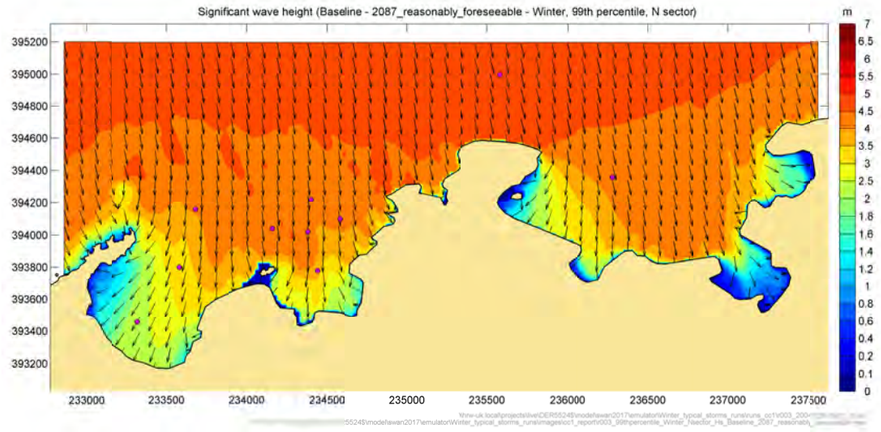

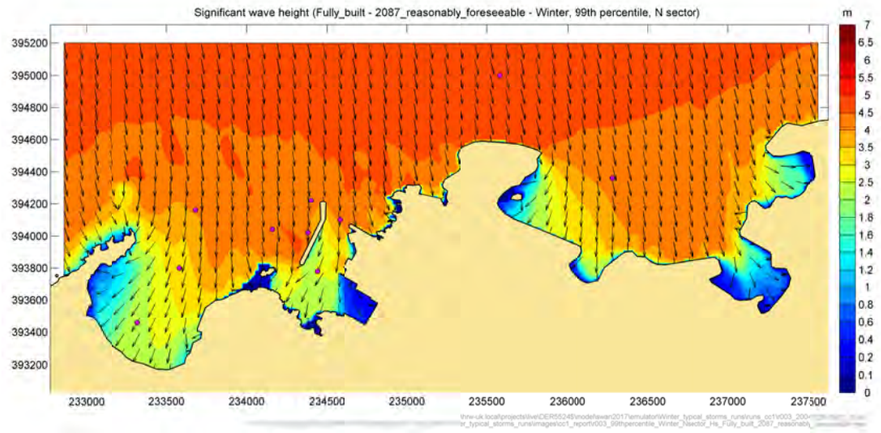

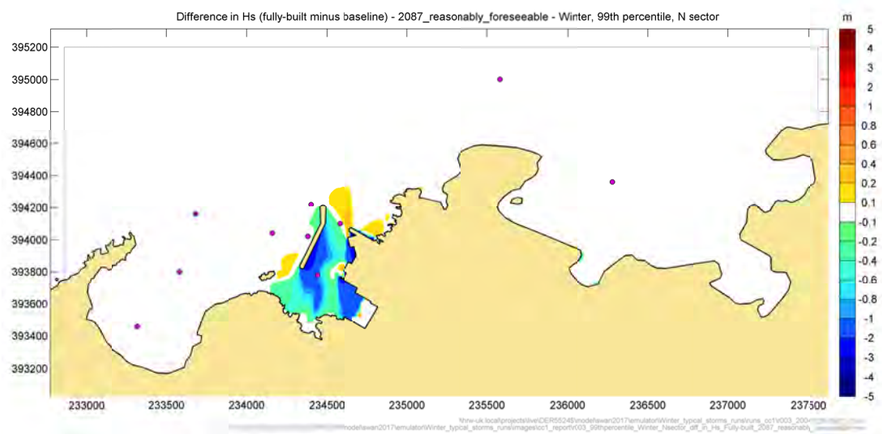

Figure 4.9: Difference in significant wave height, fully-built compared to baseline, 99th percentile winter wave condition, from the N sector, “2087 reasonably foreseeable”

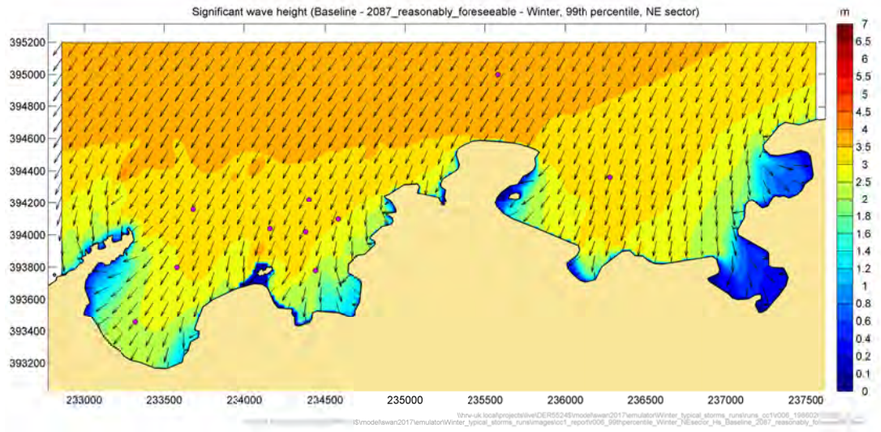

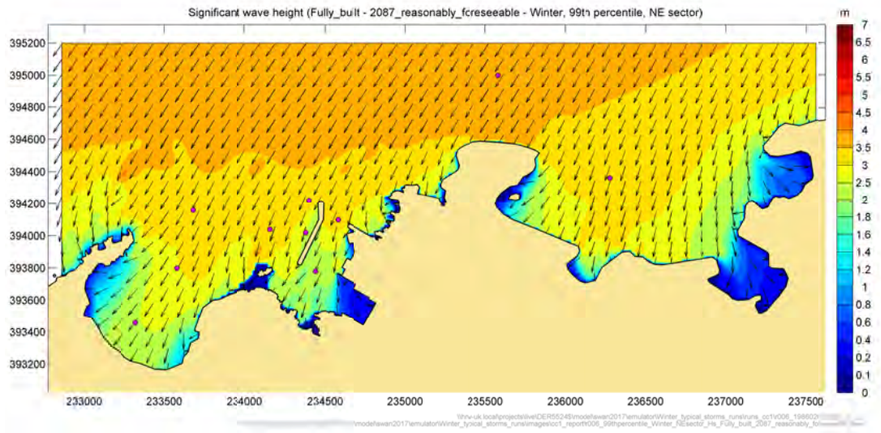

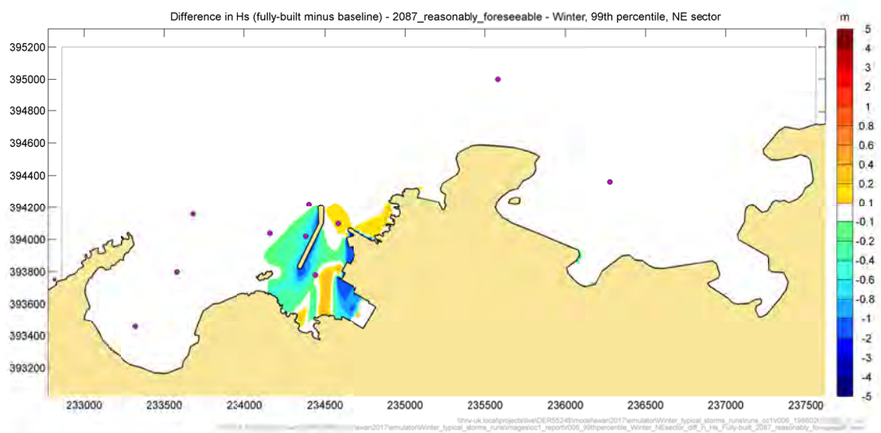

Figure 4.10: Difference in significant wave height, fully-built compared to baseline, 99th percentile winter wave condition, from the NE sector, “2087 reasonably foreseeable”

Source: HR Wallingford SWAN wave model; Wave predictions in the lee of the breakwater are included for illustration only. The HR Wallingford ARTEMIS model is used to provide reliable wave conditions behind the breakwater.

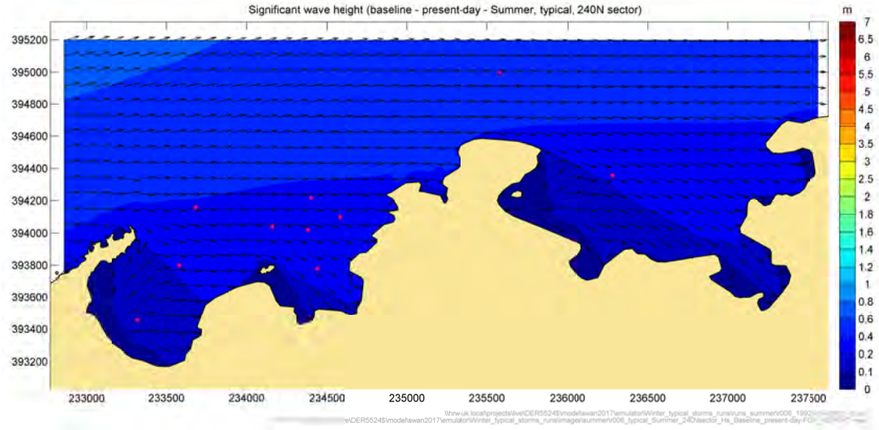

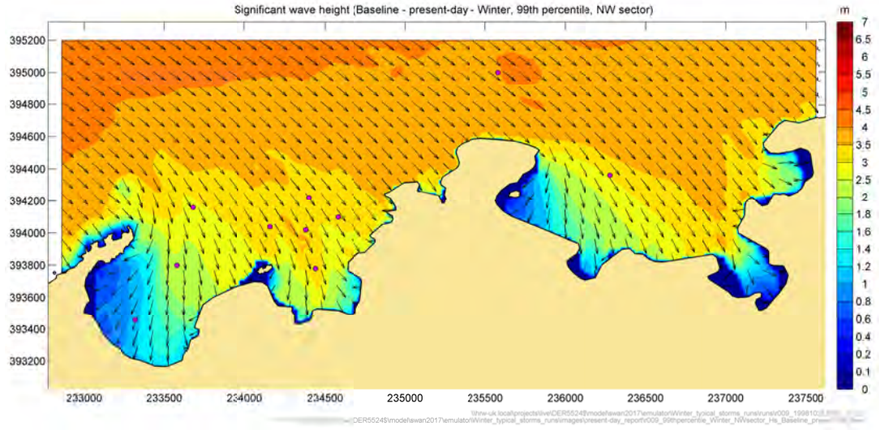

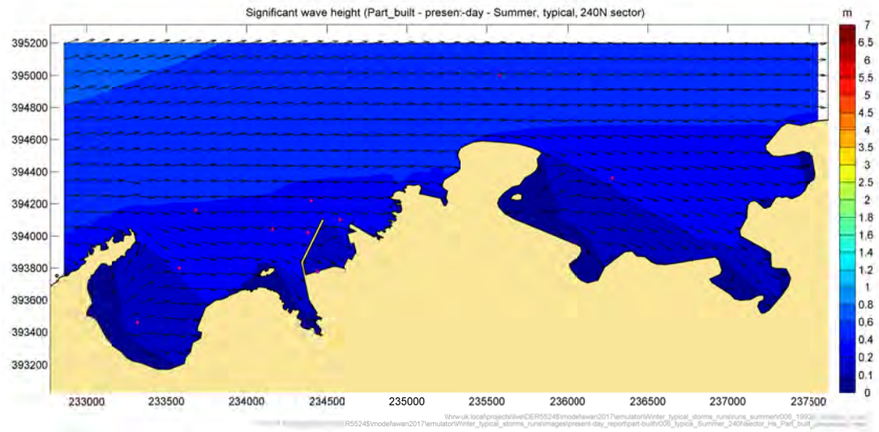

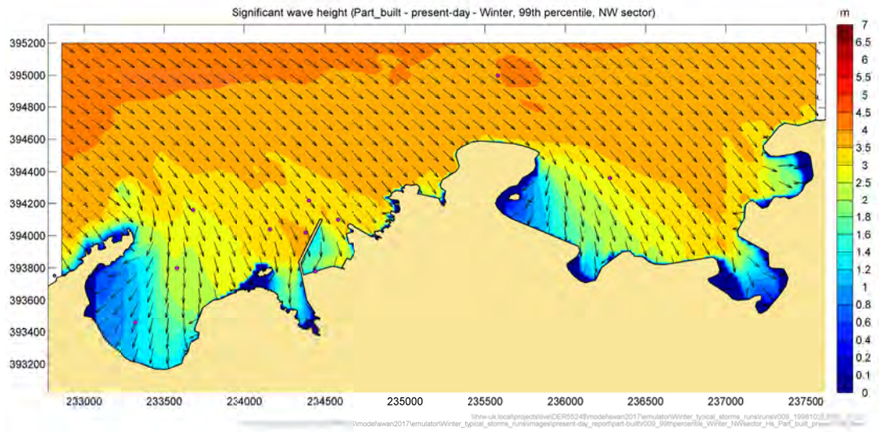

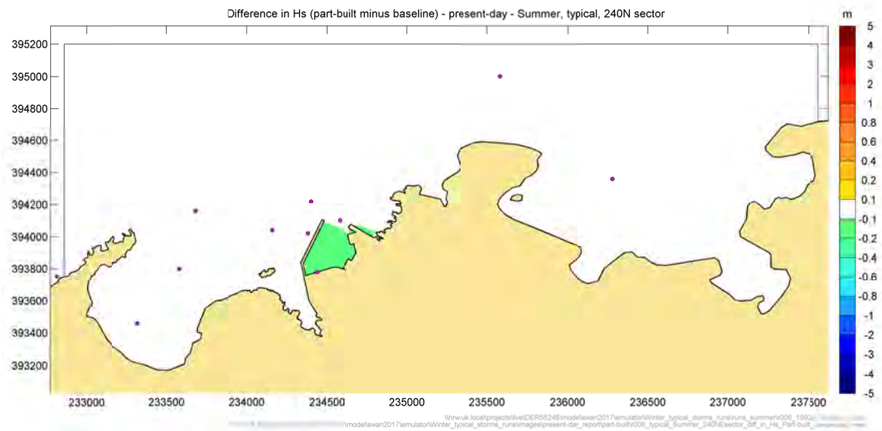

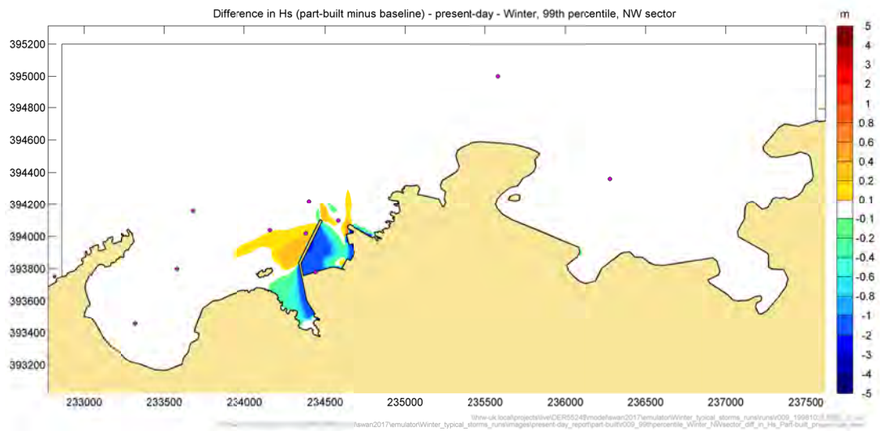

Figure 4.11: Difference in significant wave height, part-built compared to baseline, typical summer wave condition, 2023 “present-day”

Figure 4.12: Difference in significant wave height, part-built compared to baseline, 99th percentile winter wave condition, from the NW sector, “2023 present-day”

Source: HR Wallingford SWAN wave model; Wave predictions in the lee of the breakwater are included for illustration only. The HR Wallingford ARTEMIS model is used to provide reliable wave conditions behind the breakwater.

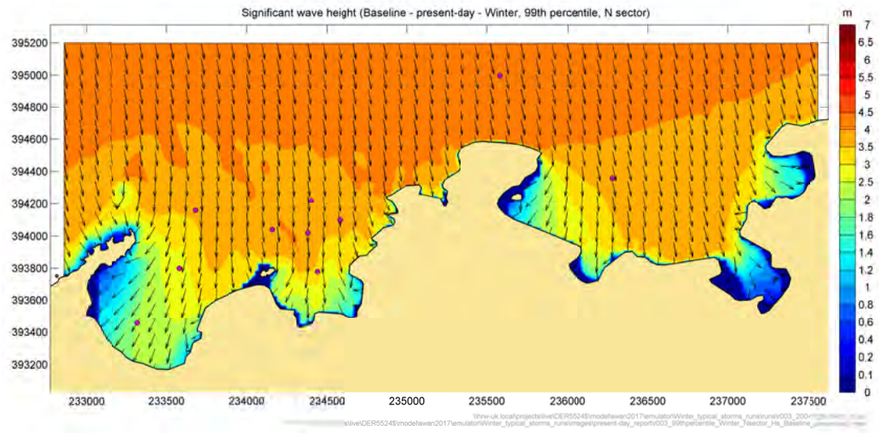

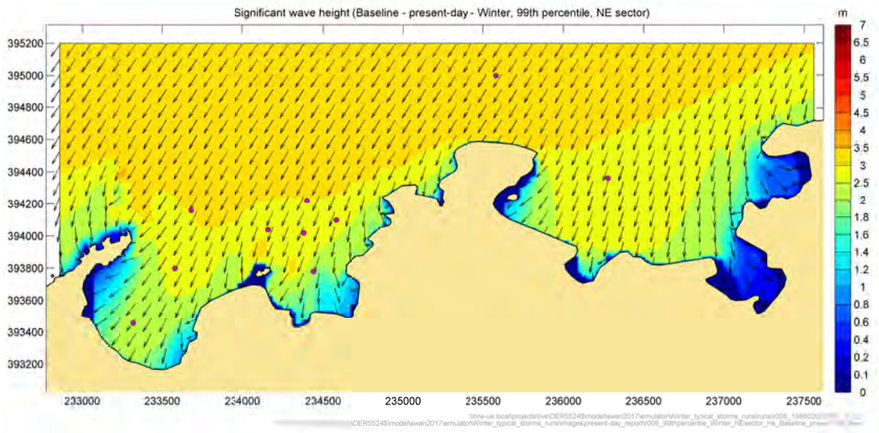

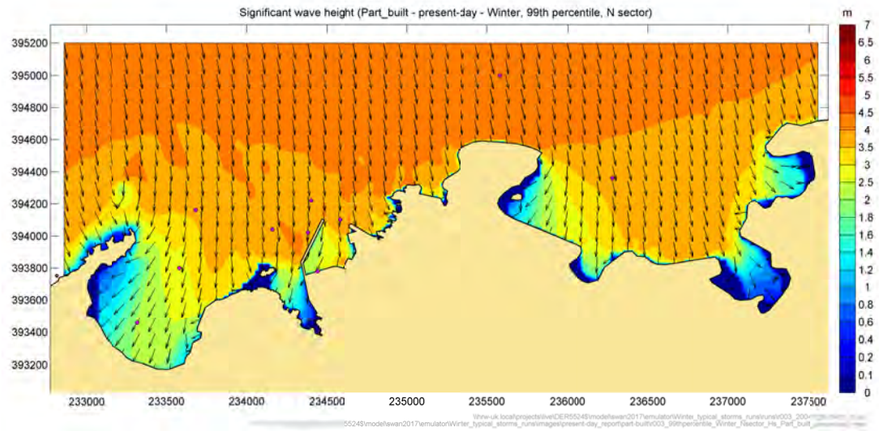

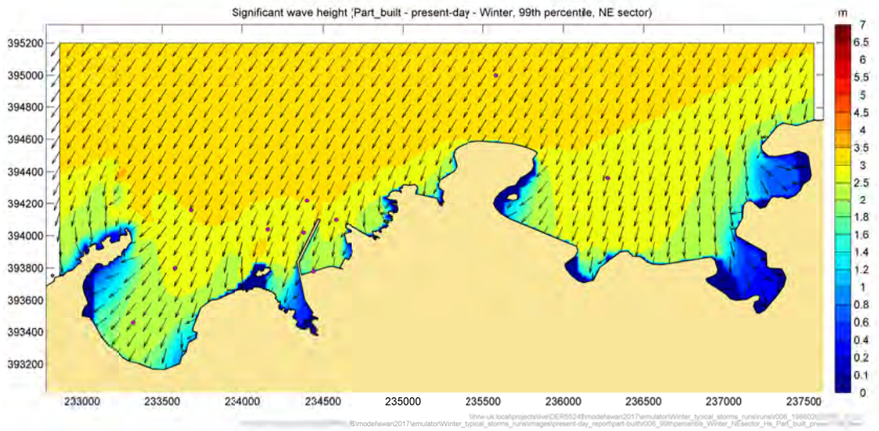

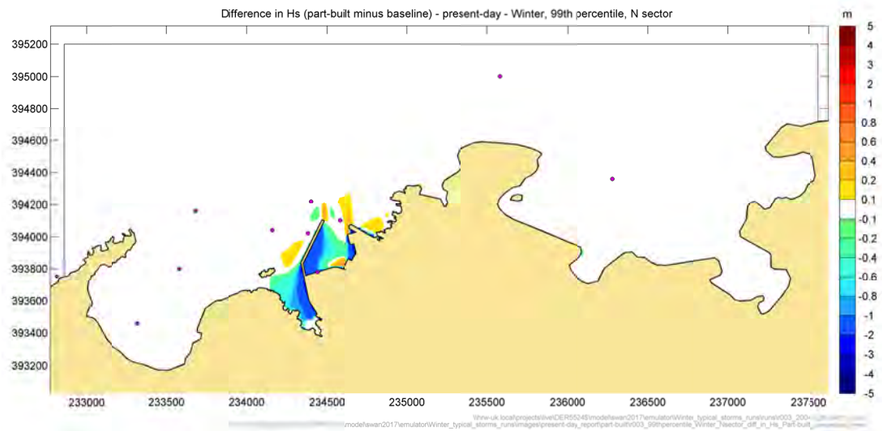

Figure 4.13: Difference in significant wave height, part-built compared to baseline, 99th percentile winter wave condition, from the N sector, "2023 present-day"

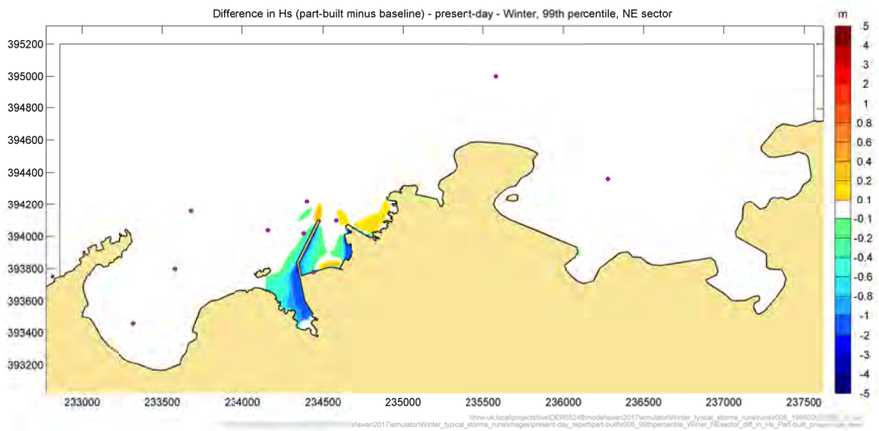

Figure 4.14: Difference in significant wave height, part-built compared to baseline, 99th percentile winter wave condition, from the NE sector, "2023 present-day"

Source: HR Wallingford SWAN wave model; Wave predictions in the lee of the breakwater are included for illustration only. The HR Wallingford ARTEMIS model is used to provide reliable wave conditions behind the breakwater.

4.5.2. Further sensitivity tests to assess refocussing of wave energy in Cemlyn Bay

In order to investigate further the refocussing of wave energy highlighted in the "2087 reasonably foreseeable" 99th winter conditions model runs, a suite of simulations was conducted to explore sensitivity to offshore wave direction at the outer model boundary.

Table 4.13 summarises the original winter present-day wave conditions at Offshore Point 3 used in the model. The "2087 reasonably foreseeable" conditions were obtained from the present-day conditions by applying a 10% increase in wave heights (and corresponding 5% in wave periods) and wind speeds to reflect the future climate change allowances. They were also run in the model, at water levels increased by 0.62m to allow for climate change. Although not originally requested, conditions from the West sector were also tested for completeness.

Table 4.13: Representative present-day Winter storm wave conditions at Offshore Point 3 and corresponding offshore wave direction at the model boundary

Sector	Event	H_s (m)	T_{m-10} (s)	Wave Direction (°N) at Point 3	Corresponding offshore wave direction (°N)	Wind Direction (°N)
NE	99th percentile	3.48	6.9	36	35	37
N	99th percentile	4.21	7.8	345	342	359
NW	99th percentile	4.03	7.5	303	290	294
W	99th percentile	3.58	7.3	275	246	260

Source: HR Wallingford analysis at Offshore Point 3

These simulations were run at a 5° interval in the offshore wave direction within the W, NW, N and NE sectors, for the "2087 reasonably foreseeable" conditions, applying the same wind conditions as for the original selected representative 99th percentile condition in the sector.

The differences in significant wave height between the fully-built layout and the baseline from the offshore wave direction sensitivity runs are shown in Figure 4.15 to Figure 4.18.

171°N

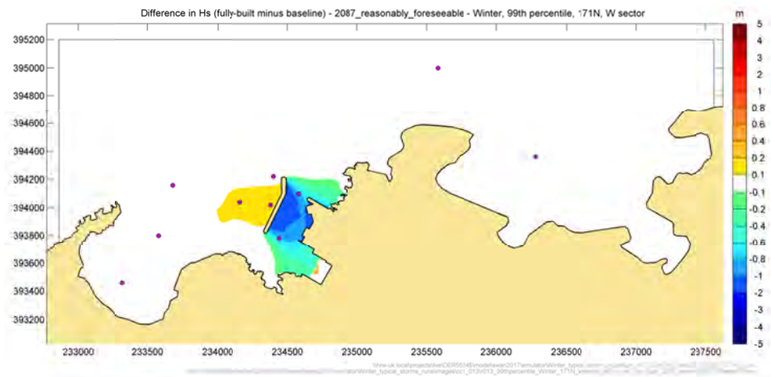

176°N

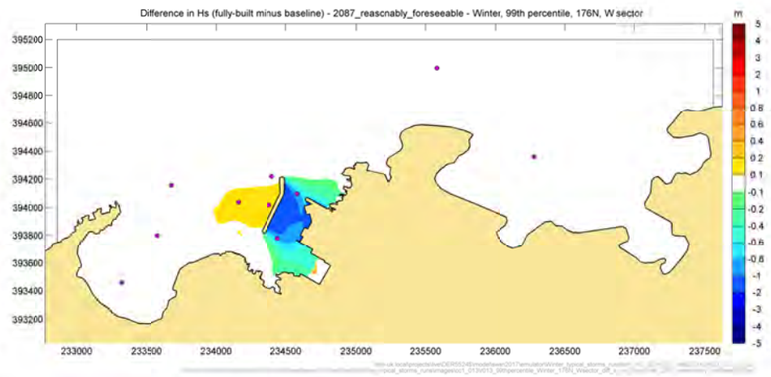

181°N

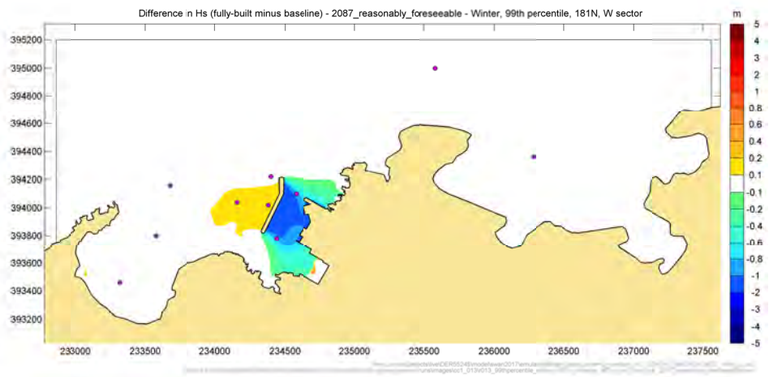

191°N

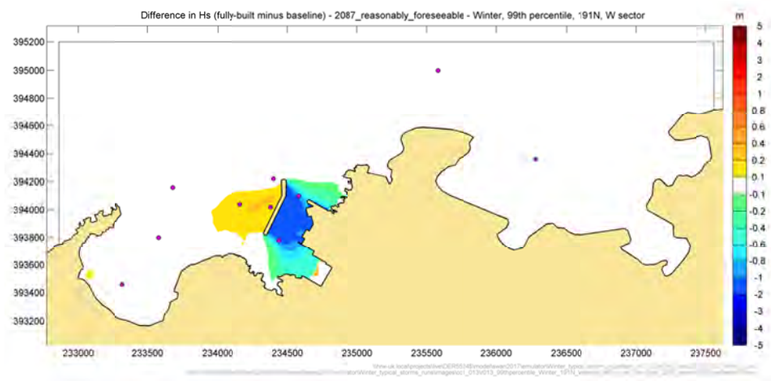

201°N

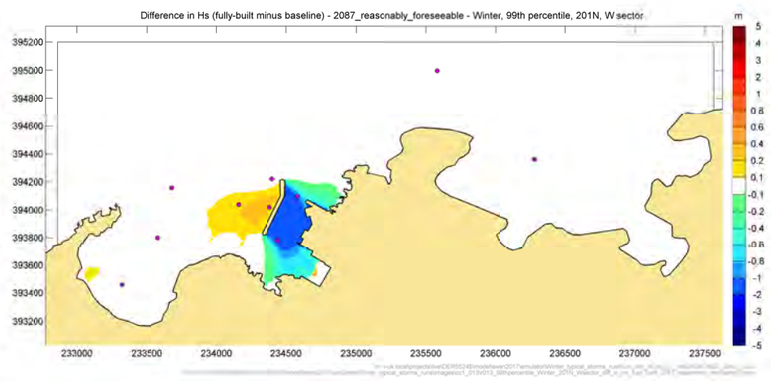

211°N

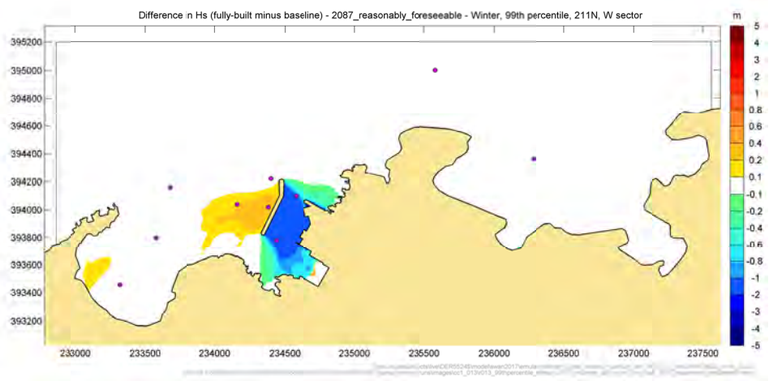

221°N

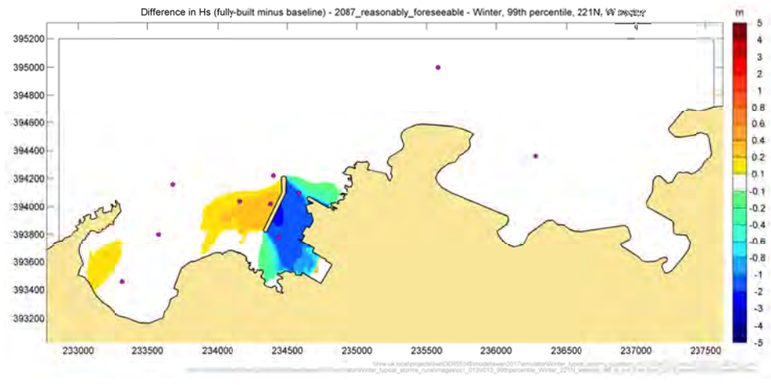

231°N

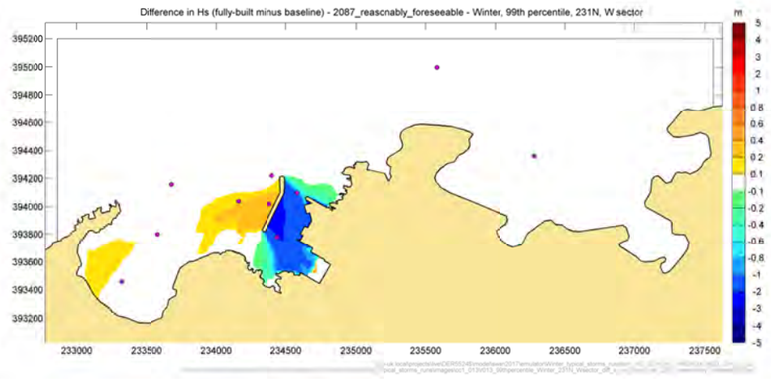

236°N

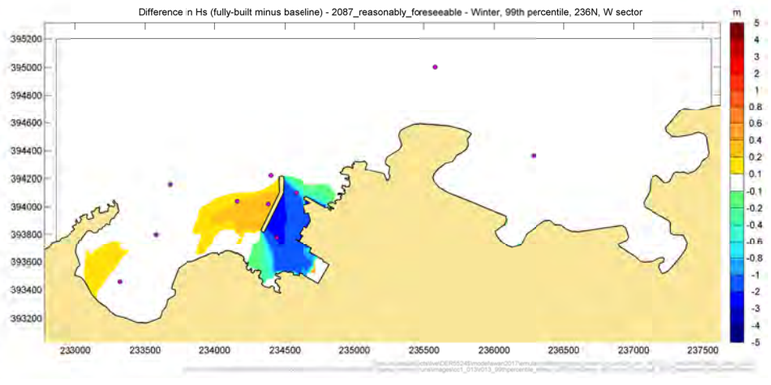

Figure 4.15: Difference in significant wave height fully-built layout compared to baseline, “2087 reasonably foreseeable” conditions, sensitivity runs offshore wave direction 171°N to 236°N

Note: the purple dots on the plots represent the location of the nearshore wave output points (Figure 4.4).

241°N

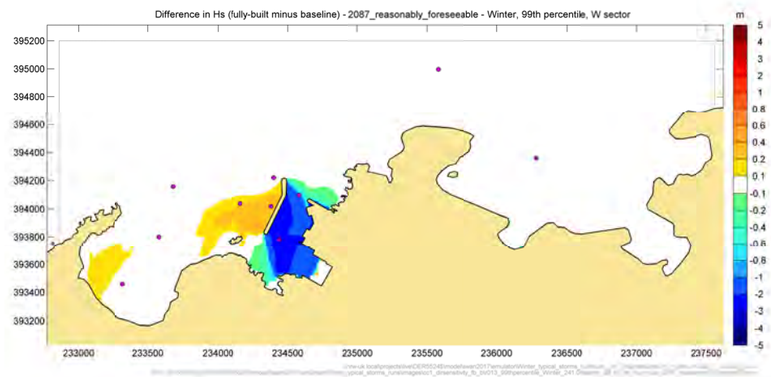

246°N

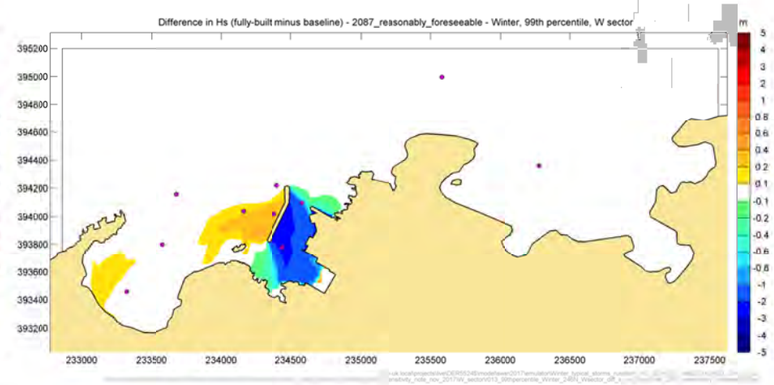

251°N

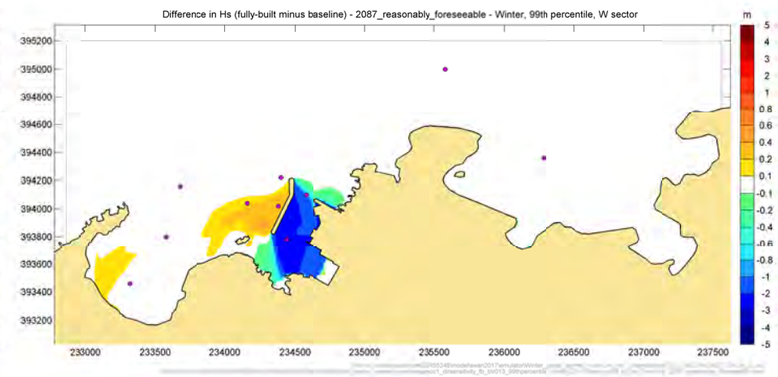

256°N

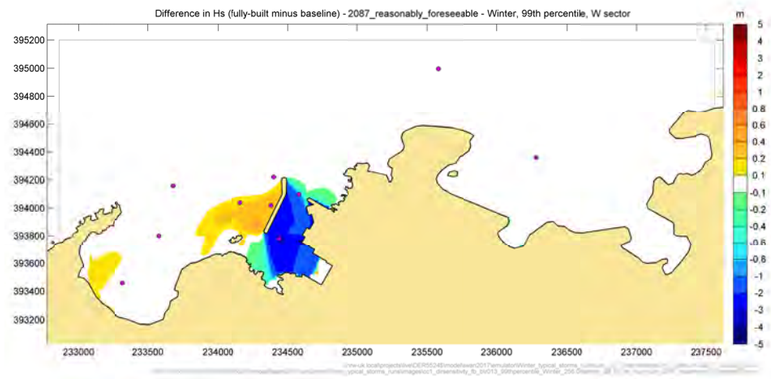

261°N

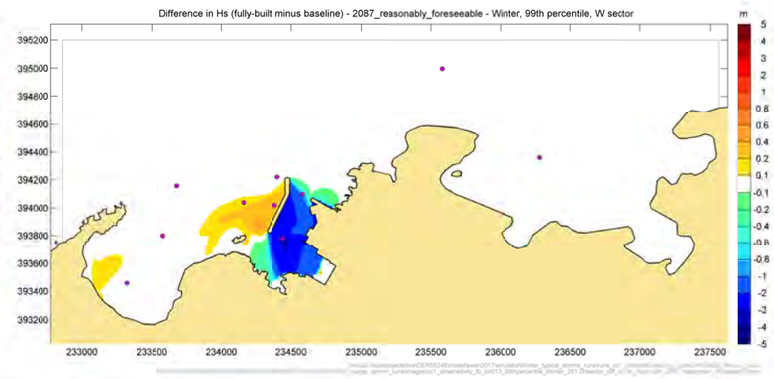

266°N

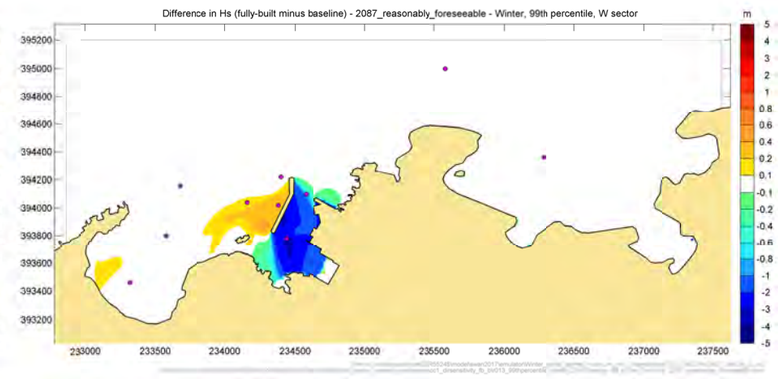

271°N

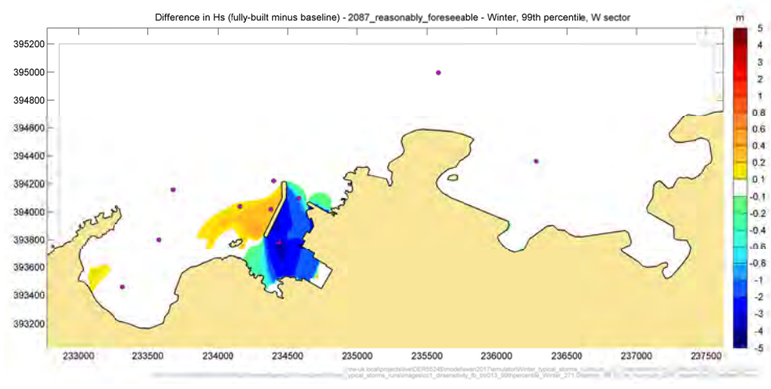

281°N

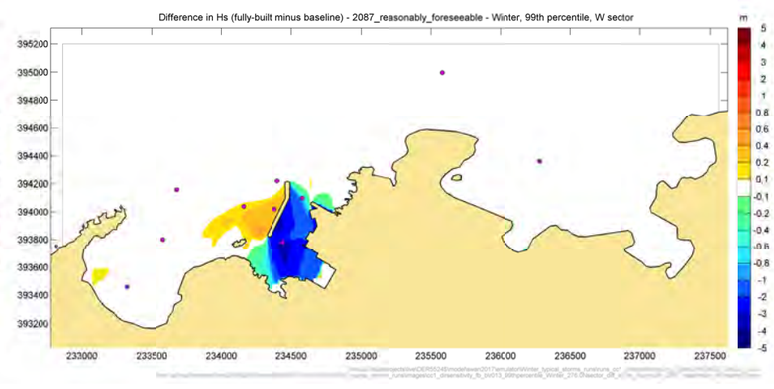

286°N

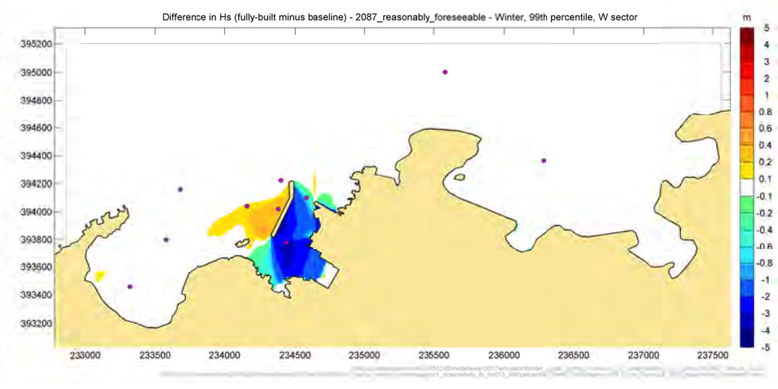

Figure 4.16: Difference in significant wave height fully-built layout compared to baseline, “2087 reasonably foreseeable” conditions, sensitivity runs offshore wave direction 245°N to 286°N

290°N

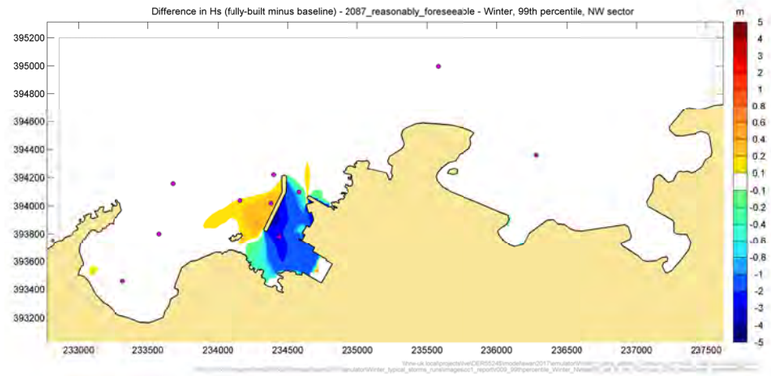

295°N

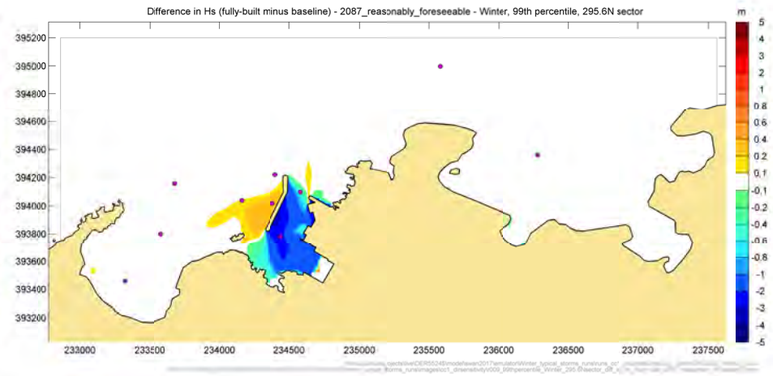

300°N

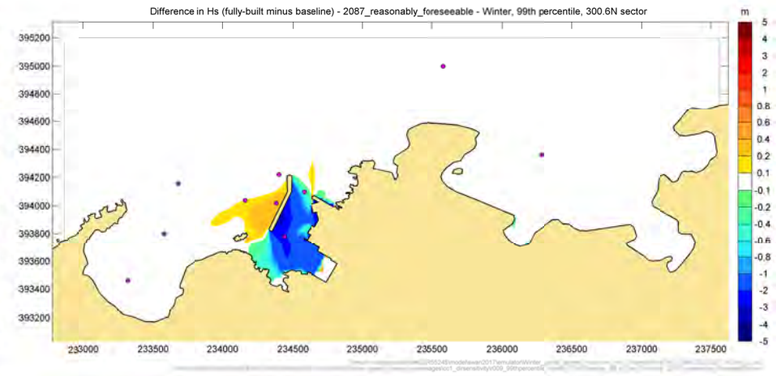

310°N

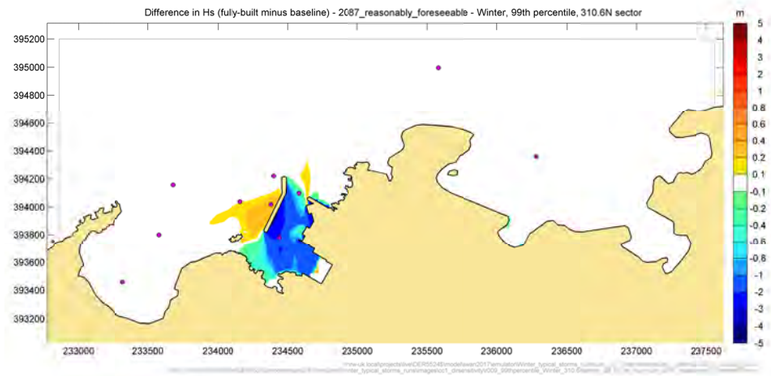

315°N

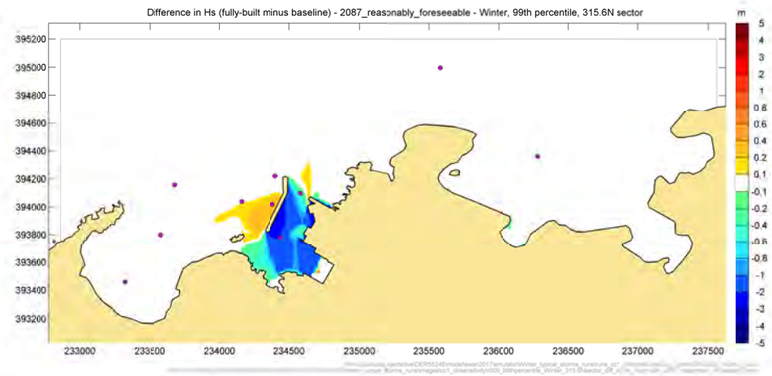

320°N

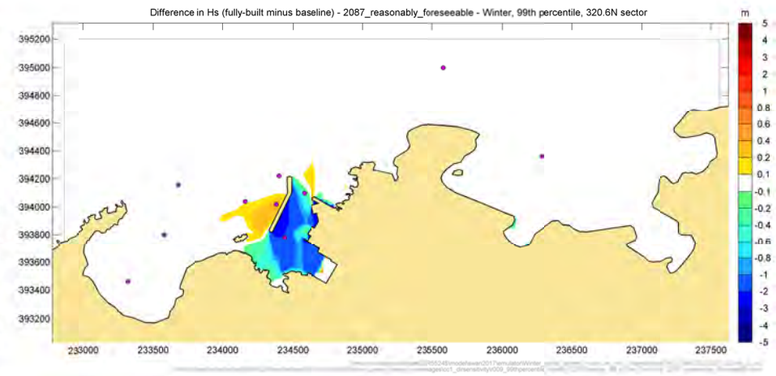

325°N

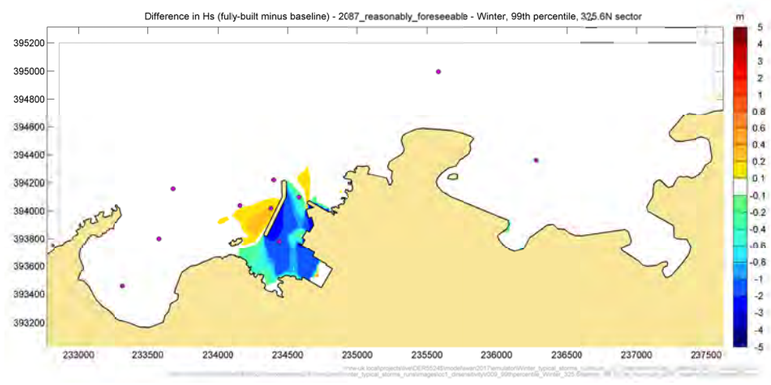

330°N

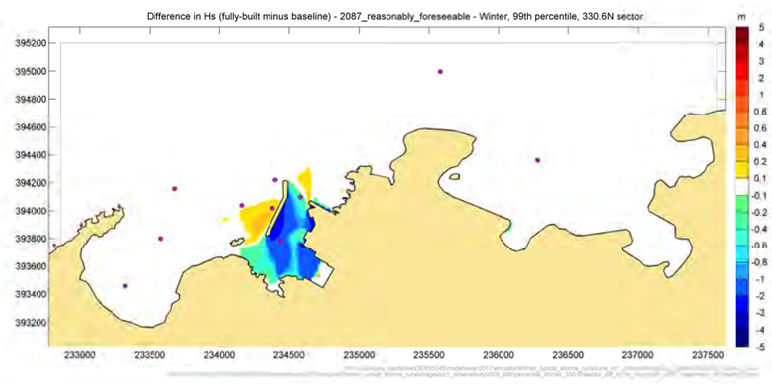

335°N

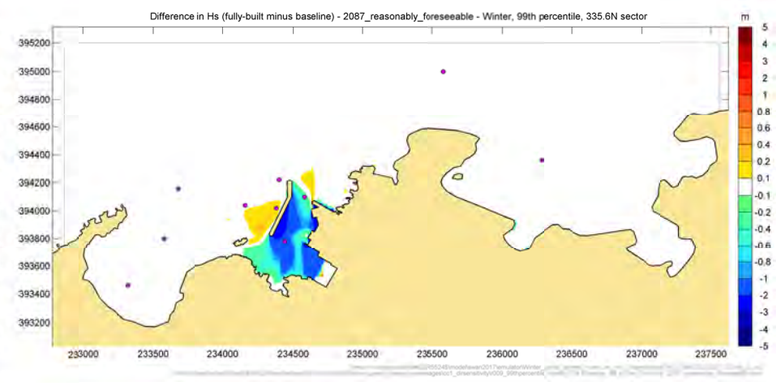

Figure 4.17: Difference in significant wave height fully-built layout compared to baseline, “2087 reasonably foreseeable” conditions, sensitivity runs offshore wave direction 295°N to 335°N

337°N

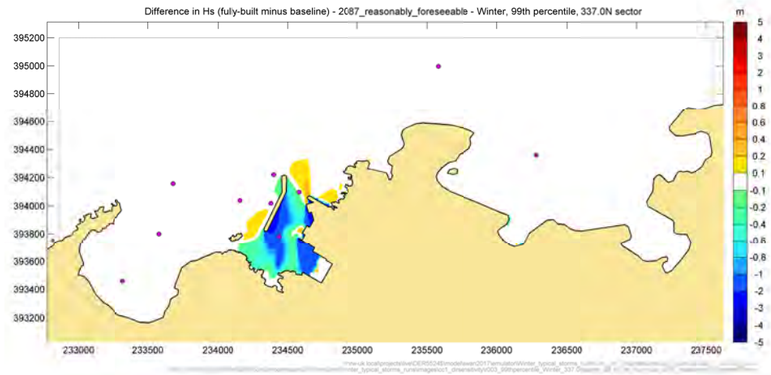

342°N

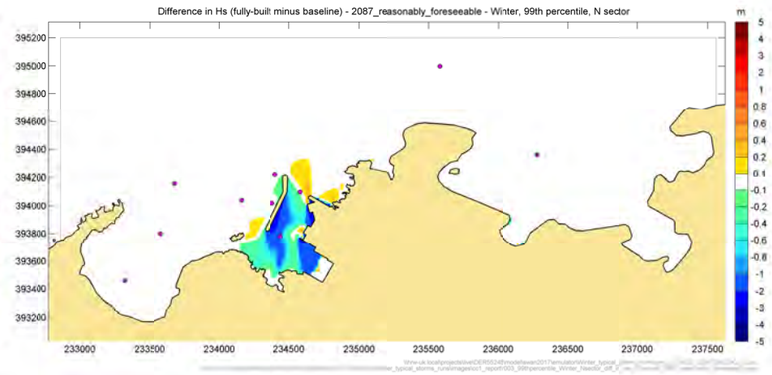

347°N

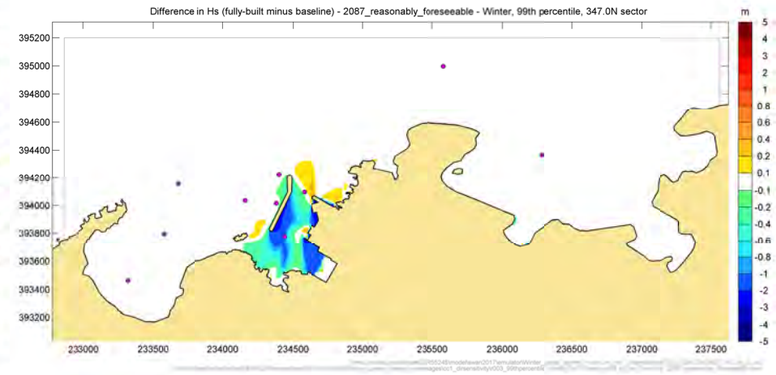

352°N

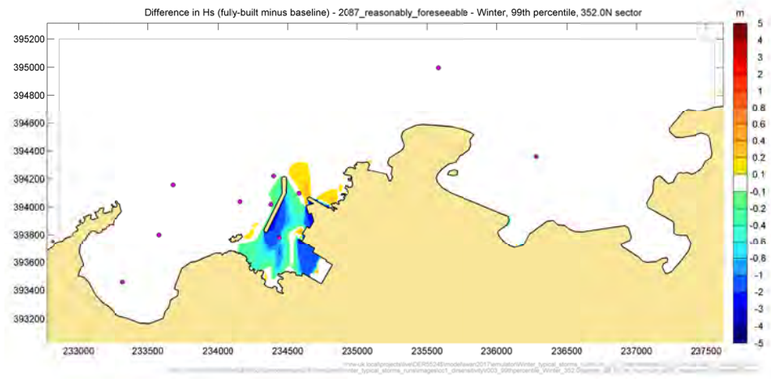

357°N

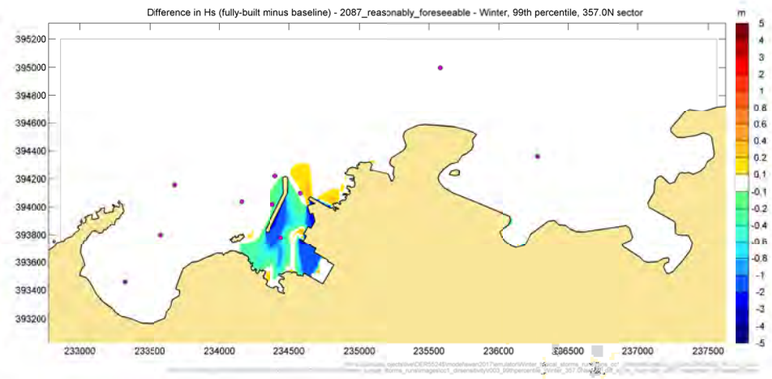

2°N

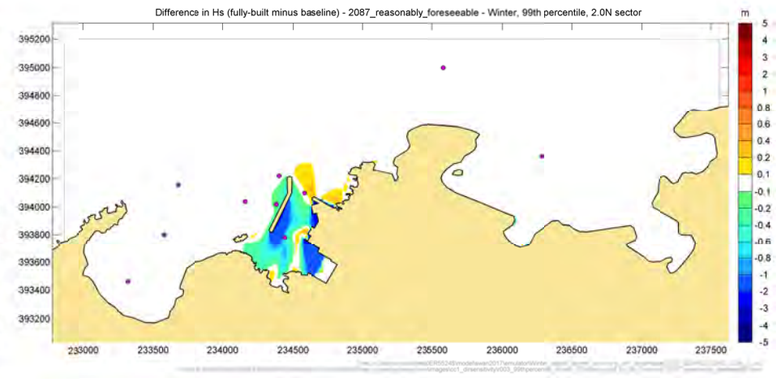

7°N

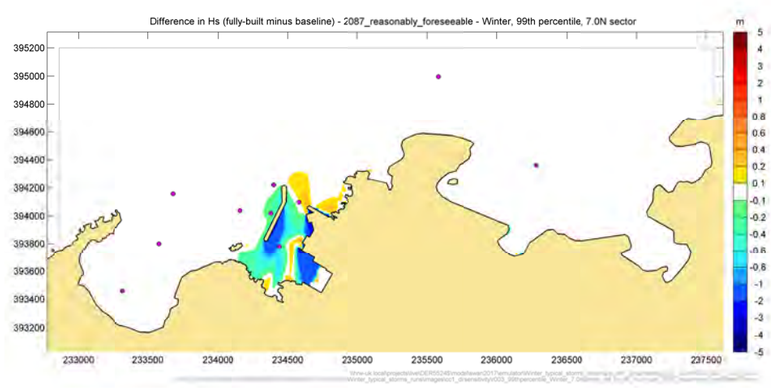

12°N

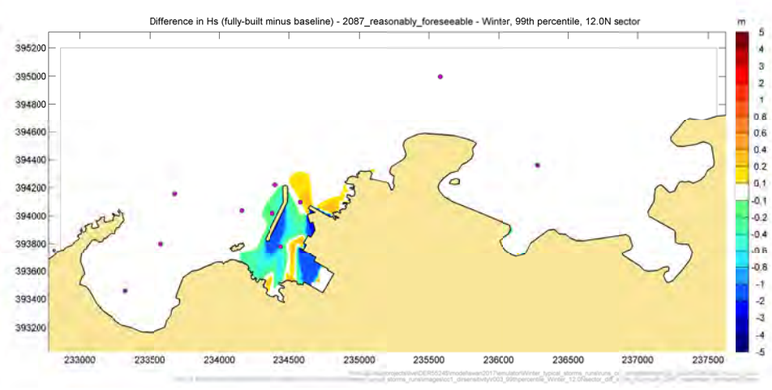

17°N

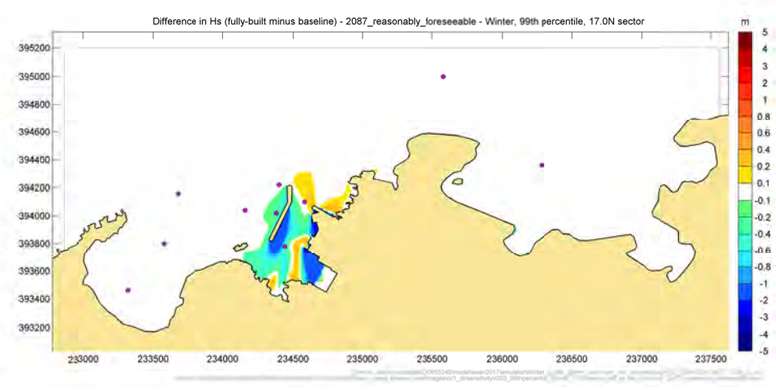

Figure 4.18: Difference in significant wave height fully-built layout compared to baseline, “2087 reasonably foreseeable” conditions, sensitivity runs offshore wave direction 337°N to 17°N

The influence of these additional directions was examined and the condition, within each 45° sector that had the largest influence on wave heights at Cemlyn Bay was chosen as the representative condition in that sector.

The effect of refocussing in Cemlyn Bay is observed for offshore wave directions from 176°N to 295°N, when the wind is from the West or North-West. Offshore conditions originating from the West sector refract towards the land. As illustrated in Figure 4.19 and Figure 4.20, varying the offshore wave direction at the boundary by 40° (from 246°N to 286°N) for the same wave conditions (significant wave height and wave period) only varies the wave direction at the Offshore Point 3 by 13°. The variation in offshore wave direction does have an effect on the magnitude of the waves at the site but less on the mean direction of the waves due to refraction.

Based on the sensitivity tests, the chosen directions for each sector are presented in Table 4.14, although results are generally similar to those from the representative directions shown in Section 4.5.

Table 4.14: Selected representative winter offshore wave directions applied at the SWAN boundary

Sector	Event	Representative Offshore Direction (°N)	Worst Direction from sensitivity study (°N)
NE	99th percentile	35	45
N	99th percentile	342	337
NW	99th percentile	290	286
W	99th percentile	246	246

Source: HR Wallingford

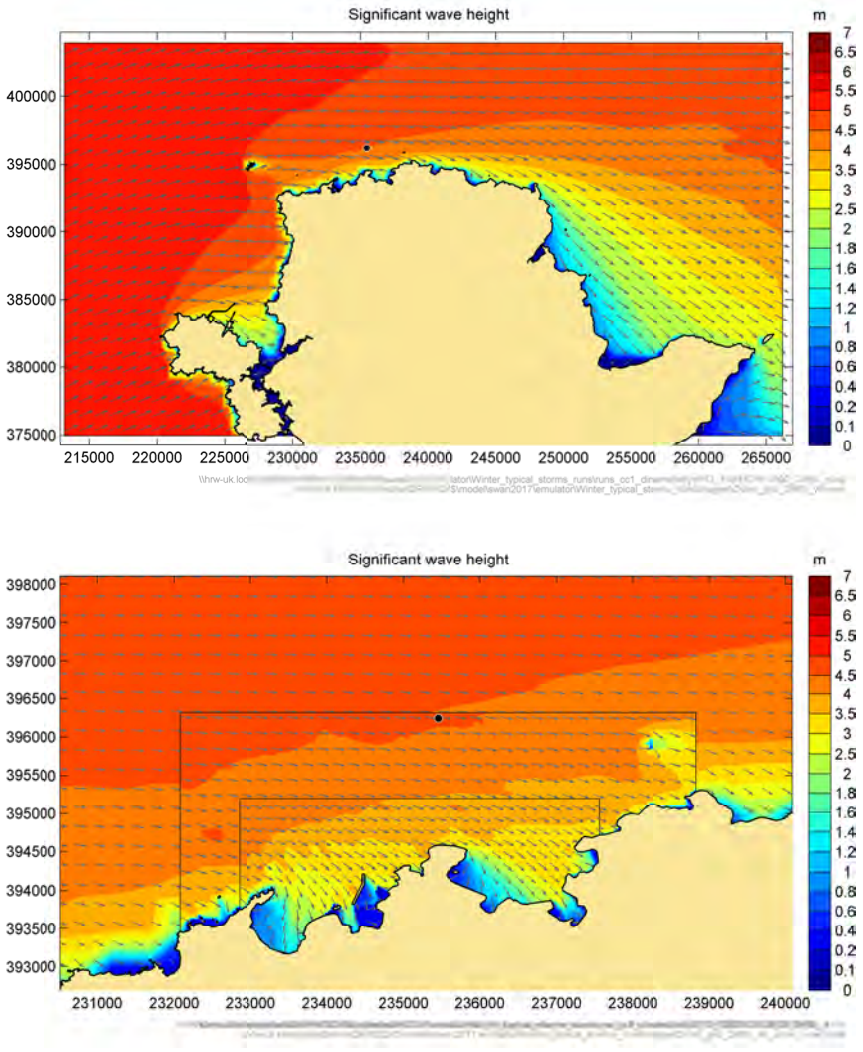

Figure 4.19: W sector conditions with offshore boundary wave direction of 246°N

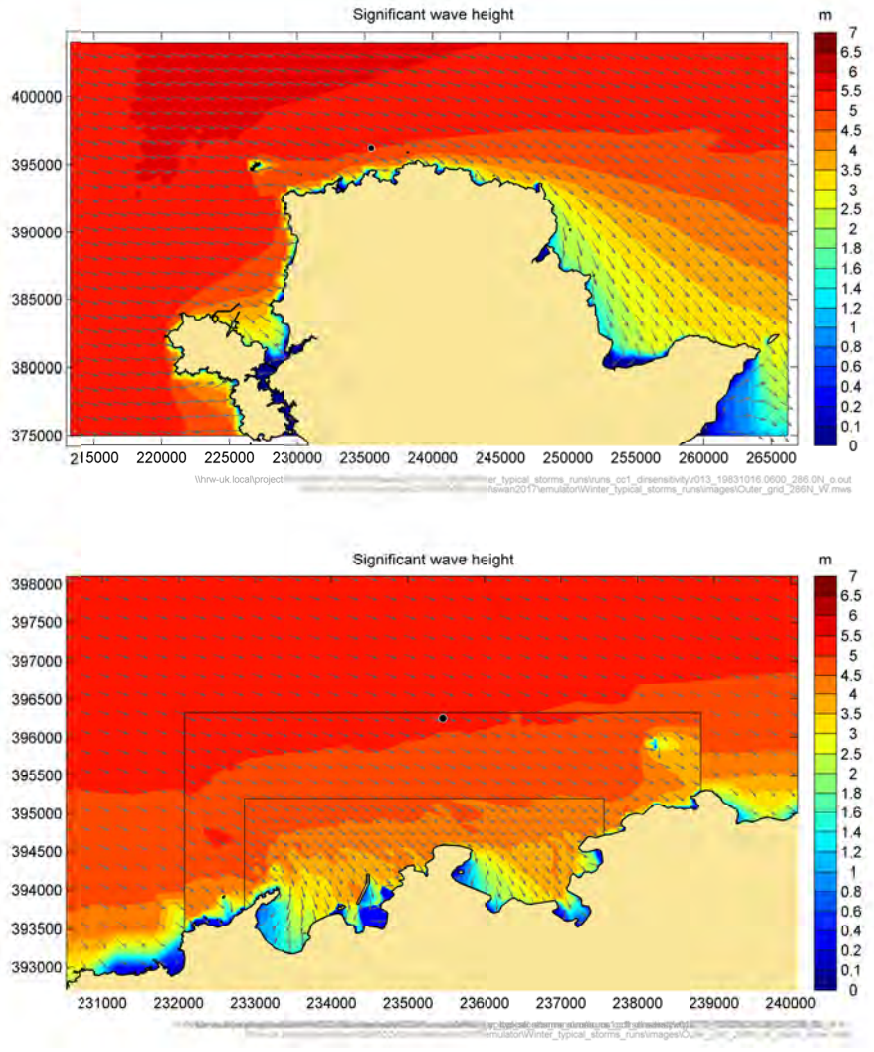

Figure 4.20: W sector conditions with offshore boundary wave direction of 286°N

4.5.3. How frequently the effect is likely to occur

To estimate how frequently a refocusing of wave energy due to the proposed marine structures in Cemlyn Bay is likely to occur, the offshore wave height that gives 10cm difference in significant wave height in Cemlyn Bay were determined for each 5° sector based on the sensitivity runs that give more than 10cm difference (i.e. with offshore wave direction from 176°N to 295°N). All occurrences in the all-year offshore climate table above these conditions were then summed up to give an estimate of the proportion of the time a difference in significant wave height of 10cm or above in Cemlyn Bay will occur.

This analysis was carried out for the "2087 reasonably foreseeable" conditions and the proportion of the time a difference in significant wave height of 10cm or above in Cemlyn Bay is estimated to be 4.9%. This is perhaps a slightly conservative estimate because the worst direction (westerly) wind was applied with all wave directions between 176°N and 291°N.

4.5.4. Selected 99th percentile Winter conditions, difference in significant wave height maps – Fully-built layout

Following the sensitivity tests to the offshore wave directions, the worst directions in each sector were selected to revise the representative 99th percentile winter "2087 reasonably foreseeable" conditions (Table 4.14). The corresponding difference plots (difference in predicted significant wave height between the fully-built layout and the baseline) from the NE, N, NW and W sectors are shown in Figure 4.21 and Figure 4.22.

Each figure is in three parts, and represents just one wave condition. The top pane of each figure shows the baseline significant wave height for the area around Wylfa, the middle pane the corresponding wave heights for the fully-built layout. The bottom pane shows the difference in significant wave height between the runs with and without structures. Yellow and orange shades show increases in significant wave height of at least 10 centimetres. Blue and green shades show reductions in wave height of at least 10 centimetres.

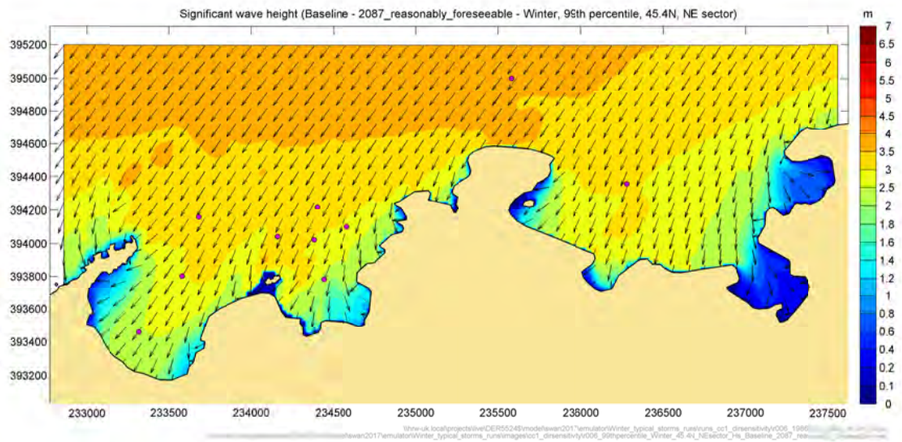

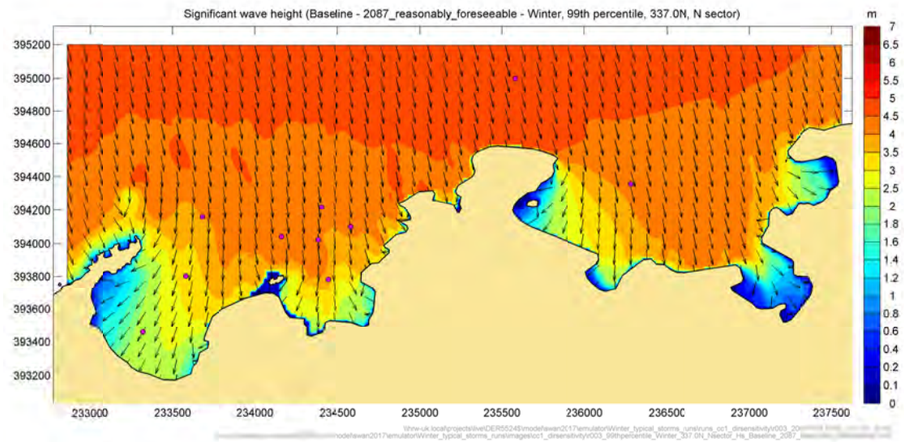

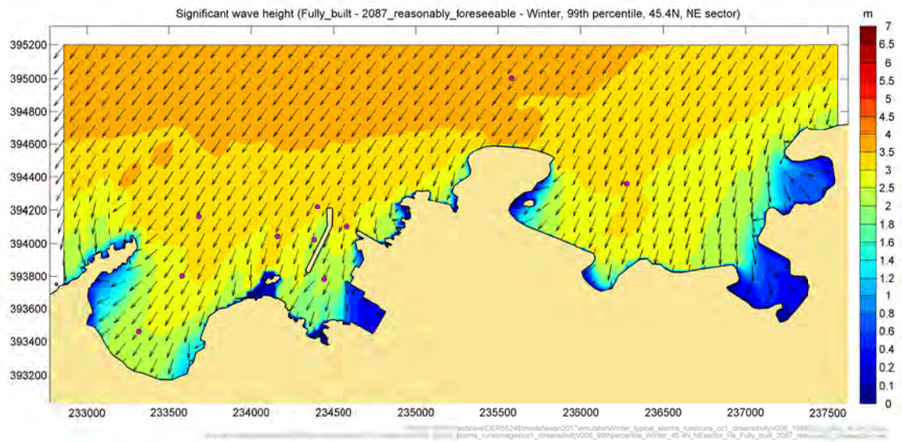

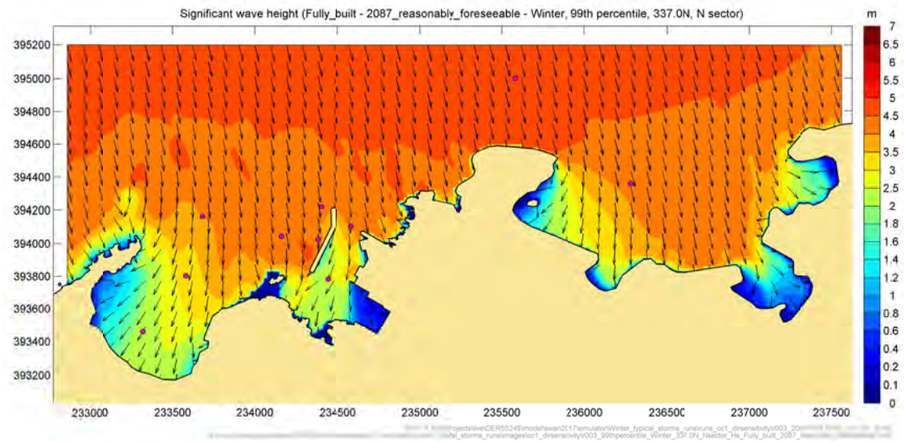

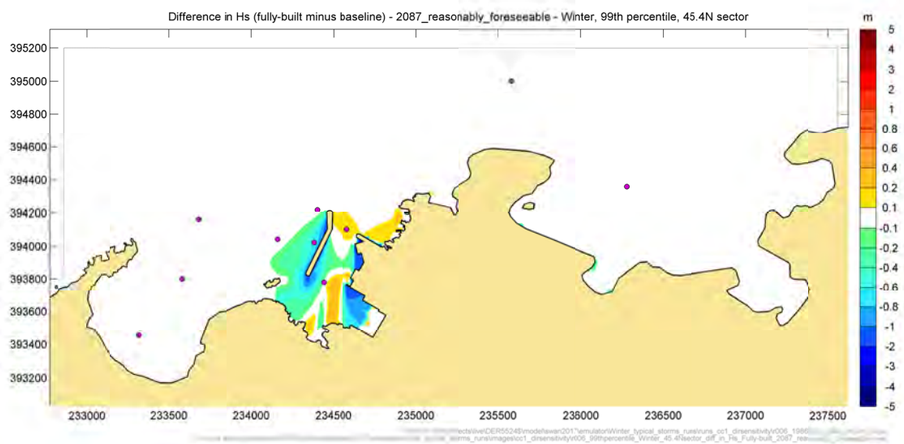

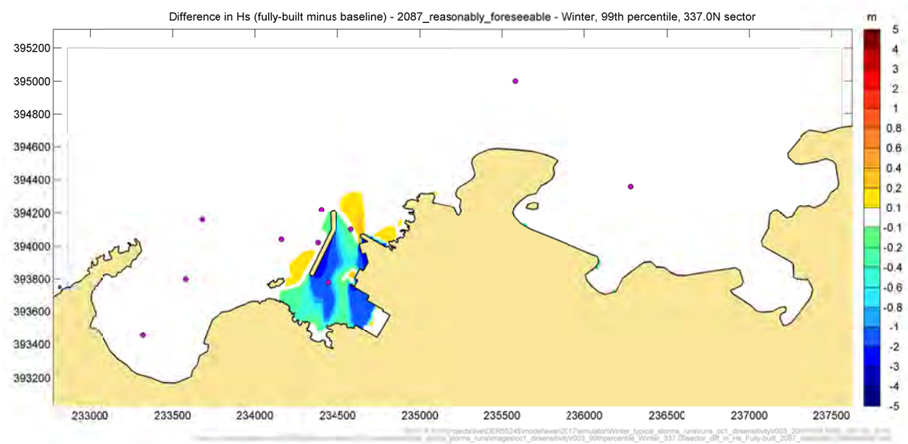

Figure 4.21: Difference in significant wave height, fully-built compared to baseline case, “2087 reasonably foreseeable conditions, NE (left) and N (right) sectors

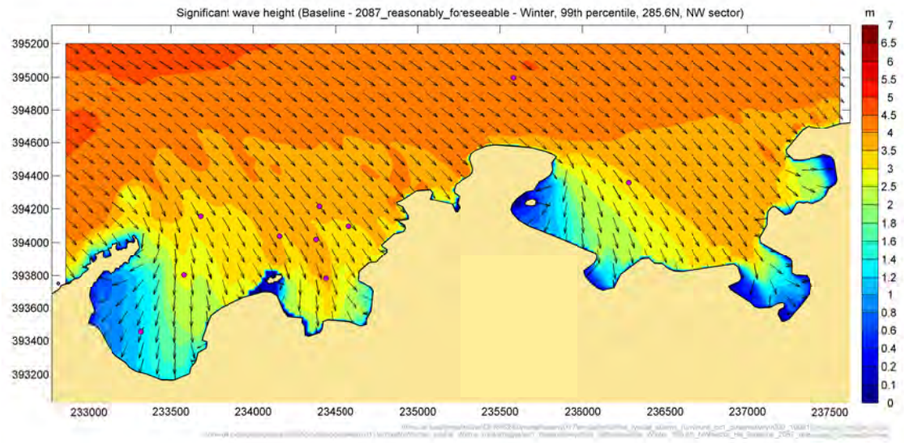

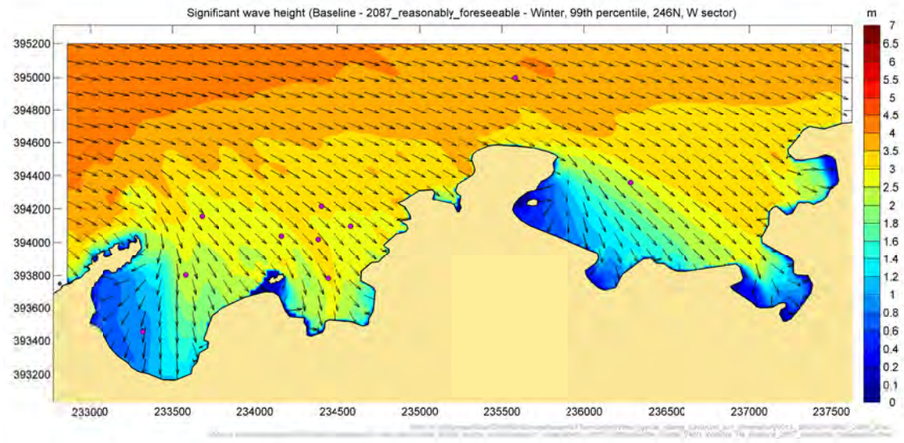

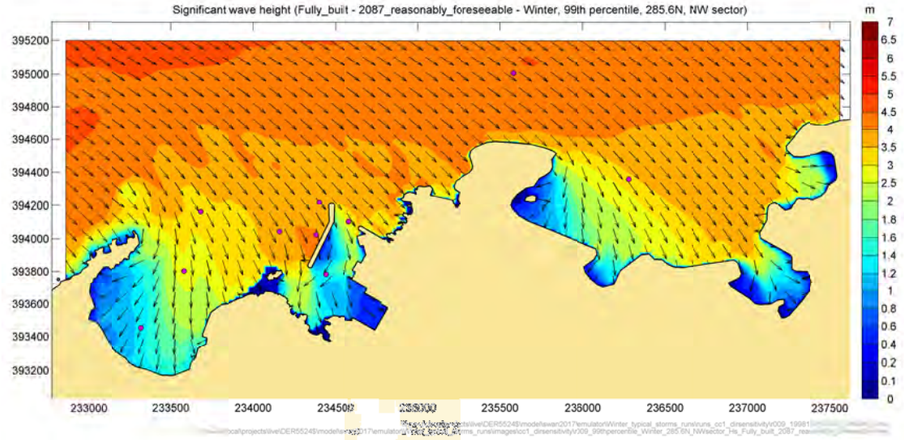

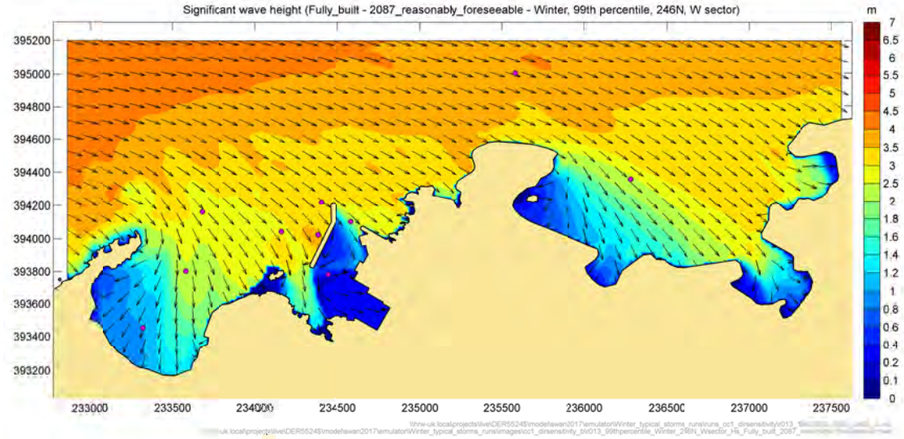

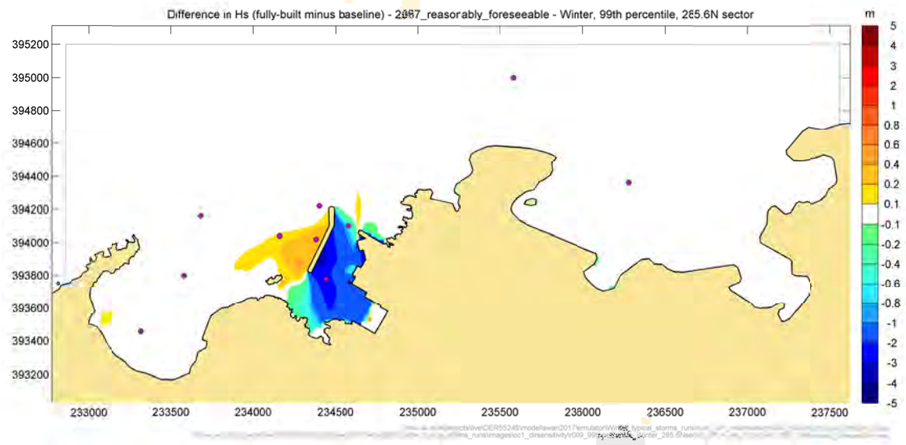

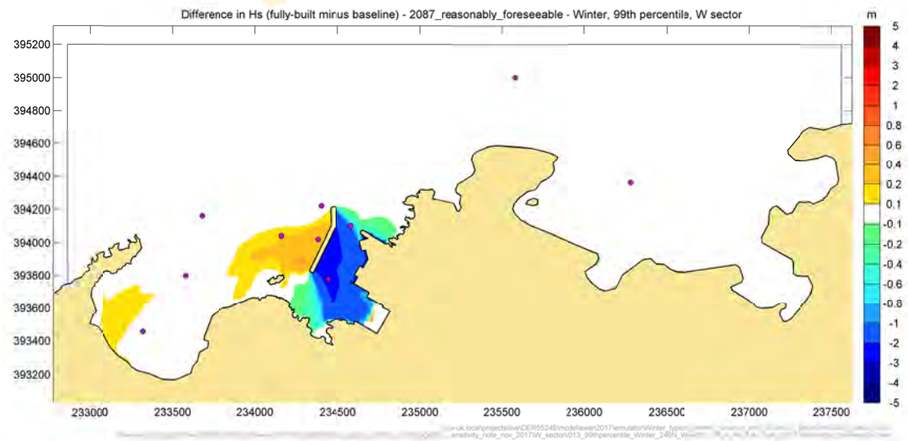

Figure 4.22: Difference in significant wave height, fully-built compared to baseline case, “2087 reasonably foreseeable conditions, NW (left) and W (right) sectors

4.5.5. Wave conditions in Cemlyn Bay

The differences in significant wave height in Cemlyn Bay due to the marine structures are predicted to be less than 20cm for the "2087 reasonably foreseeable" 99th percentile winter conditions.

To illustrate the effects of the marine structures in Cemlyn Bay, in addition to the individual winter conditions, a comparison between the annual wave climates at the nearshore wave output Point 6 (see Figure 4.4) with and without the proposed development in place is presented. Table 4.15 and Table 4.16 show the distribution of significant wave height against mean wave direction at Point 6, for the "present-day" baseline and the "present-day" fully-built layout, respectively. Table 4.17 and Table 4.18 are the corresponding distribution of significant wave height against mean wave period.

The climates show:

- Little difference in wave distributions with and without the proposed marine structures in:
  - Changes in the distribution of waves against mean wave direction are due to the shelter / blockage or the wave reflections from the Western Breakwater.
  - The distribution against mean wave periods is very similar between the two layouts.
- The distribution of large waves (H_s > 2m) against mean wave directions and mean wave periods is similar in both layouts.

The wave conditions in Cemlyn Bay can be summarised as:

- The offshore wave conditions from North / North-East give the largest waves in the Bay and very little change is predicted due to the proposed marine structures.
- Offshore wave conditions from North-West / West are sheltered by the Twyrn Cemlyn headland and give lower wave heights than the North and North-East sectors. They are the most affected by the western breakwater (increase in H_s between 10 and 20cm), but give smaller wave conditions than conditions from North / North –East.
- The main cause of focussing of wave energy in the bay is the reflections from the western breakwater.
- The proportion of the time a difference in H_s of 10cm or above in Cemlyn Bay is estimated to be 4.9%.
- The largest storms will still come from North / North-East.

Table 4.15: Annual wave climate at Point 6, baseline, "2087 reasonably foreseeable", significant wave height (Hs) against mean wave direction

			Wave direction (°N)											
			-15	15	45	75	105	135	165	195	225	255	285	315
H_{s1} (m)	H_{s2} (m)	$P(H_s>H_{s1})$	15	45	75	105	135	165	195	225	255	285	315	345
0	0.5	100.00%	15394	32201	15741	5676	4037	2864	1635	785	658	449	494	1245
0.5	1	18.82%	1388	9491	3974	41	5	<1	-	-	-	-	-	-
1	1.5	3.92%	36	2282	688	-	-	-	-	-	-	-	-	-
1.5	2	0.92%	-	512	198	-	-	-	-	-	-	-	-	-
2	2.5	0.21%	-	144	33	-	-	-	-	-	-	-	-	-
2.5	3	0.03%	-	22	2	-	-	-	-	-	-	-	-	-
3	3.5	0.00%	-	4	-	-	-	-	-	-	-	-	-	-
Percentage Occurrence			16.82%	44.66%	20.64%	5.72%	4.04%	2.86%	1.64%	0.79%	0.66%	0.45%	0.49%	1.25%

Source: HR Wallingford, SWAN wave transformation and Met Office WW3 offshore data, 1980-2015; occurrence is in parts per hundred thousand

Table 4.16: Annual wave climate at Point 6, fully-built, "2087 reasonably foreseeable", significant wave height (Hs) against mean wave direction

			Wave direction (°N)											
			-15	15	45	75	105	135	165	195	225	255	285	315
H_{s1} (m)	H_{s2} (m)	$P(H_s>H_{s1})$	15	45	75	105	135	165	195	225	255	285	315	345
0	0.5	100.00%	7638	36126	17286	7498	5823	3087	1083	535	394	283	285	627
0.5	1	19.34%	258	11219	3841	57	5	2	-	-	-	-	-	-
1	1.5	3.95%	-	2407	630	-	-	-	-	-	-	-	-	-
1.5	2	0.92%	-	547	167	-	-	-	-	-	-	-	-	-
2	2.5	0.20%	-	144	30	-	-	-	-	-	-	-	-	-
2.5	3	0.03%	-	24	2	-	-	-	-	-	-	-	-	-
3	3.5	0.00%	-	4	-	-	-	-	-	-	-	-	-	-
Percentage Occurrence			7.90%	50.47%	21.96%	7.56%	5.83%	3.09%	1.08%	0.53%	0.39%	0.28%	0.28%	0.63%

Source: HR Wallingford, SWAN wave transformation and Met Office WW3 offshore data, 1980-2015; occurrence is in parts per hundred thousand

Table 4.17: Annual wave climate at Point 6, baseline, "2087 reasonably foreseeable", significant wave height (Hs) against mean wave period

			Mean Wave Period (T_{m-10}) in Seconds													
			0	1	2	3	4	5	6	7	8	9	10	11	12	13	14
H_{s1} (m)	H_{s2} (m)	$P(H_s>H_{s1})$	1	2	3	4	5	6	7	8	9	10	11	12	13	14	15
0	0.5	100.00%	211	6193	19675	26462	18673	7179	2112	532	114	15	7	2	3	2	<1
0.5	1	18.82%	-	16	646	3890	4874	3309	1368	582	159	46	7	<1	-	-	-
1	1.5	3.92%	-	-	3	138	939	1071	573	227	37	12	5	<1	-	-	-
1.5	2	0.92%	-	-	-	<1	44	254	218	149	39	5	<1	-	-	-	-
2	2.5	0.21%	-	-	-	-	-	31	72	48	26	1	-	-	-	-	-
2.5	3	0.03%	-	-	-	-	-	-	3	12	8	2	-	-	-	-	-
3	3.5	0.00%	-	-	-	-	-	-	-	2	2	-	-	-	-	-	-
Percentage Occurrence			0.21%	6.21%	20.32%	30.49%	24.53%	11.84%	4.35%	1.55%	0.38%	0.08%	0.02%	0.00%	0.00%	0.00%	0.00%

Source: HR Wallingford, SWAN wave transformation and Met Office WW3 offshore data, 1980-2015; occurrence is in parts per hundred thousand

Table 4.18: Annual wave climate at Point 6, fully-built, "2087 reasonably foreseeable", significant wave height (Hs) against mean wave period

			Mean Wave Period (T_{m-10}) in Seconds													
			0	1	2	3	4	5	6	7	8	9	10	11	12	13	14
H_{s1} (m)	H_{s2} (m)	$P(H_s>H_{s1})$	1	2	3	4	5	6	7	8	9	10	11	12	13	14	15
0	0.5	100.00%	169	5776	19416	26722	18736	7105	2071	530	111	16	5	2	3	2	<1
0.5	1	19.34%	-	14	609	3848	5049	3574	1456	607	169	49	6	<1	-	-	-
1	1.5	3.95%	-	-	2	125	928	1099	587	240	37	13	5	<1	-	-	-
1.5	2	0.92%	-	-	-	<1	39	252	223	155	39	5	<1	-	-	-	-
2	2.5	0.20%	-	-	-	-	-	27	71	49	26	1	-	-	-	-	-
2.5	3	0.03%	-	-	-	-	-	-	3	12	9	2	-	-	-	-	-
3	3.5	0.00%	-	-	-	-	-	-	-	2	2	-	-	-	-	-	-
Percentage Occurrence			0.17%	5.79%	20.03%	30.70%	24.75%	12.06%	4.41%	1.60%	0.39%	0.09%	0.02%	0.00%	0.00%	0.00%	0.00%

Source: HR Wallingford, SWAN wave transformation and Met Office WW3 offshore data, 1980-2015; occurrence is in parts per hundred thousand

4.5.6. December 2013 storm

The comparison between the baseline and the fully-built layout was also carried out for the December 2013 storm.

Figure 4.23 shows the variation in offshore wave and wind conditions through the storm at the Met Office offshore data point. The offshore conditions from the Met Office model point corresponding to the peak of the storm are listed in Table 4.19.

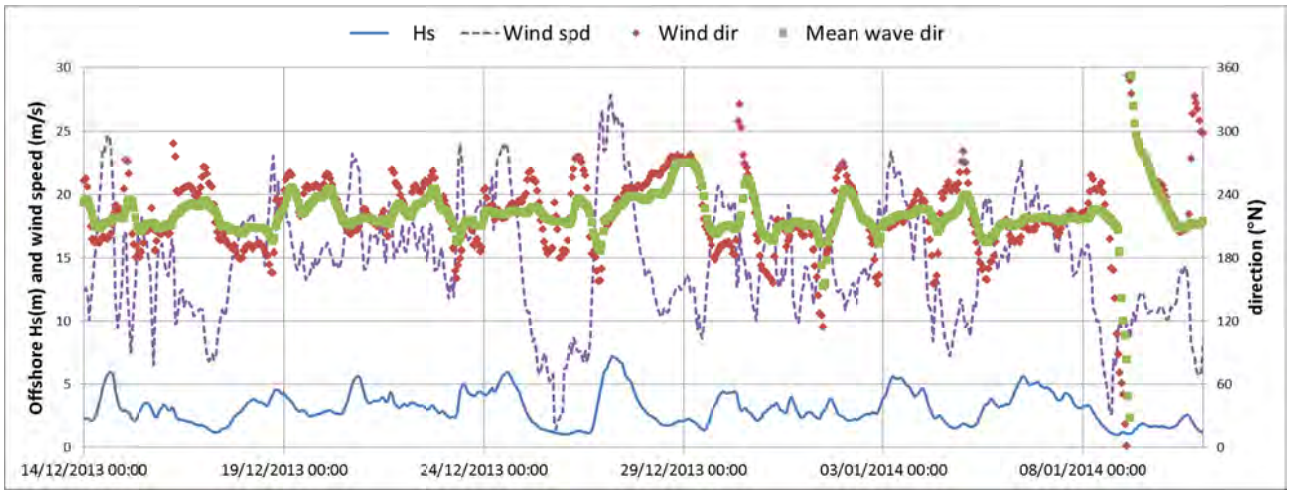

Figure 4.23: Offshore conditions from the Met Office model point data set during the December 2013 storm

Source: Met Office WW3 offshore data, 1980 - 2015

Table 4.19: Offshore conditions at the peak of the December 2013 storm

	H_s (m)	T_{m-10} (s)	Mean Wave Direction (°N)	Wind speed (m/s)	Wind direction (°N)
27/12/2013 05:00	7.24	9.5	220	27.2	217

Source: Met Office WW3 offshore data, 1980 - 2015

Predicted significant wave height through the storm event at Point 6 in Cemlyn Bay is shown in Figure 4.24 for the baseline and fully-built layout. There is only a small difference in significant wave height between the two layouts.

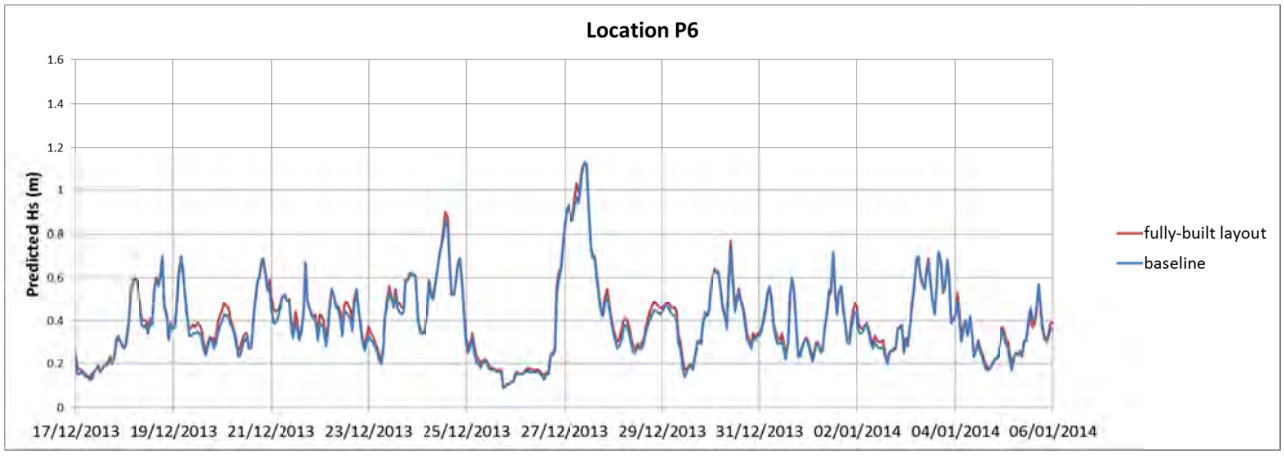

Figure 4.24: Predicted significant wave heights, baseline and fully-built layout, December 2013 storm

Source: HR Wallingford, SWAN wave transformation and Met Office WW3 offshore data, 1980 - 2015

4.5.7. Selected 99th percentile Winter conditions, difference in significant wave height maps – additional 'worst-case' construction layout

One additional part-built layout has been considered for potential impact. It is chosen to represent the "worst-case" construction layout for potential impact and consists of the full Western Breakwater in place with the cofferdam and causeway.

The resulting model layout and bathymetry is shown in Figure 4.25.

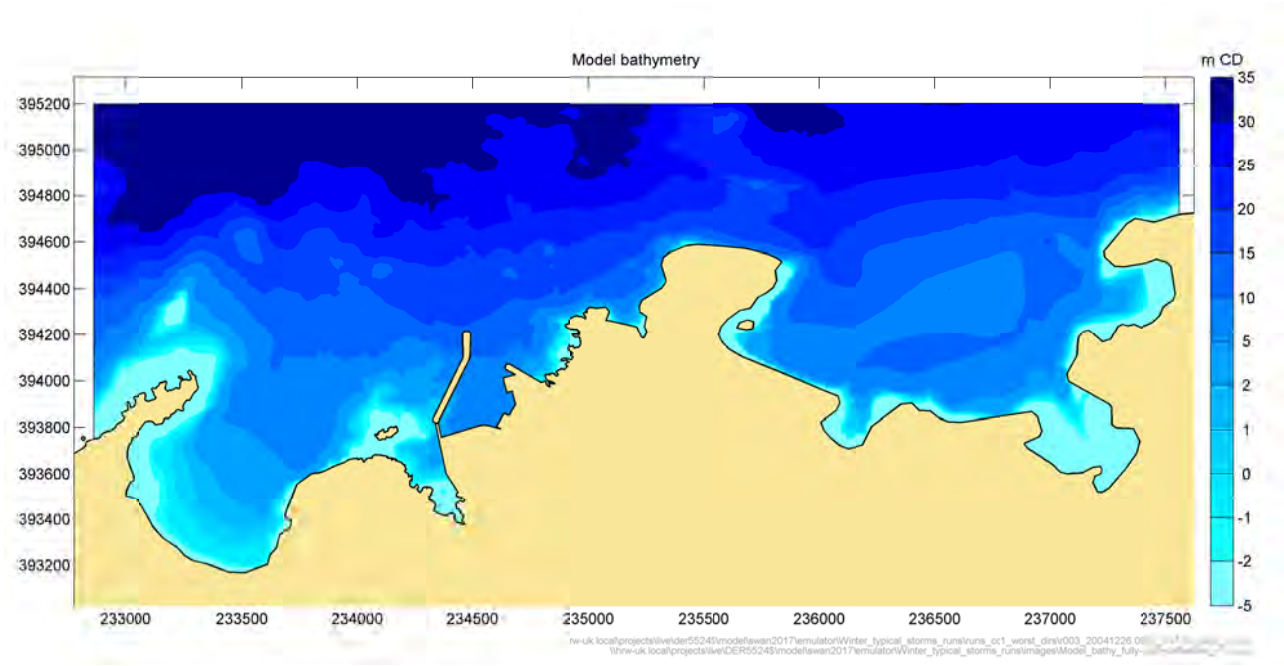

Figure 4.25: SWAN model bathymetry, "worst-case" construction layout

The difference plots (difference in predicted significant wave height between the “worst-case” construction layout and the baseline) for the selected 99th percentile winter “2087 reasonably foreseeable” conditions from the NE, N, NW and W sectors, are shown in Figure 4.26 and Figure 4.27.

Each figure is in three parts, and represents just one wave condition. The top pane of each figure shows the baseline significant wave height for the area around Wylfa, the middle pane the corresponding wave heights for the “worst-case” construction layout. The bottom pane shows the difference in significant wave height between the runs with and without structures. Yellow and orange shades show increases in significant wave height of at least 10 centimetres. Blue and green shades show reductions in wave height of at least 10 centimetres.

Figure 4.26 and Figure 4.27 are directly comparable with Figure 4.21 and Figure 4.22 for the fully-built layout. The effects in Cemlyn Bay are almost identical to the effects predicted for the fully-built layout, which is expected since the main cause of the refocussing of wave energy in Cemlyn Bay comes from the reflections from the western breakwater. The predicted differences with the “worst-case” construction layout are not higher than the ones predicted with the fully-built layout.

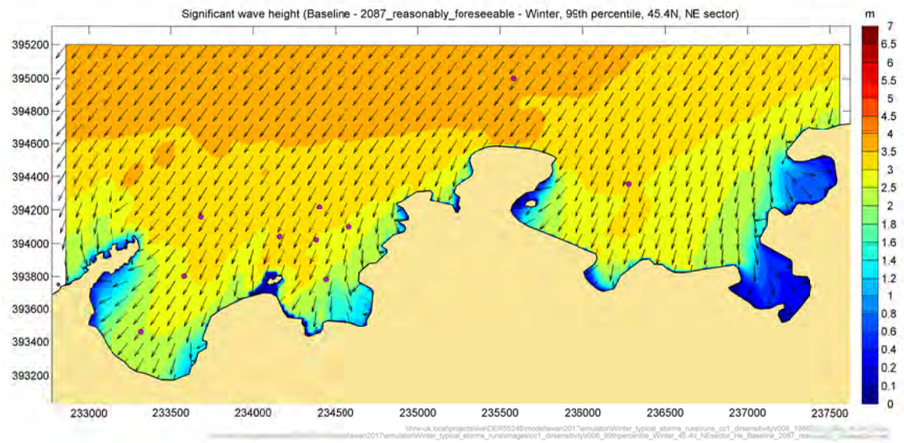

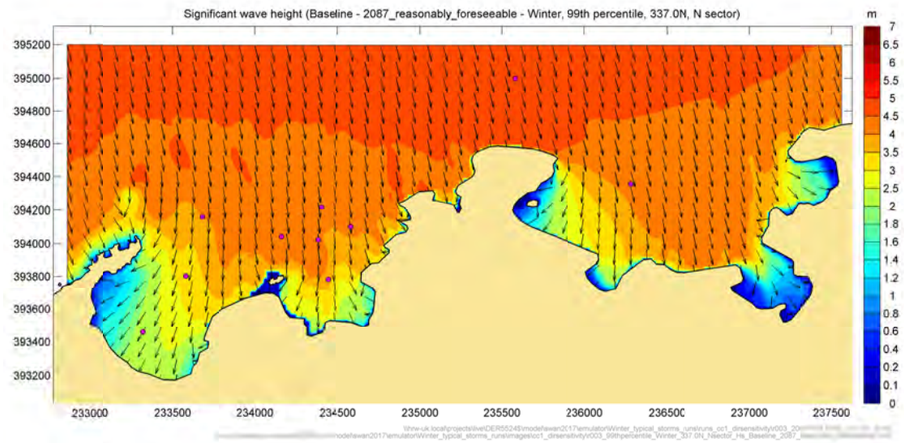

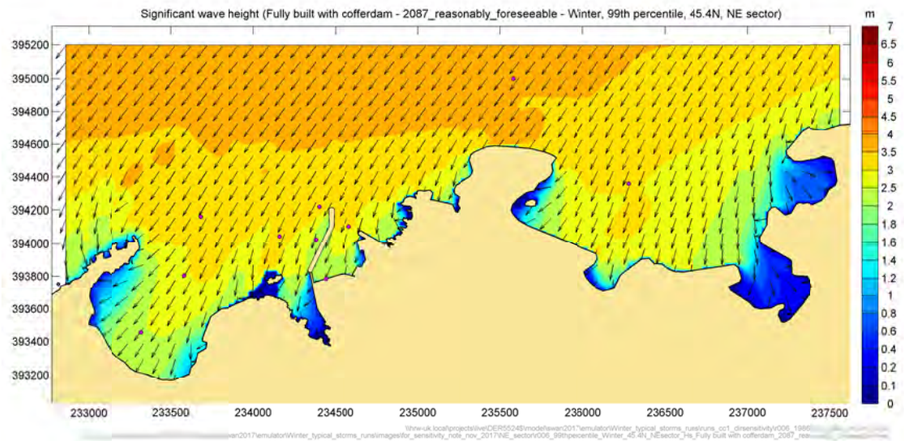

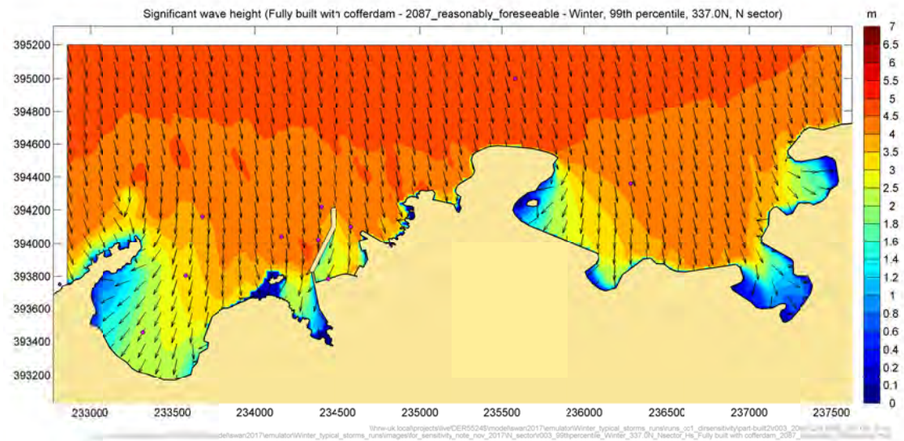

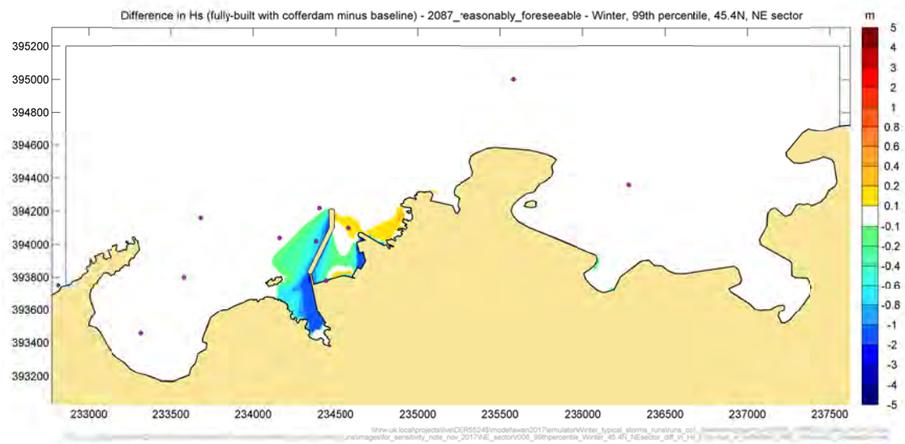

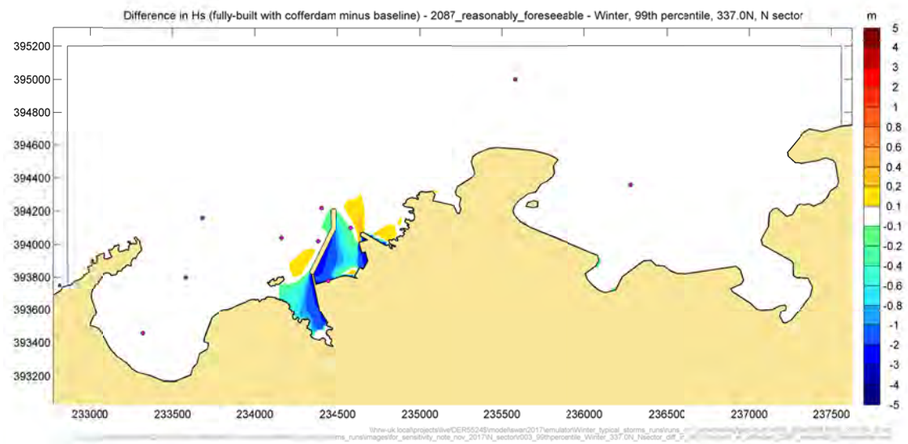

Figure 4.26: Difference in significant wave height, “worst-case” construction layout compared to baseline case, “2087 reasonably foreseeable conditions, NE (left) and N (right) sectors

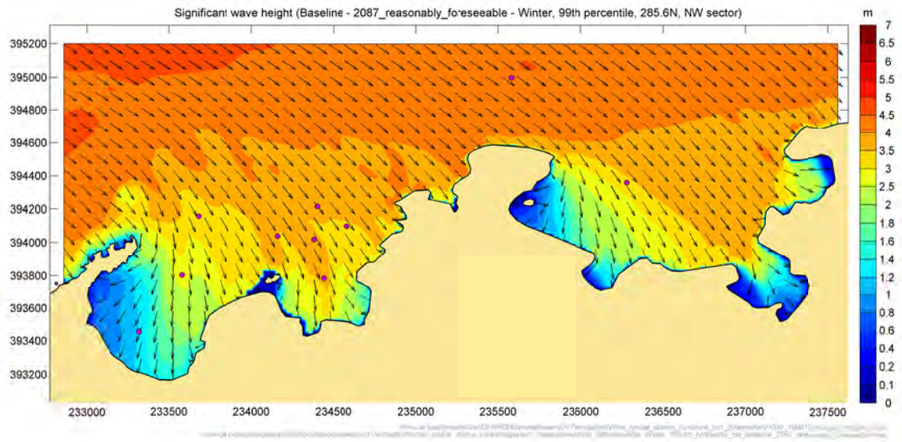

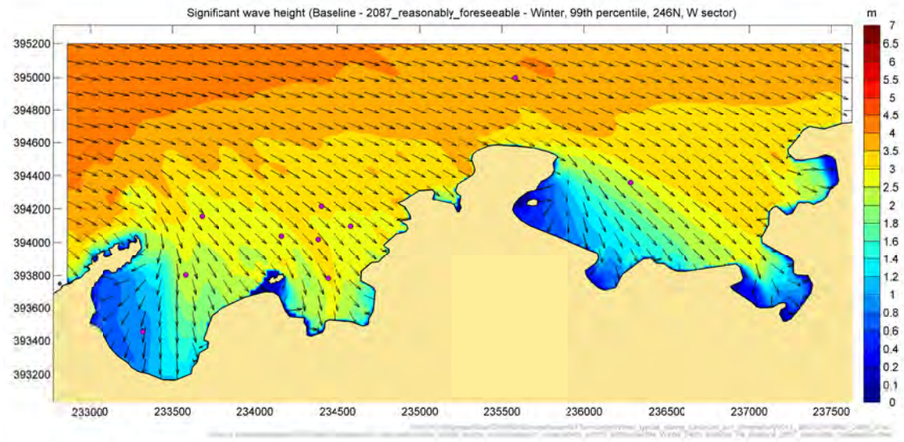

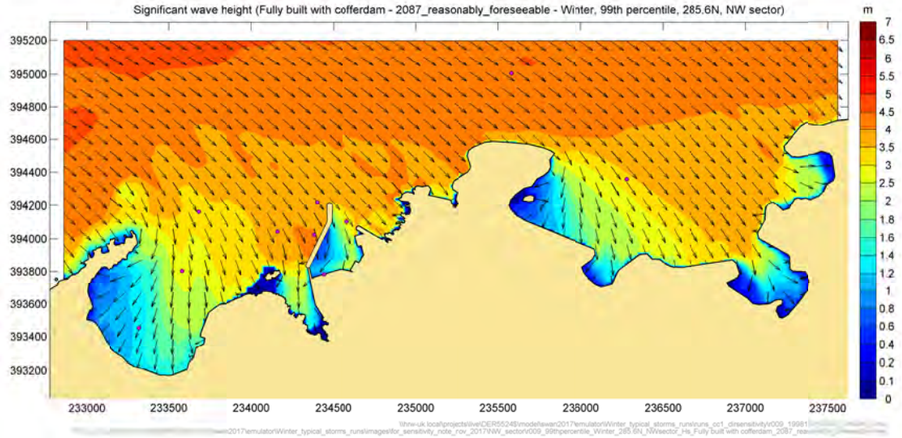

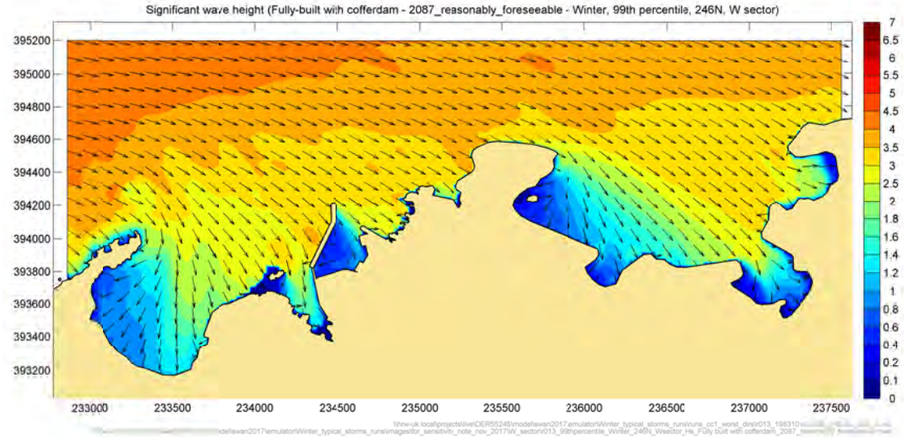

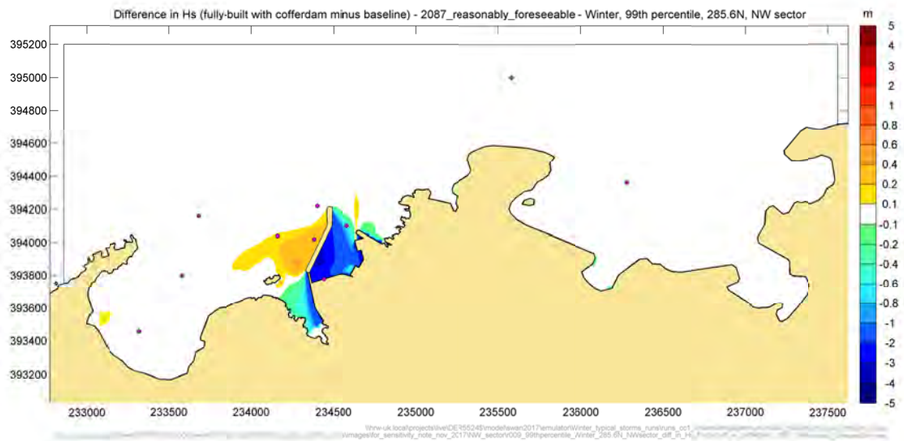

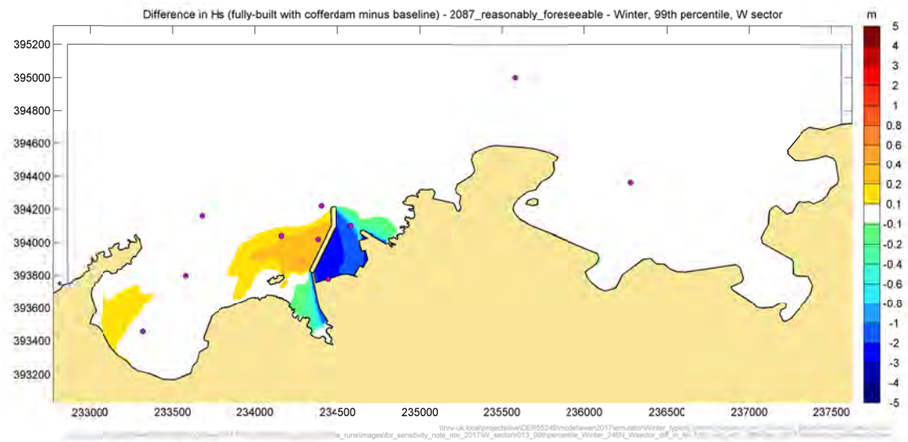

Figure 4.27: Difference in significant wave height, “worst-case” construction layout compared to baseline case, “2087 reasonably foreseeable conditions, NW (left) and W (right) sectors

For completeness, the difference plots (difference in predicted significant wave height between the “worst-case” construction layout and the baseline) for the selected 99th percentile winter “present-day” conditions are shown in Figure 4.28 and Figure 4.29. This comparison is more relevant since the construction layout will not be in place for the 2087 future conditions.

The predicted differences for the “present-day” conditions follow the same pattern as for the “2087 reasonably foreseeable” conditions, but are smaller in magnitude.

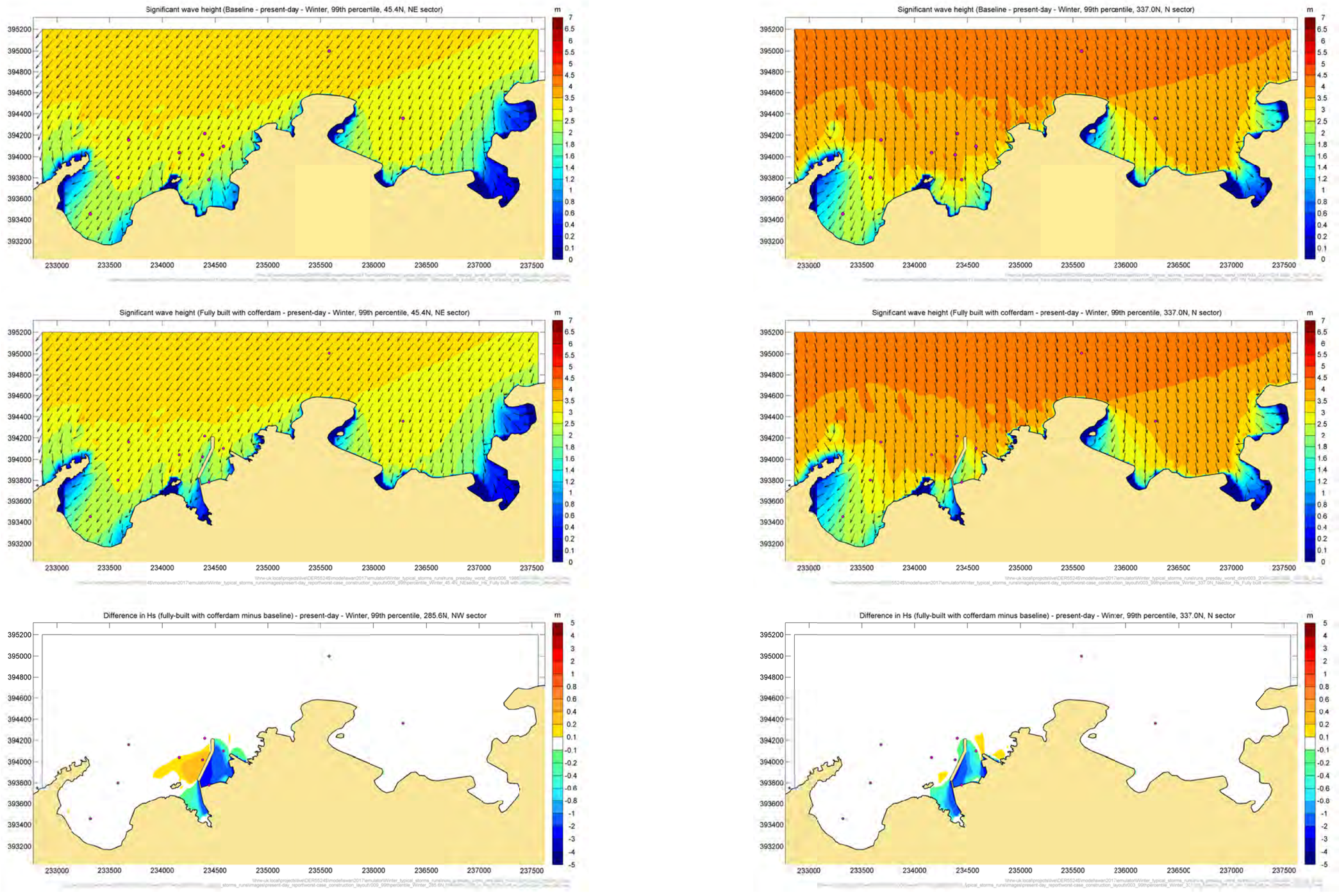

Figure 4.28: Difference in significant wave height, “worst-case” construction layout compared to baseline case, “present-day” conditions, NE (left) and N (right) sectors

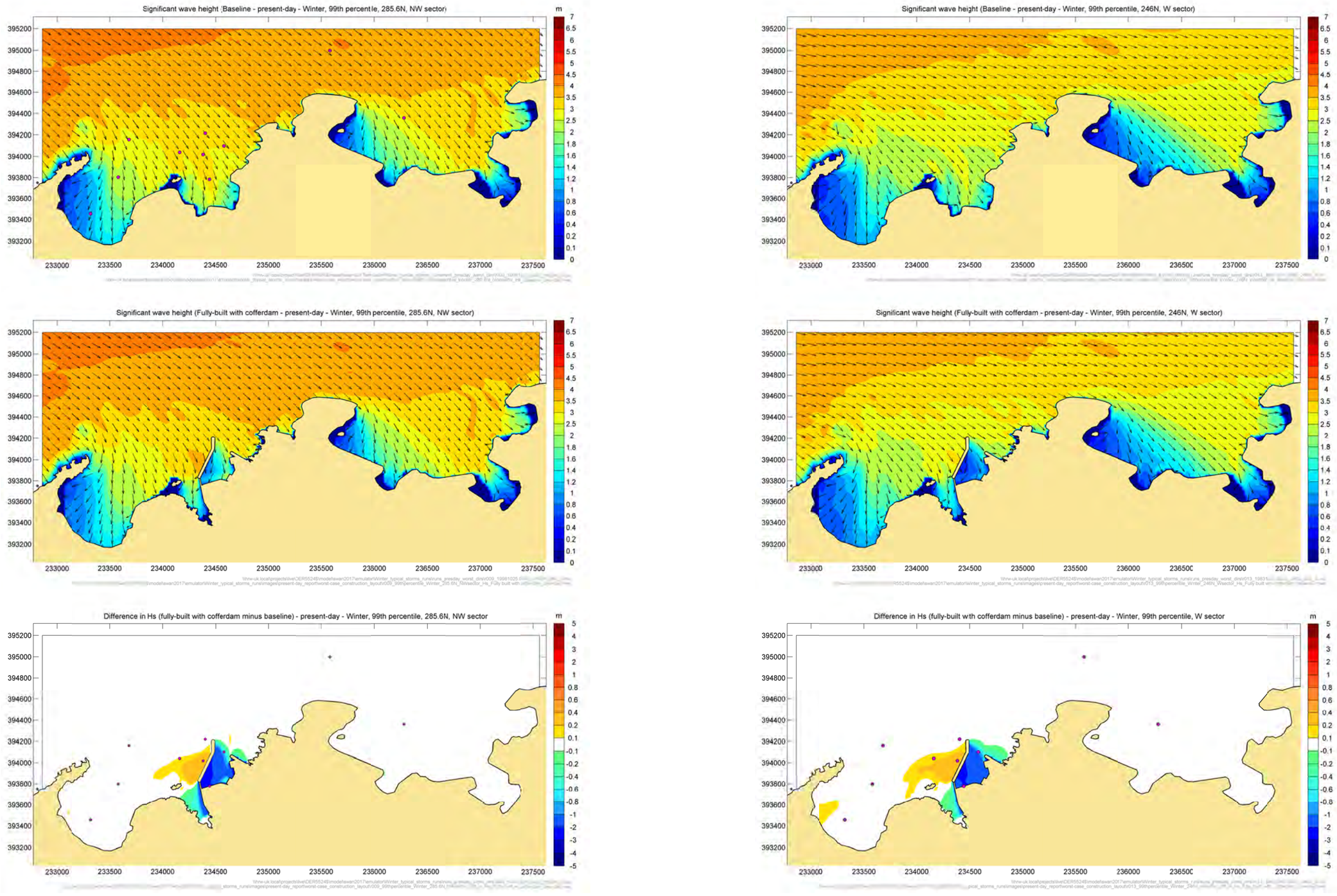

Figure 4.29: Difference in significant wave height, “worst-case” construction layout compared to baseline case, “present-day” conditions, NW (left) and W (right) sectors

5. Wave conditions inside the harbour

Although the SWAN model represents far-field diffraction and reflection of waves, it is a phase–averaged coastal area model that is not designed for use inside harbour areas where more complex wave interference between diffracted and reflected waves may occur. For modelling inside harbours, a local phase-resolving wave disturbance model is required.

Wave disturbance refers to wave conditions within a small area (up to a few kilometres across) protected from incoming waves, usually by breakwaters or headlands. In this instance it relates to the area in the lee of the Wylfa Newydd breakwaters, including the Materials Off-Loading Facility (MOLF), the cofferdam and the cooling water intake. It is required to produce wave conditions to be used to estimate overtopping rates at the two MOLF berths and at the cofferdam, to feed into a flood risk assessment.

The model runs and results from the disturbance modelling focus on marginal and joint exceedence return periods at the MOLF berths and the cofferdam for the 2087 “reasonably foreseeable”, 2087 “credible maximum” and 2187 “reasonably foreseeable” climate-changed scenarios, for the fully-built layout, and for the 2023 “present-day” climate change scenario for the part-built layout. The probabilities of occurrence of interest correspond to return periods of 5, 25, 75, 200 and 1000 years.

5.1. The ARTEMIS wave model

The ARTEMIS model is based on the finite element solution of the Mild Slope Equation. It was developed by the National Hydraulics Laboratory (LNH) of the Research and Development Division of the French Electricity Board (EDF-DER) as part of the TELEMAC finite element hydraulic modelling system. It represents transformation of random waves, including the following effects:

- wave shoaling;
- wave refraction;
- partial reflections from for example the breakwater or quays;
- wave diffraction;
- energy dissipation due to depth-limited wave breaking and seabed friction;
- wave resonance effects.

Further details of the ARTEMIS model are included in Appendix D.

5.1.1. Application of the ARTEMIS model to Wylfa

A local ARTEMIS wave disturbance model was set up to represent the waves inside the harbour area. The model was set up for the part-built layout and the fully-built layout, including the two main breakwaters and the lowering of the bed level within the harbour area relative to present-day levels.

Figure 5.1 and Figure 5.2 show the ARTEMIS model area and bathymetry which was obtained from the local surveys, supplemented with charted data points, for both layouts. The model mesh is unstructured, with a typical spatial resolution of 1.4m in order to resolve the wavelengths of the waves of interest. Note that the bathymetry to the south-west of the southern tip of the western breakwater has been refined relative to that used for the SWAN model, both because this area is critical for wave energy entering the harbour and because the ARTEMIS model grid is finer than that of the SWAN model.

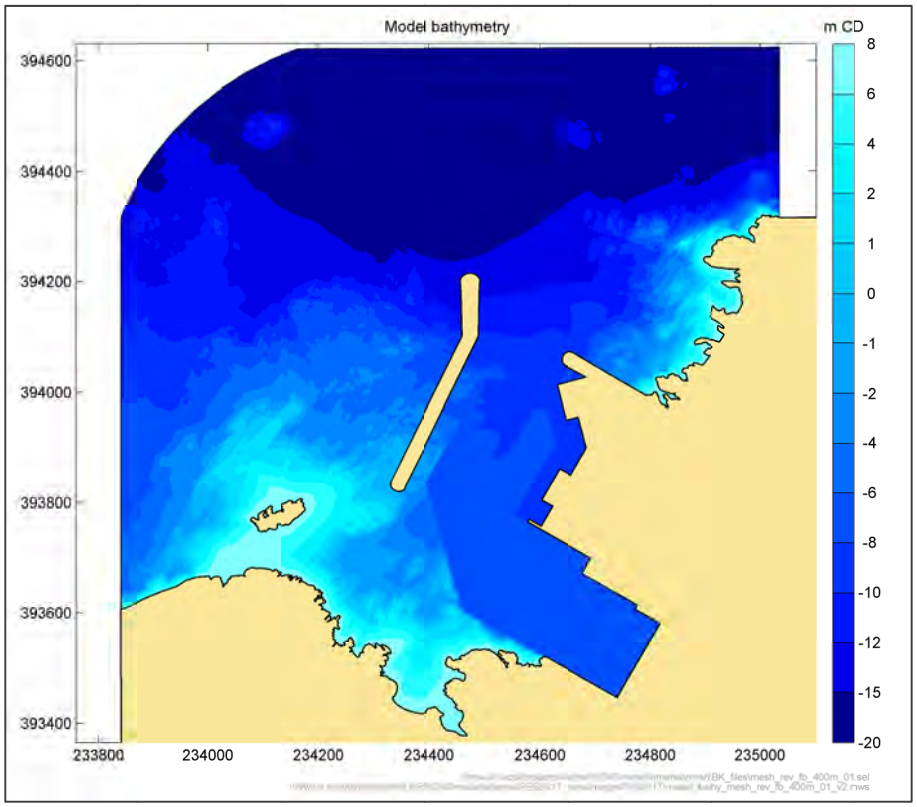

Figure 5.1: ARTEMIS model extent and bathymetry, fully-built layout

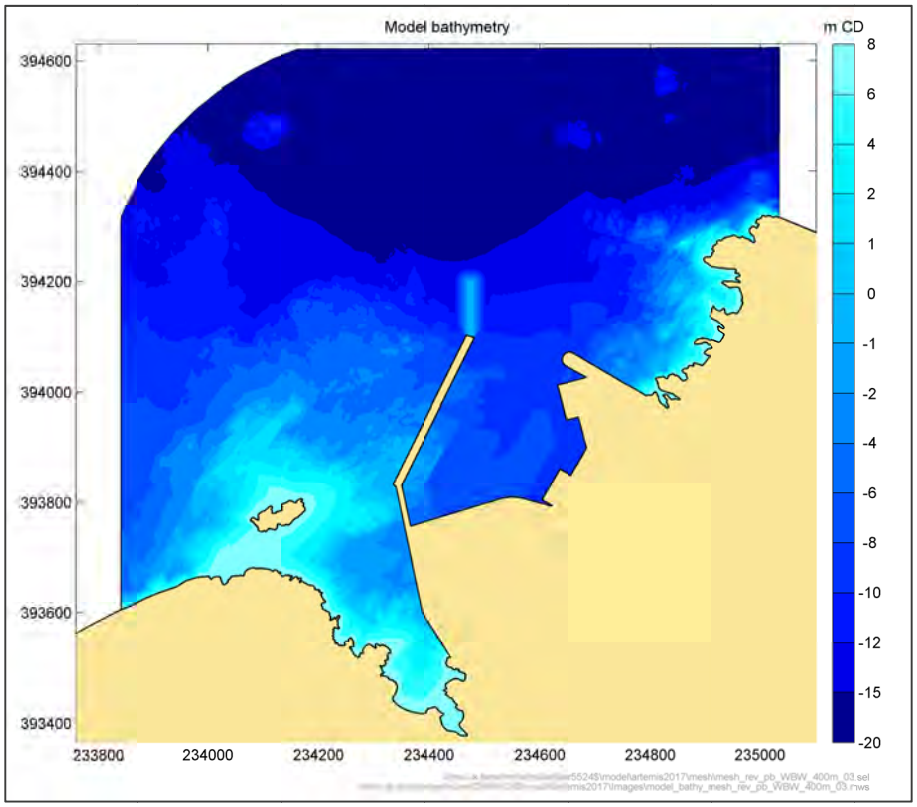

Figure 5.2: ARTEMIS model extent and bathymetry, part-built layout

5.2. Boundary wave conditions

5.2.1. Point P1 at which to estimate boundary conditions

Boundary conditions for the ARTEMIS model were extracted from the SWAN model on the ARTEMIS model boundary (Figure 5.3). Initially, two points / directions were considered as potentially leading to the greatest wave agitation in the harbour: P1 on the northern model boundary and P2 on the north-west model boundary. Selection of the more appropriate boundary point depended on some sensitivity tests.

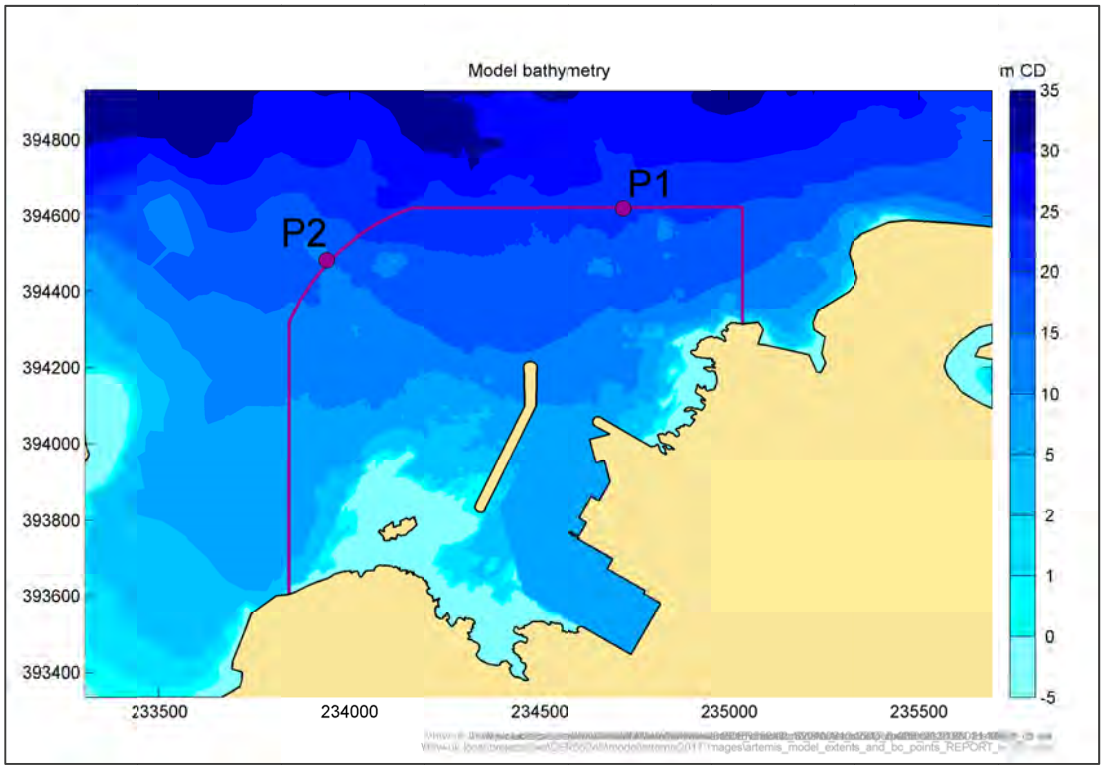

Figure 5.3: Locations of the ARTEMIS model boundary point

An earlier wave modelling study (Amec, 2015) showed that the highest waves close to the coast at Wylfa come from the north, and that they originated broadly from the north. As the harbour entrance faces north, it might be expected that the highest wave conditions within the harbour would also come from the north. However, there is the possibility that waves approaching the harbour from the north-west would also enter the harbour, through the shallow water between the southern tip of the western breakwater and the land. The sensitivity test described here was designed to check that waves from the north-west would not significantly affect the extreme wave conditions predicted within the harbour.

The four storms from the north causing the highest waves at Point P1 and the four storms from the north-west causing the highest waves at Point P2 were identified based on the SWAN model predictions for Points P1 and P2. For the fully-built layout, the wave heights within the harbour area were larger for each of the northerly storms than for any of the north-westerly storms. As a further check, the largest storm from each sector was run through ARTEMIS (for an earlier harbour design layout), both storms being run at a 1 year return period sea level. The results are shown in Figure 5.4, in which the waves for the northerly storm are significant higher within the harbour than those for the north-westerly storm. Subsequent analysis is based on waves for all sectors combined, but with the assumption that the highest waves will approach the harbour approximately from the north at Point P1.

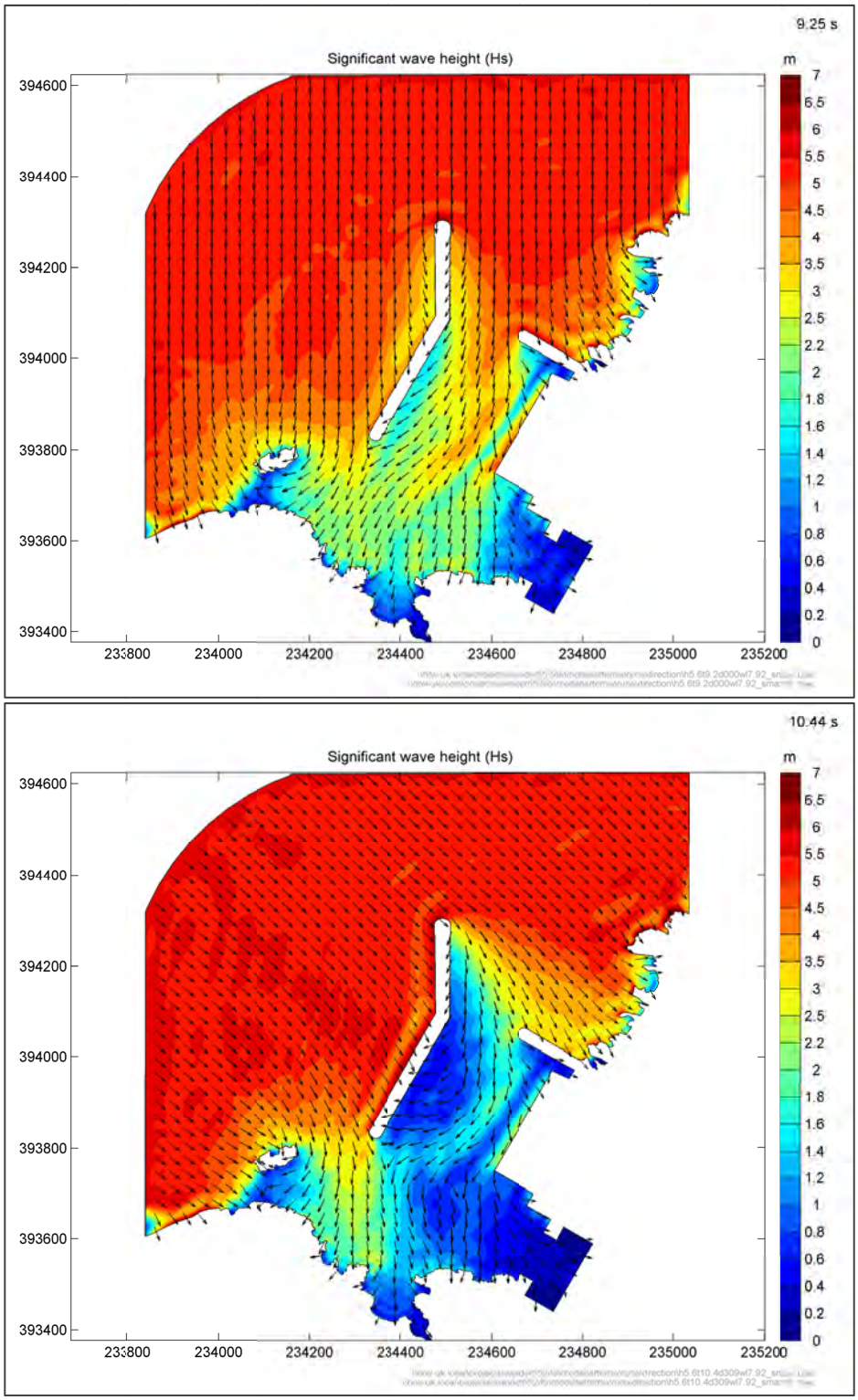

Figure 5.4: Significant wave heights from the most severe storms in the 35-year time series at Point P1 (top) from the north and (bottom) from the north-west sectors

Source: ARTEMIS model; based on an earlier harbour design (2015 layout drawings)

5.2.2. Boundary wave direction

The distribution of significant wave height against mean wave direction at Point P1 is shown in Figure 5.5. This is based on the SWAN model runs for the "2087 reasonably foreseeable" climate-changed scenario, applying partitioned offshore wave spectra, and covering only the highest ten percent of wave heights offshore.

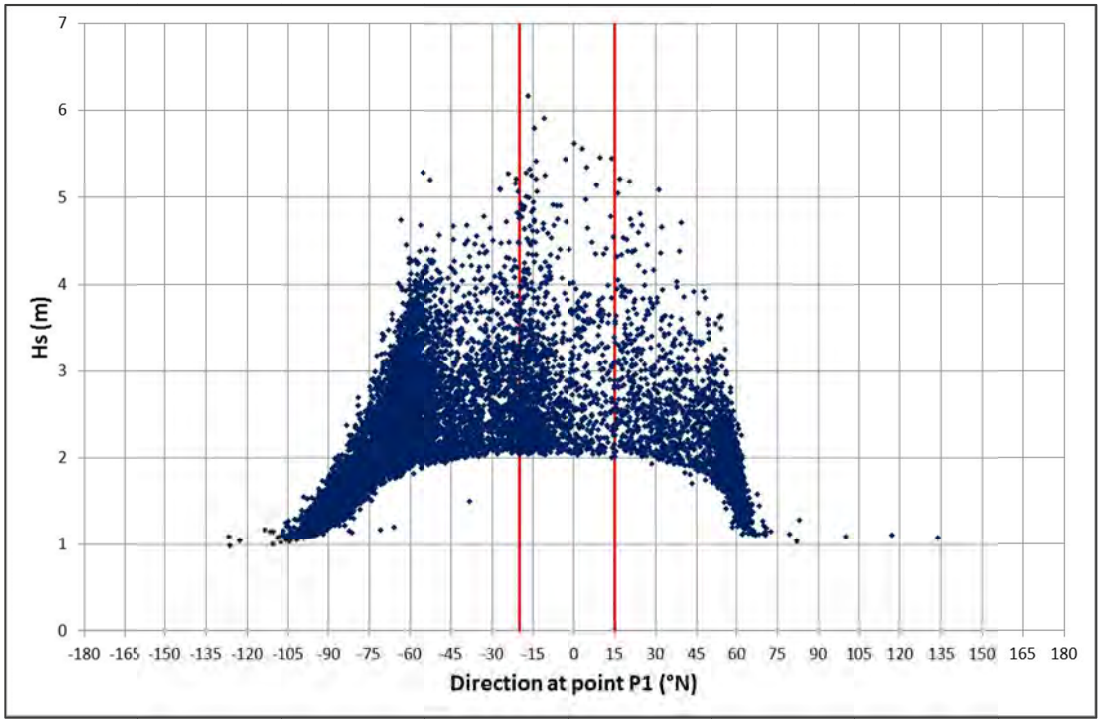

Figure 5.5: Distribution of significant wave height against mean wave direction at the ARTEMIS model boundary Point P1

Source: SWAN model runs of the highest 10% storm events offshore and Met Office WW3 offshore data, 1980-2015, including future climate change allowance

Although the prevailing wave direction is approximately north-west, the highest waves at Point P1 are predicted to come from close to north (-20°N to +15°N, as indicated by the red lines in Figure 5.5). The extreme wave conditions were tested as coming from due north at Point P1 and from directions ten degrees either side of due north. Due north was adopted as the worst case offshore direction for wave heights within the harbour.

Based on the highest four northerly wave conditions modelled with SWAN, the directional spread was found to be of order 30-35°, represented in ARTEMIS by setting model parameter S_{max} to a value of 10.

5.2.3. Boundary wave heights and periods

The derivation of wave extremes and the joint probability with high water levels at Point P1 for the "2087 reasonably foreseeable" climate-changed scenario, undertaken during earlier work, is described in Appendix E.

The tangent-based joint exceedence curves at Point P1 provide conditions to run in the ARTEMIS model. The joint exceedence curves are curves of joint extreme combinations of significant wave height and water level. The tangent-based method refers to the approach used to derive the contours, in which the joint exceedence curve for a given probability or return period is defined by the property that wave height / water level combinations exceeding the tangent to the curve at any point have the required probability of exceedence (Huseby et al., 2013). This approach ensures that for example at every point along the 200-year curve, the probability of the wave /water level combination being outside the tangent to this curve is once in 200 years. The method is described in more detail in Appendix E.2.

Present-day and future climate changed conditions were derived from the "2087 reasonably foreseeable" conditions.

The "2087 reasonably foreseeable" joint exceedence curves at P1 for return periods of 5, 25, 75, 200 and 1000 years are presented in Figure 5.6. The information is also tabulated in Table E.2 (the first row of each block of data representing the marginal extreme wave condition for that return period).

Twenty representative conditions (4 combinations of wave height and water level per return period) were selected for each climate-changed scenario, to be run in ARTEMIS, in order to transform the whole set of joint exceedence curves (shown in Figure 5.6). The twenty representative conditions run in the ARTEMIS model were selected to be sufficient to scale the joint-exceedence curves at the entrance to the joint-exceedence curves at the points inside the harbour.

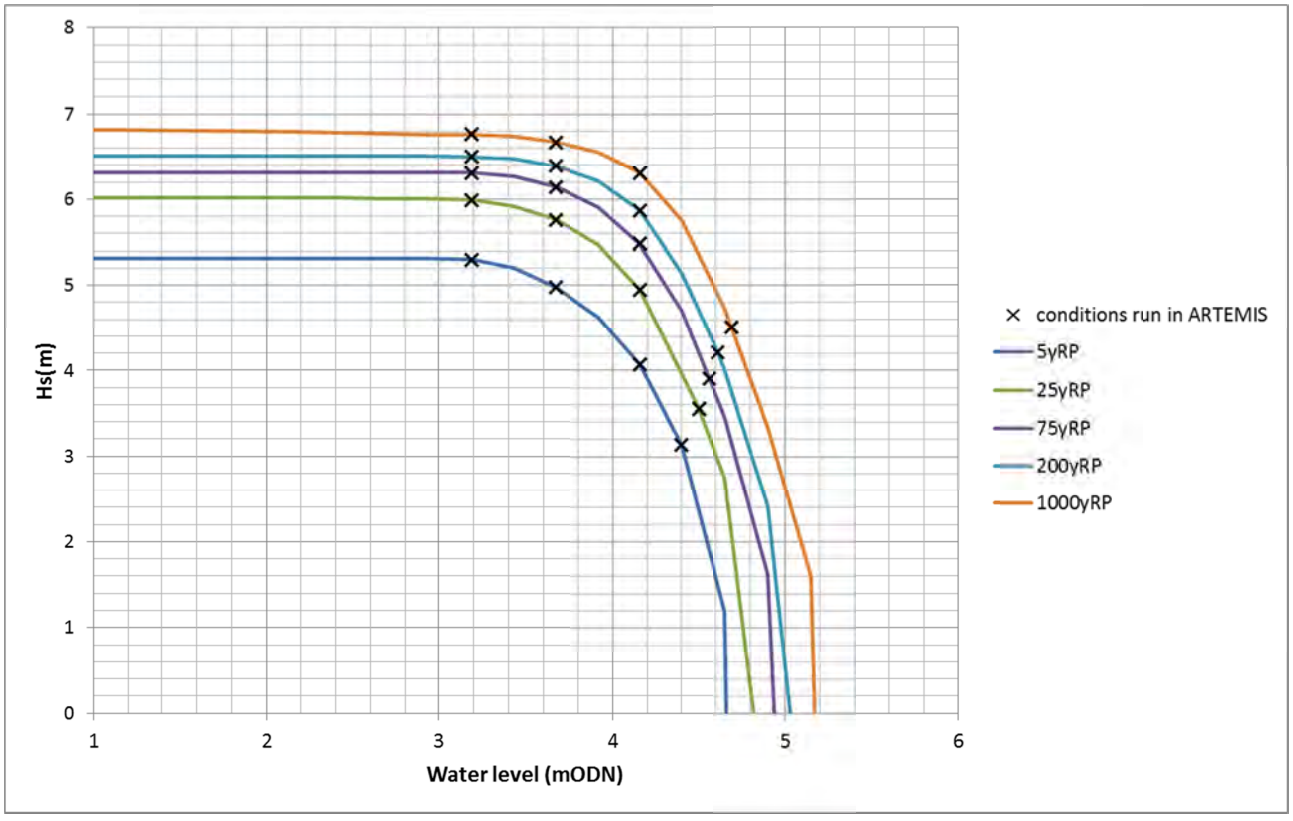

Figure 5.6: High water joint probability, Point P1, fully-built "2087 reasonably foreseeable" conditions

Source: HR Wallingford analysis; SWAN modelling

For consistency, so as to achieve best estimates of *differences* between the different climate change scenarios, the "2087 reasonably foreseeable" joint probability curves at Point P1 were used for each scenario, but with the following adjustments for the new climate-changed scenarios.

Water level

Remove the "2087 reasonably foreseeable" future climate change allowance and replace it with the relevant allowance, to account for the climate change allowances revision from UKCP09 guidance, used in earlier wave modelling work, to the Welsh Guidance 2016 used in the present modelling and summarised in Table 3.1.

Wave height

Tests showed little sensitivity of wave height at Point P1 to high-tide sea level (the water level makes more difference in shallower water closer inshore).

Therefore, wave conditions leading to the highest ten percent of wave heights at any or all of the five offshore locations (Figure 4.1) were selected to be the largest storm events for the site in the 35-year time series. These storms were run in SWAN and transformed to Point P1 at four different sea levels, with and without the wave height climate change allowance, to estimate the adjustments to apply to the "2087 reasonably foreseeable" joint probability curves at Point P1 for the new climate-changed scenarios. The four different sea levels considered are the four UKCP09 climate change scenarios (UKCIP, 2009) (used in previous modelling):

- "2087 reasonable foreseeable": 3.48mOD [1];
- "2187 reasonable foreseeable": taken as 2087 credible maximum as only a few cms difference;
- "2087 credible maximum": 4.5mOD;
- "2187 credible maximum": 6.8mOD

Sensitivity to sea level was logged in units of percentage change in wave height per additional metre of sea level. Results lay in the range -0.3%/m to +1.4%/m with an average (for high waves only) of 0.7%/m. For sea levels above that of the "2087 reasonably foreseeable" case, this result was captured in the form of a uniform adjustment of 1.0% increase per additional metre of sea level, applied to all wave heights. Sensitivity to offshore wave height was logged in units of percentage change in wave height per percentage change in offshore wave height. For the present-day case, the future climate change allowance applied to wave height (10% increase offshore) was removed by decreasing all "2087 reasonably foreseeable" wave heights by 8% (and corresponding wave periods by 3.25%).

The resulting high-water joint-exceedence curves at P1 for return periods of 5, 25, 75, 200 and 1000 years, for the "present-day", "2187 reasonably foreseeable" and "2087 credible maximum" cases, are presented in Figure 5.7 to Figure 5.9.

1 With climate change allowances based on UKCIP, 2009 guidelines, as used in previous wave modelling (HR Wallingford (2015)).

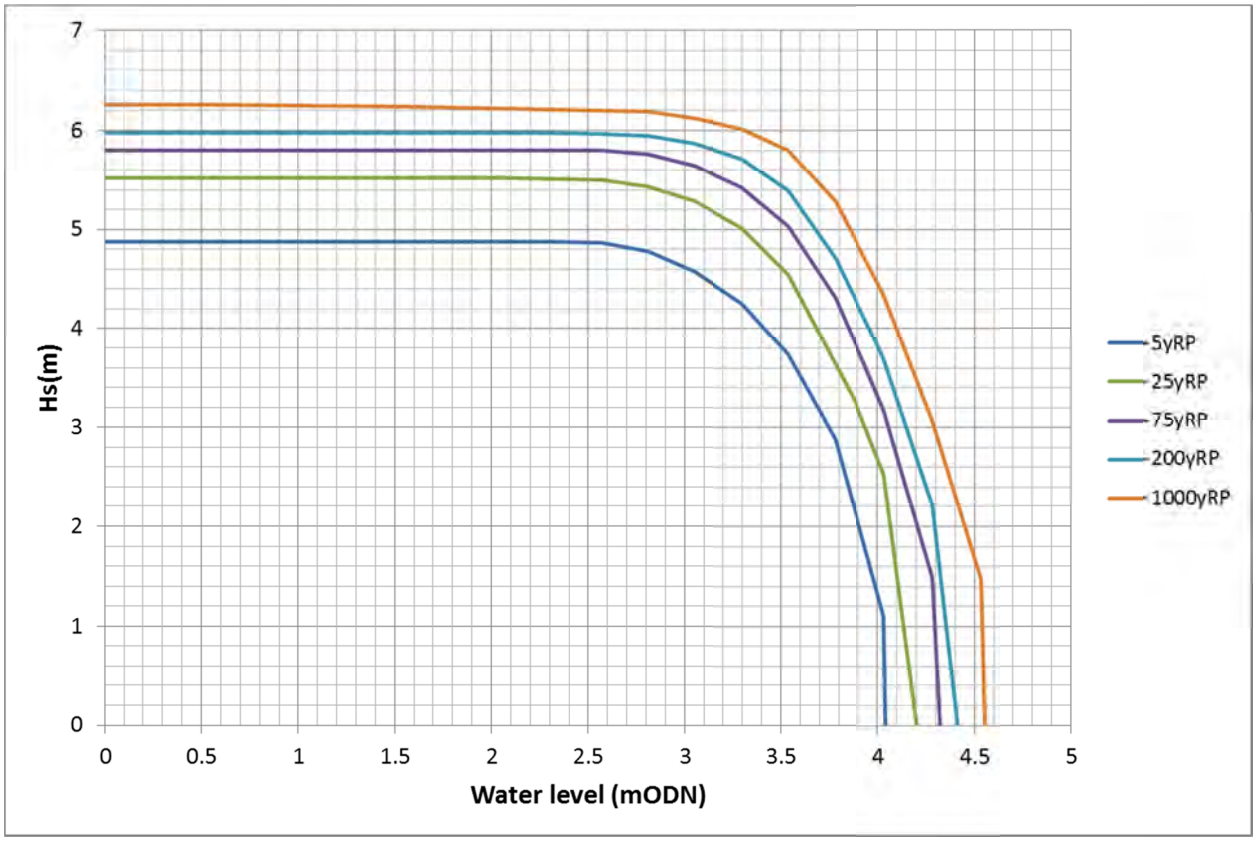

Figure 5.7: High water joint probability, Point P1, “2023 present-day” conditions

Source: HR Wallingford analysis; SWAN modelling

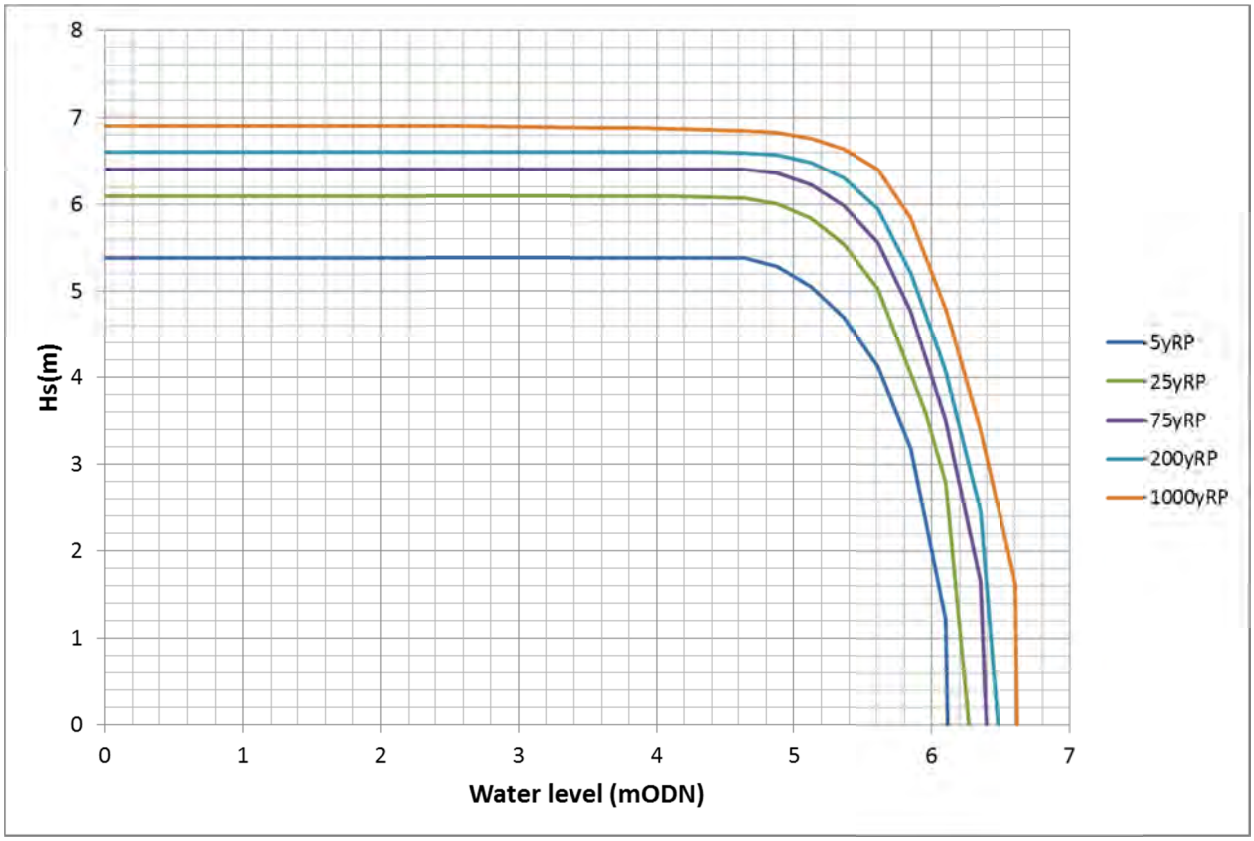

Figure 5.8: High water joint probability, Point P1, "2187 reasonably foreseeable" conditions

Source: HR Wallingford analysis; SWAN modelling

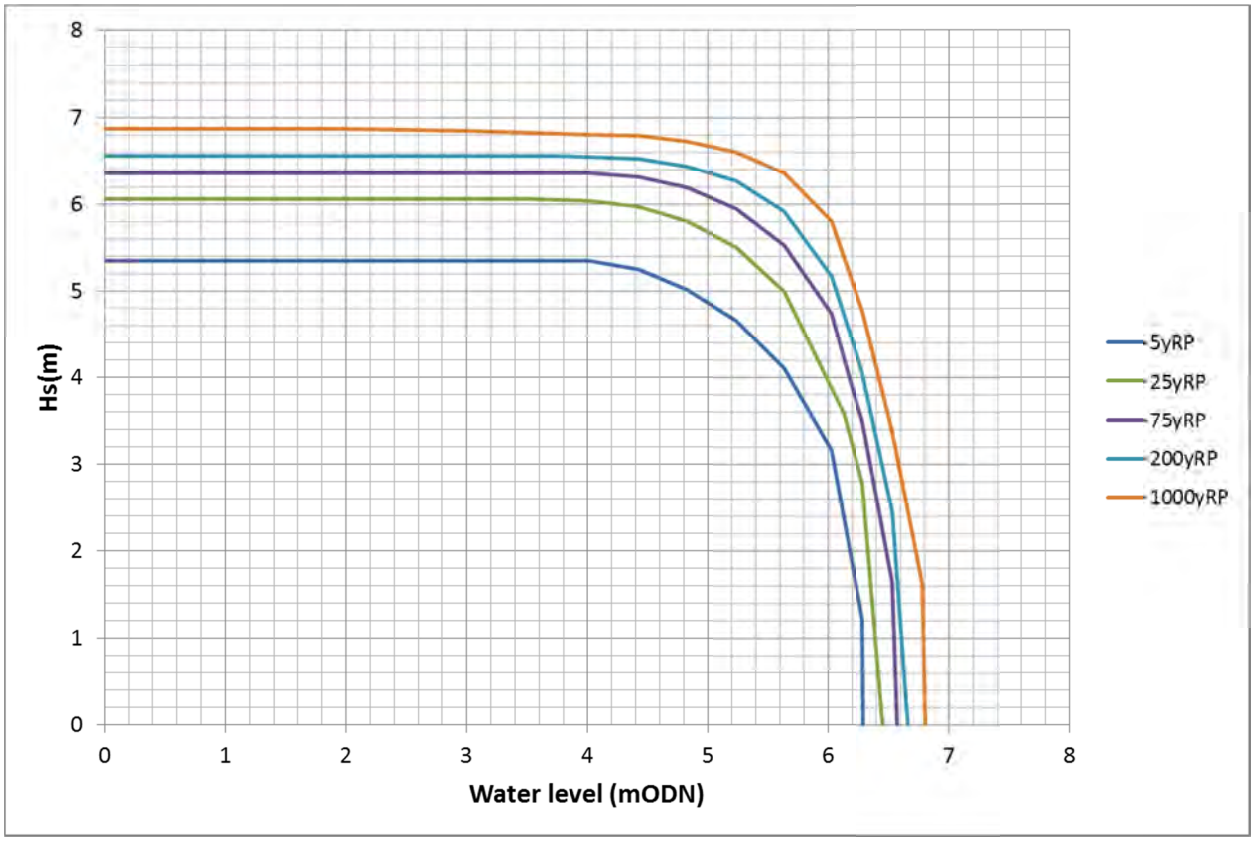

Figure 5.9: High water joint probability, Point P1, "2087 credible maximum" conditions

Source: HR Wallingford analysis; SWAN modelling

5.2.4. Transmission coefficient

In the part-built layout, the Western breakwater is partially constructed with a crest elevation of +4mAOD. The difference between the crest level and the present-day MHWS water level is only one metre. Therefore, the breakwater was represented as a partially transmissive structure in the ARTEMIS model.

The wave transmission coefficient was estimated based upon the wave conditions incident to the breakwater and an empirical relationship derived from a physical model database (HR Wallingford, 2009). A transmission coefficient of 1.0 would indicate full transmission. The transmission coefficient used in the model for the partially constructed Western breakwater is 0.35, which is a relatively conservative estimate of transmission for the MHWS present-day conditions.

5.2.5. Reflection coefficients

The reflection properties of the boundaries were represented in the ARTEMIS model by assigning appropriate wave reflection coefficients to each of the boundary types within the model, e.g. coastline, breakwaters, quays and other structures, depending on the form of the structure and the wave conditions (Allsop, 1990). A reflection coefficient of 1.0 would indicate reflection of all the incident wave energy, while a lower reflection coefficient would be indicative of some wave energy being dissipated.

The reflection coefficients used for the study are summarised in Table 5.1, and also shown in Figure 5.11 and Figure 5.12. The model runs include allowance for almost total reflection from the vertical front face of the intake structure (Figure 5.10).

Wave conditions (incident waves) are imposed at the circular segment boundary.

Table 5.1: Reflection coefficients used in the ARTEMIS model

Boundary types	Reflection coefficient
Rocky coastline	0.4
Vertical structures along the quay	0.95
CW intake	0.95
Breakwater (1:4/3 slope)	0.4
Rock revetment slope (1:1.5)	0.35
Absorbing or open structures	0.0

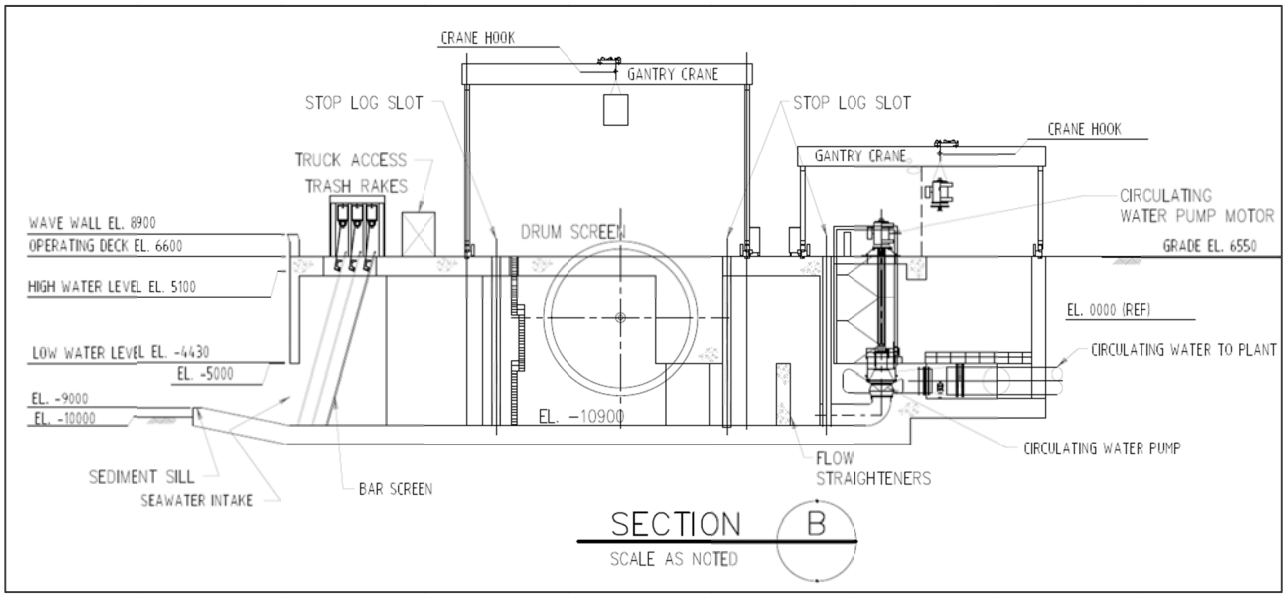

Figure 5.10: Cross-section through the intake

Source: Bechtel

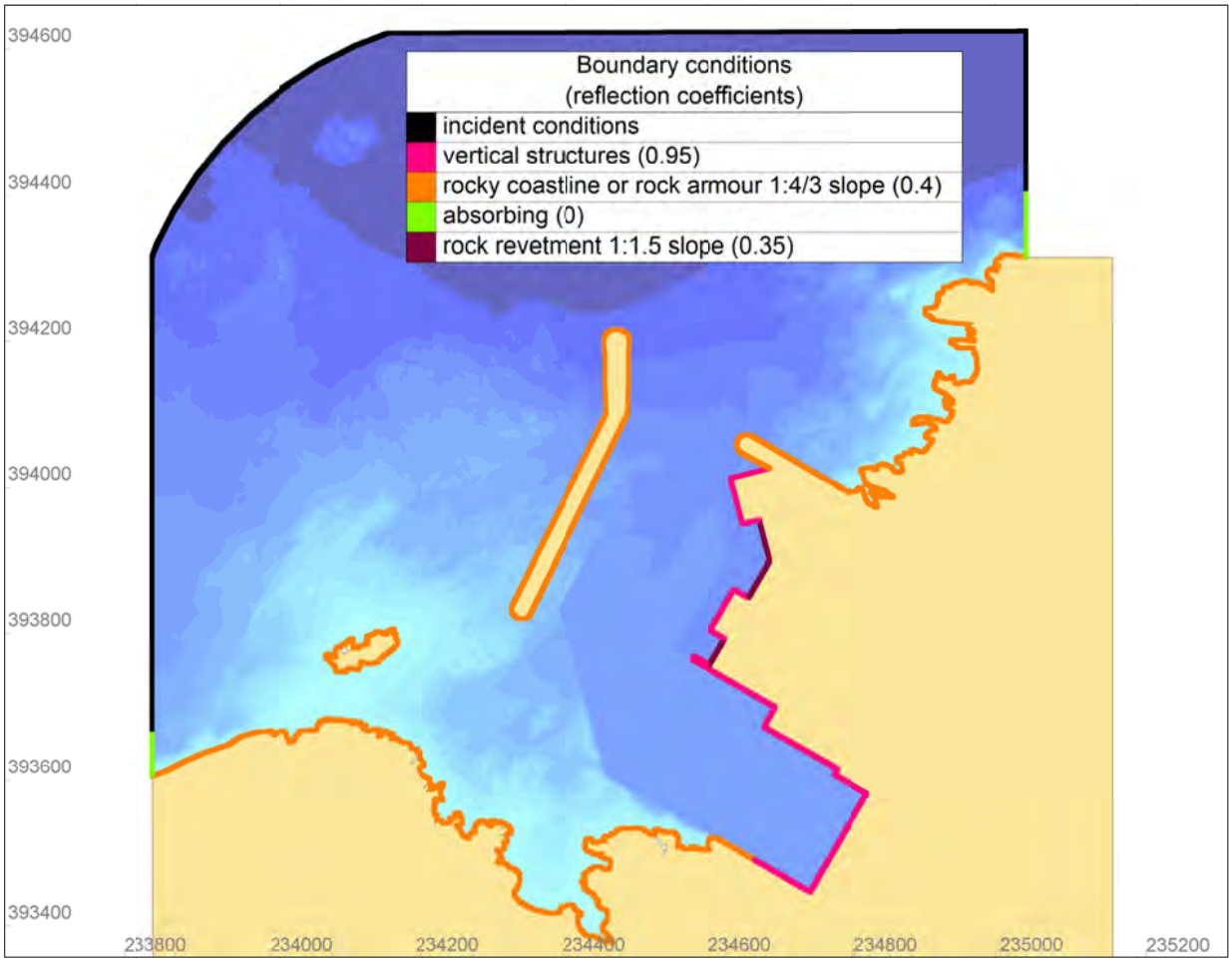

Figure 5.11: ARTEMIS model reflection coefficients and model boundaries for the fully-built layout (400m Western breakwater)

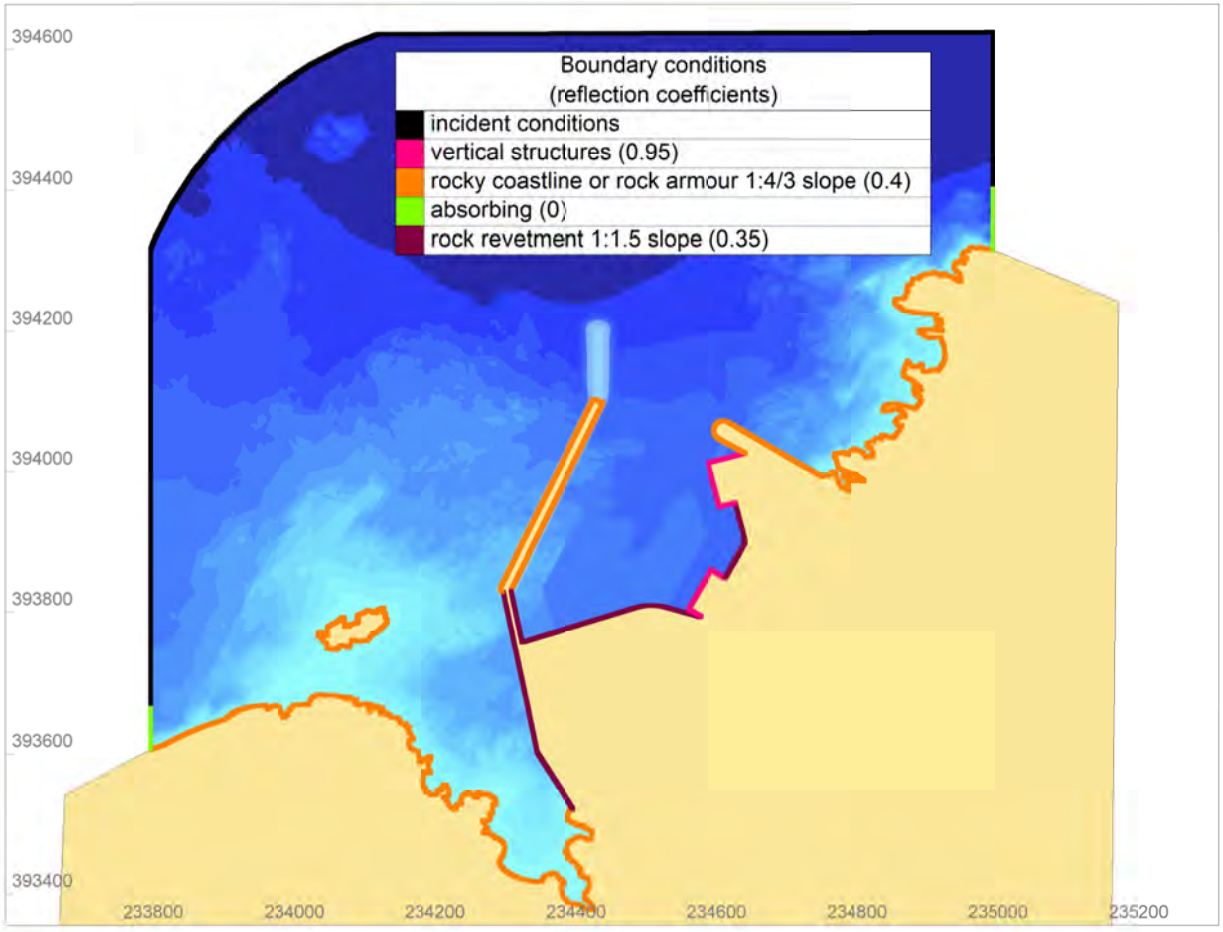

Figure 5.12: ARTEMIS model reflection coefficients and model boundaries for the part-built layout (400m Western breakwater)

5.3. Nearshore wave prediction points

Although ARTEMIS produces results across the whole model area, the greatest interest is in waves at Positions A1-A3, representative of the two MOLF quays and the cofferdam. These are shown in Figure 5.13:

- A1, the northern MOLF quay;
- A2, the southern MOLF quay;
- A3a and A3b, the cofferdam.

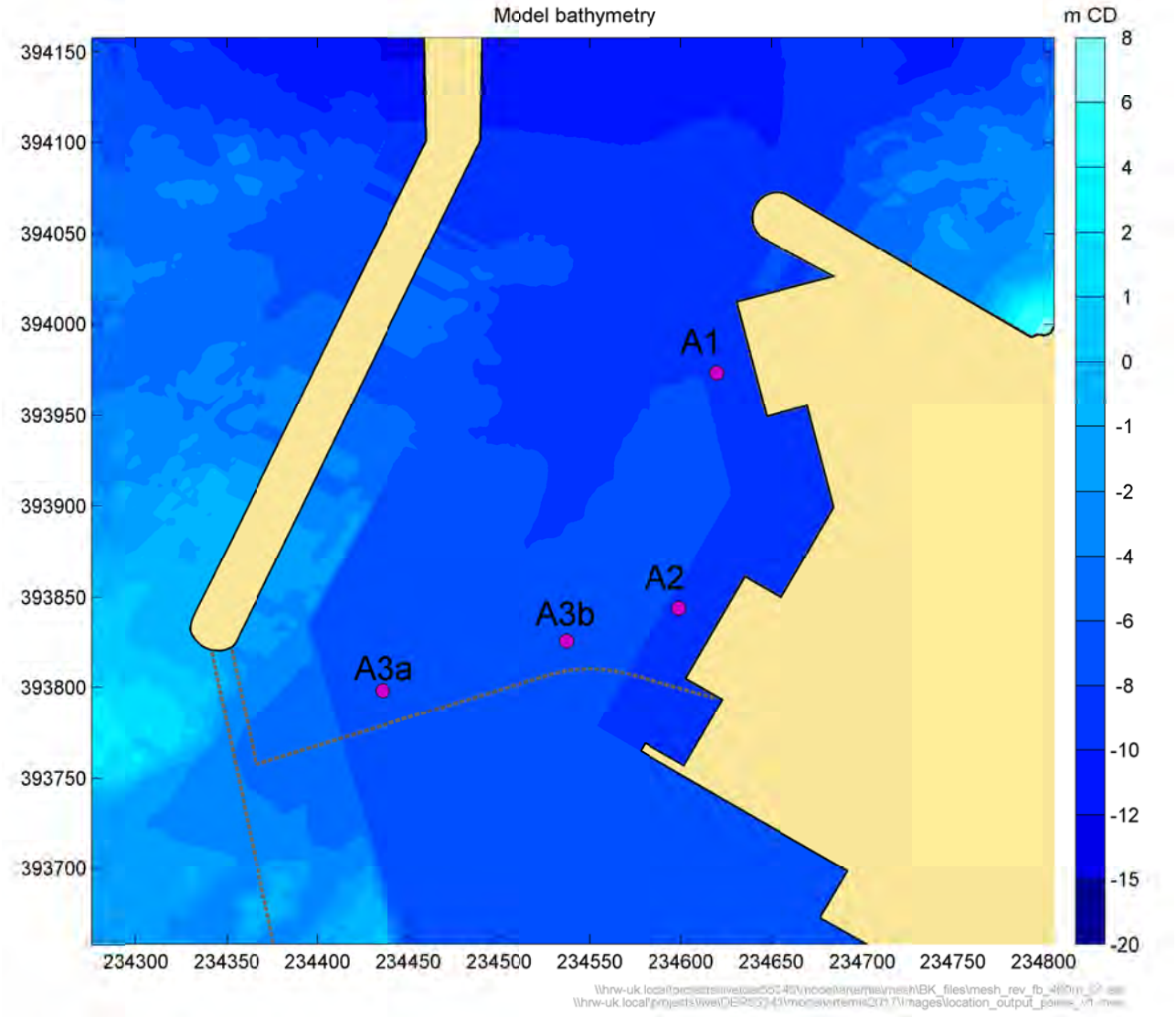

Figure 5.13: Positions at which the ARTEMIS model results are summarised

5.4. Wave extremes results

Wave and sea level conditions with joint exceedence return periods of 5, 25, 75, 200 and 1000 years on the ARTEMIS model boundary were transformed to corresponding conditions within the model area, for the harbour layouts. The list of conditions run is summarised in Table 5.2. The mean wave direction associated with the extreme runs is North, which has been selected, based on the earlier modelling, as the worst case offshore direction for wave heights within the harbour.

Table 5.2: Conditions run in the ARTEMIS model

Return Period (years)	2023 "present-day"			"2087 reasonably foreseeable"			"2187 reasonably foreseeable"			"2087 credible maximum"		
	H_s (m)	T_p (s)	Sea level (mOD)	H_s (m)	T_p (s)	Sea level (mOD)	H_s (m)	T_p (s)	Sea level (mOD)	H_s (m)	T_p (s)	Sea level (mOD)
5	4.9	9.2	2.6	5.3	9.6	3.2	5.4	9.6	4.6	5.3	9.6	4.0
5	4.6	8.9	3.1	5.0	9.3	3.7	5.1	9.3	5.1	5.0	9.3	4.8
5	3.7	8.1	3.5	4.1	8.4	4.2	4.1	8.4	5.6	4.1	8.4	5.6
5	2.9	7.1	3.8	3.1	7.4	4.4	3.2	7.4	5.9	3.2	7.4	6.0
25	5.5	9.8	2.6	6.0	10.2	3.2	6.1	10.2	4.6	6.0	10.2	4.0
25	5.3	9.6	3.1	5.8	10.0	3.7	5.8	10.0	5.1	5.8	10.0	4.8
25	4.6	8.9	3.5	5.0	9.2	4.2	5.0	9.3	5.6	5.0	9.3	5.6
25	3.3	7.6	3.9	3.6	7.8	4.5	3.6	7.9	6.0	3.6	7.9	6.1
75	5.8	10.1	2.6	6.3	10.4	3.2	6.4	10.5	4.6	6.4	10.5	4.0
75	5.6	9.9	3.1	6.1	10.3	3.7	6.2	10.4	5.1	6.2	10.3	4.8
75	5.0	9.4	3.5	5.5	9.7	4.2	5.6	9.8	5.6	5.5	9.8	5.6
75	3.6	7.9	3.9	3.9	8.2	4.6	4.0	8.3	6.0	3.9	8.2	6.2
200	6.0	10.2	2.6	6.5	10.6	3.2	6.6	10.7	4.6	6.6	10.6	4.0
200	5.9	10.1	3.1	6.4	10.5	3.7	6.5	10.6	5.1	6.4	10.5	4.8
200	5.4	9.7	3.5	5.9	10.1	4.2	6.0	10.1	5.6	5.9	10.1	5.6
200	3.9	8.2	4.0	4.2	8.5	4.6	4.3	8.6	6.1	4.2	8.5	6.2
1000	6.2	10.4	2.6	6.8	10.8	3.2	6.9	10.9	4.6	6.8	10.8	4.0
1000	6.1	10.4	3.1	6.7	10.7	3.7	6.8	10.8	5.1	6.7	10.8	4.8
1000	5.8	10.1	3.5	6.3	10.4	4.2	6.4	10.5	5.6	6.4	10.5	5.6
1000	4.1	8.5	4.1	4.5	8.8	4.7	4.6	8.9	6.1	4.5	8.8	6.3

Figure 5.14 to Figure 5.17 are example area plots of predicted significant wave heights and wave direction for the ARTEMIS model runs for the part-built and fully-built layouts, corresponding to the 1000-year wave conditions with the highest wave (first line of the 1000 year conditions in Table 5.2). Colour contours indicate significant wave height and arrows indicate mean wave direction. They highlight the variability of the predicted significant wave heights along the MOLF quays and along the cofferdam sections.

Results were extracted at the nearshore locations by averaging wave heights over circles or along a profile so as to obtain the most representative case to be used in assessing the average overtopping rate along each section of quay.

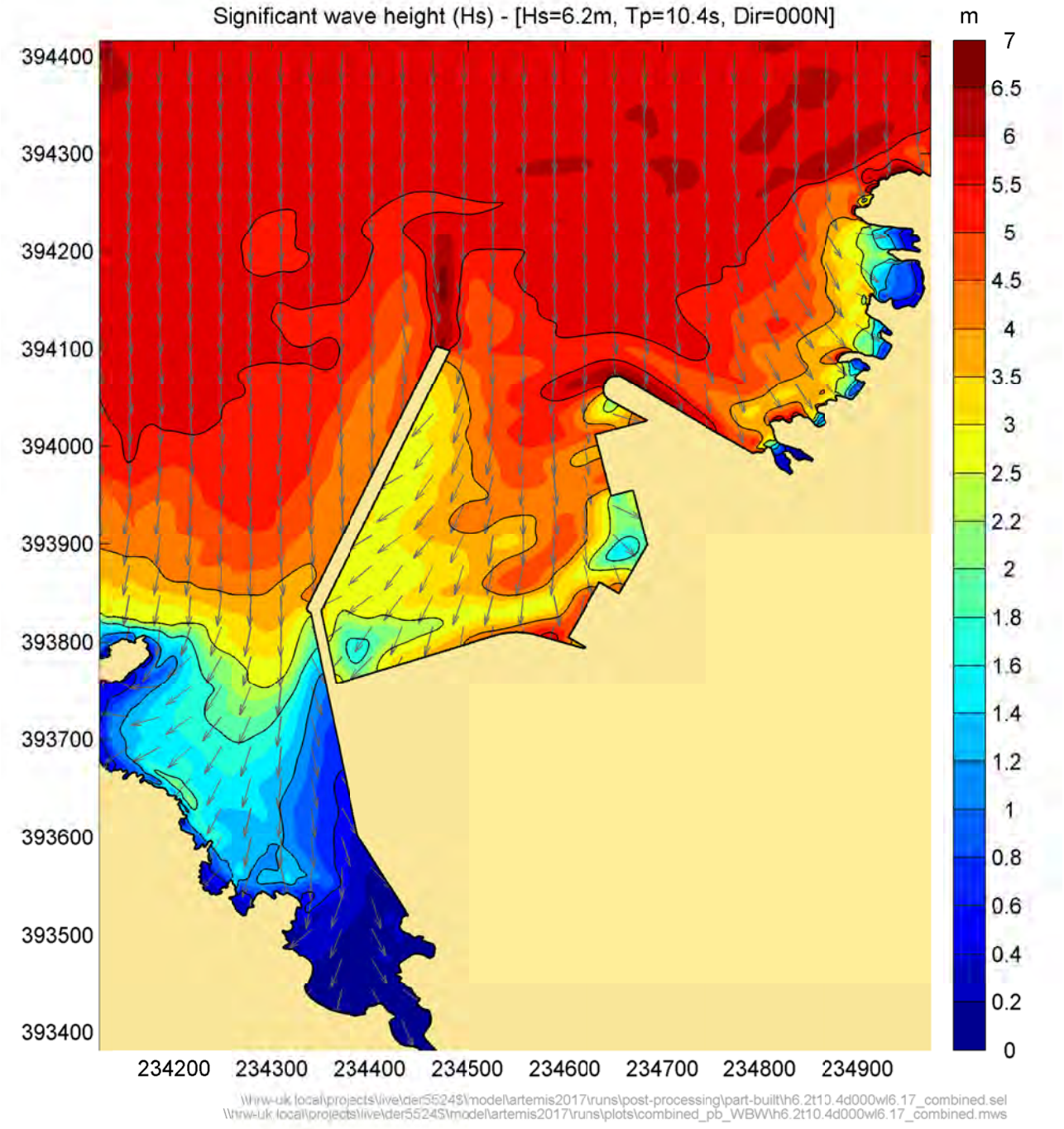

Figure 5.14: Example of predicted significant wave height and mean wave direction for the part-built layout, 1000-year present-day conditions

Source: HR Wallingford ARTEMIS modelling

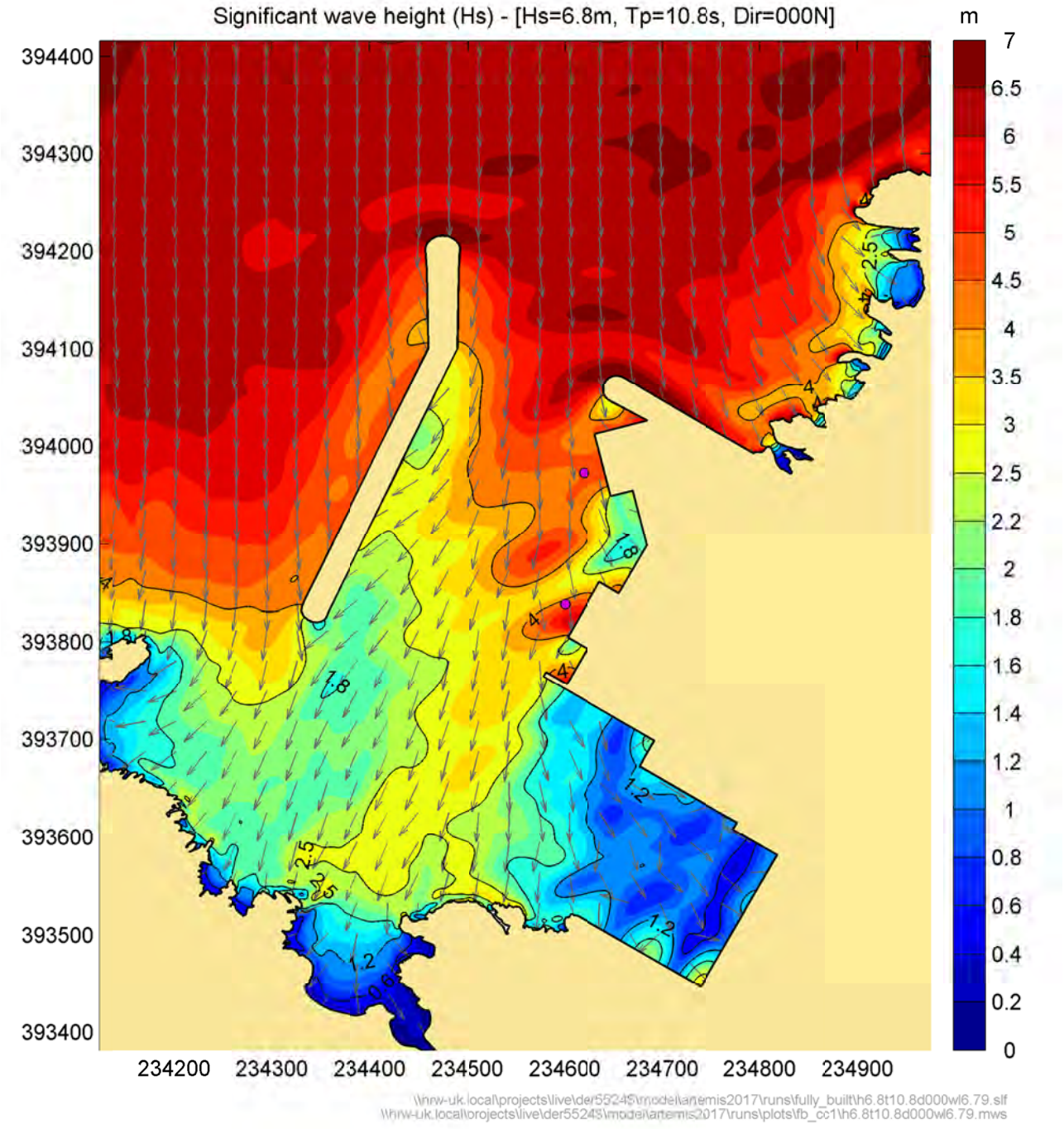

Figure 5.15: Example of predicted significant wave height and mean wave direction for the fully-built layout, 1000-year "2087 reasonably foreseeable" conditions

Source: HR Wallingford ARTEMIS modelling

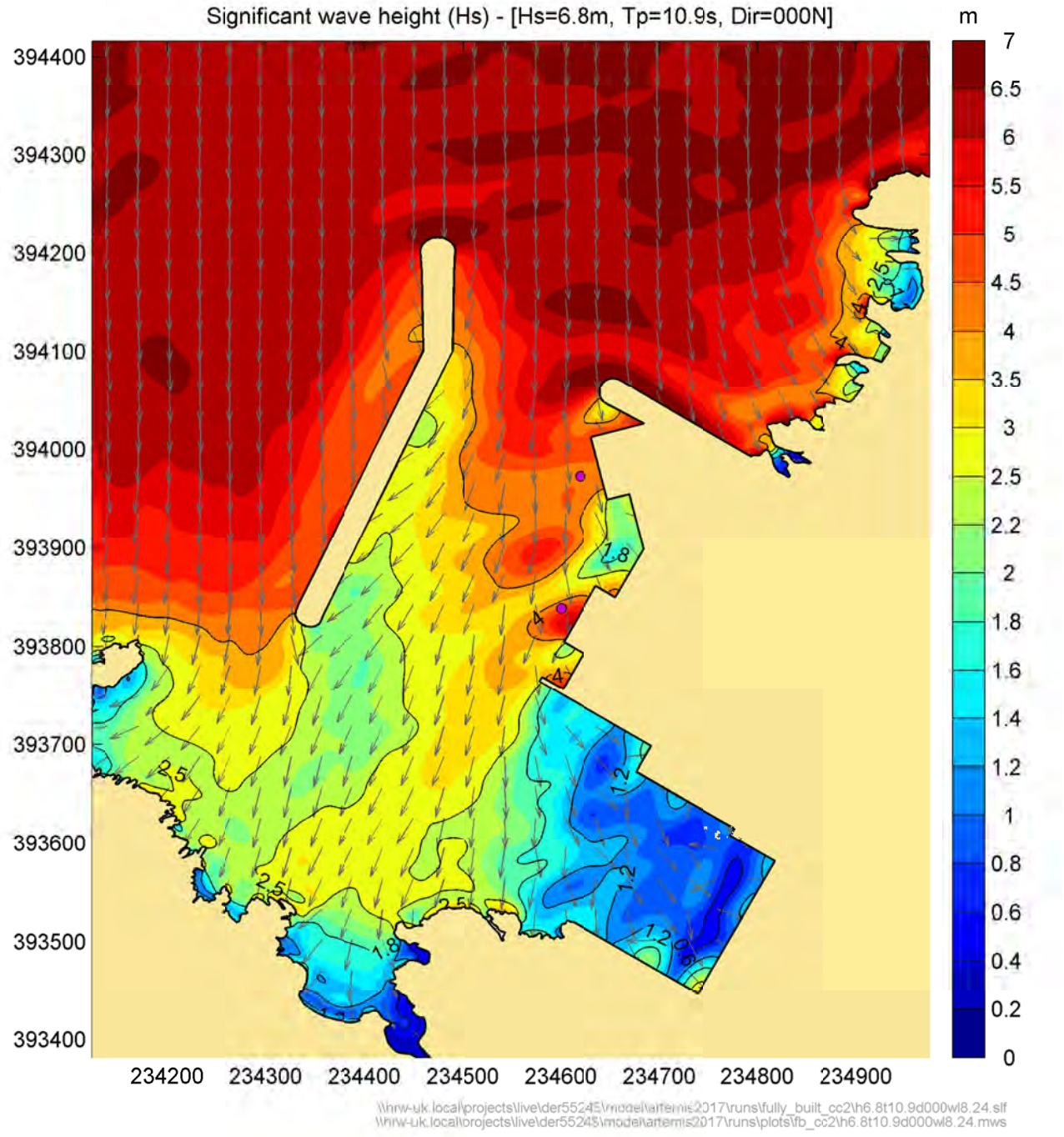

Figure 5.16: Example of predicted significant wave height and mean wave direction for the fully-built layout, 1000-year "2187 reasonably foreseeable" conditions

Source: HR Wallingford ARTEMIS modelling

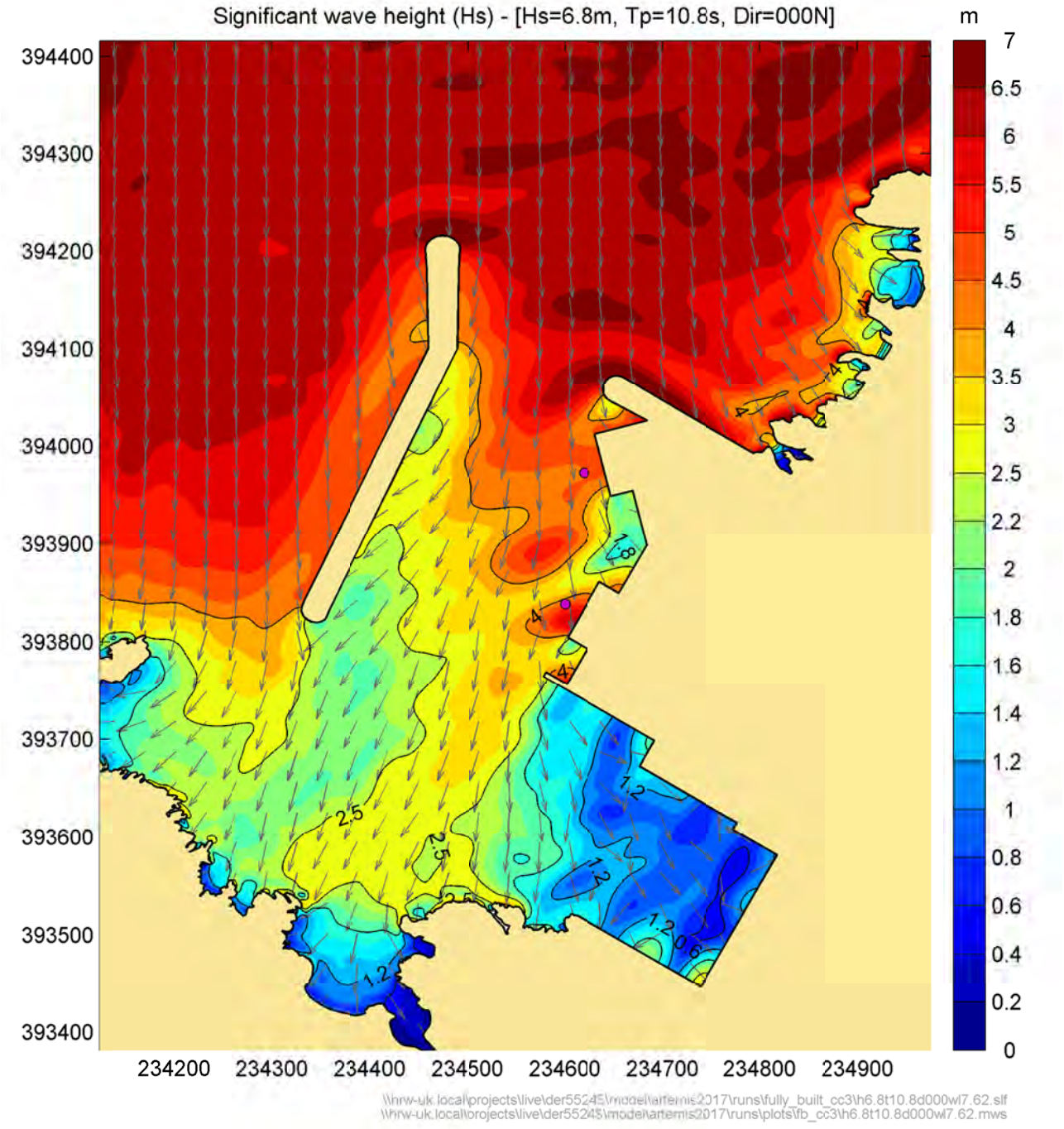

Figure 5.17: Example of predicted significant wave height and mean wave direction for the fully-built layout, 1000-year "2087 credible maximum" conditions

Source: HR Wallingford ARTEMIS modelling

5.4.1. Wave height extremes analysis

The marginal extreme wave conditions at the ARTEMIS nearshore locations are summarised in Table 5.3 to Table 5.6. The term "marginal extreme" refers to the extreme of a single variable (in this case H_s) irrespective of the value of other variables (e.g. water level). It is to distinguish between the extreme of a single variable rather than the joint probability condition.

Table 5.3 lists the "2023 present-day" extreme wave conditions for the part-built layout. Table 5.4 to Table 5.6 list the extreme wave conditions at the MOLF quays for the fully-built layout, for the "2087 reasonably foreseeable", the "2187 reasonably foreseeable" and "2087 credible maximum" scenarios.

The waves on Table 5.3 to Table 5.6 are based on the full set of runs of the ARTEMIS model from the different points along each return period joint-exceedence curve. The return periods relate to the return periods at Point P1 at the boundary of the ARTEMIS model near the entrance of the harbour.

Table 5.3: Nearshore extreme wave conditions at for the part-built layout, "2023 present-day" conditions

Return Period (years)	A1 (MOLF berth 1)		A2 (MOLF berth 2)		A3a (Cofferdam)		A3b (Cofferdam)	
	H_s (m)	T_{m-10} (s)	H_s (m)	T_{m-10} (s)	H_s (m)	T_{m-10} (s)	H_s (m)	T_{m-10} (s)
5	3.42	8.61	3.46	8.6	2.13	8.4	2.88	8.4
25	3.80	9.15	3.73	9.0	2.33	8.8	3.33	9.1
75	3.99	9.39	3.82	9.2	2.50	9.2	3.49	9.5
200	4.08	9.49	3.88	9.3	2.63	9.3	3.56	9.6
1000	4.18	9.72	3.96	9.5	2.73	9.6	3.66	9.7

Source: ARTEMIS modelling

Table 5.4: Nearshore extreme wave conditions at for the fully-built layout, "2087 reasonably foreseeable" conditions

Return Period (years)	A1 (MOLF berth 1)		A2 (MOLF berth 2)	
	H_s (m)	T_{m-10} (s)	H_s (m)	T_{m-10} (s)
5	3.42	8.9	3.26	8.8
25	3.88	9.6	3.59	9.5
75	4.06	9.8	3.81	9.7
200	4.20	10.0	3.98	10.0
1000	4.35	10.2	4.10	10.2

Source: ARTEMIS modelling

Table 5.5: Nearshore extreme wave conditions at for the fully-built layout, “2187 reasonably foreseeable” conditions

Return Period (years)	A1 (MOLF berth 1)		A2 (MOLF berth 2)	
	H_s (m)	T_{m-10} (s)	H_s (m)	T_{m-10} (s)
5	3.47	8.9	3.27	8.8
25	3.92	9.6	3.73	9.6
75	4.16	9.9	3.96	9.9
200	4.27	10.0	4.10	10.0
1000	4.40	10.2	4.22	10.2

Source: ARTEMIS modelling

Table 5.6: Nearshore extreme wave conditions at for the fully-built layout, “2087 credible maximum” conditions

RP	A1 (MOLF berth 1)		A2 (MOLF berth 2)	
	H_s (m)	T_{m-10} (s)	H_s (m)	T_{m-10} (s)
5	3.45	8.9	3.27	8.8
25	3.90	9.6	3.70	9.5
75	4.13	9.9	3.91	9.9
200	4.24	10.0	4.07	10.0
1000	4.38	10.2	4.20	10.2

Source: ARTEMIS modelling

5.4.2. Joint-probability of large waves and high sea levels

ARTEMIS results are summarised here as joint exceedence curves at the nearshore locations inside the harbour shown in Figure 5.13: A1 for the northern MOLF quay, A2 for the southern MOLF quay and A3a/b for the cofferdam.

Full sets of joint exceedence wave and sea level results are provided for the “2023 present-day” conditions for the part-built layout and for the “2087 reasonably foreseeable”, the “2187 reasonably foreseeable” and “2087 credible maximum” scenarios for the fully-built layout, including extreme wave conditions (H_s, T_{m-10}, direction) irrespective of sea level. The results are shown as joint exceedence curves in Figure 5.18 to Figure 5.21 and in Table F.1 to Table F.10 in Appendix F.

The conditions in Appendix F are the full set of results covering all joint-exceedence conditions from each return period (as plotted in Figure 5.18 to Figure 5.21). The marginal wave height extremes (i.e the univariate extreme irrespective of water level) are the conditions for each return period giving the highest wave height.

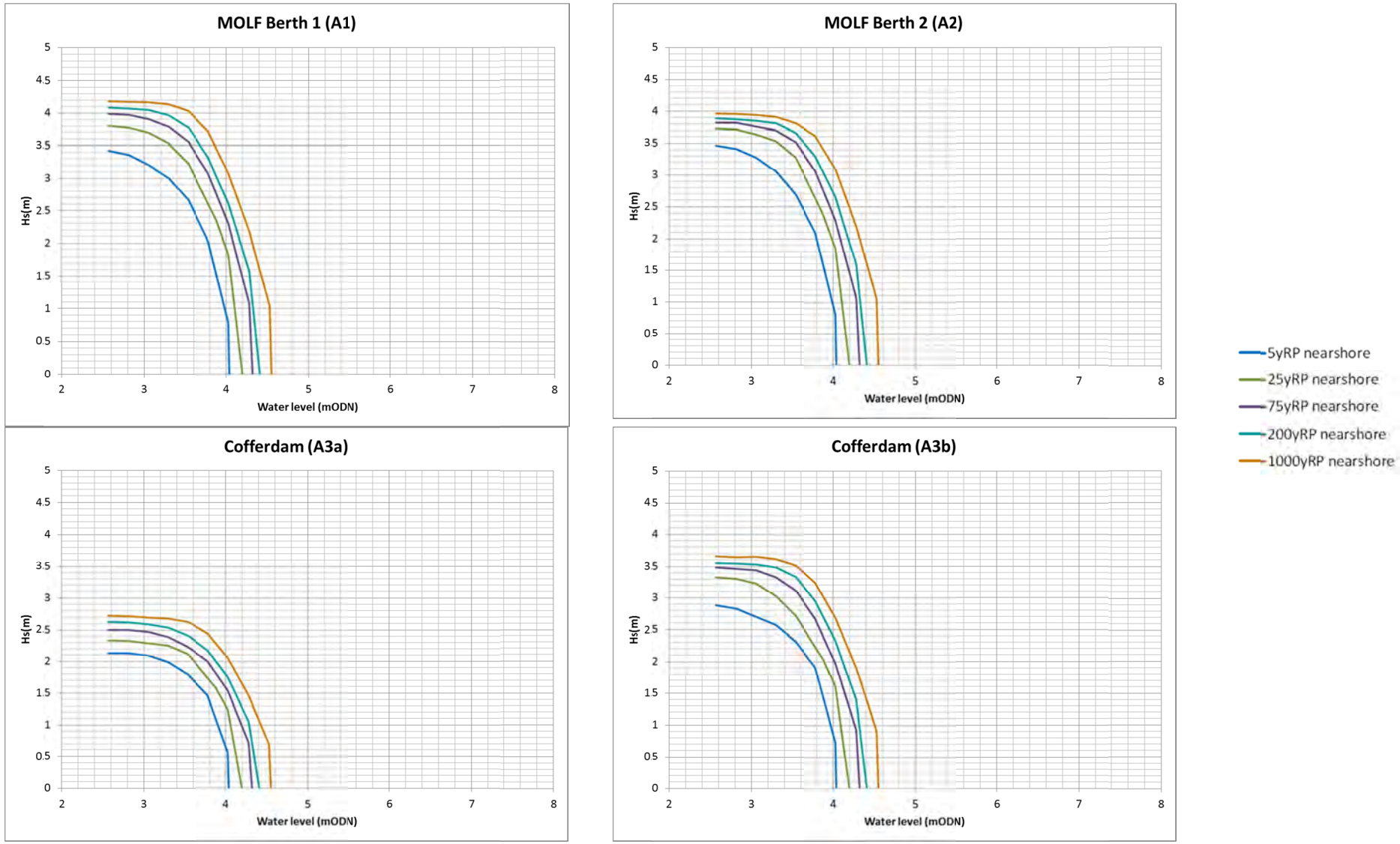

Figure 5.18: High water joint probability, MOLF and cofferdam cross-sections, part-built layout, “2023 present-day” conditions

Source: HR Wallingford analysis

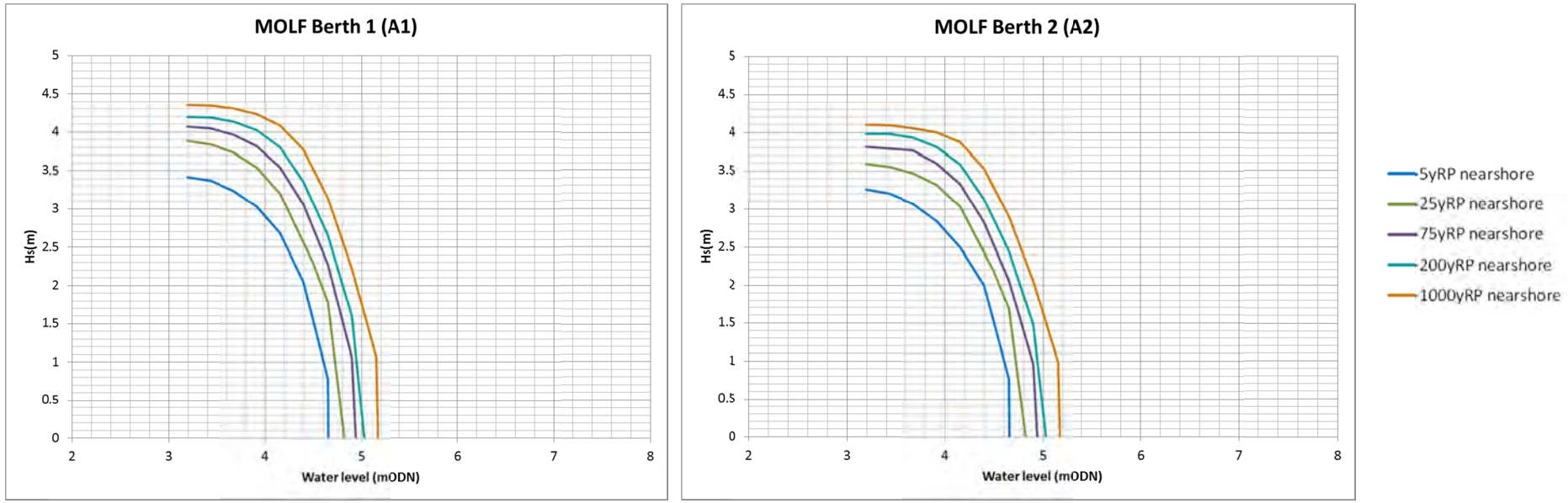

Figure 5.19: High water joint probability, MOLF and cofferdam cross-sections, fully-built layout, “2087 reasonably foreseeable” conditions

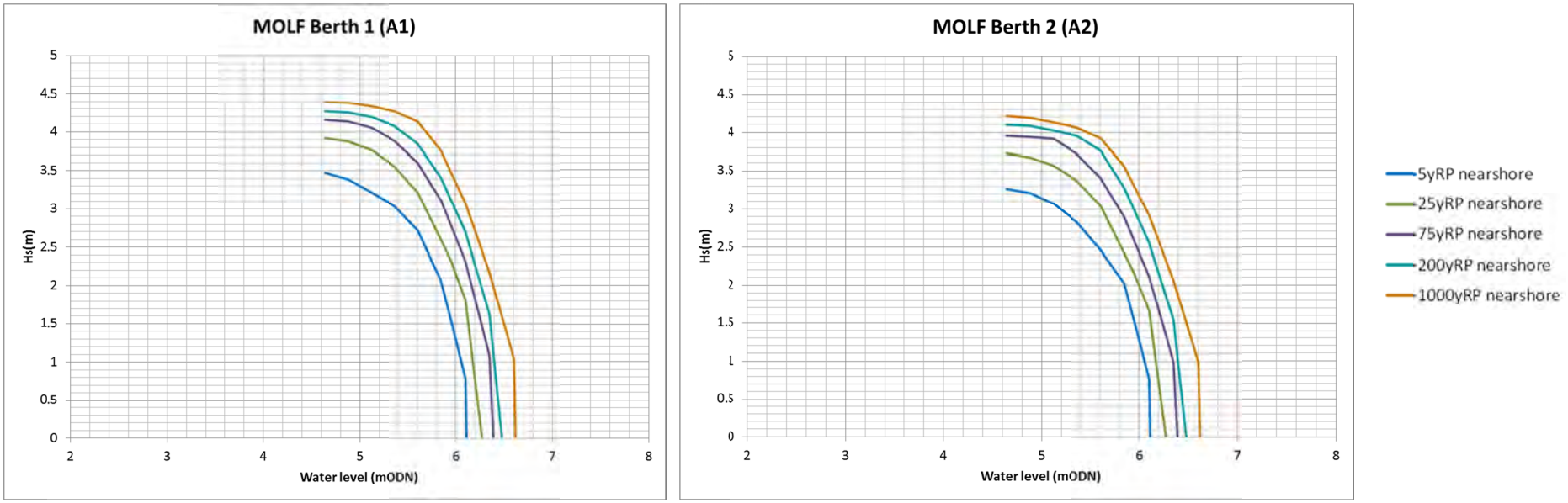

Figure 5.20: High water joint probability, MOLF and cofferdam cross-sections, fully-built layout, “2187 reasonably foreseeable” conditions

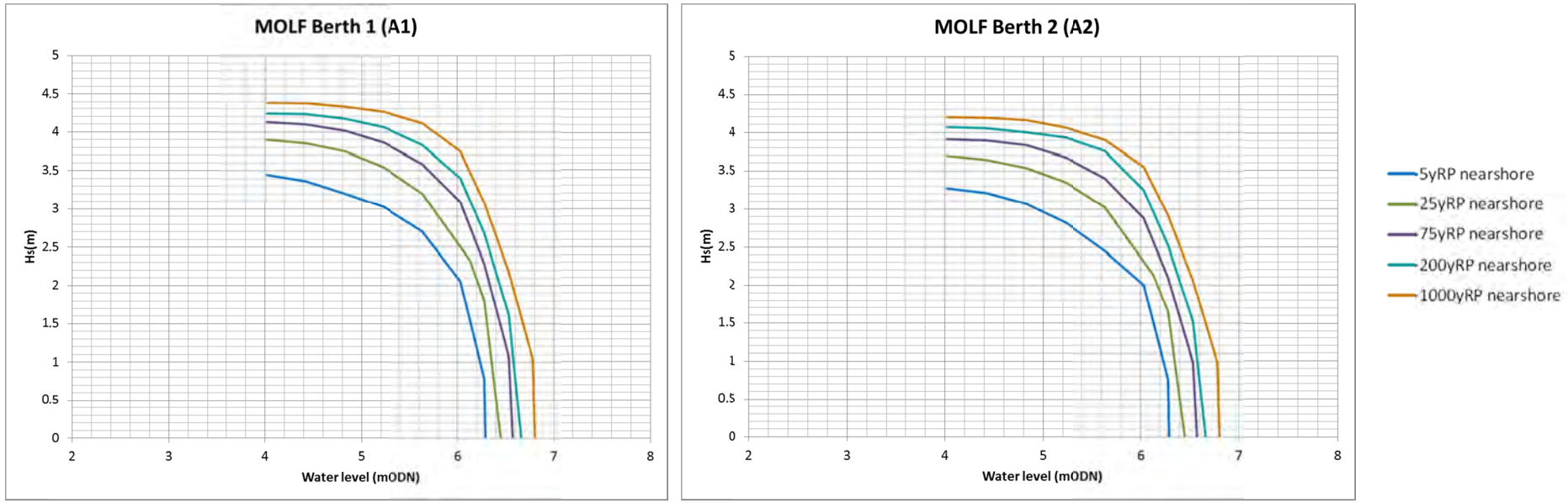

Figure 5.21: High water joint probability, MOLF and cofferdam cross-sections, fully-built layout, “2087 credible maximum” conditions

6. Overtopping rate assessment

If a wave is large enough to cross over onto the land, driven by its forward momentum, it becomes “run-up”. When run-up exceeds a structure crest level, it becomes overtopping. Overtopping magnitude is most commonly expressed as a volume (for example litres) per time (for example per second) per horizontal length (for example per metre) of structure, averaged over a period of time (for example one hour). Average overtopping rate is sensitive to wave height, wave period and the difference between the structure crest level and the still water level. It also depends on structure cross-section and roughness and on the obliquity relative to the structure of the wave attack.

Overtopping rate formulae are based on fitting curves to overtopping rates measured on structures of similar type, amongst which individual measurements might lie up to an order of magnitude outside the best estimate curves. Typically, without structure-specific measurements, the level of accuracy expected from an overtopping rate prediction is about a factor or two, although it can be higher for low rates in which only a small proportion of individual waves cause any overtopping. Peak momentary overtopping rate, possibly associated with the individual maximum wave in a sequence, can be many times greater than the average rate.

The concept of wave overtopping, and the prediction of overtopping rate, assume that the still water level (i.e. without wave action) is below the structure being overtopped. As water level increases to become close to the structure level, even to the point where the structure may be submerged even without wave action, standard overtopping rate formulae become inapplicable.

For extreme sea conditions of interest, based on the joint probability analysis results, hourly-averaged mean wave overtopping rates are estimated for points at the harbour structures and at the cofferdam.

6.1. Overtopping structure cross-sections and crest levels

6.1.1. Materials Off-Loading Facility (MOLF)

The northern MOLF quay is situated just to the south of the eastern breakwater, and faces approximately 250°N. The southern MOLF quay lies about 160m south of the northern quay, and faces approximately 300°N. The two MOLF quays and their wave prediction Positions A1 and A2 are situated as shown in Figure 5.13. For both quays, the seabed level is approximately -11.9mOD, and the overtopping rate predictions relate to water onto the +5mOD elevation platforms. Both MOLF quays are vertical block wall structures.

6.1.2. Cofferdam

Although the cofferdam would no longer be present in the fully-built layout, wave overtopping is of interest prior to its removal. The cofferdam cross-section is shown in Figure 6.1, and its wave prediction Positions A3a and A3b in Figure 5.13. The seaward-facing slope of the cofferdam is a rough 1:1.5 slope. The representative toe level for the cofferdam is taken as -10.0mOD, corresponding to the bed level at Position A3b within the ARTEMIS model. Overtopping rate predictions relate to water onto the +5mOD elevation crest of the cofferdam. Only the part-built layout and the 2023 scenario are relevant (as the cofferdam would be present only during construction).

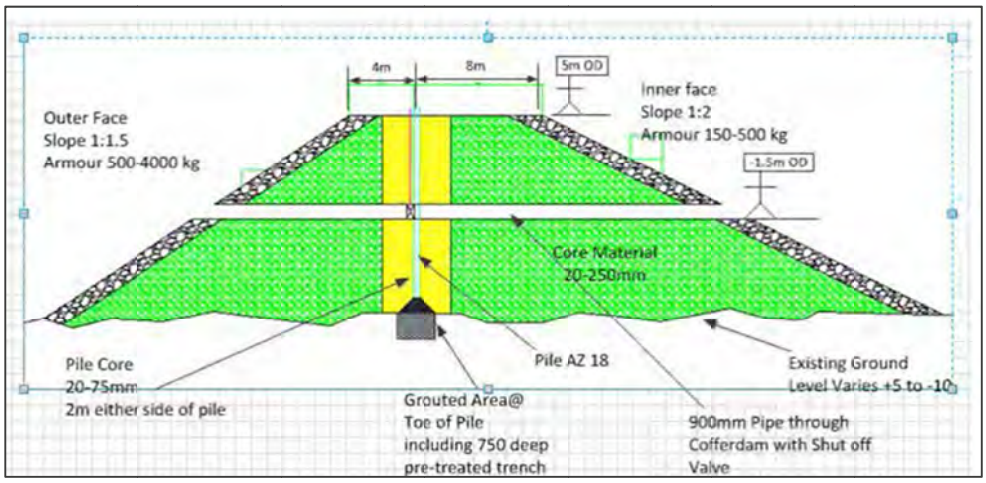

Figure 6.1: Typical cross-section for the cofferdam

Source: Diagram assembled by Horizon Nuclear Power to illustrate the cofferdam cross-section

6.2. Calculation methods

Overtopping rate (q) is estimated for the MOLF quays and for the cofferdam, for a small number of combinations of large waves and high sea levels, for each return period and climate changed scenario of interest, using the industry standard methods described in EurOtop (Pullen et al., 2007). The obliquity of the waves has been accounted for in the calculations, assuming 45° obliquity at the MOLF and 0° at the cofferdam.

Freeboard is the structure crest elevation above the still (that is without wave action) water level. For structures designed to keep overtopping to a minimum, even during extreme conditions, freeboard would be a positive value of order the same value as the largest wave heights. For structures designed to provide some protection from wave action, where high overtopping may be tolerated, freeboard may take only a small positive value, or even a negative value (meaning the structure crest is submerged).

Where the freeboard is greater than 10% of the significant wave height, standard wave overtopping formulae are used, for vertical walls for the MOLF quays, and for steep embankments for the cofferdam. Where the freeboard is a negative value greater than 30% of the incident significant wave height, the wave action causes minimal additional overtopping, on top of the continuous flow associated with inundation, and so a weiring type formula is used. Between these two limits, linear interpolation based on sea level is applied.

All calculations of overtopping and flow rate assume, effectively, that there is a dry pit behind the structure into which the overtopping water will flow (as in the case of the cofferdam). In practice, for the example where the MOLF quays are completely submerged and surrounded by water, the nett flow may be minimal.

6.3. Estimated overtopping rates at the MOLF quays

Unless breaching occurs, each overtopping “event” would persist only over a high tide, therefore with a maximum duration of, say, 3 hours, with peak overtopping occurring at high tide. Main results are in the form of spot values at high tide during an event, associated with each of the overtopping cross-sections

introduced in Section 6.1. The overtopping rate was calculated for each of the joint probability wave and water level combinations tabulated in Appendix F for the relevant scenarios. For each joint return period, the results listed in Table 6.1 relate to the joint exceedence wave and sea level condition that produces the highest overtopping at each of the MOLF quays, for the present-day 2023 case. The following parameters are given:

- the wave condition, in terms of height and period averaged over a three-hour duration, at the ARTEMIS wave prediction Point A1 or A2;
- the associated extreme sea level, in terms of high-tide peak level;
- mean (averaged over a period of, say, one hour) overtopping rate onto the structure, expressed as a volume of water per second per metre run of structure.

Table 6.1: Peak values of mean overtopping rate, for waves and sea levels with joint exceedence return periods of 5, 25, 75, 200 and 1000 years, for the MOLF quay crest levels of 5mOD, for the present-day 2023 case

Return period (years)	Northern MOLF quay				Southern MOLF quay			
	Worst case sea condition, ARTEMIS Point A1			Mean o/t rate (l/s/m)	Worst case sea condition, ARTEMIS Point A2			Mean o/t rate (l/s/m)
	H_s(s)	T_{m-10} (s)	s/l (mOD)		H_s(s)	T_{m-10} (s)	s/l (mOD)	
5	3.00	8.0	3.30	158	3.27	8.2	3.05	168
25	3.53	8.7	3.30	249	3.53	8.6	3.30	249
75	3.79	9.1	3.30	300	3.52	8.6	3.54	292
200	3.77	9.0	3.54	348	3.66	8.8	3.54	323
1000	4.03	9.4	3.54	410	3.62	8.6	3.78	371

Source: Table entries show, for each return period, the joint exceedence sea condition at the ARTEMIS Points A1 and A2 causing the highest overtopping rate: "peak" in the table title refers to conditions at high tide; "mean" in the table title refers to overtopping rate averaged over about one hour; the unit for overtopping rate is litres per second per metre horizontal distance.

Note: The accuracy of the overtopping calculations justifies only one significant figure, however as the values are being used in later calculations, in this and similar tables, more significant figures are shown.

Table 6.2 to Table 6.4 show the corresponding mean overtopping rate estimations at the peak of the tide for the reasonably foreseeable to 2087, the reasonably foreseeable to 2187, and the credible maximum to 2087 scenarios, respectively. Note that for the reasonably foreseeable to 2187, and the credible maximum to 2087 scenarios, most of the joint-exceedence wave and water level combinations are conditions where the MOLF quays would be under water (when the sea level is above the quay level) and are therefore not used in the calculations. Under these circumstances the whole MOLF platform at 5.0mOD level would be flooded by the still water level alone.

Table 6.2: Peak values of mean overtopping rate, for waves and sea levels with joint exceedence return periods of 5, 25, 75, 200 and 1000 years, for the MOLF quay crest levels of 5.0mOD, for the reasonably foreseeable 2087 climate-changed scenario

Return period (years)	Northern MOLF quay				Southern MOLF quay			
	Worst case sea condition, ARTEMIS Point A1			Mean o/t rate (l/s/m)	Worst case sea condition, ARTEMIS Point A2			Mean o/t rate (l/s/m)
	H_s(s)	T_{m-10} (s)	s/l (mOD)		H_s(s)	T_{m-10} (s)	s/l (mOD)	
5	3.03	8.3	3.92	270	2.84	8.2	3.92	232
25	3.54	9.1	3.92	388	3.32	9.0	3.92	334
75	3.54	9.0	4.16	461	3.33	8.9	4.16	404
200	3.80	9.5	4.16	533	3.59	9.4	4.16	473
1000	3.77	9.2	4.4	617	3.87	9.8	4.16	555

Source: Table entries show, for each return period, the joint exceedence sea condition at the ARTEMIS Points A1 and A2 causing the highest overtopping rate: "peak" in the table title refers to conditions at high tide; "mean" in the table title refers to overtopping rate averaged over about one hour; the unit for overtopping rate is litres per second per metre horizontal distance.

Table 6.3: Peak values of mean overtopping rate, for waves and sea levels with joint exceedence return periods of 5, 25, 75, 200 and 1000 years, for the MOLF quay crest levels of 5.0mOD, for the reasonably foreseeable 2187 climate-changed scenario

Return period (years)	Northern MOLF quay				Southern MOLF quay			
	Worst case sea condition, ARTEMIS Point A1			Mean o/t rate (l/s/m)	Worst case sea condition, ARTEMIS Point A2			Mean o/t rate (l/s/m)
	H_s(s)	T_{m-10} (s)	s/l (mOD)		H_s(s)	T_{m-10} (s)	s/l (mOD)	
5	3.30	8.7	5.00	1077	3.14	8.6	5.00	1000
25	3.82	9.5	5.00	1341	3.63	9.4	5.00	1239
75	4.09	9.8	5.00	1487	3.93	9.9	5.00	1399
200	4.22	10.0	5.00	1558	4.06	10.0	5.00	1466
1000	4.36	10.1	5.00	1634	4.16	10.1	5.00	1523

Source: Table entries show, for each return period, the joint exceedence sea condition at the ARTEMIS Points A1 and A2 causing the highest overtopping rate: "peak" in the table title refers to conditions at high tide; "mean" in the table title refers to overtopping rate averaged over about one hour; the unit for overtopping rate is litres per second per metre horizontal distance.

Table 6.4: Peak values of mean overtopping rate, for waves and sea levels with joint exceedence return periods of 5, 25, 75, 200 and 1000 years, for the MOLF quay crest levels of 5.0mOD, for the 2087 credible maximum climate-changed scenario

Return period (years)	Northern MOLF quay				Southern MOLF quay			
	Worst case sea condition, ARTEMIS Point A1			Mean o/t rate (l/s/m)	Worst case sea condition, ARTEMIS Point A2			Mean o/t rate (l/s/m)
	H_s(s)	T_{m-10} (s)	s/l (mOD)		H_s(s)	T_{m-10} (s)	s/l (mOD)	
5	3.13	8.5	5.00	993	3.01	8.5	5.00	936
25	3.71	9.4	5.00	1281	3.50	9.3	5.00	1174
75	3.98	9.7	5.00	1425	3.80	9.7	5.00	1332
200	4.15	9.9	5.00	1519	3.98	9.9	5.00	1424
1000	4.31	10.1	5.00	1608	4.14	10.1	5.00	1513

Source: Table entries show, for each return period, the joint exceedence sea condition at the ARTEMIS Points A1 and A2 causing the highest overtopping rate: "peak" in the table title refers to conditions at high tide; "mean" in the table title refers to overtopping rate averaged over about one hour; the unit for overtopping rate is litres per second per metre horizontal distance.

6.4. Estimated overtopping rates at the cofferdam

Results are presented initially in the same form as those for the MOLF quays. Table 6.5 shows the mean overtopping rate predictions at the peak of the tide for three positions along the cofferdam, for the part-built layout, for the 2023 scenario only, for the present design structure crest level of 5.0mOD.

Table 6.5: Peak values of mean overtopping rate, for waves and sea levels with joint exceedence return periods of 5, 25, 75, 200 and 1000 years, for the cofferdam, for the present-day (2023) scenario, also showing sensitivity to the cofferdam crest level

Structure	Return period (years)	Worst case sea condition, ARTEMIS point			Mean overtopping rate (l/s/m)
		H_s(s)	T_{m-10} (s)	s/l (mOD)	
West cofferdam, ARTEMIS Point A3a	5	1.99	7.8	3.30	5
	25	2.12	8.1	3.54	14
	75	2.39	8.8	3.30	21
	200	2.41	8.8	3.54	36
	1000	2.63	9.3	3.54	64
Middle cofferdam, ARTEMIS Point A3b	5	2.57	7.9	3.30	36
	25	3.23	8.9	3.05	108
	75	3.33	9.0	3.30	182
	200	3.34	9.0	3.54	258
	1000	3.52	9.4	3.54	340
East cofferdam,	5	3.27	8.2	3.05	117
	25	3.53	8.6	3.30	252

Structure	Return period	Worst case sea condition, ARTEMIS point			Mean overtopping
ARTEMIS Point A2	75	3.52	8.6	3.54	339
	200	3.66	8.8	3.54	415
	1000	3.81	9.2	3.54	505

Source: Table entries show, for each return period, the joint exceedence sea condition at the relevant ARTEMIS point causing the highest overtopping rate: "peak" in the table title refers to conditions at high tide; "mean" in the table title refers to overtopping rate averaged over about one hour; the unit for overtopping rate is litres per second per metre horizontal distance.

The overtopping rates are higher than would be acceptable for a permanent embankment, particularly at the eastern end of the cofferdam, and some damage may occur even during the 5 year return period conditions. It is possible, therefore, that the cofferdam crest level will need to be raised, at least along parts of its length. For illustrative purposes, Table 6.6 shows the mean overtopping rate predictions at the peak of the tide for the eastern part of the cofferdam, again for the part-built layout and the 2023 scenario only, for alternative structure crest levels of 6 and 7mOD. (For convenience the results for the 5.0mOD crest level, copied from Table 6.5, are also listed in Table 6.6.)

Table 6.6: Peak values of mean overtopping rate, for waves and sea levels with joint exceedence return periods of 5, 25, 75, 200 and 1000 years, for the eastern part of the cofferdam, for the present-day (2023) scenario, illustrating sensitivity to the cofferdam crest level

Structure	Return period (years)	Worst case condition, ARTEMIS Point A2			Mean overtopping rate (l/s/m)
		H_s(s)	T_{m-10} (s)	s/l (mOD)	
Cofferdam crest level +5mOD (from Table 6.5)	5	3.27	8.2	3.05	117
	25	3.53	8.6	3.30	252
	75	3.52	8.6	3.54	339
	200	3.66	8.8	3.54	415
	1000	3.81	9.2	3.54	505
Sensitivity tests					
Cofferdam crest level +6mOD	5	3.27	8.2	3.05	29
	25	3.53	8.6	3.30	69
	75	3.70	8.9	3.30	93
	200	3.66	8.8	3.54	118
	1000	3.81	9.2	3.54	151
Cofferdam crest level +7mOD	5	3.41	8.5	2.81	7
	25	3.53	8.6	3.30	19
	75	3.70	8.9	3.30	27
	200	3.81	9.1	3.30	34
	1000	3.81	9.2	3.54	45

Source: Table entries show, for each return period, the joint exceedence sea condition causing the highest overtopping rate: "peak" in the table title refers to conditions at high tide; "mean" in the table title refers to overtopping rate averaged over about one hour; the unit for overtopping rate is litres per second per metre horizontal distance.

6.5. Variation over time and overtopping volume within a single flood event at the cofferdam

Thus far, the extreme sea levels and joint extreme sea levels with waves have focussed on the peak levels during a marine flood event. Actually, the flood risk would vary during an event, both with tidal level over the course of a few hours, and wave by wave. In order to represent this variation in a fairly simple way, for example for use as boundary conditions to inundation modelling, the following approach is applied to sample overtopping rate results.

Assume that the event will last only a few hours, over the peak of a tide (and by inference assuming that the flood water would have cleared by the time of the next high tide, making it a separate "event").

Assume that the derived extreme wave condition is of 3-hour duration (as it is in the offshore source data) and that it occurs at high tide (already an assumption in the approach adopted for the joint probability analysis).

Assume that surge occurring at high tide (not necessarily the peak surge, which may occur away from high tide) persists for the same three hours.

That leaves only the astronomical tide to be adjusted. To a reasonable approximation, as the site has a fairly high tidal range, tidal variation will approximately follow a sine wave, with an amplitude somewhere between Mean High Water Springs at Cemaes Bay (for lower return period sea levels) and Highest Astronomical Tide at Cemaes Bay (for higher return period sea levels). These two sine waves are plotted in Figure 6.2, showing sea level in metres relative to its peak level, as a function of time from a few hours before high tide to a few hours after high tide.

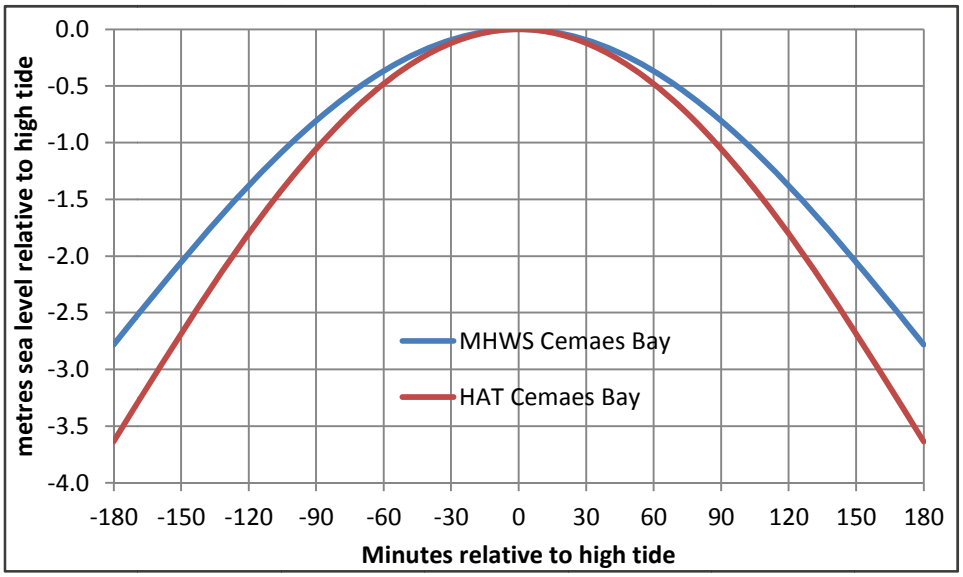

Figure 6.2: Example estimations of time variation of sea level during a marine flood event, based on MHWS and HAT at Cemaes Bay

This variation is then applied to the peak extreme sea level for an event, continuing the time (before and after the peak) until the water level is no longer of interest. The MHWS curve would be more conservative (giving a lower rate of change of sea level with time) but the HAT curve may be more realistic for high return period extreme events.

Consider the peak overtopping rates in Table 6.5 and Table 6.6 estimated for a 5-year joint exceedence return period at the cofferdam, idealised as shown in Figure 6.3.

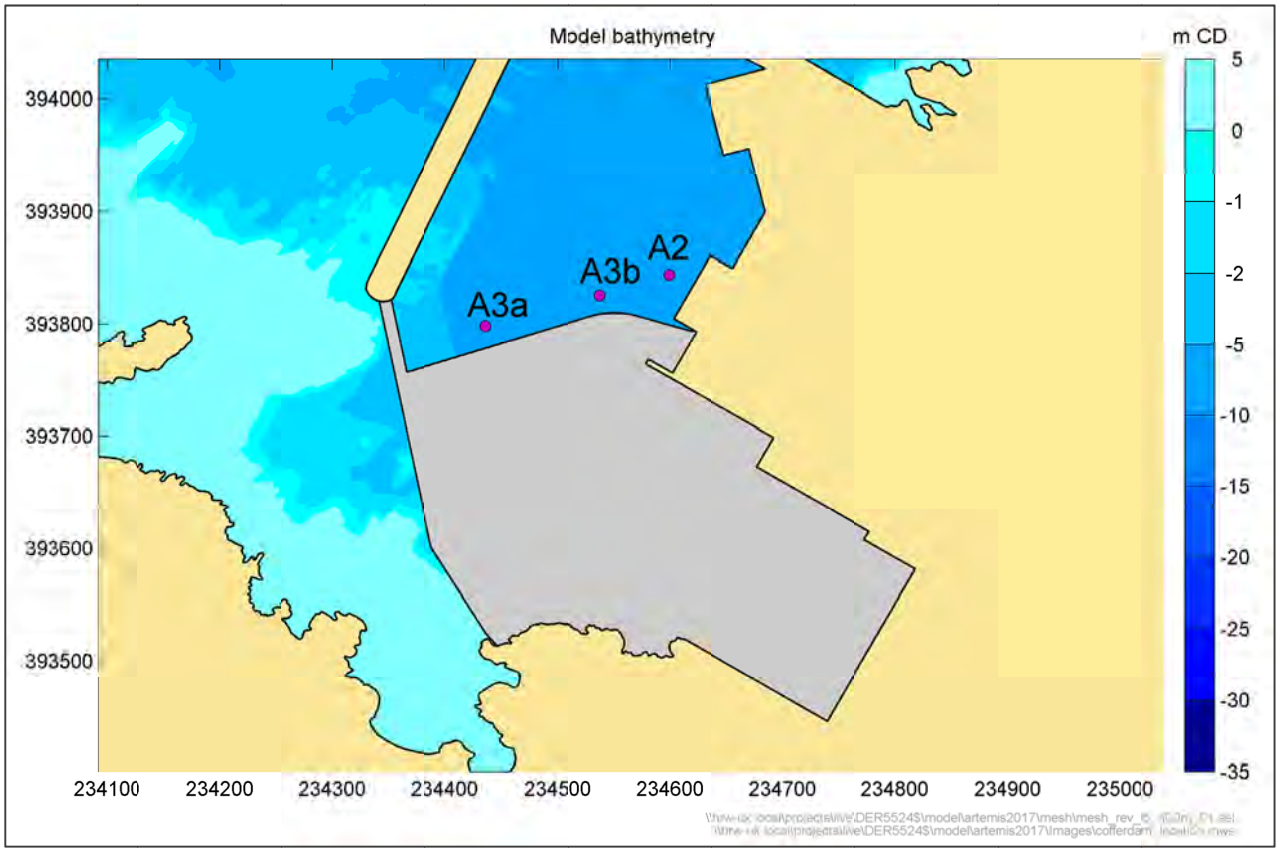

Figure 6.3: The cofferdam, the ARTEMIS model wave prediction points and the dry area protected

The rates are higher for the east part of the cofferdam than for the west and middle parts. The events represented here are based upon the sea conditions causing the greatest overtopping over the east part of the cofferdam (the 5-year return period rows in Table 6.6), matched in Table 6.7 with the wave conditions *during the same event* at the west and middle parts. Applying the MHWS curve in Figure 6.2 to the peak sea level, re-calculating the mean overtopping rate at 15-minute intervals through the tide, and summing the volumes from three hours before high tide to three hours after high tide, gives the through-tide overtopping rates listed in Table 6.7 (in units of metres cubed per high tide per metre run of wall). Assuming these rates to apply along 130, 75 and 65m lengths of the cofferdam (and that no additional overtopping comes from the southern MOLF quay) gives the through-tide overtopping volumes listed in Table 6.7 (in units of metres cubed per high tide). Spreading these volumes equally over the approximately 420m by 210m area enclosed by the cofferdams, and assuming the area to be flat to complete this illustrative calculation, gives the average through-tide flood depths listed in Table 6.7. Finally, the bottom row of Table 6.7 sums the component flood depths to give the estimated average flood depths in the otherwise dry area protected by the cofferdam, for structure crest levels of 5, 6 and 7mOD.

Table 6.7: Overtopping of the cofferdam during the 5-year return period event, for the part-built layout and present-day 2023 conditions

	Crest level 5.0mOD, sea level 3.05mOD	Crest level 6.0mOD, sea level 3.05mOD	Crest level 7.0mOD, sea level 2.81mOD
West cofferdam, ARTEMIS Point A3a, assumed 130m length			
H_s(s)	2.09	2.09	2.13
T_{m-10} (s)	8.11	8.11	8.29
Peak o/t rate (l/s/m)	4.6	0.51	0.04
Through tide o/t rate (m^3/tide/m)	33	3.7	0.3
Through tide volume (m^3/tide/130m)	4303	479	39
Depth in cofferdam dry area (m)	0.05	0.01	0.00
Middle cofferdam, ARTEMIS Point A3b, assumed 75m length			
H_s(s)	2.70	2.82	2.82
T_{m-10} (s)	8.20	8.36	8.36
Peak o/t rate (l/s/m)	33	8.9	1.18
Through tide o/t rate (m^3/tide/m)	271	75	10
Through tide volume (m^3/tide/75m)	20288	5613	742
Depth in cofferdam dry area (m)	0.23	0.06	0.01
East cofferdam, ARTEMIS Point A2, assumed 65m length			
H_s(s)	3.27	3.27	3.41
T_{m-10} (s)	8.25	8.25	8.46
Peak o/t rate (l/s/m)	117	29	7.4
Through tide o/t rate (m^3/tide/m)	1061	260	68
Through tide volume (m^3/tide/65m)	68961	16902	4417
Depth in cofferdam dry area (m)	0.78	0.19	0.05
Accumulated average depth (m) of water behind the cofferdam, through tide			
	1.06	**0.26**	**0.06**

Note: In places, figures are given to an unrealistic level of precision to facilitate tracing of the calculations.

7. References

Allsop, N.W.H. (1990). Reflection performance of rock armoured slopes in random waves. International Conference on Coastal Engineering, Delft.

Amec Foster Wheeler Environment & Infrastructure UK Ltd (Amec, 2015). Wylfa Newydd: Nuclear safety, meteorological and hydrological hazards assessment (NSMHHA). Amec Foster Wheeler Environment & Infrastructure report 200383-000-000-RPT-0003 to Horizon Nuclear Power, dated 31 July 2015.

Booij, N., Ris, R.C. and Holthuijsen, L.H. (1999). A third-generation wave model for coastal regions: 1. Model description and validation. Journal of Geophysical Research, Vol. 104, pp7649-7666, dated 15 April 1999.

Camus, P., Mendez, F.J., Medina, R., Tomas, A. and Izaguirre, C. (2013). High resolution downscaled ocean waves (dow) reanalysis in coastal areas. Coastal Engineering, 72(0): 56-68.

Environment Agency (2011). Coastal flood boundary conditions for UK mainland and islands: Project SC060064/R2: Design sea levels. Environment Agency research report.

Environment Agency (2016). Investigating coastal flood forecasting: Good practice framework. Environment Agency Report SC140007.

Gouldby, B., Mendez, F., Guanche, Y., Rueda, A. and Minguez, R. (2014). A methodology for deriving extreme nearshore sea conditions for structural design and flood risk analysis. Elsevier, Coastal Engineering.

HR Wallingford (2009). Wave transmission through structures, Report, IT582, 2009.

HR Wallingford (2013). Wylfa, Anglesey: Proposed new nuclear power plant: Marine study report. HR Wallingford report EBR5141-RT003-R03-00 to Amec, dated 13 December 2013.

HR Wallingford (2015). Wylfa Newydd: Further wave modelling, Phase 1. HR Wallingford Report DER5524-RT001-R01-00 to Amec FW, dated 18 December 2015.

HR Wallingford (2015b). State of the Nation Flood Risk Analysis: SWAN 2D calibration reports. HR Wallingford Report MCR5289-RT012 series, May 2015.

Huseby et al (2013). A new approach to environmental contours for ocean engineering applications based on direct Monte Carlo simulations. Ocean Engineering 60:124–135, March 2013.

Pullen, T., Allsop, N.W.H., Bruce, T., Kortenhaus, A., Schuttrumpf, H. & van der Meer J.W. (2007). EurOtop: Wave overtopping of sea defences and related structures: Assessment manual. *(www.overtopping-manual.com).*

United Kingdom Climate Impacts Programme (UKCIP, 2009). UK climate projections: Marine & coastal projections. United Kingdom Climate Impacts Programme report, ISBN 978 1 906360 04 7, 2009.

Welsh government (2016). Flood consequence assessments: Climate change allowances.

Appendices

A. Construction design and management regulations (CDM, 2015)

The Construction (Design and Management) Regulations 2015 (CDM 2015) require a designer to avoid foreseeable risks to those involved in construction and future use of the structure, and in doing so, they should eliminate hazards (so far as is reasonably practicable, taking into account other design considerations) and reduce and control risks associated with those hazards which remain. It is essential that, where required to do so, a principal designer and principal contractor are appointed to fulfil their respective duties under the CDM 2015. It is also essential to highlight and record the impacts of the works on health, safety and welfare which should feed into the Health and Safety File (if required). Further details of the requirements of CDM 2015 can be found on:

http://www.hse.gov.uk/construction/cdm/2015/index.htm

This project comprises modelling and desk study elements which may ultimately be used by others in the design process. No design work, as defined in the CDM 2015, has been undertaken by HR Wallingford. It is assumed that the appointed principal designer will review the information produced in this study when discharging his duties under the CDM 2015.

B. The SWAN wave transformation model

HR Wallingford
Working with water

The SWAN wave transformation model

1. Introduction

SWAN is a computational spectral wave transformation model. It can be used to obtain realistic estimates of wave parameters in coastal areas, lakes and estuaries from given wind, seabed, and current conditions. The model has been developed by the Technical University of Delft (TU Delft).

SWAN is based on a fully spectral representation of the wave action balance equation (or energy balance in the absence of currents) with all physical processes modelled explicitly. No a priori limitations are imposed on the spectral evolution. This makes SWAN (Simulating WAves Nearshore) a third-generation wave model.

The model has been used successfully at numerous sites around the UK and in other parts of the world. It is designed to represent the following wave propagation processes:

- refraction due to spatial variations in seabed and current,
- shoaling due to spatial variations in seabed and current,
- blocking and reflections by opposing currents,
- transmission through, blockage by or reflection from obstacles (such as coastlines or breakwaters).

The following wave generation and dissipation processes are also represented in SWAN:

- generation by wind,
- dissipation by whitecapping,
- dissipation by depth-induced wave breaking,
- dissipation by seabed friction,
- wave-wave interactions (quadruplets and triads),
- obstacles.

Diffraction is not represented in SWAN, so the model should not be used in areas where variations in wave height are large within a horizontal scale of a few wavelengths. Because of this, the wave field computed by SWAN will generally not be accurate in the immediate vicinity of obstacles.

The SWAN wave model has been conceived to be a computationally feasible third-generation spectral wave model for waves in shallow water (including the surf zone) with ambient currents.

2. The SWAN wave model

The SWAN model represents the waves in terms of the two-dimensional wave action density spectrum $N(\sigma,\vartheta)$, even when nonlinear phenomena dominate (e.g., in the surf zone). The independent variables are the relative frequency σ (as observed in a frame of reference moving with the action propagation velocity) and the wave direction ϑ (the direction normal to the wave crest of each spectral component). The action density is equal to the energy density divided by the relative frequency: $N(\sigma,\vartheta) = E(\sigma,\vartheta)/\sigma$.

In SWAN the two-dimensional wave action density spectrum may vary in time and space. Its evolution is described by the spectral action balance equation, which for Cartesian coordinates is (e.g. Hasselmann et al., 1973):

$$\frac{\partial}{\partial t}N+\frac{\partial}{\partial x}C_x N+\frac{\partial}{\partial y}C_y N+\frac{\partial}{\partial \sigma}C_\sigma N+\frac{\partial}{\partial \vartheta}C_\vartheta N=\frac{S(\sigma,\vartheta)}{\sigma} \quad (1)$$

The first term in the left-hand side represents the local rate of change of action density in time. The second and third term represent propagation of action in geographical $x-$ and $y-$space (with propagation velocities C_x and C_y respectively). The fourth term represents shifting of the relative frequency due to variations in depths and currents in time (with propagation velocity C_σ in $\sigma-$space). The fifth term represents propagation of action in $\vartheta-$space (depth-induced and current-induced refraction) with propagation velocity C_ϑ. The expressions for these propagation speeds are taken from linear wave theory. The term $S(\sigma,\vartheta)$ at the right hand side of the action balance equation is the source term representing the effects of generation, dissipation and non-linear wave-wave interactions.

The formulations for the generation, the dissipation and the quadruplet wave-wave interactions are taken from the WAM model (WAM Cycle3, WAMDI group, 1988, and optionally WAM Cycle4, Komen et al., 1994). These are supplemented with a spectral version of the dissipation model for depth-induced breaking of Battjes and Janssen (1978) and a more recently formulated discrete interaction approximation for the triad wave-wave interactions (Eldeberky and Battjes, 1995).

Transfer of wind energy to the waves

The transfer of wind energy to the waves is described in SWAN with a resonance mechanism (Phillips, 1957) and a feed-back mechanism (Miles, 1957). The corresponding source term for these mechanisms is commonly described as the sum of linear and exponential growth:

$$S_{in}(\sigma,\vartheta)=A+B\times E(\sigma,\vartheta) \quad (2)$$

in which A and B depend on wave frequency and direction, and wind speed and direction. The effects of currents are accounted for in SWAN by using the apparent local wind speed and direction. The expression for the term A is due to Cavaleri and Malanotte-Rizzoli (1981, revised by Tolman, 1992). Two optional expressions for the coefficient B are used in the model. The first is due to Snyder et al. (1981), re-scaled in terms of friction velocity by Komen et al. (1984). The second expression is due to Janssen (1991) and accounts explicitly for the interaction between the wind and the waves by considering atmospheric boundary layer effects and the roughness length of the sea surface.

Whitecapping

Whitecapping is primarily controlled by the steepness of the waves. In presently operating third-generation wave models (including SWAN) the whitecapping formulations are based on a pulse-based model (Hasselmann, 1974), as adapted by the WAMDI group (1988):

$$S_{ds,w}(\sigma,\vartheta)=-\Gamma\tilde{\sigma}\frac{\tilde{k}}{\tilde{k}}E(\sigma,\vartheta) \quad (3)$$

where Γ is a steepness dependent coefficient, k is wave number and $\tilde{\sigma}$ and $\tilde{k}$ denote a mean frequency and a mean wave number, respectively (cf. the WAMDI group, 1988). The value of Γ depends on the wind input formulation that is used. Since two expressions are used for the wind input in SWAN, two values for Γ are used. The first is due to Komen et al. (1984), and is used in SWAN when the wind input coefficient of Komen et al. (1984) is used. The second expression is an adaptation of this expression based on Janssen (1991). It is used when the wind input term of Janssen (1991) is used.

Depth-induced dissipation

Depth induced-dissipation may be caused by seabed friction, by seabed motion, by percolation or by back-scattering on seabed irregularities. For continental shelf seas with sandy seabeds, the dominant mechanism appears to be seabed friction, which can generally be represented as:

$$S_{ds,b}(\sigma,\vartheta) = -c_{bed}\frac{\sigma^2}{g^2\,\sinh^2(kd)}E(\sigma,\vartheta) \qquad (4)$$

in which c_{bed} is a seabed friction coefficient. A large number of models has been proposed. Hasselmann et al. (JONSWAP, 1973) suggested use of an empirically obtained constant. This seems to perform well in many different conditions as long as a suitable value is chosen (typically different for swell and wind sea; Bouws and Komen, 1983). A nonlinear formulation based on drag has been proposed by Hasselmann and Collins (1968), which was later simplified by Collins (1972), and is also implemented in SWAN. More complicated, eddy viscosity models have been developed by Madsen et al. (1988). The effect of a mean current on the wave energy dissipation due to seabed friction is not taken into account in SWAN.

Depth-induced wave breaking

Although the process of depth-induced wave breaking is still poorly understood and little is known about its spectral modelling, the total dissipation (i.e. integrated over the spectrum) can be well modelled with the dissipation of a bore applied to the breaking waves in a random field. And laboratory observations show that the shape of initially uni-modal spectra propagating across simple (barred) beach profiles is fairly insensitive to depth-induced breaking. This has led Eldeberky and Battjes (1995) to formulate a spectral version of the bore model of Battjes and Janssen (1978) which conserves the spectral shape. Their expression has been expanded in the SWAN model to include direction:

$$S_{ds,br}(\sigma\vartheta) = \frac{D_{tot}}{E_{tot}}E(\sigma(\vartheta) \qquad (5)$$

in which E_{tot} is the total wave energy and D_{tot} (which is negative) is the rate of dissipation of the total energy due to wave breaking according to Battjes and Janssen (1978). The value of D_{tot} depends critically on the breaking parameter $\gamma = H_{\max}/d$ (in which $H_{\max}$ is the maximum possible individual wave height in the local water depth d). In SWAN γ has a constant value (default is 0.73 corresponding to the mean value of the data set of Battjes and Stive, 1985).

Wave transmission

SWAN can estimate wave transmission through a structure such as a breakwater. Since obstacles usually have a plan area that is too small to be resolved by the bathymetric grid, in SWAN, an obstacle is modelled as a line. The transmission coefficient is defined as the ratio of the (significant) wave height at the downwave side of the breakwater over the (significant) wave height at the upwave side. If the crest of the

breakwater is such that waves can pass over, the transmission coefficient is taken from Goda et al. (1967) and is expressed as a function of wave height and freeboard (difference in crest level and water level).

Note that a change in wave frequency is to be expected as well as a change in wave height, since often the process above the breakwater is highly non-linear. But given the little information available, SWAN assumes that the frequencies remain unchanged over an obstacle (only the energy scale of the spectrum is affected and not the spectral shape).

Nonlinear wave-wave interactions

In deep water, quadruplet wave-wave interactions dominate the evolution of the spectrum. They transfer wave energy from the spectral peak to lower frequencies (thus moving the peak frequency to lower values) and to higher frequencies (where the energy is dissipated by whitecapping). In very shallow water, triad wave-wave interactions transfer energy from lower frequencies to higher frequencies often resulting in higher harmonics (Beji and Battjes, 1993; low-frequency energy generation by triad wave-wave interactions is not considered here).

A full computation of the **quadruplet wave-wave interactions** is extremely time consuming and not convenient in any operational wave model. A number of techniques, based on parametric methods or other types of approximations have been proposed to improve computational speed. In SWAN the computations are carried out with the Discrete Interaction Approximation (DIA) of Hasselmann et al. (1985). Eldeberky and Battjes (1995) introduced a discrete triad approximation (DTA) for co-linear waves, obtained by considering only the dominant self-self **triad interactions**. Their model has been verified with flume observations of long-crested, random waves breaking over a submerged bar (Beji and Battjes, 1993) and over a barred beach (Arcilla et al., 1994). A slightly different version, the Lumped Triad Approximation (LTA) was later derived by Eldeberky (1996) and is used in SWAN.

Cycle III of SWAN is stationary and optionally non-stationary, formulated in Cartesian (recommended only for small scales) or spherical (small scales and large scales) coordinates. The stationary mode should be used only for waves with a relatively short residence time in the computational area under consideration (i.e. small travel time of the waves through the region compared to the time scale of the geophysical conditions: wave boundary conditions, wind, tides and storm surge). A quasi-stationary approach can be taken with stationary SWAN computations in a time-varying sequence of stationary conditions.

The current version of SWAN can be used on any scale relevant for wind generated surface gravity waves, as the model now uses more accurate numerical propagation schemes and can compute on spherical co-ordinates (longitude, latitude), allowing calculations in laboratory situations, coastal regions, shelf seas and oceans. However, SWAN is specifically developed for coastal applications, which would usually not require such flexibility in scale. And it must be emphasized that on oceanic scales SWAN is certainly less efficient on oceanic scales than WAVEWATCH III and probably also less efficient than WAM.

Fully implicit numerical schemes are used in the SWAN model for propagation in both geographic and spectral spaces (an iterative, forward-marching, four-sweep technique due to Ris et al., 1994). This scheme is unconditionally stable in contrast with the explicit schemes of conventional spectral wave models.

HR Wallingford
Working with water

Typical results

1. Colour contour plots of significant wave height, H_s, and vector plots of mean wave direction over the model area.
2. Tables of H_s, T_z, T_p and mean direction at a selection of inshore locations. For example the model can be used to investigate which offshore wave conditions lead to the worst inshore wave heights at a particular site.
3. SWAN also calculates fields of wave-induced forces per unit surface area, wave orbital velocities, and a variety of other parameters. Such results can be used directly as input into a sediment transport model.
4. 2D (frequency and direction) spectrum at a selection of inshore location. Information of this type would normally be required as input to a numerical harbour model or a mathematical model of beach processes. In addition this information would also be needed at the wave paddle positions in a physical model in order to generate the correct random wave sequence for design studies.

References

Battjes, J.A. and J.P.F.M. Janssen, 1978: Energy loss and set-up due to breaking of random waves, *Proc. 16 th Int. Conf. Coastal Engineerin*g, ASCE, 569-587.

Booij, N., L.H. Holthuijsen and R.C. Ris, 1996, The "SWAN" wave model for shallow water, *Proc. 25th Int. Conf. Coastal Engineering.,* Orlando, pp. 668-676.

Collins, J.I., 1972: Prediction of shallow water spectra, *J. Geophys. Re*s., 77, No. 15, 2693-2707.

Eldeberky, Y., 1996: Nonlinear transformation of wave spectra in the nearshore zone, *Ph.D. thesi*s, Delft University of Technology, Department of Civil Engineering, The Netherlands.

Eldeberky, Y. and J.A. Battjes, 1995: Parameterization of triad interactions in wave energy models, *Proc. Coastal Dynamics Conf. '9*5, Gdansk, Poland, 140-148.

Goda, Y, H. Takeda and Y. Moriya, 1967: Laboratory investigation of wave transmission over breakwater*s, Rep. port and Harbour Res. Ins*t., 13 (from Seelig, 1979).

Hasselmann, K., T.P. Barnett, E. Bouws, H. Carlson, D.E. Cartwright, K. Enke, J.A. Ewing, H. Gienapp, D.E. Hasselmann, P. Kruseman, A. Meerburg, P. Müller, D.J. Olbers, K. Richter, W. Sell and H. Walden, 1973: Measurements of wind-wave growth and swell decay during the Joint North Sea Wave Project (JONSWAP), *Dtsch. Hydrogr.* Z. Suppl., 12, A8.

Hasselmann, S., K. Hasselmann, J.H. Allender and T.P. Barnett, 1985: Computations and parameterizations of the nonlinear energy transfer in a gravity wave spectrum. Part II: Parameterizations of the nonlinear transfer for application in wave models, *J. Phys. Oceanogr*., 15, 11, 1378-1391.

Janssen, P.A.E.M., 1991: Quasi-linear theory of wind-wave generation applied to wave forecasting, *J. Phys. Oceanogr*., 21, 1631-1642.

Komen, G.J., S. Hasselmann, and K. Hasselmann, 1984: On the existence of a fully developed wind-sea spectrum, *J. Phys. Oceanogr*., 14, 1271-1285.

Komen, G.J., Cavaleri, L., Donelan, M., Hasselmann, K., Hasselmann, S. and P.A.E.M. Janssen, 1994: *Dynamics and Modelling of Ocean Wave*s, Cambridge University Press, 532 p.

Madsen, O.S., Y.-K. Poon and H.C. Graber, 1988: Spectral wave attenuation by seabed friction: Theory, *Proc. 21 th Int. Conf. Coastal Engineerin*g, ASCE, 492-504.

Ris, R.C., N. Booij and L.H. Holthuijsen, 1999, A third-generation wave model for coastal regions, Part II: Verification, *J.Geoph.Research,* 104, C4, 7667-7681.

Tolman, H.J., 1992: Effects of numerics on the physics in a third-generation wind-wave model, *J. Phys. Oceanog*r., 22, 10, 1095-1111.

WAMDI group, 1988: The WAM model - a third generation ocean wave prediction model, *J. Phys. Oceanog*r., 18, 1775-1810.

C. Nearshore wave climates (present-day conditions)

The wave modelling underlying these wave climates was undertaken at actual sea levels appropriate to each record, with no mark up of offshore wave and wind conditions beyond that determined during the wave model calibration, and no allowance for uncertainty. Present-day wave roses and frequency tables are presented for the nearshore output locations (see Figure 4.4) for the baseline, part-built and fully-built layouts. Note that Point 9 is not provided for the part-built and fully-built layouts as a local phase-resolving wave disturbance model is required for modelling inside the harbour.

Seasonal (summer and winter) wave climates are presented for Points 2, 3, 4 and 6. Frequency tables (annual and seasonal) are also provided at the nearshore points in digital format.

Occurrence is in parts per hundred thousand in all frequency tables.

C.1. Annual conditions

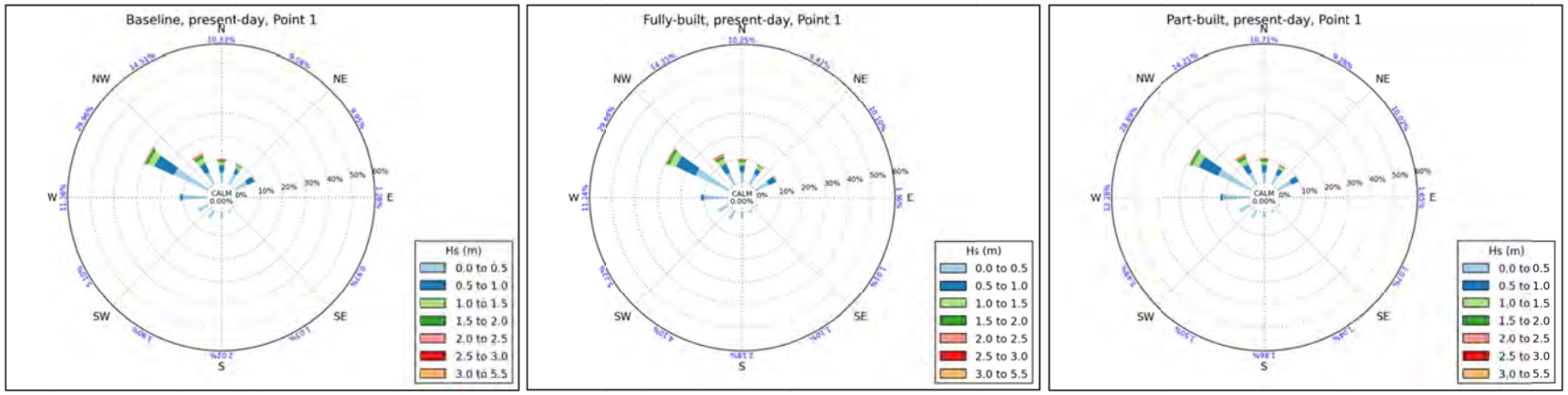

Figure C.1: Annual wave roses for nearshore prediction Point 1, present-day, baseline, part-built and fully-built layouts

Source: HR Wallingford, SWAN wave transformation and Met Office WW3 offshore data, 1980-2015

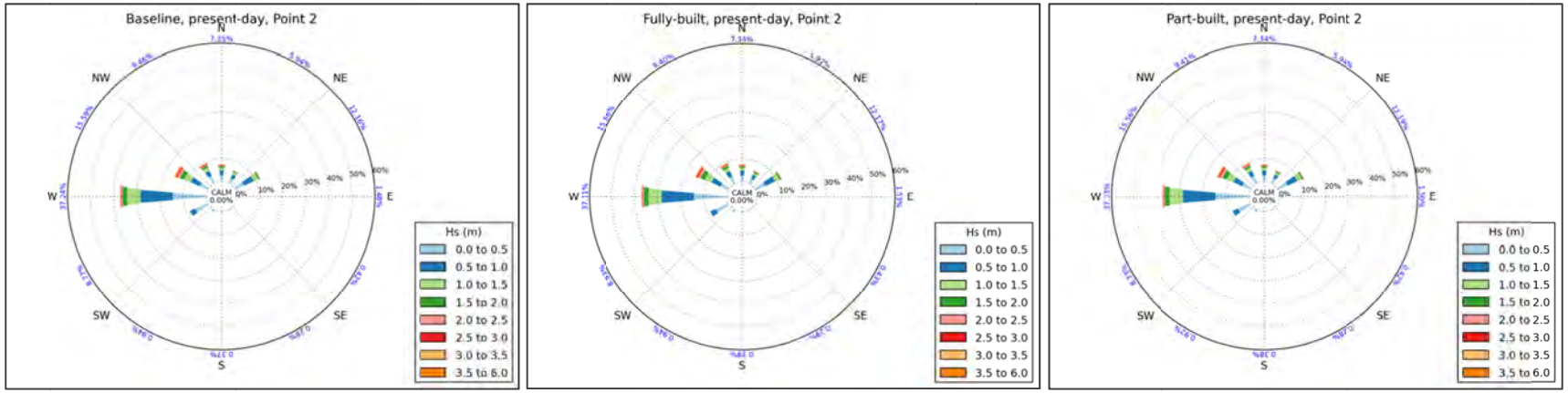

Figure C.2: Annual wave roses for nearshore prediction Point 2, present-day, baseline, part-built and fully-built layouts

Source: HR Wallingford, SWAN wave transformation and Met Office WW3 offshore data, 1980-2015

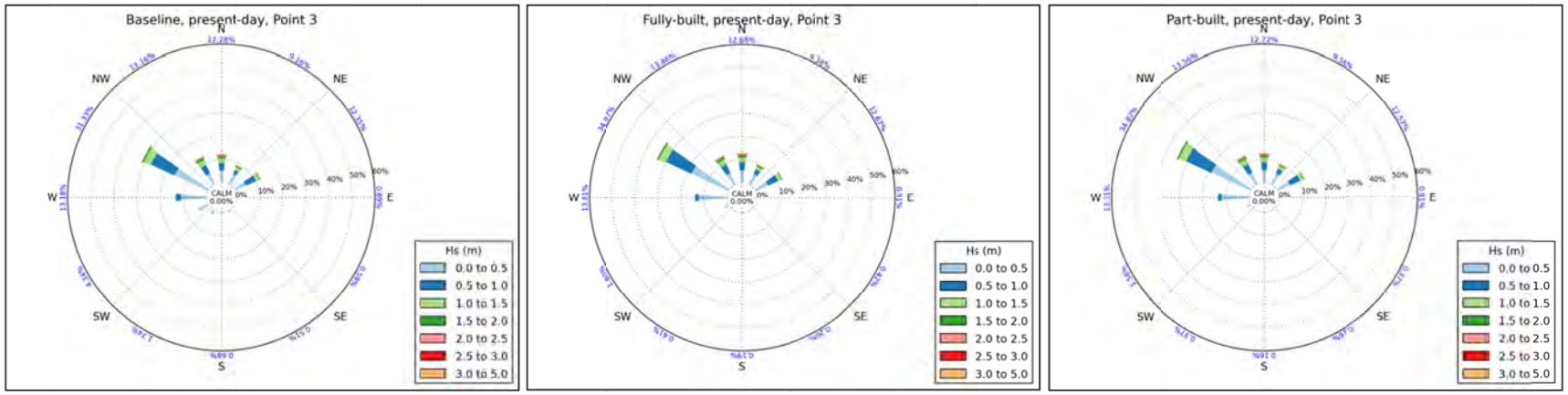

Figure C.3: Annual wave roses for nearshore prediction Point 3, present-day, baseline, part-built and fully-built layouts

Source: HR Wallingford, SWAN wave transformation and Met Office WW3 offshore data, 1980-2015

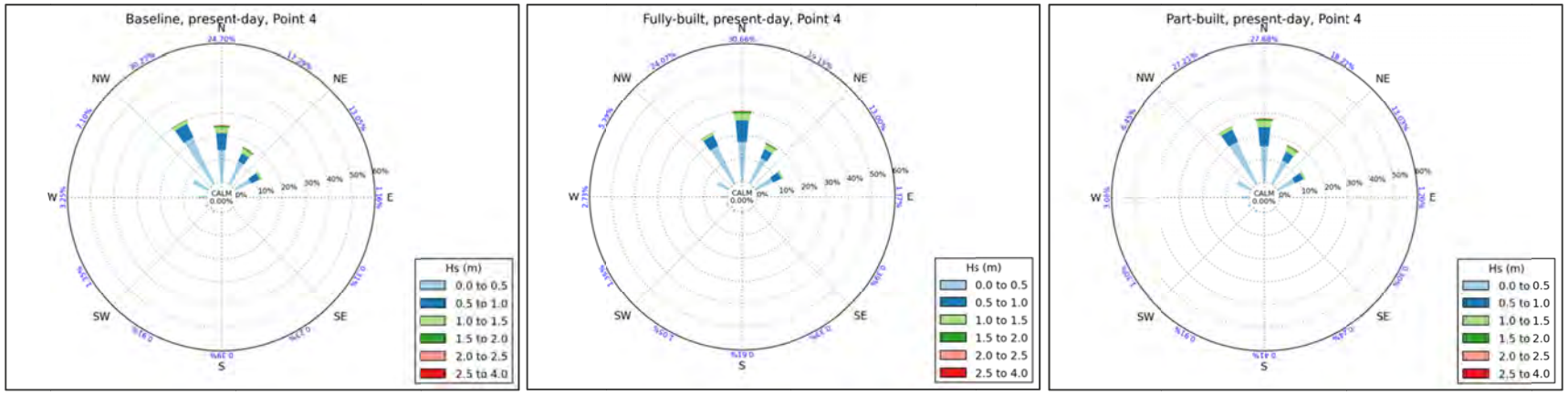

Figure C.4: Annual wave roses for nearshore prediction Point 4, present-day, baseline, part-built and fully-built layouts

Source: HR Wallingford, SWAN wave transformation and Met Office WW3 offshore data, 1980-2015

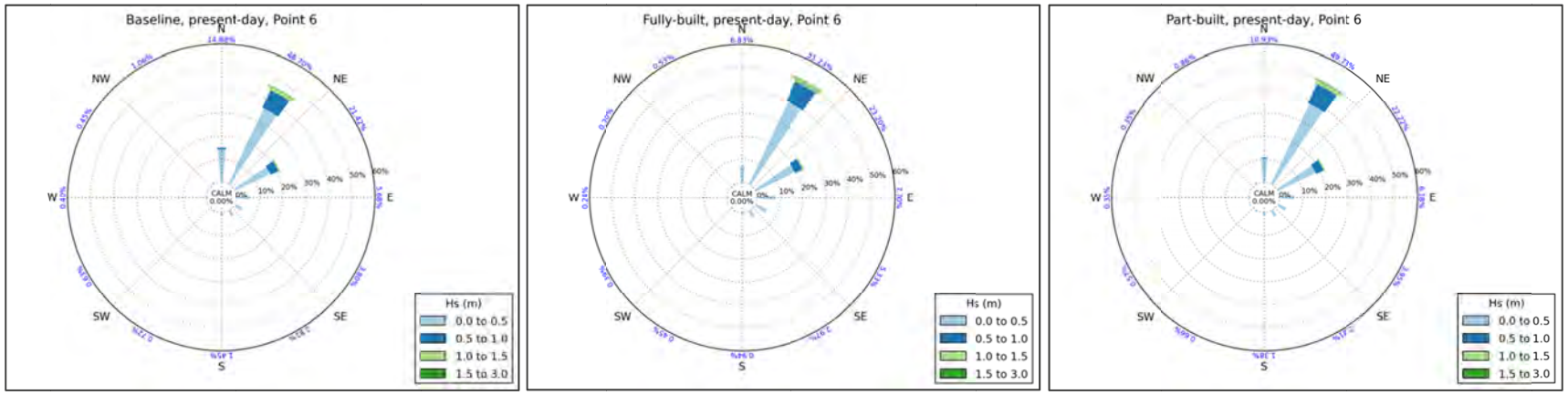

Figure C.5: Annual wave roses for nearshore prediction Point 6, present-day, baseline, part-built and fully-built layouts

Source: HR Wallingford, SWAN wave transformation and Met Office WW3 offshore data, 1980-2015

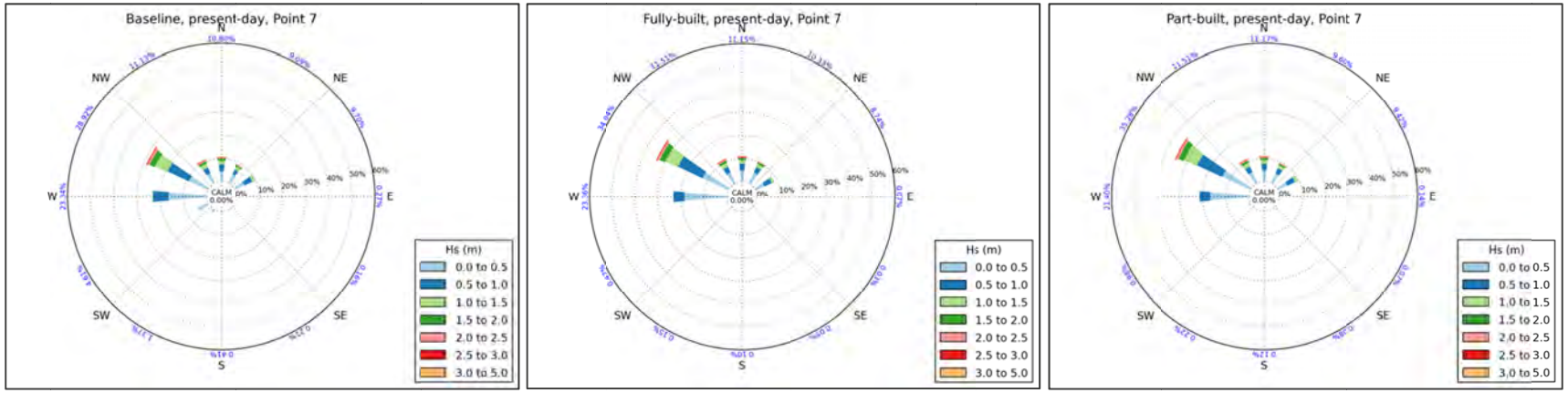

Figure C.6: Annual wave roses for nearshore prediction Point 7, present-day, baseline, part-built and fully-built layouts

Source: HR Wallingford, SWAN wave transformation and Met Office WW3 offshore data, 1980-2015

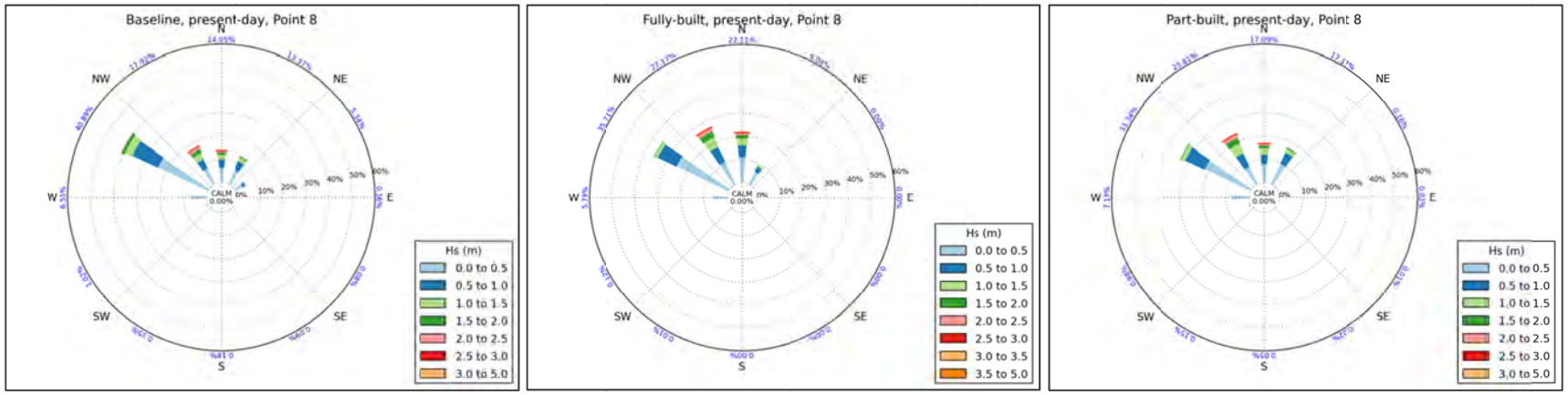

Figure C.7: Annual wave roses for nearshore prediction Point 8, present-day, baseline, part-built and fully-built layouts

Source: HR Wallingford, SWAN wave transformation and Met Office WW3 offshore data, 1980-2015

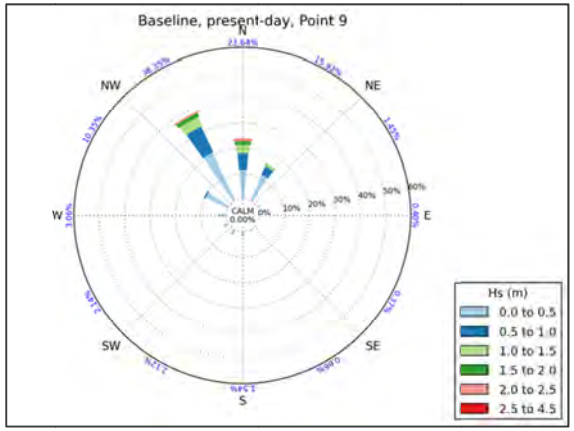

Figure C.8: Annual wave roses for nearshore prediction Point 9, present-day, baseline, part-built and fully-built layouts

Source: HR Wallingford, SWAN wave transformation and Met Office WW3 offshore data, 1980-2015

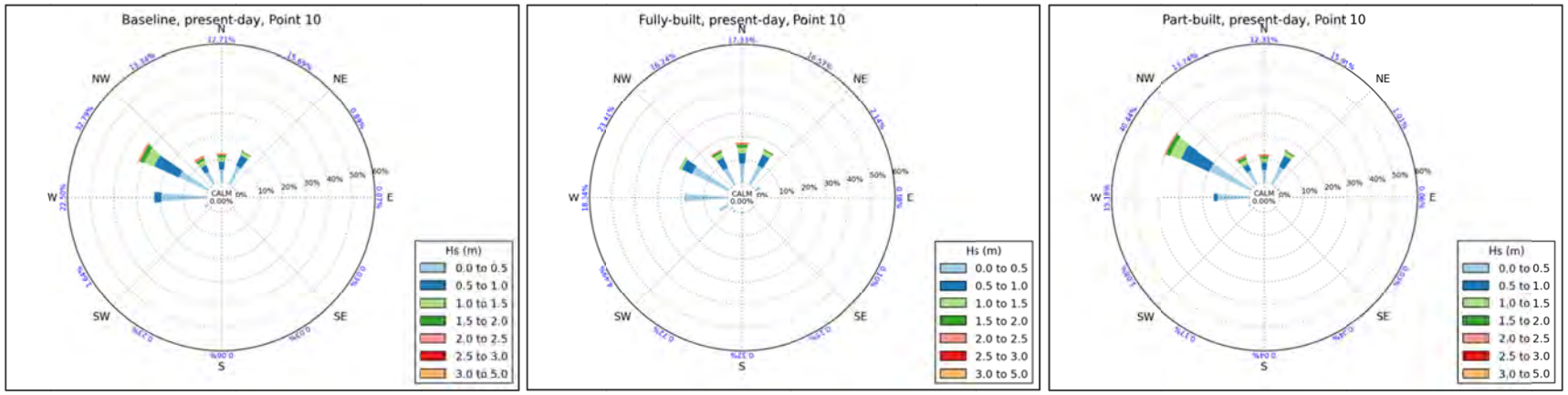

Figure C.9: Annual wave roses for nearshore prediction Point 10, present-day, baseline, part-built and fully-built layouts

Source: HR Wallingford, SWAN wave transformation and Met Office WW3 offshore data, 1980-2015

Table C.1: Annual wave climate at Point 1, baseline, 2023 "present day", significant wave height (H_s) against mean wave direction

			Wave direction											
			-15	15	45	75	105	135	165	195	225	255	285	315
H_{s1} (m)	H_{s2} (m)	$P(H_s>H_{s1})$	15	45	75	105	135	165	195	225	255	285	315	345
0	0.5	100.00%	4622	5104	6119	1265	956	1032	2015	3895	5062	10382	16205	5720
0.5	1	37.62%	2735	2428	3325	20	11	2	3	6	37	977	9256	4094
1	1.5	14.73%	1653	1363	443	-	-	-	-	-	-	-	2913	2468
1.5	2	5.89%	702	485	58	-	-	-	-	-	-	-	1119	1201
2	2.5	2.32%	326	163	6	-	-	-	-	-	-	-	344	567
2.5	3	0.92%	164	31	1	-	-	-	-	-	-	-	107	263
3	3.5	0.35%	80	6	-	-	-	-	-	-	-	-	15	122
3.5	4	0.13%	33	2	-	-	-	-	-	-	-	-	2	52
4	4.5	0.04%	10	<1	-	-	-	-	-	-	-	-	-	20
4.5	5	0.01%	5	-	-	-	-	-	-	-	-	-	-	5
5	5.5	0.00%	<1	-	-	-	-	-	-	-	-	-	-	1
	Percentage Occurrence		10.33%	9.58%	9.95%	1.28%	0.97%	1.03%	2.02%	3.90%	5.10%	11.36%	29.96%	14.51%

Source: HR Wallingford, SWAN wave transformation and Met Office WW3 offshore data, 1980-2015; occurrence is in parts per hundred thousand

Table C.2: Annual wave climate at Point 1, fully-built, 2023 "present day", significant wave height (H_s) against mean wave direction

			Wave direction											
			-15	15	45	75	105	135	165	195	225	255	285	315
H_{s1} (m)	H_{s2} (m)	$P(H_s>H_{s1})$	15	45	75	105	135	165	195	225	255	285	315	345
0	0.5	100.00%	4549	4980	6271	1333	998	1097	2173	4090	5174	10195	15869	5599
0.5	1	37.67%	2753	2394	3314	28	10	3	4	6	43	1049	9281	4080
1	1.5	14.71%	1631	1363	443	-	-	-	-	-	-	-	2932	2459
1.5	2	5.88%	700	483	62	-	-	-	-	-	-	-	1130	1182
2	2.5	2.32%	326	161	6	-	-	-	-	-	-	-	344	566
2.5	3	0.92%	162	31	1	-	-	-	-	-	-	-	107	264
3	3.5	0.35%	78	6	-	-	-	-	-	-	-	-	17	124
3.5	4	0.13%	33	2	-	-	-	-	-	-	-	-	2	51
4	4.5	0.04%	10	<1	-	-	-	-	-	-	-	-	-	20
4.5	5	0.01%	5	-	-	-	-	-	-	-	-	-	-	5
5	5.5	0.00%	<1	-	-	-	-	-	-	-	-	-	-	1
	Percentage Occurrence		10.25%	9.42%	10.10%	1.36%	1.01%	1.10%	2.18%	4.10%	5.22%	11.24%	29.68%	14.35%

Source: HR Wallingford, SWAN wave transformation and Met Office WW3 offshore data, 1980-2015; occurrence is in parts per hundred thousand

Table C.3: Annual wave climate at Point 1, part-built, 2023 “present day”, significant wave height (H_s) against mean wave direction

			Wave direction											
			-15	15	45	75	105	135	165	195	225	255	285	315
H_{s1} (m)	H_{s2} (m)	$P(H_s>H_{s1})$	15	45	75	105	135	165	195	225	255	285	315	345
0	0.5	100.00%	4441	4639	6613	1613	1057	1037	1855	3491	5463	11279	15508	5492
0.5	1	37.51%	3016	2562	3067	33	12	7	4	6	29	1002	9034	4017
1	1.5	14.72%	1848	1466	287	-	-	-	-	-	-	-	2845	2394
1.5	2	5.88%	767	436	42	-	-	-	-	-	-	-	1068	1251
2	2.5	2.32%	333	144	6	-	-	-	-	-	-	-	326	593
2.5	3	0.92%	170	28	1	-	-	-	-	-	-	-	98	268
3	3.5	0.35%	85	4	-	-	-	-	-	-	-	-	14	121
3.5	4	0.13%	38	2	-	-	-	-	-	-	-	-	2	48
4	4.5	0.04%	11	<1	-	-	-	-	-	-	-	-	-	19
4.5	5	0.01%	5	-	-	-	-	-	-	-	-	-	-	4
5	5.5	0.00%	<1	-	-	-	-	-	-	-	-	-	-	1
	Percentage Occurrence			10.71%	9.28%	10.02%	1.65%	1.07%	1.04%	1.86%	3.50%	5.49%	12.28%	28.89%

Source: HR Wallingford, SWAN wave transformation and Met Office WW3 offshore data, 1980-2015; occurrence is in parts per hundred thousand

Table C.4: Annual wave climate at Point 1, baseline, 2023 "present day", significant wave height (H_s) against mean wave period (T_{m-10})

			Mean Wave Period (T_{m-10}) in Seconds													
			0	1	2	3	4	5	6	7	8	9	10	11	12	13
H_{s1} (m)	H_{s2} (m)	$P(H_s>H_{s1})$	1	2	3	4	5	6	7	8	9	10	11	12	13	14
0	0.5	100.00%	24	4278	22792	24463	9036	1544	183	34	12	3	4	3	<1	1
0.5	1	37.62%	-	8	360	8879	10605	2236	684	114	8	-	-	-	-	-
1	1.5	14.73%	-	-	6	149	5423	2988	206	51	18	<1	-	-	-	-
1.5	2	5.89%	-	-	<1	4	233	2854	441	24	5	3	-	-	-	-
2	2.5	2.32%	-	-	-	-	4	527	817	52	3	1	-	-	-	-
2.5	3	0.92%	-	-	-	-	-	7	421	129	6	2	-	-	-	-
3	3.5	0.35%	-	-	-	-	-	-	49	167	5	2	-	-	-	-
3.5	4	0.13%	-	-	-	-	-	-	1	69	18	1	-	-	-	-
4	4.5	0.04%	-	-	-	-	-	-	-	4	26	-	-	-	-	-
4.5	5	0.01%	-	-	-	-	-	-	-	<1	8	<1	-	-	-	-
5	5.5	0.00%	-	-	-	-	-	-	-	-	1	<1	-	-	-	-
	Percentage Occurrence		0.02%	4.29%	23.16%	33.50%	25.30%	10.16 %	2.80%	0.64%	0.11%	0.01%	0.00%	0.00%	0.00%	0.00%

Source: HR Wallingford, SWAN wave transformation and Met Office WW3 offshore data, 1980 - 2015; occurrence is in parts per hundred thousand

Table C.5: Annual wave climate at Point 1, fully-built, 2023 "present day", significant wave height (H_s) against mean wave period (T_{m-10})

H_{s1} (m)	H_{s2} (m)	$P(H_s>H_{s1})$	Mean Wave Period (T_{m-10}) in Seconds													
			0	1	2	3	4	5	6	7	8	9	10	11	12	13
			1	2	3	4	5	6	7	8	9	10	11	12	13	14
0	0.5	100.00%	27	4775	22803	24459	8604	1421	183	30	13	4	6	2	<1	1
0.5	1	37.67%	-	7	378	8753	10783	2259	671	107	7	-	-	-	-	-
1	1.5	14.71%	-	-	6	126	5663	2761	201	54	16	1	-	-	-	-
1.5	2	5.88%	-	-	<1	2	236	2858	429	24	5	2	-	-	-	-
2	2.5	2.32%	-	-	-	-	2	570	777	49	4	1	-	-	-	-
2.5	3	0.92%	-	-	-	-	-	6	428	123	6	2	-	-	-	-
3	3.5	0.35%	-	-	-	-	-	-	46	171	5	2	-	-	-	-
3.5	4	0.13%	-	-	-	-	-	-	1	70	16	1	-	-	-	-
4	4.5	0.04%	-	-	-	-	-	-	-	4	25	-	-	-	-	-
4.5	5	0.01%	-	-	-	-	-	-	-	<1	8	<1	-	-	-	-
5	5.5	0.00%	-	-	-	-	-	-	-	-	1	<1	-	-	-	-
	Percentage Occurrence		0.03%	4.78%	23.19%	33.34%	25.29%	9.87%	2.74%	0.63%	0.11%	0.01%	0.01%	0.00%	0.00%	0.00%

Source: HR Wallingford, SWAN wave transformation and Met Office WW3 offshore data, 1980 - 2015; occurrence is in parts per hundred thousand

Table C.6: Annual wave climate at Point 1, part-built, 2023 "present day", significant wave height (H_s) against mean wave period (T_{m-10})

H_{s1} (m)	H_{s2} (m)	$P(H_s>H_{s1})$	Mean Wave Period (T_{m-10}) in Seconds													
			0	1	2	3	4	5	6	7	8	9	10	11	12	13
			1	2	3	4	5	6	7	8	9	10	11	12	13	14
0	0.5	100.00%	29	4759	22836	24467	8625	1516	190	38	14	5	5	2	<1	1
0.5	1	37.51%	-	6	369	8719	10709	2175	691	112	8	-	-	-	-	-
1	1.5	14.72%	-	-	6	117	5677	2764	206	52	16	1	-	-	-	-
1.5	2	5.88%	-	-	<1	2	231	2871	427	24	5	2	-	-	-	-
2	2.5	2.32%	-	-	-	-	2	572	773	49	4	1	-	-	-	-
2.5	3	0.92%	-	-	-	-	-	6	427	123	6	2	-	-	-	-
3	3.5	0.35%	-	-	-	-	-	-	46	169	5	2	-	-	-	-
3.5	4	0.13%	-	-	-	-	-	-	1	71	16	1	-	-	-	-
4	4.5	0.04%	-	-	-	-	-	-	-	4	25	-	-	-	-	-
4.5	5	0.01%	-	-	-	-	-	-	-	<1	8	<1	-	-	-	-
5	5.5	0.00%	-	-	-	-	-	-	-	-	1	<1	-	-	-	-
	Percentage Occurrence		0.03%	4.76%	23.21%	33.31%	25.24%	9.90%	2.76%	0.64%	0.11%	0.02%	0.01%	0.00%	0.00%	0.00%

Source: HR Wallingford, SWAN wave transformation and Met Office WW3 offshore data, 1980 - 2015; occurrence is in parts per hundred thousand

Table C.7: Annual wave climate at Point 2, baseline, 2023 “present day”, significant wave height (H_s) against mean wave direction

			Wave direction											
			-15	15	45	75	105	135	165	195	225	255	285	315
H_{s1} (m)	H_{s2} (m)	$P(H_s>H_{s1})$	15	45	75	105	135	165	195	225	255	285	315	345
0	0.5	100.00%	2609	2370	4537	1026	322	216	290	778	6004	14450	3944	3413
0.5	1	60.04%	2160	1684	4612	429	92	61	79	150	2449	14046	4211	2447
1	1.5	27.62%	1300	939	2059	24	3	4	5	17	309	5776	3126	1582
1.5	2	12.48%	633	489	642	<1	-	-	-	-	7	2009	1874	901
2	2.5	5.92%	308	255	231	-	-	-	-	-	-	663	1193	498
2.5	3	2.77%	153	115	71	-	-	-	-	-	-	225	685	303
3	3.5	1.22%	107	49	7	-	-	-	-	-	-	46	382	154
3.5	4	0.48%	45	19	2	-	-	-	-	-	-	14	140	80
4	4.5	0.18%	19	16	-	-	-	-	-	-	-	7	30	44
4.5	5	0.06%	9	2	-	-	-	-	-	-	-	1	5	23
5	5.5	0.02%	6	1	-	-	-	-	-	-	-	-	1	7
5.5	6	0.00%	2	-	-	-	-	-	-	-	-	-	-	3
	Percentage Occurrence		7.35%	5.94%	12.16%	1.48%	0.42%	0.28%	0.37%	0.94%	8.77%	37.24%	15.59%	9.46%

Source: HR Wallingford, SWAN wave transformation and Met Office WW3 offshore data, 1980-2015; occurrence is in parts per hundred thousand

Table C.8: Annual wave climate at Point 2, fully-built, 2023 "present day", significant wave height (H_s) against mean wave direction

			Wave direction											
			-15	15	45	75	105	135	165	195	225	255	285	315
H_{s1} (m)	H_{s2} (m)	$P(H_s>H_{s1})$	15	45	75	105	135	165	195	225	255	285	315	345
0	0.5	100.00%	2576	2344	4558	1057	333	220	301	759	6111	14330	3935	3374
0.5	1	60.10%	2162	1685	4595	442	96	66	80	157	2464	14047	4213	2438
1	1.5	27.66%	1310	943	2064	25	4	4	5	19	346	5747	3116	1574
1.5	2	12.50%	637	488	640	<1	-	-	-	-	7	2033	1872	898
2	2.5	5.92%	311	255	233	-	-	-	-	-	-	662	1187	499
2.5	3	2.78%	157	116	71	-	-	-	-	-	-	226	682	301
3	3.5	1.22%	108	49	7	-	-	-	-	-	-	45	383	156
3.5	4	0.48%	46	19	2	-	-	-	-	-	-	13	140	80
4	4.5	0.18%	19	16	-	-	-	-	-	-	-	7	30	44
4.5	5	0.06%	9	2	-	-	-	-	-	-	-	1	5	22
5	5.5	0.02%	6	1	-	-	-	-	-	-	-	-	1	8
5.5	6	0.00%	2	-	-	-	-	-	-	-	-	-	-	3
	Percentage Occurrence		7.34%	5.92%	12.17%	1.53%	0.43%	0.29%	0.39%	0.94%	8.93%	37.11%	15.56%	9.40%

Source: HR Wallingford, SWAN wave transformation and Met Office WW3 offshore data, 1980-2015; occurrence is in parts per hundred thousand

Table C.9: Annual wave climate at Point 2, part-built, 2023 "present day", significant wave height (H_s) against mean wave direction

			Wave direction											
			-15	15	45	75	105	135	165	195	225	255	285	315
H_{s1} (m)	H_{s2} (m)	$P(H_s>H_{s1})$	15	45	75	105	135	165	195	225	255	285	315	345
0	0.5	100.00%	2586	2378	4565	1034	322	217	295	757	5949	14444	3934	3385
0.5	1	60.14%	2155	1678	4608	437	96	60	84	149	2457	14136	4199	2436
1	1.5	27.64%	1308	942	2061	25	3	4	4	18	315	5782	3126	1580
1.5	2	12.47%	635	488	643	<1	-	-	-	-	7	2016	1869	899
2	2.5	5.91%	306	255	234	-	-	-	-	-	-	662	1186	498
2.5	3	2.77%	156	114	70	-	-	-	-	-	-	226	685	299
3	3.5	1.22%	108	49	7	-	-	-	-	-	-	45	382	157
3.5	4	0.48%	45	19	2	-	-	-	-	-	-	13	140	79
4	4.5	0.18%	19	16	-	-	-	-	-	-	-	7	30	44
4.5	5	0.06%	9	2	-	-	-	-	-	-	-	1	5	23
5	5.5	0.02%	6	1	-	-	-	-	-	-	-	-	1	7
5.5	6	0.00%	2	-	-	-	-	-	-	-	-	-	-	3
	Percentage Occurrence		7.34%	5.94%	12.19%	1.50%	0.42%	0.28%	0.38%	0.92%	8.73%	37.33%	15.56%	9.41%

Source: HR Wallingford, SWAN wave transformation and Met Office WW3 offshore data, 1980-2015; occurrence is in parts per hundred thousand

Table C.10: Annual wave climate at Point 2, baseline, 2023 "present day", significant wave height (H_s) against mean wave period (T_{m-10})

			Mean Wave Period (T_{m-10}) in Seconds												
			0	1	2	3	4	5	6	7	8	9	10	11	12
H_{s1} (m)	H_{s2} (m)	$P(H_s>H_{s1})$	1	2	3	4	5	6	7	8	9	10	11	12	13
0	0.5	100.00%	<1	442	12942	19108	6167	1069	180	31	10	3	5	2	<1
0.5	1	60.04%	-	-	620	14811	14659	2132	176	22	<1	-	-	-	-
1	1.5	27.62%	-	-	2	836	9894	3453	879	77	3	-	-	-	-
1.5	2	12.48%	-	-	-	8	1771	4111	456	186	23	-	-	-	-
2	2.5	5.92%	-	-	-	-	46	2556	472	51	22	2	-	-	-
2.5	3	2.77%	-	-	-	<1	-	383	1100	61	7	<1	-	-	-
3	3.5	1.22%	-	-	-	-	-	5	585	143	7	4	-	-	-
3.5	4	0.48%	-	-	-	-	-	<1	59	230	8	<1	-	-	-
4	4.5	0.18%	-	-	-	-	-	-	1	99	13	2	-	-	-
4.5	5	0.06%	-	-	-	-	-	-	<1	17	21	2	<1	-	-
5	5.5	0.02%	-	-	-	-	-	-	-	1	19	1	-	-	-
	Percentage Occurrence		0.00%	0.44%	13.56%	34.76%	32.54%	13.71%	3.91%	0.92%	0.13%	0.01%	0.01%	0.00%	0.00%

Source: HR Wallingford, SWAN wave transformation and Met Office WW3 offshore data, 1980-2015; occurrence is in parts per hundred thousand

Table C.11: Annual wave climate at Point 2, fully-built, 2023 "present day", significant wave height (H_s) against mean wave period (T_{m-10})

			Mean Wave Period (T_{m-10}) in Seconds												
			0	1	2	3	4	5	6	7	8	9	10	11	12
H_{s1} (m)	H_{s2} (m)	$P(H_s>H_{s1})$	1	2	3	4	5	6	7	8	9	10	11	12	13
0	0.5	100.00%	<1	465	13097	18978	6060	1069	179	29	12	3	5	2	<1
0.5	1	60.10%	-	-	635	14875	14639	2106	169	21	<1	-	-	-	-
1	1.5	27.66%	-	-	2	842	9899	3490	852	68	3	-	-	-	-
1.5	2	12.50%	-	-	-	8	1742	4138	480	186	23	-	-	-	-
2	2.5	5.92%	-	-	-	-	45	2550	476	54	21	2	-	-	-
2.5	3	2.78%	-	-	-	<1	-	380	1103	59	8	<1	-	-	-
3	3.5	1.22%	-	-	-	-	-	5	589	143	7	4	-	-	-
3.5	4	0.48%	-	-	-	-	-	<1	59	232	7	<1	-	-	-
4	4.5	0.18%	-	-	-	-	-	-	1	100	13	2	-	-	-
4.5	5	0.06%	-	-	-	-	-	-	<1	16	21	2	<1	-	-
5	5.5	0.02%	-	-	-	-	-	-	-	2	19	1	-	-	-
	Percentage Occurrence		0.00%	0.46%	13.73%	34.70%	32.38%	13.74%	3.91%	0.91%	0.13%	0.01%	0.01%	0.00%	0.00%

Source: HR Wallingford, SWAN wave transformation and Met Office WW3 offshore data, 1980-2015; occurrence is in parts per hundred thousand

Table C.12: Annual wave climate at Point 2, part-built, 2023 "present day", significant wave height (H_s) against mean wave period (T_{m-10})

			Mean Wave Period (T_{m-10}) in Seconds												
			0	1	2	3	4	5	6	7	8	9	10	11	12
H_{s1} (m)	H_{s2} (m)	$P(H_s>H_{s1})$	1	2	3	4	5	6	7	8	9	10	11	12	13
0	0.5	100.00%	<1	479	13116	18918	6030	1078	188	31	13	2	5	2	<1
0.5	1	60.14%	-	-	614	14826	14721	2136	176	22	<1	-	-	-	-
1	1.5	27.64%	-	-	2	806	9887	3521	872	76	3	-	-	-	-
1.5	2	12.47%	-	-	-	8	1680	4197	466	185	22	-	-	-	-
2	2.5	5.91%	-	-	-	-	46	2539	483	51	21	2	-	-	-
2.5	3	2.77%	-	-	-	<1	-	355	1125	61	8	<1	-	-	-
3	3.5	1.22%	-	-	-	-	-	5	589	143	6	4	-	-	-
3.5	4	0.48%	-	-	-	-	-	<1	58	231	7	<1	-	-	-
4	4.5	0.18%	-	-	-	-	-	-	1	100	13	2	-	-	-
4.5	5	0.06%	-	-	-	-	-	-	<1	16	21	2	<1	-	-
5	5.5	0.02%	-	-	-	-	-	-	-	1	19	1	-	-	-
	Percentage Occurrence		0.00%	0.48%	13.73%	34.56%	32.36%	13.83%	3.96%	0.92%	0.13%	0.01%	0.01%	0.00%	0.00%

Source: HR Wallingford, SWAN wave transformation and Met Office WW3 offshore data, 1980-2015; occurrence is in parts per hundred thousand

Table C.13: Annual wave climate at Point 3, baseline, 2023 “present day”, significant wave height (H_s) against mean wave direction

			Wave direction											
			-15	15	45	75	105	135	165	195	225	255	285	315
H_{s1} (m)	H_{s2} (m)	$P(H_s>H_{s1})$	15	45	75	105	135	165	195	225	255	285	315	345
0	0.5	100.00%	5129	4696	5412	669	590	503	675	1732	4221	10996	15906	5003
0.5	1	44.47%	3367	2252	4842	16	3	3	4	5	115	2178	11381	4133
1	1.5	16.17%	2075	1259	1620	<1	-	-	-	-	-	2	3226	2274
1.5	2	5.71%	947	577	367	-	-	-	-	-	-	-	681	1156
2	2.5	1.99%	400	241	82	-	-	-	-	-	-	-	126	457
2.5	3	0.68%	208	83	24	-	-	-	-	-	-	-	12	114
3	3.5	0.24%	107	36	1	-	-	-	-	-	-	-	2	27
3.5	4	0.07%	36	14	-	-	-	-	-	-	-	-	-	2
4	4.5	0.02%	9	4	-	-	-	-	-	-	-	-	-	-
4.5	5	0.00%	2	2	-	-	-	-	-	-	-	-	-	-
	Percentage Occurrence		12.28%	9.16%	12.35%	0.69%	0.59%	0.51%	0.68%	1.74%	4.34%	13.18%	31.33%	13.16%

Source: HR Wallingford, SWAN wave transformation and Met Office WW3 offshore data, 1980-2015; occurrence is in parts per hundred thousand

Table C.14: Annual wave climate at Point 3, fully-built, 2023 “present day”, significant wave height (H_s) against mean wave direction

			Wave direction											
			-15	15	45	75	105	135	165	195	225	255	285	315
H_{s1} (m)	H_{s2} (m)	$P(H_s>H_{s1})$	15	45	75	105	135	165	195	225	255	285	315	345
0	0.5	100.00%	5282	4883	5852	893	413	201	185	403	1795	12293	17789	5288
0.5	1	44.72%	3476	2263	4793	18	2	3	2	2	7	1518	12098	4120
1	1.5	16.42%	2146	1267	1579	-	-	-	-	-	-	2	3347	2272
1.5	2	5.81%	986	587	352	-	-	-	-	-	-	-	702	1181
2	2.5	2.00%	418	245	77	-	-	-	-	-	-	-	123	455
2.5	3	0.68%	211	86	19	-	-	-	-	-	-	-	10	110
3	3.5	0.24%	110	35	1	-	-	-	-	-	-	-	2	28
3.5	4	0.07%	35	14	-	-	-	-	-	-	-	-	-	2
4	4.5	0.02%	10	3	-	-	-	-	-	-	-	-	-	-
4.5	5	0.00%	2	2	-	-	-	-	-	-	-	-	-	-
	Percentage Occurrence		12.68%	9.38%	12.67%	0.91%	0.42%	0.20%	0.19%	0.41%	1.80%	13.81%	34.07%	13.46%

Source: HR Wallingford, SWAN wave transformation and Met Office WW3 offshore data, 1980-2015; occurrence is in parts per hundred thousand

Table C.15: Annual wave climate at Point 3, part-built, 2023 “present day”, significant wave height (H_s) against mean wave direction

			Wave direction											
			-15	15	45	75	105	135	165	195	225	255	285	315
H_{s1} (m)	H_{s2} (m)	$P(H_s>H_{s1})$	15	45	75	105	135	165	195	225	255	285	315	345
0	0.5	100.00%	5337	5028	5792	798	371	158	162	372	1576	11785	18580	5380
0.5	1	44.66%	3479	2283	4758	12	1	3	2	1	6	1520	12088	4115
1	1.5	16.39%	2138	1274	1568	-	-	-	-	-	-	2	3301	2298
1.5	2	5.81%	987	591	355	-	-	-	-	-	-	-	708	1173
2	2.5	2.00%	414	244	77	-	-	-	-	-	-	-	126	454
2.5	3	0.68%	212	88	19	-	-	-	-	-	-	-	11	111
3	3.5	0.24%	108	36	1	-	-	-	-	-	-	-	2	27
3.5	4	0.07%	35	14	-	-	-	-	-	-	-	-	-	2
4	4.5	0.02%	9	4	-	-	-	-	-	-	-	-	-	-
4.5	5	0.00%	2	2	-	-	-	-	-	-	-	-	-	-
	Percentage Occurrence		12.72%	9.56%	12.57%	0.81%	0.37%	0.16%	0.16%	0.37%	1.58%	13.31%	34.82%	13.56%

Source: HR Wallingford, SWAN wave transformation and Met Office WW3 offshore data, 1980-2015; occurrence is in parts per hundred thousand

Table C.16: Annual wave climate at Point 3, baseline, 2023 "present day", significant wave height (H_s) against mean wave period (T_{m-10})

			Mean Wave Period (T_{m-10}) in Seconds													
			0	1	2	3	4	5	6	7	8	9	10	11	12	13
H_{s1} (m)	H_{s2} (m)	$P(H_s>H_{s1})$	1	2	3	4	5	6	7	8	9	10	11	12	13	14
0	0.5	100.00%	3	1814	19190	23996	8608	1536	294	62	16	4	4	3	3	<1
0.5	1	44.47%	-	3	474	11162	12425	3188	923	115	7	<1	-	-	-	-
1	1.5	16.17%	-	-	3	276	6294	3181	487	178	37	2	-	-	-	-
1.5	2	5.71%	-	-	-	5	354	2693	572	77	24	3	-	-	-	-
2	2.5	1.99%	-	-	-	-	4	469	717	97	13	5	-	-	-	-
2.5	3	0.68%	-	-	-	-	-	11	311	106	10	2	-	-	-	-
3	3.5	0.24%	-	-	-	-	-	-	37	128	4	3	<1	-	-	-
3.5	4	0.07%	-	-	-	-	-	-	<1	29	22	-	-	-	-	-
4	4.5	0.02%	-	-	-	-	-	-	-	3	9	1	-	-	-	-
4.5	5	0.00%	-	-	-	-	-	-	-	-	4	-	-	-	-	-
	Percentage Occurrence		0.00%	1.82%	19.67%	35.44%	27.68%	11.08%	3.34%	0.80%	0.14%	0.02%	0.00%	0.00%	0.00%	0.00%

Source: HR Wallingford, SWAN wave transformation and Met Office WW3 offshore data, 1980-2015; occurrence is in parts per hundred thousand

Table C.17: Annual wave climate at Point 3, fully-built, 2023 "present day", significant wave height (H_s) against mean wave period (T_{m-10})

			Mean Wave Period (T_{m-10}) in Seconds													
			0	1	2	3	4	5	6	7	8	9	10	11	12	13
H_{s1} (m)	H_{s2} (m)	$P(H_s>H_{s1})$	1	2	3	4	5	6	7	8	9	10	11	12	13	14
0	0.5	100.00%	2	1821	19294	23945	8414	1443	273	56	15	4	4	3	3	<1
0.5	1	44.72%	-	3	461	11469	12308	3111	841	102	5	<1	-	-	-	-
1	1.5	16.42%	-	-	3	249	6572	3108	476	171	32	2	-	-	-	-
1.5	2	5.81%	-	-	-	5	364	2780	563	74	21	2	-	-	-	-
2	2.5	2.00%	-	-	-	<1	4	478	726	92	14	4	-	-	-	-
2.5	3	0.68%	-	-	-	-	-	10	316	101	9	2	-	-	-	-
3	3.5	0.24%	-	-	-	-	-	-	38	131	3	3	<1	-	-	-
3.5	4	0.07%	-	-	-	-	-	-	<1	29	21	-	-	-	-	-
4	4.5	0.02%	-	-	-	-	-	-	-	3	10	-	-	-	-	-
4.5	5	0.00%	-	-	-	-	-	-	-	-	4	-	-	-	-	-
	Percentage Occurrence		0.00%	1.82%	19.76%	35.67%	27.66%	10.93%	3.23%	0.76%	0.13%	0.02%	0.00%	0.00%	0.00%	0.00%

Source: HR Wallingford, SWAN wave transformation and Met Office WW3 offshore data, 1980-2015; occurrence is in parts per hundred thousand

Table C.18: Annual wave climate at Point 3, part-built, 2023 "present day", significant wave height (H_s) against mean wave period (T_{m-10})

			Mean Wave Period (T_{m-10}) in Seconds													
			0	1	2	3	4	5	6	7	8	9	10	11	12	13
H_{s1} (m)	H_{s2} (m)	$P(H_s>H_{s1})$	1	2	3	4	5	6	7	8	9	10	11	12	13	14
0	0.5	100.00%	2	1791	19252	23902	8512	1504	287	59	16	4	4	3	3	<1
0.5	1	44.66%	-	2	452	11370	12290	3147	888	112	6	<1	-	-	-	-
1	1.5	16.39%	-	-	3	248	6531	3113	475	175	35	2	-	-	-	-
1.5	2	5.81%	-	-	-	5	362	2782	565	75	22	2	-	-	-	-
2	2.5	2.00%	-	-	-	<1	3	475	726	93	13	5	-	-	-	-
2.5	3	0.68%	-	-	-	-	-	10	320	100	10	2	-	-	-	-
3	3.5	0.24%	-	-	-	-	-	-	37	130	4	3	<1	-	-	-
3.5	4	0.07%	-	-	-	-	-	-	<1	28	22	-	-	-	-	-
4	4.5	0.02%	-	-	-	-	-	-	-	3	10	-	-	-	-	-
4.5	5	0.00%	-	-	-	-	-	-	-	-	4	-	-	-	-	-
	Percentage Occurrence		0.00%	1.79%	19.71%	35.53%	27.70%	11.03%	3.30%	0.78%	0.14%	0.02%	0.00%	0.00%	0.00%	0.00%

Source: HR Wallingford, SWAN wave transformation and Met Office WW3 offshore data, 1980-2015; occurrence is in parts per hundred thousand

Table C.19: Annual wave climate at Point 4, baseline, 2023 “present day”, significant wave height (H_s) against mean wave direction

			Wave direction											
			-15	15	45	75	105	135	165	195	225	255	285	315
H_{s1} (m)	H_{s2} (m)	$P(H_s>H_{s1})$	15	45	75	105	135	165	195	225	255	285	315	345
0	0.5	100.00%	13795	10913	7847	1157	309	228	394	912	1348	3244	6939	21906
0.5	1	31.01%	7395	3742	4202	3	<1	-	-	-	-	2	158	6642
1	1.5	8.86%	2506	1859	802	-	-	-	-	-	-	-	-	1525
1.5	2	2.17%	749	519	146	-	-	-	-	-	-	-	-	182
2	2.5	0.57%	217	182	48	-	-	-	-	-	-	-	-	11
2.5	3	0.12%	38	56	3	-	-	-	-	-	-	-	-	2
3	3.5	0.02%	4	13	-	-	-	-	-	-	-	-	-	-
3.5	4	0.00%	-	3	-	-	-	-	-	-	-	-	-	-
	Percentage Occurrence		24.70%	17.29%	13.05%	1.16%	0.31%	0.23%	0.39%	0.91%	1.35%	3.25%	7.10%	30.27%

Source: HR Wallingford, SWAN wave transformation and Met Office WW3 offshore data, 1980-2015; occurrence is in parts per hundred thousand

Table C.20: Annual wave climate at Point 4, fully-built, 2023 "present day", significant wave height (H_s) against mean wave direction

			Wave direction											
			-15	15	45	75	105	135	165	195	225	255	285	315
H_{s1} (m)	H_{s2} (m)	$P(H_s>H_{s1})$	15	45	75	105	135	165	195	225	255	285	315	345
0	0.5	100.00%	17288	12080	8172	1363	394	327	612	1049	1350	2723	5169	17812
0.5	1	31.66%	9266	4195	3966	4	<1	<1	<1	-	-	5	124	5013
1	1.5	9.09%	3005	2052	691	-	-	-	-	-	-	-	-	1113
1.5	2	2.23%	841	558	125	-	-	-	-	-	-	-	-	125
2	2.5	0.58%	218	195	40	-	-	-	-	-	-	-	-	6
2.5	3	0.12%	41	54	2	-	-	-	-	-	-	-	-	<1
3	3.5	0.02%	5	14	-	-	-	-	-	-	-	-	-	-
3.5	4	0.00%	-	3	-	-	-	-	-	-	-	-	-	-
	Percentage Occurrence		30.66%	19.15%	13.00%	1.37%	0.39%	0.33%	0.61%	1.05%	1.35%	2.73%	5.29%	24.07%

Source: HR Wallingford, SWAN wave transformation and Met Office WW3 offshore data, 1980-2015; occurrence is in parts per hundred thousand

Table C.21: Annual wave climate at Point 4, part-built, 2023 "present day", significant wave height (H_s) against mean wave direction

			Wave direction											
			-15	15	45	75	105	135	165	195	225	255	285	315
H_{s1} (m)	H_{s2} (m)	$P(H_s>H_{s1})$	15	45	75	105	135	165	195	225	255	285	315	345
0	0.5	100.00%	15480	11365	8062	1197	299	238	410	905	1298	3056	6303	20049
0.5	1	31.34%	8344	4055	4060	2	1	-	-	-	-	3	143	5736
1	1.5	8.99%	2784	1986	728	-	-	-	-	-	-	-	-	1280
1.5	2	2.22%	817	553	132	-	-	-	-	-	-	-	-	139
2	2.5	0.58%	216	196	42	-	-	-	-	-	-	-	-	7
2.5	3	0.11%	38	53	3	-	-	-	-	-	-	-	-	1
3	3.5	0.02%	4	14	-	-	-	-	-	-	-	-	-	-
3.5	4	0.00%	-	3	-	-	-	-	-	-	-	-	-	-
	Percentage Occurrence		27.68%	18.22%	13.03%	1.20%	0.30%	0.24%	0.41%	0.91%	1.30%	3.06%	6.45%	27.21%

Source: HR Wallingford, SWAN wave transformation and Met Office WW3 offshore data, 1980-2015; occurrence is in parts per hundred thousand

Table C.22: Annual wave climate at Point 4, baseline, 2023 "present day", significant wave height (H_s) against mean wave period (T_{m-10})

			Mean Wave Period (T_{m-10}) in Seconds												
			0	1	2	3	4	5	6	7	8	9	10	11	12
H_{s1} (m)	H_{s2} (m)	$P(H_s>H_{s1})$	1	2	3	4	5	6	7	8	9	10	11	12	13
0	0.5	100.00%	47	4449	21645	26563	12417	3065	643	122	22	6	7	3	1
0.5	1	31.01%	-	10	794	6544	9177	3719	1410	418	69	5	-	-	-
1	1.5	8.86%	-	-	1	161	2448	2977	843	193	53	15	1	-	-
1.5	2	2.17%	-	-	<1	-	83	737	569	185	13	7	<1	-	-
2	2.5	0.57%	-	-	-	-	2	63	216	150	19	5	3	-	-
2.5	3	0.12%	-	-	-	-	-	-	28	42	25	2	2	-	-
3	3.5	0.02%	-	-	-	-	-	-	-	11	5	<1	-	-	-
3.5	4	0.00%	-	-	-	-	-	-	-	<1	2	-	-	-	-
4	4.5	0.00%	-	-	-	-	-	-	-	-	-	-	-	-	-
4.5	5	0.00%	-	-	-	-	-	-	-	-	-	-	-	-	-
	Percentage Occurrence		0.05%	4.46%	22.44%	33.27%	24.13%	10.56%	3.71%	1.12%	0.21%	0.04%	0.01%	0.00%	0.00%

Source: HR Wallingford, SWAN wave transformation and Met Office WW3 offshore data, 1980-2015; occurrence is in parts per hundred thousand

Table C.23: Annual wave climate at Point 4, fully-built, 2023 "present day", significant wave height (H_s) against mean wave period (T_{m-10})

			Mean Wave Period (T_{m-10}) in Seconds												
			0	1	2	3	4	5	6	7	8	9	10	11	12
H_{s1} (m)	H_{s2} (m)	$P(H_s>H_{s1})$	1	2	3	4	5	6	7	8	9	10	11	12	13
0	0.5	100.00%	29	4242	21897	26549	12053	2835	585	111	21	6	7	3	1
0.5	1	31.66%	-	8	685	6744	9540	3730	1404	397	61	5	-	-	-
1	1.5	9.09%	-	-	<1	140	2544	3093	829	185	54	16	-	-	-
1.5	2	2.23%	-	-	-	<1	75	769	604	181	12	7	<1	-	-
2	2.5	0.58%	-	-	-	-	1	60	226	147	19	4	2	-	-
2.5	3	0.12%	-	-	-	-	-	-	26	45	23	2	2	-	-
3	3.5	0.02%	-	-	-	-	-	-	-	12	6	<1	<1	-	-
3.5	4	0.00%	-	-	-	-	-	-	-	<1	2	-	-	-	-
4	4.5	0.00%	-	-	-	-	-	-	-	-	-	-	-	-	-
4.5	5	0.00%	-	-	-	-	-	-	-	-	-	-	-	-	-
	Percentage Occurrence		0.03%	4.25%	22.58%	33.43%	24.21%	10.49%	3.67%	1.08%	0.20%	0.04%	0.01%	0.00%	0.00%

Source: HR Wallingford, SWAN wave transformation and Met Office WW3 offshore data, 1980-2015; occurrence is in parts per hundred thousand

Table C.24: Annual wave climate at Point 4, part-built, 2023 "present day", significant wave height (H_s) against mean wave period (T_{m-10})

			Mean Wave Period (T_{m-10}) in Seconds												
			0	1	2	3	4	5	6	7	8	9	10	11	12
H_{s1} (m)	H_{s2} (m)	$P(H_s>H_{s1})$	1	2	3	4	5	6	7	8	9	10	11	12	13
0	0.5	100.00%	38	4199	21534	26616	12444	3051	625	119	20	6	7	3	1
0.5	1	31.34%	-	8	741	6644	9285	3731	1430	423	75	5	-	-	-
1	1.5	8.99%	-	-	1	149	2496	3031	839	194	50	16	1	-	-
1.5	2	2.22%	-	-	-	<1	80	766	583	190	12	7	<1	-	-
2	2.5	0.58%	-	-	-	-	1	65	222	145	20	4	3	-	-
2.5	3	0.11%	-	-	-	-	-	-	26	41	24	2	1	-	-
3	3.5	0.02%	-	-	-	-	-	-	-	11	5	<1	<1	-	-
3.5	4	0.00%	-	-	-	-	-	-	-	<1	2	-	-	-	-
4	4.5	0.00%	-	-	-	-	-	-	-	-	-	-	-	-	-
4.5	5	0.00%	-	-	-	-	-	-	-	-	-	-	-	-	-
	Percentage Occurrence		0.04%	4.21%	22.28%	33.41%	24.31%	10.64%	3.73%	1.13%	0.21%	0.04%	0.01%	0.00%	0.00%

Source: HR Wallingford, SWAN wave transformation and Met Office WW3 offshore data, 1980-2015; occurrence is in parts per hundred thousand

Table C.25: Annual wave climate at Point 5, baseline, 2023 “present day”, significant wave height (H_s) against mean wave direction

			Wave direction											
			-15	15	45	75	105	135	165	195	225	255	285	315
H_{s1} (m)	H_{s2} (m)	$P(H_s>H_{s1})$	15	45	75	105	135	165	195	225	255	285	315	345
0	0.5	100.00%	6326	6922	4032	196	158	80	69	122	449	4648	28498	7248
0.5	1	41.25%	3318	3506	2283	-	<1	-	<1	<1	-	34	11874	4111
1	1.5	16.13%	1967	1713	185	-	-	-	-	-	-	-	3462	2273
1.5	2	6.53%	904	668	8	-	-	-	-	-	-	-	1136	1196
2	2.5	2.61%	403	243	-	-	-	-	-	-	-	-	286	641
2.5	3	1.04%	243	61	-	-	-	-	-	-	-	-	66	298
3	3.5	0.37%	124	13	-	-	-	-	-	-	-	-	14	101
3.5	4	0.12%	66	7	-	-	-	-	-	-	-	-	1	15
4	4.5	0.03%	21	<1	-	-	-	-	-	-	-	-	-	4
4.5	5	0.01%	7	-	-	-	-	-	-	-	-	-	-	-
	Percentage Occurrence		13.38%	13.13%	6.51%	0.20%	0.16%	0.08%	0.07%	0.12%	0.45%	4.68%	45.34%	15.89%

Source: HR Wallingford, SWAN wave transformation and Met Office WW3 offshore data, 1980 - 2015; occurrence is in parts per hundred thousand

Table C.26: Annual wave climate at Point 5, fully-built, 2023 "present day", significant wave height (H_s) against mean wave direction

			Wave direction											
			-15	15	45	75	105	135	165	195	225	255	285	315
H_{s1} (m)	H_{s2} (m)	$P(H_s>H_{s1})$	15	45	75	105	135	165	195	225	255	285	315	345
0	0.5	100.00%	6993	7910	2642	166	123	203	273	542	1544	7356	22470	100.00%
0.5	1	42.83%	3824	5108	481	-	-	<1	1	6	5	160	10099	42.83%
1	1.5	17.14%	2280	1832	7	-	-	-	-	-	-	-	2561	17.14%
1.5	2	7.10%	1021	660	<1	-	-	-	-	-	-	-	542	7.10%
2	2.5	2.88%	484	235	-	-	-	-	-	-	-	-	88	2.88%
2.5	3	1.12%	273	58	-	-	-	-	-	-	-	-	10	1.12%
3	3.5	0.40%	140	15	-	-	-	-	-	-	-	-	1	0.40%
3.5	4	0.13%	70	8	-	-	-	-	-	-	-	-	<1	0.13%
4	4.5	0.03%	23	1	-	-	-	-	-	-	-	-	-	0.03%
4.5	5	0.01%	7	-	-	-	-	-	-	-	-	-	-	0.01%
	Percentage Occurrence		15.11%	15.83%	3.13%	0.17%	0.12%	0.20%	0.27%	0.55%	1.55%	7.52%	35.77%	19.78%

Source: HR Wallingford, SWAN wave transformation and Met Office WW3 offshore data, 1980 - 2015; occurrence is in parts per hundred thousand

Table C.27: Annual wave climate at Point 5, part-built, 2023 “present day”, significant wave height (H_s) against mean wave direction

			Wave direction											
			-15	15	45	75	105	135	165	195	225	255	285	315
H_{s1} (m)	H_{s2} (m)	$P(H_s>H_{s1})$	15	45	75	105	135	165	195	225	255	285	315	345
0	0.5	100.00%	6640	7020	3560	229	229	238	319	700	2297	8744	21224	6537
0.5	1	42.26%	3568	4421	1392	-	-	1	1	2	5	98	10943	4982
1	1.5	16.85%	2154	1888	22	-	-	-	-	-	-	-	3052	2771
1.5	2	6.96%	960	682	<1	-	-	-	-	-	-	-	884	1582
2	2.5	2.85%	470	248	-	-	-	-	-	-	-	-	160	864
2.5	3	1.11%	264	61	-	-	-	-	-	-	-	-	31	357
3	3.5	0.40%	136	15	-	-	-	-	-	-	-	-	4	114
3.5	4	0.13%	68	8	-	-	-	-	-	-	-	-	-	16
4	4.5	0.04%	23	1	-	-	-	-	-	-	-	-	-	3
4.5	5	0.01%	8	-	-	-	-	-	-	-	-	-	-	-
	Percentage Occurrence		14.29%	14.35%	4.97%	0.23%	0.23%	0.24%	0.32%	0.70%	2.30%	8.84%	36.30%	17.23%

Source: HR Wallingford, SWAN wave transformation and Met Office WW3 offshore data, 1980 - 2015; occurrence is in parts per hundred thousand

Table C.28: Annual wave climate at Point 5, baseline, 2023 "present day", significant wave height (H_s) against mean wave period (T_{m-10})

			Mean Wave Period (T_{m-10}) in Seconds													
			0	1	2	3	4	5	6	7	8	9	10	11	12	13
H_{s1} (m)	H_{s2} (m)	$P(H_s>H_{s1})$	1	2	3	4	5	6	7	8	9	10	11	12	13	14
0	0.5	100.00%	8	2173	19091	23865	10464	2464	504	124	33	7	6	5	2	2
0.5	1	41.25%	-	3	303	8703	11594	3048	1246	218	10	1	-	-	-	-
1	1.5	16.13%	-	-	4	117	5167	3410	493	292	105	12	-	-	-	-
1.5	2	6.53%	-	-	-	3	173	2913	708	83	22	10	1	-	-	-
2	2.5	2.61%	-	-	-	<1	3	399	1003	151	12	5	-	-	-	-
2.5	3	1.04%	-	-	-	-	-	5	365	273	17	4	3	-	-	-
3	3.5	0.37%	-	-	-	-	-	-	10	211	23	5	2	-	-	-
3.5	4	0.12%	-	-	-	-	-	-	<1	32	54	2	<1	-	-	-
4	4.5	0.03%	-	-	-	-	-	-	-	1	21	3	<1	-	-	-
4.5	5	0.01%	-	-	-	-	-	-	-	<1	4	3	-	-	-	-
	Percentage Occurrence		0.01%	2.18%	19.40%	32.69%	27.40%	12.24%	4.33%	1.39%	0.30%	0.05%	0.01%	0.01%	0.00%	0.00%

Source: HR Wallingford, SWAN wave transformation and Met Office WW3 offshore data, 1980 - 2015; occurrence is in parts per hundred thousand

Table C.29: Annual wave climate at Point 5, fully-built, 2023 "present day", significant wave height (H_s) against mean wave period (T_{m-10})

			Mean Wave Period (T_{m-10}) in Seconds													
			0	1	2	3	4	5	6	7	8	9	10	11	12	13
H_{s1} (m)	H_{s2} (m)	$P(H_s>H_{s1})$	1	2	3	4	5	6	7	8	9	10	11	12	13	14
0	0.5	100.00%	5	1742	17975	23473	10765	2550	497	111	29	7	5	6	2	1
0.5	1	42.83%	-	4	352	9314	11513	3041	1249	203	11	<1	-	-	-	-
1	1.5	17.14%	-	-	5	169	5937	3005	505	322	96	7	-	-	-	-
1.5	2	7.10%	-	-	-	4	275	3209	597	77	33	14	2	-	-	-
2	2.5	2.88%	-	-	-	<1	4	536	1081	130	12	6	-	-	-	-
2.5	3	1.12%	-	-	-	-	-	6	430	259	13	4	4	-	-	-
3	3.5	0.40%	-	-	-	-	-	-	13	231	21	4	2	-	-	-
3.5	4	0.13%	-	-	-	-	-	-	<1	36	55	3	<1	-	-	-
4	4.5	0.03%	-	-	-	-	-	-	-	<1	22	4	<1	-	-	-
4.5	5	0.01%	-	-	-	-	-	-	-	-	4	3	-	-	-	-
	Percentage Occurrence		0.01%	1.75%	18.33%	32.96%	28.49%	12.35%	4.37%	1.37%	0.30%	0.05%	0.01%	0.01%	0.00%	0.00%

Source: HR Wallingford, SWAN wave transformation and Met Office WW3 offshore data, 1980 - 2015; occurrence is in parts per hundred thousand

Table C.30: Annual wave climate at Point 5, part-built, 2023 "present day", significant wave height (H_s) against mean wave period (T_{m-10})

			Mean Wave Period (T_{m-10}) in Seconds													
			0	1	2	3	4	5	6	7	8	9	10	11	12	13
H_{s1} (m)	H_{s2} (m)	$P(H_s>H_{s1})$	1	2	3	4	5	6	7	8	9	10	11	12	13	14
0	0.5	100.00%	6	1779	18299	23593	10808	2557	524	117	33	7	5	4	4	1
0.5	1	42.26%	-	4	306	9133	11420	3025	1284	231	10	<1	-	-	-	-
1	1.5	16.85%	-	-	4	141	5689	3155	474	307	107	10	-	-	-	-
1.5	2	6.96%	-	-	-	4	229	3143	610	80	29	13	2	-	-	-
2	2.5	2.85%	-	-	-	<1	3	506	1076	137	14	5	-	-	-	-
2.5	3	1.11%	-	-	-	-	-	5	417	268	15	4	4	-	-	-
3	3.5	0.40%	-	-	-	-	-	-	14	228	21	6	2	-	-	-
3.5	4	0.13%	-	-	-	-	-	-	<1	36	54	2	<1	-	-	-
4	4.5	0.04%	-	-	-	-	-	-	-	1	22	4	<1	-	-	-
4.5	5	0.01%	-	-	-	-	-	-	-	<1	5	3	-	-	-	-
	Percentage Occurrence		0.01%	1.78%	18.61%	32.87%	28.15%	12.39%	4.40%	1.41%	0.31%	0.05%	0.01%	0.00%	0.00%	0.00%

Source: HR Wallingford, SWAN wave transformation and Met Office WW3 offshore data, 1980 - 2015; occurrence is in parts per hundred thousand

Table C.31: Annual wave climate at Point 6, baseline, 2023 “present day”, significant wave height (H_s) against mean wave direction

			Wave direction											
			-15	15	45	75	105	135	165	195	225	255	285	315
H_{s1} (m)	H_{s2} (m)	$P(H_s>H_{s1})$	15	45	75	105	135	165	195	225	255	285	315	345
0	0.5	100.00%	14177	36245	17164	5663	3796	2807	1452	720	632	400	454	1059
0.5	1	15.43%	697	8524	3675	19	1	<1	-	-	-	-	-	-
1	1.5	2.51%	6	1583	469	-	-	-	-	-	-	-	-	-
1.5	2	0.46%	-	270	96	-	-	-	-	-	-	-	-	-
2	2.5	0.09%	-	65	12	-	-	-	-	-	-	-	-	-
2.5	3	0.01%	-	11	1	-	-	-	-	-	-	-	-	-
	Percentage Occurrence		14.88%	46.70%	21.42%	5.68%	3.80%	2.81%	1.45%	0.72%	0.63%	0.40%	0.45%	1.06%

Source: HR Wallingford, SWAN wave transformation and Met Office WW3 offshore data, 1980-2015; occurrence is in parts per hundred thousand

Table C.32: Annual wave climate at Point 6, fully-built, 2023 "present day", significant wave height (H_s) against mean wave direction

			Wave direction											
			-15	15	45	75	105	135	165	195	225	255	285	315
H_{s1} (m)	H_{s2} (m)	$P(H_s>H_{s1})$	15	45	75	105	135	165	195	225	255	285	315	345
0	0.5	100.00%	6766	39648	19086	7675	5333	2969	938	446	388	239	199	529
0.5	1	15.78%	61	9574	3587	23	2	<1	-	-	-	-	-	-
1	1.5	2.54%	-	1643	439	-	-	-	-	-	-	-	-	-
1.5	2	0.45%	-	291	76	-	-	-	-	-	-	-	-	-
2	2.5	0.09%	-	66	9	-	-	-	-	-	-	-	-	-
2.5	3	0.01%	-	11	<1	-	-	-	-	-	-	-	-	-
	Percentage Occurrence		6.83%	51.23%	23.20%	7.70%	5.33%	2.97%	0.94%	0.45%	0.39%	0.24%	0.20%	0.53%

Source: HR Wallingford, SWAN wave transformation and Met Office WW3 offshore data, 1980-2015; occurrence is in parts per hundred thousand

Table C.33: Annual wave climate at Point 6, part-built, 2023 “present day”, significant wave height (H_s) against mean wave direction

			Wave direction											
			-15	15	45	75	105	135	165	195	225	255	285	315
H_{s1} (m)	H_{s2} (m)	$P(H_s>H_{s1})$	15	45	75	105	135	165	195	225	255	285	315	345
0	0.5	100.00%	10702	38499	18101	6158	3946	2806	1382	664	573	351	350	864
0.5	1	15.60%	233	9243	3570	18	2	<1	-	-	-	-	-	-
1	1.5	2.54%	-	1635	446	-	-	-	-	-	-	-	-	-
1.5	2	0.46%	-	282	88	-	-	-	-	-	-	-	-	-
2	2.5	0.09%	-	63	12	-	-	-	-	-	-	-	-	-
2.5	3	0.01%	-	11	1	-	-	-	-	-	-	-	-	-
	Percentage Occurrence		10.93%	49.73%	22.22%	6.18%	3.95%	2.81%	1.38%	0.66%	0.57%	0.35%	0.35%	0.86%

Source: HR Wallingford, SWAN wave transformation and Met Office WW3 offshore data, 1980-2015; occurrence is in parts per hundred thousand

Table C.34: Annual wave climate at Point 6, baseline, 2023 "present day", significant wave height (H_s) against mean wave period (T_{m-10})

			Mean Wave Period (T_{m-10}) in Seconds													
			0	1	2	3	4	5	6	7	8	9	10	11	12	13
H_{s1} (m)	H_{s2} (m)	$P(H_s>H_{s1})$	1	2	3	4	5	6	7	8	9	10	11	12	13	14
0	0.5	100.00%	189	6378	21391	28119	19466	6759	1783	393	70	12	4	2	2	<1
0.5	1	15.43%	1	7	390	3288	4323	3130	1235	413	103	26	2	-	-	-
1	1.5	2.51%	-	-	<1	38	556	803	446	184	24	5	2	-	-	-
1.5	2	0.46%	-	-	-	-	13	125	129	75	24	<1	-	-	-	-
2	2.5	0.09%	-	-	-	-	-	12	30	20	15	-	-	-	-	-
2.5	3	0.01%	-	-	-	-	-	-	-	10	2	-	-	-	-	-
3	3.5	0.00%	-	-	-	-	-	-	-	-	-	-	-	-	-	-
3.5	4	0.00%	-	-	-	-	-	-	-	-	-	-	-	-	-	-
4	4.5	0.00%	-	-	-	-	-	-	-	-	-	-	-	-	-	-
4.5	5	0.00%	-	-	-	-	-	-	-	-	-	-	-	-	-	-
	Percentage Occurrence		0.19%	6.38%	21.78%	31.45%	24.36%	10.83%	3.62%	1.09%	0.24%	0.04%	0.01%	0.00%	0.00%	0.00%

Source: HR Wallingford, SWAN wave transformation and Met Office WW3 offshore data, 1980-2015; occurrence is in parts per hundred thousand

Table C.35: Annual wave climate at Point 6, fully-built, 2023 "present day", significant wave height (H_s) against mean wave period (T_{m-10})

			Mean Wave Period (T_{m-10}) in Seconds													
			0	1	2	3	4	5	6	7	8	9	10	11	12	13
H_{s1} (m)	H_{s2} (m)	$P(H_s>H_{s1})$	1	2	3	4	5	6	7	8	9	10	11	12	13	14
0	0.5	100.00%	158	6059	21238	28402	19482	6678	1733	384	63	13	4	2	2	<1
0.5	1	15.78%	<1	6	358	3266	4442	3315	1283	443	106	26	1	-	-	-
1	1.5	2.54%	-	-	<1	38	544	820	459	187	25	6	3	-	-	-
1.5	2	0.45%	-	-	-	-	11	123	132	74	26	<1	-	-	-	-
2	2.5	0.09%	-	-	-	-	-	12	29	20	14	-	-	-	-	-
2.5	3	0.01%	-	-	-	-	-	-	-	10	2	-	-	-	-	-
3	3.5	0.00%	-	-	-	-	-	-	-	-	-	-	-	-	-	-
3.5	4	0.00%	-	-	-	-	-	-	-	-	-	-	-	-	-	-
4	4.5	0.00%	-	-	-	-	-	-	-	-	-	-	-	-	-	-
4.5	5	0.00%	-	-	-	-	-	-	-	-	-	-	-	-	-	-
	Percentage Occurrence		0.16%	6.06%	21.60%	31.71%	24.48%	10.95%	3.64%	1.12%	0.24%	0.05%	0.01%	0.00%	0.00%	0.00%

Source: HR Wallingford, SWAN wave transformation and Met Office WW3 offshore data, 1980-2015; occurrence is in parts per hundred thousand

Table C.36: Annual wave climate at Point 6, part-built, 2023 “present day”, significant wave height (H_s) against mean wave period (T_{m-10})

			Mean Wave Period (T_{m-10}) in Seconds													
			0	1	2	3	4	5	6	7	8	9	10	11	12	13
H_{s1} (m)	H_{s2} (m)	$P(H_s>H_{s1})$	1	2	3	4	5	6	7	8	9	10	11	12	13	14
0	0.5	100.00%	157	5967	20938	28076	19713	7082	1924	438	81	12	5	2	2	<1
0.5	1	15.60%	1	8	407	3300	4273	3197	1285	457	109	27	2	-	-	-
1	1.5	2.54%	-	-	<1	39	565	799	450	189	29	5	4	-	-	-
1.5	2	0.46%	-	-	-	-	13	126	128	76	26	<1	-	-	-	-
2	2.5	0.09%	-	-	-	-	-	12	30	20	14	-	-	-	-	-
2.5	3	0.01%	-	-	-	-	-	-	-	10	2	-	-	-	-	-
3	3.5	0.00%	-	-	-	-	-	-	-	-	-	-	-	-	-	-
3.5	4	0.00%	-	-	-	-	-	-	-	-	-	-	-	-	-	-
4	4.5	0.00%	-	-	-	-	-	-	-	-	-	-	-	-	-	-
4.5	5	0.00%	-	-	-	-	-	-	-	-	-	-	-	-	-	-
	Percentage Occurrence		0.16%	5.97%	21.35%	31.41%	24.56%	11.22%	3.82%	1.19%	0.26%	0.04%	0.01%	0.00%	0.00%	0.00%

Source: HR Wallingford, SWAN wave transformation and Met Office WW3 offshore data, 1980-2015; occurrence is in parts per hundred thousand

Table C.37: Annual wave climate at Point 7, baseline, 2023 “present day”, significant wave height (H_s) against mean wave direction

			Wave direction											
			-15	15	45	75	105	135	165	195	225	255	285	315
H_{s1} (m)	H_{s2} (m)	$P(H_s>H_{s1})$	15	45	75	105	135	165	195	225	255	285	315	345
0	0.5	100.00%	4511	4186	4741	266	162	210	412	1364	4529	16307	9029	4695
0.5	1	49.59%	2853	2436	3757	1	-	<1	-	3	84	6719	10207	2708
1	1.5	20.82%	1740	1368	1005	-	-	-	-	-	-	315	5802	1794
1.5	2	8.80%	837	690	178	-	-	-	-	-	-	3	2452	969
2	2.5	3.67%	454	294	12	-	-	-	-	-	-	-	997	547
2.5	3	1.36%	209	78	4	-	-	-	-	-	-	-	351	268
3	3.5	0.45%	112	23	-	-	-	-	-	-	-	-	67	112
3.5	4	0.14%	54	14	-	-	-	-	-	-	-	-	10	29
4	4.5	0.03%	16	2	-	-	-	-	-	-	-	-	1	6
4.5	5	0.01%	10	-	-	-	-	-	-	-	-	-	-	-
	Percentage Occurrence		10.80%	9.09%	9.70%	0.27%	0.16%	0.21%	0.41%	1.37%	4.61%	23.34%	28.92%	11.13%

Source: HR Wallingford, SWAN wave transformation and Met Office WW3 offshore data, 1980 2015; occurrence is in parts per hundred thousand

Table C.38: Annual wave climate at Point 7, fully-built, 2023 “present day”, significant wave height (H_s) against mean wave direction

			Wave direction											
			-15	15	45	75	105	135	165	195	225	255	285	315
H_{s1} (m)	H_{s2} (m)	$P(H_s>H_{s1})$	15	45	75	105	135	165	195	225	255	285	315	345
0	0.5	100.00%	4778	5088	4122	70	35	50	99	151	460	18471	12457	5159
0.5	1	49.06%	2928	2655	3491	-	-	-	-	<1	5	4802	11791	2713
1	1.5	20.67%	1748	1403	961	-	-	-	-	-	-	85	5979	1763
1.5	2	8.74%	830	741	149	-	-	-	-	-	-	<1	2407	938
2	2.5	3.67%	455	313	15	-	-	-	-	-	-	-	982	540
2.5	3	1.36%	217	86	3	-	-	-	-	-	-	-	349	256
3	3.5	0.45%	111	29	-	-	-	-	-	-	-	-	67	109
3.5	4	0.14%	53	15	-	-	-	-	-	-	-	-	10	26
4	4.5	0.04%	17	2	-	-	-	-	-	-	-	-	<1	6
4.5	5	0.01%	10	-	-	-	-	-	-	-	-	-	-	-
	Percentage Occurrence		11.15%	10.33 %	8.74%	0.07%	0.03%	0.05%	0.10%	0.15%	0.47%	23.36%	34.04%	11.51%

Source: HR Wallingford, SWAN wave transformation and Met Office WW3 offshore data, 1980 2015; occurrence is in parts per hundred thousand

Table C.39: Annual wave climate at Point 7, part-built, 2023 “present day”, significant wave height (H_s) against mean wave direction

			Wave direction											
			-15	15	45	75	105	135	165	195	225	255	285	315
H_{s1} (m)	H_{s2} (m)	$P(H_s>H_{s1})$	15	45	75	105	135	165	195	225	255	285	315	345
0	0.5	100.00%	4826	4625	4416	139	68	81	121	225	977	16667	13498	5196
0.5	1	49.16%	2871	2475	3752	<1	-	-	-	-	2	4631	12021	2701
1	1.5	20.71%	1742	1338	1049	-	-	-	-	-	-	102	5954	1738
1.5	2	8.78%	850	713	185	-	-	-	-	-	-	<1	2405	944
2	2.5	3.69%	461	316	19	-	-	-	-	-	-	-	988	535
2.5	3	1.37%	220	88	4	-	-	-	-	-	-	-	341	262
3	3.5	0.45%	116	27	-	-	-	-	-	-	-	-	67	106
3.5	4	0.14%	53	15	-	-	-	-	-	-	-	-	10	24
4	4.5	0.04%	19	2	-	-	-	-	-	-	-	-	<1	5
4.5	5	0.01%	10	-	-	-	-	-	-	-	-	-	-	-
	Percentage Occurrence		11.17%	9.60%	9.42%	0.14%	0.07%	0.08%	0.12%	0.22%	0.98%	21.40%	35.28%	11.51%

Source: HR Wallingford, SWAN wave transformation and Met Office WW3 offshore data, 1980 2015; occurrence is in parts per hundred thousand

Table C.40: Annual wave climate at Point 7, baseline, 2023 "present day", significant wave height (H_s) against mean wave period (T_{m-10})

			Mean Wave Period (T_{m-10}) in Seconds													
			0	1	2	3	4	5	6	7	8	9	10	11	12	13
H_{s1} (m)	H_{s2} (m)	$P(H_s>H_{s1})$	1	2	3	4	5	6	7	8	9	10	11	12	13	14
0	0.5	100.00%	2	1353	17790	21909	7460	1437	346	80	19	7	4	4	2	<1
0.5	1	49.59%	-	3	426	12210	12525	2982	571	47	4	-	-	-	-	-
1	1.5	20.82%	-	-	3	261	8195	2533	773	237	22	<1	-	-	-	-
1.5	2	8.80%	-	-	-	6	722	3967	325	72	33	4	-	-	-	-
2	2.5	3.67%	-	-	-	1	9	1344	881	57	11	<1	-	-	-	-
2.5	3	1.36%	-	-	-	-	<1	30	754	114	7	4	-	-	-	-
3	3.5	0.45%	-	-	-	-	-	-	106	195	12	2	-	-	-	-
3.5	4	0.14%	-	-	-	-	-	-	2	87	13	3	<1	-	-	-
4	4.5	0.03%	-	-	-	-	-	-	-	6	18	<1	-	-	-	-
4.5	5	0.01%	-	-	-	-	-	-	-	<1	8	1	-	-	-	-
	Percentage Occurrence		0.00%	1.36%	18.22%	34.39%	28.91%	12.29%	3.76%	0.90%	0.15%	0.02%	0.00%	0.00%	0.00%	0.00%

Source: HR Wallingford, SWAN wave transformation and Met Office WW3 offshore data, 1980 2015; occurrence is in parts per hundred thousand

Table C.41: Annual wave climate at Point 7, fully-built, 2023 "present day", significant wave height (H_s) against mean wave period (T_{m-10})

			Mean Wave Period (T_{m-10}) in Seconds													
			0	1	2	3	4	5	6	7	8	9	10	11	12	13
H_{s1} (m)	H_{s2} (m)	$P(H_s>H_{s1})$	1	2	3	4	5	6	7	8	9	10	11	12	13	14
0	0.5	100.00%	2	1280	16793	22876	7978	1535	354	83	20	7	3	5	2	<1
0.5	1	49.06%	-	3	367	11990	12207	3121	642	51	4	-	-	-	-	-
1	1.5	20.67%	-	-	4	368	8155	2354	772	260	25	1	-	-	-	-
1.5	2	8.74%	-	-	-	4	1055	3570	333	68	31	3	-	-	-	-
2	2.5	3.67%	-	-	-	1	9	1418	808	57	11	<1	-	-	-	-
2.5	3	1.36%	-	-	-	-	<1	44	748	106	8	4	-	-	-	-
3	3.5	0.45%	-	-	-	-	-	-	113	190	12	2	-	-	-	-
3.5	4	0.14%	-	-	-	-	-	-	2	87	11	3	<1	-	-	-
4	4.5	0.04%	-	-	-	-	-	-	-	7	18	<1	-	-	-	-
4.5	5	0.01%	-	-	-	-	-	-	-	<1	8	1	-	-	-	-
	Percentage Occurrence		0.00%	1.28%	17.16%	35.24%	29.41%	12.04%	3.77%	0.91%	0.15%	0.02%	0.00%	0.01%	0.00%	0.00%

Source: HR Wallingford, SWAN wave transformation and Met Office WW3 offshore data, 1980 2015; occurrence is in parts per hundred thousand

Table C.42: Annual wave climate at Point 7, part-built, 2023 "present day", significant wave height (H_s) against mean wave period (T_{m-10})

			Mean Wave Period (T_{m-10}) in Seconds													
			0	1	2	3	4	5	6	7	8	9	10	11	12	13
H_{s1} (m)	H_{s2} (m)	$P(H_s>H_{s1})$	1	2	3	4	5	6	7	8	9	10	11	12	13	14
0	0.5	100.00%	2	1253	17313	22310	8010	1487	347	81	18	7	3	5	2	<1
0.5	1	49.16%	-	3	363	11781	12551	3062	639	51	4	-	-	-	-	-
1	1.5	20.71%	-	-	3	230	8074	2572	751	266	27	1	-	-	-	-
1.5	2	8.78%	-	-	-	3	688	3968	338	64	32	3	-	-	-	-
2	2.5	3.69%	-	-	-	1	10	1336	900	61	11	<1	-	-	-	-
2.5	3	1.37%	-	-	-	-	<1	28	755	120	8	4	-	-	-	-
3	3.5	0.45%	-	-	-	-	-	-	104	198	11	2	-	-	-	-
3.5	4	0.14%	-	-	-	-	-	-	2	83	14	3	<1	-	-	-
4	4.5	0.04%	-	-	-	-	-	-	-	6	19	<1	-	-	-	-
4.5	5	0.01%	-	-	-	-	-	-	-	<1	8	1	-	-	-	-
	Percentage Occurrence		0.00%	1.26%	17.68%	34.32%	29.33%	12.45%	3.84%	0.93%	0.15%	0.02%	0.00%	0.00%	0.00%	0.00%

Source: HR Wallingford, SWAN wave transformation and Met Office WW3 offshore data, 1980 2015; occurrence is in parts per hundred thousand

Table C.43: Annual wave climate at Point 8, baseline, 2023 “present day”, significant wave height (Hs) against mean wave direction

			Wave direction											
			-15	15	45	75	105	135	165	195	225	255	285	315
H_{s1} (m)	H_{s2} (m)	$P(H_s>H_{s1})$	15	45	75	105	135	165	195	225	255	285	315	345
0	0.5	100.00%	6397	6607	3883	161	85	90	177	349	1020	6463	23855	7452
0.5	1	43.46%	3466	4282	1411	<1	-	-	-	<1	<1	83	12135	4336
1	1.5	17.75%	2182	1708	44	-	-	-	-	-	-	-	3364	2855
1.5	2	7.60%	992	531	-	-	-	-	-	-	-	-	1277	1574
2	2.5	3.22%	545	183	-	-	-	-	-	-	-	-	218	1151
2.5	3	1.13%	297	35	-	-	-	-	-	-	-	-	38	405
3	3.5	0.35%	121	19	-	-	-	-	-	-	-	-	4	122
3.5	4	0.08%	42	4	-	-	-	-	-	-	-	-	-	25
4	4.5	0.01%	9	-	-	-	-	-	-	-	-	-	-	3
4.5	5	0.00%	1	-	-	-	-	-	-	-	-	-	-	-
	Percentage Occurrence		14.05%	13.37%	5.34%	0.16%	0.08%	0.09%	0.18%	0.35%	1.02%	6.55%	40.89%	17.92%

Source: HR Wallingford, SWAN wave transformation and Met Office WW3 offshore data, 1980 2015; occurrence is in parts per hundred thousand

Table C.44: Annual wave climate at Point 8, fully-built, 2023 “present day”, significant wave height (Hs) against mean wave direction

			Wave direction											
			-15	15	45	75	105	135	165	195	225	255	285	315
H_{s1} (m)	H_{s2} (m)	$P(H_s>H_{s1})$	15	45	75	105	135	165	195	225	255	285	315	345
0	0.5	100.00%	10904	5988	3	1	4	<1	2	11	121	5721	24926	10693
0.5	1	41.63%	5294	2246	-	-	-	-	-	-	-	69	8992	7144
1	1.5	17.88%	2981	565	-	-	-	-	-	-	-	-	1539	4498
1.5	2	8.30%	1392	179	-	-	-	-	-	-	-	-	244	2540
2	2.5	3.94%	771	63	-	-	-	-	-	-	-	-	8	1547
2.5	3	1.55%	510	21	-	-	-	-	-	-	-	-	4	494
3	3.5	0.52%	169	12	-	-	-	-	-	-	-	-	-	190
3.5	4	0.15%	70	2	-	-	-	-	-	-	-	-	-	48
4	4.5	0.03%	16	-	-	-	-	-	-	-	-	-	-	14
4.5	5	0.00%	2	-	-	-	-	-	-	-	-	-	-	2
	Percentage Occurrence		22.11%	9.08%	0.00%	0.00%	0.00%	0.00%	0.00%	0.01%	0.12%	5.79%	35.71%	27.17%

Source: HR Wallingford, SWAN wave transformation and Met Office WW3 offshore data, 1980 2015; occurrence is in parts per hundred thousand

Table C.45: Annual wave climate at Point 8, part-built, 2023 “present day”, significant wave height (Hs) against mean wave direction

			Wave direction										
			-15	15	45	75	105	135	165	195	225	255	285	315
H_{s1} (m)	H_{s2} (m)	$P(H_s>H_{s1})$	15	45	75	105	135	165	195	225	255	285	315	345
0	0.5	100.00%	7976	9682	156	23	14	16	45	153	982	7112	21886	8221
0.5	1	43.73%	4097	5238	<1	-	-	-	-	-	-	83	9269	6437
1	1.5	18.61%	2568	1552	-	-	-	-	-	-	-	-	1824	4293
1.5	2	8.37%	1206	475	-	-	-	-	-	-	-	-	334	2581
2	2.5	3.78%	644	166	-	-	-	-	-	-	-	-	22	1524
2.5	3	1.42%	401	37	-	-	-	-	-	-	-	-	4	501
3	3.5	0.48%	134	18	-	-	-	-	-	-	-	-	-	199
3.5	4	0.13%	51	6	-	-	-	-	-	-	-	-	-	46
4	4.5	0.02%	14	2	-	-	-	-	-	-	-	-	-	7
4.5	5	0.00%	1	-	-	-	-	-	-	-	-	-	-	-
	Percentage Occurrence		17.09%	17.17%	0.16%	0.02%	0.01%	0.02%	0.05%	0.15%	0.98%	7.19%	33.34%	23.81%

Source: HR Wallingford, SWAN wave transformation and Met Office WW3 offshore data, 1980 2015; occurrence is in parts per hundred thousand

Table C.46: Annual wave climate at Point 8, baseline, 2023 "present day", significant wave height (H_s) against mean wave period (T_{m-10})

			Mean Wave Period (T_{m-10}) in Seconds													
			0	1	2	3	4	5	6	7	8	9	10	11	12	13
H_{s1} (m)	H_{s2} (m)	$P(H_s>H_{s1})$	1	2	3	4	5	6	7	8	9	10	11	12	13	14
0	0.5	100.00%	6	1651	17202	22720	11224	2830	661	174	45	10	7	5	3	1
0.5	1	43.46%	-	3	316	8845	11182	3589	1464	288	23	2	-	-	-	-
1	1.5	17.75%	-	-	4	137	5417	3358	655	461	113	7	<1	-	-	-
1.5	2	7.60%	-	-	-	4	257	3209	663	126	88	24	2	-	-	-
2	2.5	3.22%	-	-	-	<1	5	630	1232	198	21	10	1	-	-	-
2.5	3	1.13%	-	-	-	-	-	5	330	402	30	7	<1	-	-	-
3	3.5	0.35%	-	-	-	-	-	-	8	187	62	4	5	-	-	-
3.5	4	0.08%	-	-	-	-	-	-	<1	21	37	12	1	-	-	-
4	4.5	0.01%	-	-	-	-	-	-	-	<1	7	2	2	<1	-	-
4.5	5	0.00%	-	-	-	-	-	-	-	-	<1	<1	-	-	-	-
	Percentage Occurrence		0.01%	1.65%	17.52%	31.71%	28.09%	13.62%	5.01%	1.86%	0.43%	0.08%	0.02%	0.01%	0.00%	0.00%

Source: HR Wallingford, SWAN wave transformation and Met Office WW3 offshore data, 1980 2015; occurrence is in parts per hundred thousand

Table C.47: Annual wave climate at Point 8, fully-built, 2023 "present day", significant wave height (H_s) against mean wave period (T_{m-10})

			Mean Wave Period (T_{m-10}) in Seconds													
			0	1	2	3	4	5	6	7	8	9	10	11	12	13
H_{s1} (m)	H_{s2} (m)	$P(H_s>H_{s1})$	1	2	3	4	5	6	7	8	9	10	11	12	13	14
0	0.5	100.00%	5	1186	13635	24426	13227	4366	1086	322	78	25	6	8	3	2
0.5	1	41.63%	-	4	242	7154	9992	3966	1841	484	58	3	2	-	-	-
1	1.5	17.88%	-	-	3	192	5337	2643	718	520	159	10	<1	-	-	-
1.5	2	8.30%	-	-	-	3	628	2808	603	156	114	42	2	-	-	-
2	2.5	3.94%	-	-	-	-	18	1124	1057	138	29	19	5	-	-	-
2.5	3	1.55%	-	-	-	<1	-	25	566	396	32	7	2	-	-	-
3	3.5	0.52%	-	-	-	-	-	<1	32	259	69	7	3	<1	-	-
3.5	4	0.15%	-	-	-	-	-	-	<1	57	51	7	3	-	-	-
4	4.5	0.03%	-	-	-	-	-	-	-	5	15	8	2	-	-	-
4.5	5	0.00%	-	-	-	-	-	-	-	-	<1	1	2	<1	-	-
	Percentage Occurrence		0.01%	1.19%	13.88%	31.77%	29.20%	14.93%	5.90%	2.34%	0.61%	0.13%	0.03%	0.01%	0.00%	0.00%

Source: HR Wallingford, SWAN wave transformation and Met Office WW3 offshore data, 1980 2015; occurrence is in parts per hundred thousand

Table C.48: Annual wave climate at Point 8, part-built, 2023 "present day", significant wave height (H_s) against mean wave period (T_{m-10})

			Mean Wave Period (T_{m-10}) in Seconds													
			0	1	2	3	4	5	6	7	8	9	10	11	12	13
H_{s1} (m)	H_{s2} (m)	$P(H_s>H_{s1})$	1	2	3	4	5	6	7	8	9	10	11	12	13	14
0	0.5	100.00%	4	1171	14964	22828	12261	3865	875	207	60	13	6	6	4	1
0.5	1	43.73%	-	5	304	8748	10229	3738	1678	384	35	3	1	-	-	-
1	1.5	18.61%	-	-	4	268	5821	2763	747	510	114	8	<1	-	-	-
1.5	2	8.37%	-	-	-	5	578	3079	607	164	119	42	3	-	-	-
2	2.5	3.78%	-	-	-	1	16	1068	1069	157	30	11	4	-	-	-
2.5	3	1.42%	-	-	-	<1	-	18	541	345	29	8	<1	-	-	-
3	3.5	0.48%	-	-	-	-	-	-	26	253	59	8	5	-	-	-
3.5	4	0.13%	-	-	-	-	-	-	<1	51	43	7	1	-	-	-
4	4.5	0.02%	-	-	-	-	-	-	-	2	14	4	2	<1	-	-
4.5	5	0.00%	-	-	-	-	-	-	-	-	<1	<1	-	-	-	-
	Percentage Occurrence		0.00%	1.18%	15.27%	31.85%	28.91%	14.53%	5.54%	2.07%	0.50%	0.11%	0.02%	0.01%	0.00%	0.00%

Source: HR Wallingford, SWAN wave transformation and Met Office WW3 offshore data, 1980 2015; occurrence is in parts per hundred thousand

Table C.49: Annual wave climate at Point 9, baseline, 2023 “present day”, significant wave height (Hs) against mean wave direction

			Wave direction											
			-15	15	45	75	105	135	165	195	225	255	285	315
H_{s1} (m)	H_{s2} (m)	$P(H_s>H_{s1})$	15	45	75	105	135	165	195	225	255	285	315	345
0	0.5	100.00%	11619	11458	1448	401	369	662	1535	2122	2139	3040	9683	20818
0.5	1	34.71%	6237	3546	5	-	<1	-	<1	<1	5	20	652	11335
1	1.5	12.90%	3391	682	-	-	-	-	-	-	-	-	13	3963
1.5	2	4.86%	1476	202	-	-	-	-	-	-	-	-	-	1621
2	2.5	1.56%	665	25	-	-	-	-	-	-	-	-	-	475
2.5	3	0.39%	191	7	-	-	-	-	-	-	-	-	-	110
3	3.5	0.08%	52	-	-	-	-	-	-	-	-	-	-	23
3.5	4	0.01%	7	-	-	-	-	-	-	-	-	-	-	2
4	4.5	0.00%	-	-	-	-	-	-	-	-	-	-	-	<1
	Percentage Occurrence		23.64%	15.92%	1.45%	0.40%	0.37%	0.66%	1.54%	2.12%	2.14%	3.06%	10.35%	38.35%

Source: HR Wallingford, SWAN wave transformation and Met Office WW3 offshore data, 1980-2015; occurrence is in parts per hundred thousand

Table C.50: Annual wave climate at Point 9, baseline, 2023 "present day", significant wave height (H_s) against mean wave period (T_{m-10})

			Mean Wave Period (T_{m-10}) in Seconds													
			0	1	2	3	4	5	6	7	8	9	10	11	12	13
H_{s1} (m)	H_{s2} (m)	$P(H_s>H_{s1})$	1	2	3	4	5	6	7	8	9	10	11	12	13	14
0	0.5	100.00%	31	2858	19461	23863	13055	4447	1156	297	86	23	6	9	2	<1
0.5	1	34.71%	-	4	238	6120	9570	3425	1728	608	98	9	1	-	-	-
1	1.5	12.90%	-	-	2	74	2833	3482	898	532	196	30	1	-	-	-
1.5	2	4.86%	-	-	-	2	122	1693	994	344	91	44	9	-	-	-
2	2.5	1.56%	-	-	-	<1	<1	142	575	343	76	20	8	-	-	-
2.5	3	0.39%	-	-	-	-	-	-	45	213	44	4	2	<1	-	-
3	3.5	0.08%	-	-	-	-	-	-	<1	30	35	6	2	2	-	-
3.5	4	0.01%	-	-	-	-	-	-	-	-	5	2	2	-	-	-
4	4.5	0.00%	-	-	-	-	-	-	-	-	-	-	-	<1	-	-
4.5	5	0.00%	-	-	-	-	-	-	-	-	-	-	-	-	-	-
	Percentage Occurrence		0.03%	2.86%	19.70%	30.06%	25.58%	13.19%	5.40%	2.37%	0.63%	0.14%	0.03%	0.01%	0.00%	0.00%

Source: HR Wallingford, SWAN wave transformation and Met Office WW3 offshore data, 1980-2015; occurrence is in parts per hundred thousand

Table C.51: Annual wave climate at Point 10, baseline, 2023 “present day”, significant wave height (H_s) against mean wave direction

			Wave direction											
			-15	15	45	75	105	135	165	195	225	255	285	315
H_{s1} (m)	H_{s2} (m)	$P(H_s>H_{s1})$	15	45	75	105	135	165	195	225	255	285	315	345
0	0.5	100.00%	5661	8727	890	73	31	33	55	230	1635	19483	13797	6038
0.5	1	43.35%	3371	4983	4	-	-	-	-	<1	9	3014	11855	3081
1	1.5	17.03%	1961	1446	-	-	-	-	-	-	-	7	4638	2084
1.5	2	6.89%	905	404	-	-	-	-	-	-	-	-	1760	1157
2	2.5	2.67%	422	110	-	-	-	-	-	-	-	-	528	609
2.5	3	1.00%	213	20	-	-	-	-	-	-	-	-	183	247
3	3.5	0.33%	99	3	-	-	-	-	-	-	-	-	24	104
3.5	4	0.10%	61	1	-	-	-	-	-	-	-	-	3	14
4	4.5	0.02%	13	<1	-	-	-	-	-	-	-	-	-	4
4.5	5	0.01%	7	-	-	-	-	-	-	-	-	-	-	-
	Percentage Occurrence		12.71%	15.69%	0.89%	0.07%	0.03%	0.03%	0.06%	0.23%	1.64%	22.50%	32.79%	13.34%

Source: HR Wallingford, SWAN wave transformation and Met Office WW3 offshore data, 1980-2015; occurrence is in parts per hundred thousand

Table C.52: Annual wave climate at Point 10, fully-built, 2023 "present day", significant wave height (H_s) against mean wave direction

			Wave direction											
			-15	15	45	75	105	135	165	195	225	255	285	315
H_{s1} (m)	H_{s2} (m)	$P(H_s>H_{s1})$	15	45	75	105	135	165	195	225	255	285	315	345
0	0.5	100.00%	8339	8892	1962	185	102	149	319	720	4485	18144	17528	7762
0.5	1	31.41%	4372	5218	176	-	-	-	<1	2	10	194	4768	4911
1	1.5	11.76%	2484	1763	2	-	-	-	-	-	-	-	884	2104
1.5	2	4.53%	1180	515	-	-	-	-	-	-	-	-	193	936
2	2.5	1.70%	493	143	-	-	-	-	-	-	-	-	27	394
2.5	3	0.64%	265	30	-	-	-	-	-	-	-	-	9	98
3	3.5	0.24%	111	4	-	-	-	-	-	-	-	-	-	31
3.5	4	0.09%	63	2	-	-	-	-	-	-	-	-	-	4
4	4.5	0.03%	16	<1	-	-	-	-	-	-	-	-	-	1
4.5	5	0.01%	7	-	-	-	-	-	-	-	-	-	-	-
	Percentage Occurrence		17.33%	16.57%	2.14%	0.18%	0.10%	0.15%	0.32%	0.72%	4.49%	18.34%	23.41%	16.24%

Source: HR Wallingford, SWAN wave transformation and Met Office WW3 offshore data, 1980-2015; occurrence is in parts per hundred thousand

Table C.53: Annual wave climate at Point 10, part-built, 2023 “present day”, significant wave height (H_s) against mean wave direction

			Wave direction										
			-15	15	45	75	105	135	165	195	225	255	285	315
H_{s1} (m)	H_{s2} (m)	$P(H_s>H_{s1})$	15	45	75	105	135	165	195	225	255	285	315	345
0	0.5	100.00%	5541	8321	1000	55	34	36	37	166	1084	13545	19826	6529
0.5	1	43.83%	3120	5279	14	-	-	-	-	-	<1	1634	13252	2984
1	1.5	17.54%	1917	1613	-	-	-	-	-	-	-	-	4908	2153
1.5	2	6.95%	866	485	-	-	-	-	-	-	-	-	1777	1177
2	2.5	2.65%	449	164	-	-	-	-	-	-	-	-	564	589
2.5	3	0.88%	230	36	-	-	-	-	-	-	-	-	89	219
3	3.5	0.31%	123	8	-	-	-	-	-	-	-	-	19	84
3.5	4	0.07%	44	2	-	-	-	-	-	-	-	-	1	7
4	4.5	0.02%	13	<1	-	-	-	-	-	-	-	-	-	<1
4.5	5	0.00%	4	-	-	-	-	-	-	-	-	-	-	-
	Percentage Occurrence		12.31%	15.91%	1.01%	0.06%	0.03%	0.04%	0.04%	0.17%	1.08%	15.18%	40.44%	13.74%

Source: HR Wallingford, SWAN wave transformation and Met Office WW3 offshore data, 1980-2015; occurrence is in parts per hundred thousand

Table C.54: Annual wave climate at Point 10, baseline, 2023 "present day", significant wave height (H_s) against mean wave period (T_{m-10})

			Mean Wave Period (T_{m-10}) in Seconds													
			0	1	2	3	4	5	6	7	8	9	10	11	12	13
H_{s1} (m)	H_{s2} (m)	$P(H_s>H_{s1})$	1	2	3	4	5	6	7	8	9	10	11	12	13	14
0	0.5	100.00%	7	1836	19053	23942	9436	1859	388	93	19	8	3	5	2	1
0.5	1	43.35%	-	3	371	10075	11859	2917	983	108	3	<1	-	-	-	-
1	1.5	17.03%	-	-	7	186	6510	2685	442	248	52	3	-	-	-	-
1.5	2	6.89%	-	-	-	3	393	3322	428	58	18	5	-	-	-	-
2	2.5	2.67%	-	-	-	1	4	648	942	63	8	3	-	-	-	-
2.5	3	1.00%	-	-	-	-	-	6	464	182	8	4	-	-	-	-
3	3.5	0.33%	-	-	-	-	-	-	31	184	12	3	-	-	-	-
3.5	4	0.10%	-	-	-	-	-	-	1	48	28	2	<1	-	-	-
4	4.5	0.02%	-	-	-	-	-	-	-	2	15	<1	-	-	-	-
4.5	5	0.01%	-	-	-	-	-	-	-	<1	5	1	-	-	-	-
	Percentage Occurrence		0.01%	1.84%	19.43%	34.21%	28.20%	11.44%	3.68%	0.99%	0.17%	0.03%	0.00%	0.01%	0.00%	0.00%

Source: HR Wallingford, SWAN wave transformation and Met Office WW3 offshore data, 1980-2015; occurrence is in parts per hundred thousand

Table C.55: Annual wave climate at Point 10, fully-built, 2023 "present day", significant wave height (H_s) against mean wave period (T_{m-10})

			Mean Wave Period (T_{m-10}) in Seconds													
			0	1	2	3	4	5	6	7	8	9	10	11	12	13
H_{s1} (m)	H_{s2} (m)	$P(H_s>H_{s1})$	1	2	3	4	5	6	7	8	9	10	11	12	13	14
0	0.5	100.00%	56	4555	20586	25903	13100	3612	647	93	19	6	4	4	<1	1
0.5	1	31.41%	<1	7	295	5587	9624	2553	1114	393	71	5	-	-	-	-
1	1.5	11.76%	-	-	2	122	3276	3231	468	89	34	14	<1	-	-	-
1.5	2	4.53%	-	-	<1	3	136	1752	792	125	7	7	2	-	-	-
2	2.5	1.70%	-	-	-	-	2	205	638	193	18	2	1	-	-	-
2.5	3	0.64%	-	-	-	-	<1	3	191	189	13	5	2	-	-	-
3	3.5	0.24%	-	-	-	-	-	-	8	117	20	<1	<1	-	-	-
3.5	4	0.09%	-	-	-	-	-	-	<1	16	51	1	-	-	-	-
4	4.5	0.03%	-	-	-	-	-	-	-	<1	15	2	-	-	-	-
4.5	5	0.01%	-	-	-	-	-	-	-	-	3	4	-	-	-	-
	Percentage Occurrence		0.06%	4.56%	20.88%	31.62%	26.14%	11.36%	3.86%	1.22%	0.25%	0.05%	0.01%	0.00%	0.00%	0.00%

Source: HR Wallingford, SWAN wave transformation and Met Office WW3 offshore data, 1980-2015; occurrence is in parts per hundred thousand

Table C.56: Annual wave climate at Point 10, part-built, 2023 "present day", significant wave height (H_s) against mean wave period (T_{m-10})

			Mean Wave Period (T_{m-10}) in Seconds													
			0	1	2	3	4	5	6	7	8	9	10	11	12	13
H_{s1} (m)	H_{s2} (m)	$P(H_s>H_{s1})$	1	2	3	4	5	6	7	8	9	10	11	12	13	14
0	0.5	100.00%	3	1338	16748	24076	11062	2341	466	99	21	8	4	5	2	
0.5	1	43.83%	-	3	290	9932	11353	3265	1221	210	8	<1	-	-	-	
1	1.5	17.54%	-	-	4	190	6524	2936	563	300	69	5	-	-	-	
1.5	2	6.95%	-	-	-	4	412	3222	530	94	35	8	-	-	-	
2	2.5	2.65%	-	-	-	<1	4	660	948	133	13	7	-	-	-	
2.5	3	0.88%	-	-	-	-	-	4	392	163	10	3	2	-	-	
3	3.5	0.31%	-	-	-	-	-	-	32	182	15	4	<1	-	-	
3.5	4	0.07%	-	-	-	-	-	-	<1	25	27	<1	<1	-	-	
4	4.5	0.02%	-	-	-	-	-	-	-	2	11	1	-	-	-	
4.5	5	0.00%	-	-	-	-	-	-	-	<1	4	-	-	-	-	
	Percentage Occurrence		0.00%	1.34%	17.04%	34.20%	29.36%	12.43%	4.15%	1.21%	0.21%	0.04%	0.01%	0.01%	0.00%	0.00%

Source: HR Wallingford, SWAN wave transformation and Met Office WW3 offshore data, 1980-2015; occurrence is in parts per hundred thousand

C.2. Summer (Apr-Sep) conditions

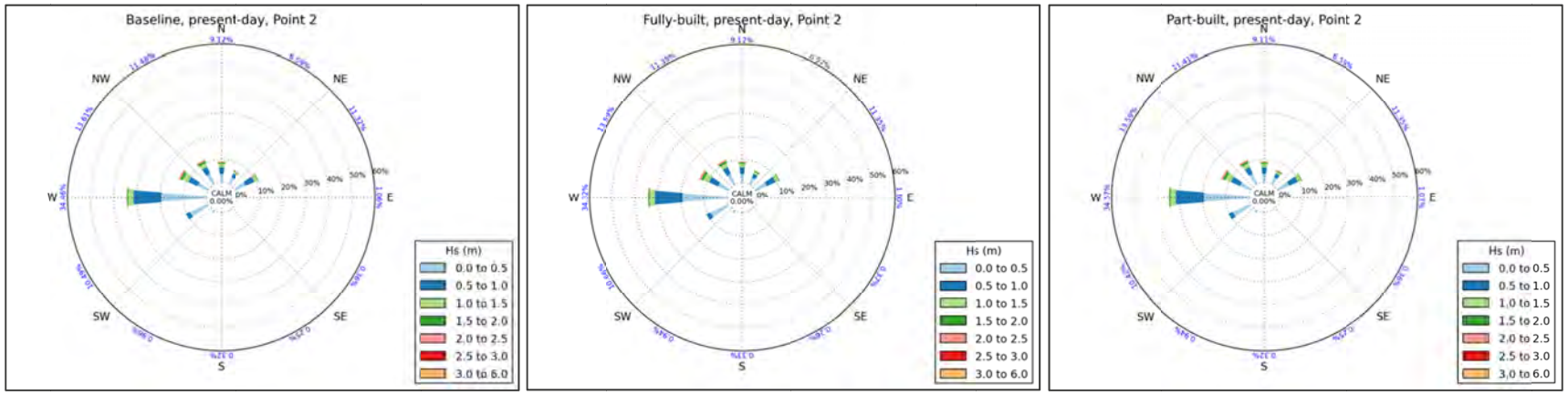

Figure C.10: Summer wave roses for nearshore prediction Point 2, present-day, baseline, part-built and fully-built layouts

Source: HR Wallingford, SWAN wave transformation and Met Office WW3 offshore data, 1980-2015

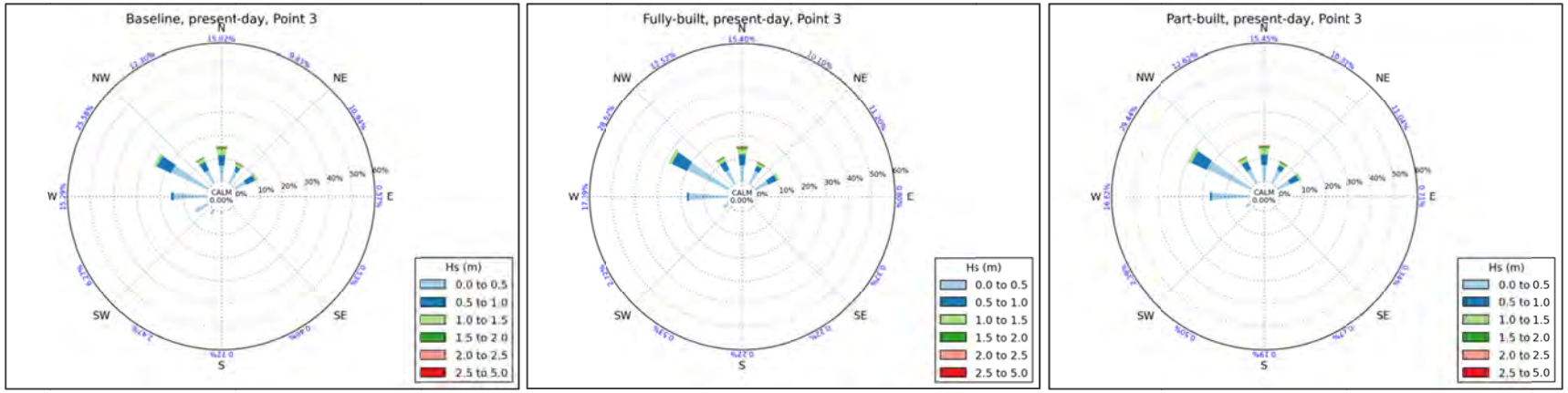

Figure C.11: Summer wave roses for nearshore prediction Point 3, present-day, baseline, part-built and fully-built layouts

Source: HR Wallingford, SWAN wave transformation and Met Office WW3 offshore data, 1980-2015

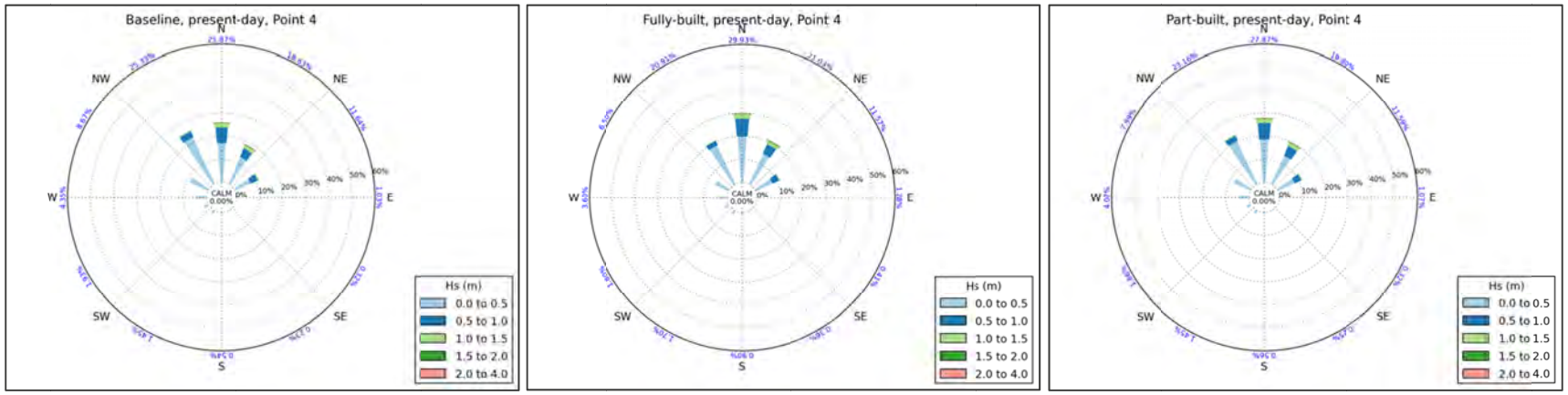

Figure C.12: Summer wave roses for nearshore prediction Point 4, present-day, baseline, part-built and fully-built layouts

Source: HR Wallingford, SWAN wave transformation and Met Office WW3 offshore data, 1980-2015

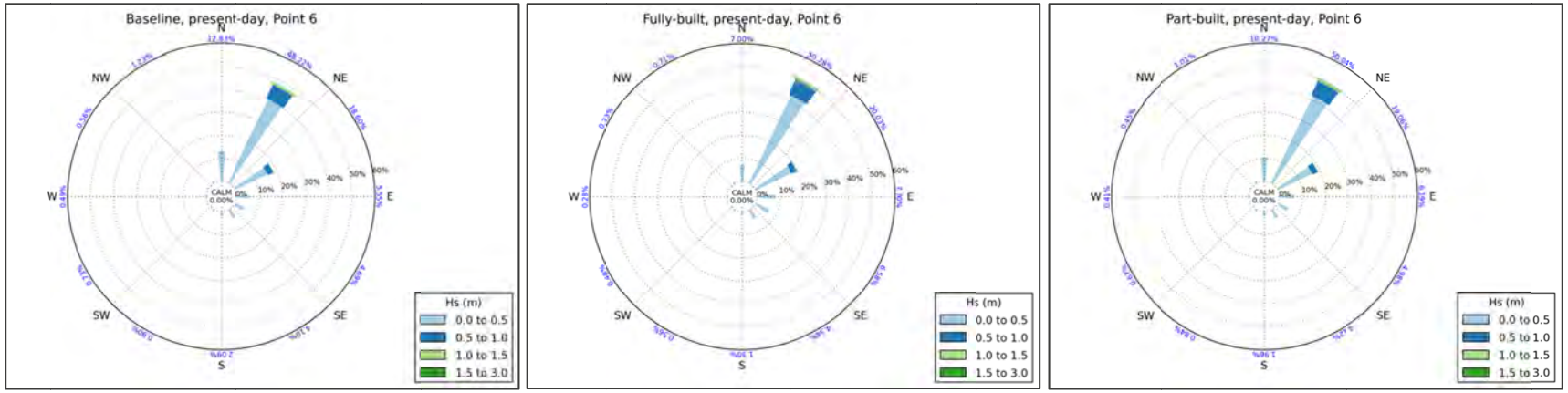

Figure C.13: Summer wave roses for nearshore prediction Point 6, present-day, baseline, part-built and fully-built layouts

Source: HR Wallingford, SWAN wave transformation and Met Office WW3 offshore data, 1980-2015

Table C.57: Summer wave climate at Point 2, baseline, 2023 “present day”, significant wave height (Hs) against mean wave direction

			Wave direction											
			-15	15	45	75	105	135	165	195	225	255	285	315
			15	45	75	105	135	165	195	225	255	285	315	345
H_{s1} (m)	H_{s2} (m)	$P(H_s>H_{s1})$												
0	0.5	100.00%	3719	3194	5269	879	308	227	284	878	8477	19461	4983	4952
0.5	1	47.37%	2949	1843	4145	177	51	28	33	76	1933	12062	4323	3206
1	1.5	16.54%	1543	818	1468	-	-	-	-	1	75	2301	2570	1818
1.5	2	5.95%	476	386	342	-	-	-	-	-	1	501	1064	890
2	2.5	2.29%	266	160	57	-	-	-	-	-	-	123	477	367
2.5	3	0.84%	106	109	30	-	-	-	-	-	-	11	159	140
3	3.5	0.29%	52	48	4	-	-	-	-	-	-	1	30	93
3.5	4	0.06%	5	11	1	-	-	-	-	-	-	-	4	12
4	4.5	0.03%	2	17	-	-	-	-	-	-	-	-	-	-
4.5	5	0.01%	1	2	-	-	-	-	-	-	-	-	-	-
5	5.5	0.00%	2	1	-	-	-	-	-	-	-	-	-	-
5.5	6	0.00%	-	-	-	-	-	-	-	-	-	-	-	-
	Percentage Occurrence		9.12%	6.59%	11.32%	1.06%	0.36%	0.25%	0.32%	0.96%	10.49%	34.46%	13.61%	11.48%

Source: HR Wallingford, SWAN wave transformation and Met Office WW3 offshore data, 19802015

Table C.58: Summer wave climate at Point 2, fully-built, 2023 “present day”, significant wave height (Hs) against mean wave direction

			Wave direction											
			-15	15	45	75	105	135	165	195	225	255	285	315
			15	45	75	105	135	165	195	225	255	285	315	345
H_{s1} (m)	H_{s2} (m)	$P(H_s>H_{s1})$												
0	0.5	100.00%	3687	3165	5302	914	317	231	298	860	8599	19316	4987	4894
0.5	1	47.43%	2958	1844	4139	182	51	29	33	79	1962	12066	4324	3195
1	1.5	16.57%	1555	824	1475	-	-	-	-	1	100	2296	2559	1809
1.5	2	5.95%	482	385	342	-	-	-	-	-	1	505	1062	883
2	2.5	2.29%	269	161	57	-	-	-	-	-	-	123	468	370
2.5	3	0.84%	111	109	30	-	-	-	-	-	-	11	158	135
3	3.5	0.29%	52	48	4	-	-	-	-	-	-	1	30	94
3.5	4	0.06%	5	11	1	-	-	-	-	-	-	-	4	12
4	4.5	0.03%	2	17	-	-	-	-	-	-	-	-	-	-
4.5	5	0.01%	1	2	-	-	-	-	-	-	-	-	-	-
5	5.5	0.00%	2	1	-	-	-	-	-	-	-	-	-	-
5.5	6	0.00%	-	-	-	-	-	-	-	-	-	-	-	-
	Percentage Occurrence		9.12%	6.57%	11.35%	1.10%	0.37%	0.26%	0.33%	0.94%	10.66%	34.32%	13.59%	11.39%

Source: HR Wallingford, SWAN wave transformation and Met Office WW3 offshore data, 1980-2015

Table C.59: Summer wave climate at Point 2, part-built, 2023 “present day”, significant wave height (Hs) against mean wave direction

			Wave direction											
			-15	15	45	75	105	135	165	195	225	255	285	315
			15	45	75	105	135	165	195	225	255	285	315	345
H_{s1} (m)	H_{s2} (m)	$P(H_s>H_{s1})$												
0	0.5	100.00%	3698	3199	5296	893	308	229	282	863	8392	19459	4984	4908
0.5	1	47.49%	2950	1833	4149	181	51	25	38	75	1953	12156	4308	3193
1	1.5	16.58%	1551	823	1470	-	-	-	-	1	78	2316	2573	1817
1.5	2	5.95%	478	385	345	-	-	-	-	-	1	502	1065	886
2	2.5	2.29%	265	161	58	-	-	-	-	-	-	124	472	367
2.5	3	0.84%	110	109	29	-	-	-	-	-	-	11	158	135
3	3.5	0.29%	53	48	4	-	-	-	-	-	-	1	30	95
3.5	4	0.06%	4	11	1	-	-	-	-	-	-	-	4	12
4	4.5	0.03%	2	17	-	-	-	-	-	-	-	-	-	-
4.5	5	0.01%	1	2	-	-	-	-	-	-	-	-	-	-
5	5.5	0.00%	2	1	-	-	-	-	-	-	-	-	-	-
5.5	6	0.00%	-	-	-	-	-	-	-	-	-	-	-	-
	Percentage Occurrence		9.11%	6.59%	11.35%	1.07%	0.36%	0.25%	0.32%	0.94%	10.42%	34.57%	13.59%	11.41%

Source: HR Wallingford, SWAN wave transformation and Met Office WW3 offshore data, 1980-2015

Table C.60: Summer wave climate at Point 2, baseline, 2023 "present day", significant wave height (H_s) against mean wave period (T_{m-10})

			Mean Wave Period (Tm-10) in Seconds												
			0	1	2	3	4	5	6	7	8	9	10	11	12
			1	2	3	4	5	6	7	8	9	10	11	12	13
H_{s1} (m)	H_{s2} (m)	$P(H_s>H_{s1})$													
0	0.5	100.00%	1	647	19023	25408	6655	751	97	22	12	4	7	2	1
0.5	1	47.37%	-	-	722	16087	12846	1128	39	4	-	-	-	-	-
1	1.5	16.54%	-	-	-	794	7953	1668	172	6	-	-	-	-	-
1.5	2	5.95%	-	-	-	5	1156	2428	53	17	-	-	-	-	-
2	2.5	2.29%	-	-	-	-	23	1292	126	2	5	-	-	-	-
2.5	3	0.84%	-	-	-	1	-	162	388	1	2	-	-	-	-
3	3.5	0.29%	-	-	-	-	-	2	210	16	-	-	-	-	-
3.5	4	0.06%	-	-	-	-	-	-	17	16	-	-	-	-	-
4	4.5	0.03%	-	-	-	-	-	-	-	19	-	-	-	-	-
4.5	5	0.01%	-	-	-	-	-	-	-	2	1	-	-	-	-
5	5.5	0.00%	-	-	-	-	-	-	-	-	3	-	-	-	-
	Percentage Occurrence		0.00%	0.65%	19.75%	42.30%	28.63%	7.43%	1.10%	0.11%	0.02%	0.00%	0.01%	0.00%	0.00%

Source: HR Wallingford, SWAN wave transformation and Met Office WW3 offshore data, 1980-2015

Table C.61: Summer wave climate at Point 2, fully-built, 2023 "present day", significant wave height (H_s) against mean wave period (T_{m-10})

			Mean Wave Period (Tm-10) in Seconds												
			0	1	2	3	4	5	6	7	8	9	10	11	12
			1	2	3	4	5	6	7	8	9	10	11	12	13
H_{s1} (m)	H_{s2} (m)	$P(H_s>H_{s1})$													
0	0.5	100.00%	1	684	19239	25212	6530	761	95	20	14	4	7	2	1
0.5	1	47.43%	-	-	735	16155	12819	1112	36	4	-	-	-	-	-
1	1.5	16.57%	-	-	-	799	7939	1707	167	6	-	-	-	-	-
1.5	2	5.95%	-	-	-	5	1136	2448	57	15	-	-	-	-	-
2	2.5	2.29%	-	-	-	-	24	1291	125	2	5	-	-	-	-
2.5	3	0.84%	-	-	-	1	-	163	386	1	2	-	-	-	-
3	3.5	0.29%	-	-	-	-	-	2	211	16	-	-	-	-	-
3.5	4	0.06%	-	-	-	-	-	-	17	16	-	-	-	-	-
4	4.5	0.03%	-	-	-	-	-	-	-	19	-	-	-	-	-
4.5	5	0.01%	-	-	-	-	-	-	-	2	1	-	-	-	-
5	5.5	0.00%	-	-	-	-	-	-	-	-	3	-	-	-	-
	Percentage Occurrence		0.00%	0.68%	19.97%	42.17%	28.45%	7.48%	1.09%	0.10%	0.03%	0.00%	0.01%	0.00%	0.00%

Source: HR Wallingford, SWAN wave transformation and Met Office WW3 offshore data, 1980-2015

Table C.62: Summer wave climate at Point 2, part-built, 2023 "present day", significant wave height (H_s) against mean wave period (T_{m-10})

			Mean Wave Period (Tm-10) in Seconds												
			0	1	2	3	4	5	6	7	8	9	10	11	12
			1	2	3	4	5	6	7	8	9	10	11	12	13
H_{s1} (m)	H_{s2} (m)	$P(H_s>H_{s1})$													
0	0.5	100.00%	1	710	19244	25145	6498	763	102	19	15	3	7	3	1
0.5	1	47.49%	-	-	728	16135	12866	1140	40	4	-	-	-	-	-
1	1.5	16.58%	-	-	-	781	7951	1721	169	6	-	-	-	-	-
1.5	2	5.95%	-	-	-	5	1080	2503	57	15	-	-	-	-	-
2	2.5	2.29%	-	-	-	-	24	1287	128	2	5	-	-	-	-
2.5	3	0.84%	-	-	-	1	-	149	397	1	2	-	-	-	-
3	3.5	0.29%	-	-	-	-	-	2	213	16	-	-	-	-	-
3.5	4	0.06%	-	-	-	-	-	-	16	16	-	-	-	-	-
4	4.5	0.03%	-	-	-	-	-	-	-	19	-	-	-	-	-
4.5	5	0.01%	-	-	-	-	-	-	-	2	1	-	-	-	-
5	5.5	0.00%	-	-	-	-	-	-	-	-	3	-	-	-	-
	Percentage Occurrence		0.00%	0.71%	19.97%	42.07%	28.42%	7.57%	1.12%	0.10%	0.03%	0.00%	0.01%	0.00%	0.00%

Source: HR Wallingford, SWAN wave transformation and Met Office WW3 offshore data, 1980-2015

Table C.63: Summer wave climate at Point 3, baseline, 2023 “present day”, significant wave height (Hs) against mean wave direction

			Wave direction											
			-15	15	45	75	105	135	165	195	225	255	285	315
			15	45	75	105	135	165	195	225	255	285	315	345
H_{s1} (m)	H_{s2} (m)	$P(H_s>H_{s1})$												
0	0.5	100.00%	6939	5794	5551	564	529	463	723	2471	6210	14108	17498	6213
0.5	1	32.94%	4514	2287	4168	11	-	-	2	2	65	1179	6809	3880
1	1.5	10.02%	2388	1037	1071	-	-	-	-	-	-	-	1142	1649
1.5	2	2.73%	813	411	130	-	-	-	-	-	-	-	125	469
2	2.5	0.78%	251	176	14	-	-	-	-	-	-	-	5	79
2.5	3	0.26%	108	82	10	-	-	-	-	-	-	-	-	8
3	3.5	0.05%	5	23	-	-	-	-	-	-	-	-	-	1
3.5	4	0.02%	1	15	-	-	-	-	-	-	-	-	-	-
4	4.5	0.01%	1	4	-	-	-	-	-	-	-	-	-	-
4.5	5	0.00%	-	-	-	-	-	-	-	-	-	-	-	-
	Percentage Occurrence		15.02%	9.83%	10.94%	0.57%	0.53%	0.46%	0.72%	2.47%	6.27%	15.29%	25.58%	12.30%

Source: HR Wallingford, SWAN wave transformation and Met Office WW3 offshore data, 1980-2015

Table C.64: Summer wave climate at Point 3, fully-built, 2023 “present day”, significant wave height (Hs) against mean wave direction

			Wave direction											
			-15	15	45	75	105	135	165	195	225	255	285	315
			15	45	75	105	135	165	195	225	255	285	315	345
H_{s1} (m)	H_{s2} (m)	$P(H_s>H_{s1})$												
0	0.5	100.00%	7085	5978	5946	795	373	217	220	529	2719	16583	19881	6486
0.5	1	33.19%	4648	2331	4093	7	-	-	-	2	1	811	7290	3831
1	1.5	10.17%	2455	1062	1027	-	-	-	-	-	-	-	1213	1643
1.5	2	2.77%	838	426	123	-	-	-	-	-	-	-	126	473
2	2.5	0.79%	260	177	11	-	-	-	-	-	-	-	5	77
2.5	3	0.26%	109	87	4	-	-	-	-	-	-	-	-	6
3	3.5	0.05%	5	23	-	-	-	-	-	-	-	-	-	1
3.5	4	0.02%	1	15	-	-	-	-	-	-	-	-	-	-
4	4.5	0.01%	2	3	-	-	-	-	-	-	-	-	-	-
4.5	5	0.00%	-	-	-	-	-	-	-	-	-	-	-	-
	Percentage Occurrence		15.40%	10.10%	11.20%	0.80%	0.37%	0.22%	0.22%	0.53%	2.72%	17.39%	28.52%	12.52%

Source: HR Wallingford, SWAN wave transformation and Met Office WW3 offshore data, 1980-2015

Table C.65: Summer wave climate at Point 3, part-built, 2023 “present day”, significant wave height (Hs) against mean wave direction

			Wave direction											
			-15	15	45	75	105	135	165	195	225	255	285	315
			15	45	75	105	135	165	195	225	255	285	315	345
H_{s1} (m)	H_{s2} (m)	$P(H_s>H_{s1})$												
0	0.5	100.00%	7147	6168	5812	710	343	172	193	500	2383	15998	20879	6560
0.5	1	33.14%	4640	2361	4060	3	-	-	-	1	2	825	7233	3829
1	1.5	10.18%	2445	1066	1024	-	-	-	-	-	-	-	1197	1669
1.5	2	2.78%	840	424	125	-	-	-	-	-	-	-	126	476
2	2.5	0.79%	256	176	11	-	-	-	-	-	-	-	5	78
2.5	3	0.26%	110	88	5	-	-	-	-	-	-	-	-	7
3	3.5	0.05%	5	23	-	-	-	-	-	-	-	-	-	1
3.5	4	0.02%	1	15	-	-	-	-	-	-	-	-	-	-
4	4.5	0.01%	1	4	-	-	-	-	-	-	-	-	-	-
4.5	5	0.00%	-	-	-	-	-	-	-	-	-	-	-	-
	Percentage Occurrence		15.45%	10.32%	11.04%	0.71%	0.34%	0.17%	0.19%	0.50%	2.39%	16.82%	29.44%	12.62%

Source: HR Wallingford, SWAN wave transformation and Met Office WW3 offshore data, 1980-2015

Table C.66: Summer wave climate at Point 3, baseline, 2023 “present day”, significant wave height (Hs) against mean wave period (Tm-10)

			Mean Wave Period (Tm-10) in Seconds													
			0	1	2	3	4	5	6	7	8	9	10	11	12	13
			1	2	3	4	5	6	7	8	9	10	11	12	13	14
H_{s1} (m)	H_{s2} (m)	$P(H_s>H_{s1})$														
0	0.5	100.00%	4	2745	26853	28608	7677	980	136	26	11	7	6	4	4	1
0.5	1	32.94%	-	5	548	11477	9425	1286	165	10	-	-	-	-	-	-
1	1.5	10.02%	-	-	-	268	5266	1683	55	16	-	-	-	-	-	-
1.5	2	2.73%	-	-	-	4	239	1590	108	-	6	-	-	-	-	-
2	2.5	0.78%	-	-	-	-	3	275	246	-	1	-	-	-	-	-
2.5	3	0.26%	-	-	-	-	-	8	186	13	-	-	-	-	-	-
3	3.5	0.05%	-	-	-	-	-	-	17	13	-	-	-	-	-	-
3.5	4	0.02%	-	-	-	-	-	-	-	15	1	-	-	-	-	-
4	4.5	0.01%	-	-	-	-	-	-	-	2	3	-	-	-	-	-
4.5	5	0.00%	-	-	-	-	-	-	-	-	-	-	-	-	-	-
	Percentage Occurrence		0.00%	2.75%	27.40%	40.36%	22.61%	5.82%	0.91%	0.09%	0.02%	0.01%	0.01%	0.00%	0.00%	0.00%

Source: HR Wallingford, SWAN wave transformation and Met Office WW3 offshore data, 1980-2015

Table C.67: Summer wave climate at Point 3, fully-built, 2023 “present day”, significant wave height (Hs) against mean wave period (Tm-10)

			Mean Wave Period (Tm-10) in Seconds													
			0	1	2	3	4	5	6	7	8	9	10	11	12	13
			1	2	3	4	5	6	7	8	9	10	11	12	13	14
H_{s1} (m)	H_{s2} (m)	$P(H_s>H_{s1})$														
0	0.5	100.00%	4	2773	27011	28498	7414	926	127	24	11	7	6	4	4	1
0.5	1	33.19%	-	5	545	11760	9309	1242	145	8	-	-	-	-	-	-
1	1.5	10.17%	-	-	1	238	5487	1602	57	15	-	-	-	-	-	-
1.5	2	2.77%	-	-	-	4	249	1625	101	-	6	-	-	-	-	-
2	2.5	0.79%	-	-	-	1	2	284	242	-	1	-	-	-	-	-
2.5	3	0.26%	-	-	-	-	-	7	189	11	-	-	-	-	-	-
3	3.5	0.05%	-	-	-	-	-	-	17	13	-	-	-	-	-	-
3.5	4	0.02%	-	-	-	-	-	-	-	15	1	-	-	-	-	-
4	4.5	0.01%	-	-	-	-	-	-	-	2	3	-	-	-	-	-
4.5	5	0.00%	-	-	-	-	-	-	-	-	-	-	-	-	-	-
	Percentage Occurrence		0.00%	2.78%	27.56%	40.50%	22.46%	5.69%	0.88%	0.09%	0.02%	0.01%	0.01%	0.00%	0.00%	0.00%

Source: HR Wallingford, SWAN wave transformation and Met Office WW3 offshore data, 1980-2015

Table C.68: Summer wave climate at Point 3, part-built, 2023 “present day”, significant wave height (Hs) against mean wave period (Tm-10)

			Mean Wave Period (Tm-10) in Seconds													
			0	1	2	3	4	5	6	7	8	9	10	11	12	13
			1	2	3	4	5	6	7	8	9	10	11	12	13	14
H_{s1} (m)	H_{s2} (m)	$P(H_s>H_{s1})$														
0	0.5	100.00%	3	2725	26960	28477	7541	963	134	26	12	7	6	3	5	1
0.5	1	33.14%	-	4	538	11684	9300	1263	156	10	-	-	-	-	-	-
1	1.5	10.18%	-	-	1	241	5464	1622	56	16	-	-	-	-	-	-
1.5	2	2.78%	-	-	-	4	248	1631	102	-	6	-	-	-	-	-
2	2.5	0.79%	-	-	-	1	2	282	241	-	1	-	-	-	-	-
2.5	3	0.26%	-	-	-	-	-	8	192	11	-	-	-	-	-	-
3	3.5	0.05%	-	-	-	-	-	-	17	13	-	-	-	-	-	-
3.5	4	0.02%	-	-	-	-	-	-	-	15	1	-	-	-	-	-
4	4.5	0.01%	-	-	-	-	-	-	-	2	3	-	-	-	-	-
4.5	5	0.00%	-	-	-	-	-	-	-	-	-	-	-	-	-	-
	Percentage Occurrence		0.00%	2.73%	27.50%	40.41%	22.56%	5.77%	0.90%	0.09%	0.02%	0.01%	0.01%	0.00%	0.01%	0.00%

Source: HR Wallingford, SWAN wave transformation and Met Office WW3 offshore data, 1980-2015

Table C.69: Summer wave climate at Point 4, baseline, 2023 “present day”, significant wave height (Hs) against mean wave direction

			Wave direction											
			-15	15	45	75	105	135	165	195	225	255	285	315
			15	45	75	105	135	165	195	225	255	285	315	345
H_{s1} (m)	H_{s2} (m)	$P(H_s>H_{s1})$												
0	0.5	100.00%	16813	12936	7704	1033	324	233	542	1450	1928	4348	8623	22077
0.5	1	21.99%	6875	3866	3405	1	-	-	-	-	-	-	46	2824
1	1.5	4.97%	1808	1339	516	-	-	-	-	-	-	-	-	421
1.5	2	0.89%	317	329	12	-	-	-	-	-	-	-	-	6
2	2.5	0.22%	52	113	6	-	-	-	-	-	-	-	-	-
2.5	3	0.05%	1	36	-	-	-	-	-	-	-	-	-	-
3	3.5	0.01%	-	13	-	-	-	-	-	-	-	-	-	-
3.5	4	0.00%	-	1	-	-	-	-	-	-	-	-	-	-
	Percentage Occurrence		25.87%	18.63%	11.64%	1.03%	0.32%	0.23%	0.54%	1.45%	1.93%	4.35%	8.67%	25.33%

Source: HR Wallingford, SWAN wave transformation and Met Office WW3 offshore data, 1980-2015

Table C.70: Summer wave climate at Point 4, fully-built, 2023 “present day”, significant wave height (Hs) against mean wave direction

			Wave direction											
			-15	15	45	75	105	135	165	195	225	255	285	315
			15	45	75	105	135	165	195	225	255	285	315	345
H_{s1} (m)	H_{s2} (m)	$P(H_s>H_{s1})$												
0	0.5	100.00%	20035	14572	7991	1282	406	365	896	1700	1796	3600	6475	18509
0.5	1	22.37%	7586	4455	3137	1	-	-	-	-	-	-	25	2084
1	1.5	5.08%	1939	1493	430	-	-	-	-	-	-	-	-	317
1.5	2	0.91%	321	349	10	-	-	-	-	-	-	-	-	3
2	2.5	0.22%	51	116	5	-	-	-	-	-	-	-	-	-
2.5	3	0.05%	1	35	-	-	-	-	-	-	-	-	-	-
3	3.5	0.01%	-	14	-	-	-	-	-	-	-	-	-	-
3.5	4	0.00%	-	1	-	-	-	-	-	-	-	-	-	-
	Percentage Occurrence		29.93%	21.03%	11.57%	1.28%	0.41%	0.36%	0.90%	1.70%	1.80%	3.60%	6.50%	20.91%

Source: HR Wallingford, SWAN wave transformation and Met Office WW3 offshore data, 1980-2015

Table C.71: Summer wave climate at Point 4, part-built, 2023 “present day”, significant wave height (Hs) against mean wave direction

			Wave direction											
			-15	15	45	75	105	135	165	195	225	255	285	315
			15	45	75	105	135	165	195	225	255	285	315	345
H_{s1} (m)	H_{s2} (m)	$P(H_s>H_{s1})$												
0	0.5	100.00%	18430	13572	7855	1071	317	251	563	1452	1858	4073	7956	20410
0.5	1	22.19%	7201	4280	3260	1	-	-	-	-	-	-	32	2383
1	1.5	5.03%	1864	1438	462	-	-	-	-	-	-	-	-	366
1.5	2	0.90%	320	347	11	-	-	-	-	-	-	-	-	3
2	2.5	0.22%	51	118	5	-	-	-	-	-	-	-	-	-
2.5	3	0.05%	1	34	-	-	-	-	-	-	-	-	-	-
3	3.5	0.01%	-	14	-	-	-	-	-	-	-	-	-	-
3.5	4	0.00%	-	1	-	-	-	-	-	-	-	-	-	-
	Percentage Occurrence		27.87%	19.80%	11.59%	1.07%	0.32%	0.25%	0.56%	1.45%	1.86%	4.07%	7.99%	23.16%

Source: HR Wallingford, SWAN wave transformation and Met Office WW3 offshore data, 1980-2015

Table C.72: Summer wave climate at Point 4, baseline, 2023 “present day”, significant wave height (Hs) against mean wave period (Tm-10)

			Mean Wave Period (Tm-10) in Seconds												
			0	1	2	3	4	5	6	7	8	9	10	11	12
			1	2	3	4	5	6	7	8	9	10	11	12	13
H_{s1} (m)	H_{s2} (m)	$P(H_s>H_{s1})$													
0	0.5	100.00%	59	6794	29021	29941	10123	1715	274	48	13	7	11	5	1
0.5	1	21.99%	-	13	934	7026	7334	1391	282	34	3	-	-	-	-
1	1.5	4.97%	-	-	1	172	1927	1806	164	6	6	2	-	-	-
1.5	2	0.89%	-	-	1	-	59	379	209	16	-	-	-	-	-
2	2.5	0.22%	-	-	-	-	2	48	109	13	-	-	-	-	-
2.5	3	0.05%	-	-	-	-	-	-	21	13	3	-	-	-	-
3	3.5	0.01%	-	-	-	-	-	-	-	11	2	-	-	-	-
3.5	4	0.00%	-	-	-	-	-	-	-	-	1	-	-	-	-
4	4.5	0.00%	-	-	-	-	-	-	-	-	-	-	-	-	-
4.5	5	0.00%	-	-	-	-	-	-	-	-	-	-	-	-	-
	Percentage Occurrence		0.06%	6.81%	29.96%	37.14%	19.44%	5.34%	1.06%	0.14%	0.03%	0.01%	0.01%	0.01%	0.00%

Source: HR Wallingford, SWAN wave transformation and Met Office WW3 offshore data, 1980-2015

Table C.73: Summer wave climate at Point 4, fully-built, 2023 “present day”, significant wave height (Hs) against mean wave period (Tm-10)

			Mean Wave Period (Tm-10) in Seconds												
			0	1	2	3	4	5	6	7	8	9	10	11	12
			1	2	3	4	5	6	7	8	9	10	11	12	13
H_{s1} (m)	H_{s2} (m)	$P(H_s>H_{s1})$													
0	0.5	100.00%	33	6500	29391	29985	9776	1605	255	45	12	8	11	5	1
0.5	1	22.37%	-	10	813	7247	7547	1370	269	32	1	-	-	-	-
1	1.5	5.08%	-	-	-	147	2009	1847	159	7	7	2	-	-	-
1.5	2	0.91%	-	-	-	1	54	398	214	15	-	-	-	-	-
2	2.5	0.22%	-	-	-	-	1	48	111	12	-	-	-	-	-
2.5	3	0.05%	-	-	-	-	-	-	22	11	3	-	-	-	-
3	3.5	0.01%	-	-	-	-	-	-	-	12	2	-	-	-	-
3.5	4	0.00%	-	-	-	-	-	-	-	-	1	-	-	-	-
4	4.5	0.00%	-	-	-	-	-	-	-	-	-	-	-	-	-
4.5	5	0.00%	-	-	-	-	-	-	-	-	-	-	-	-	-
	Percentage Occurrence		0.03%	6.51%	30.20%	37.38%	19.39%	5.27%	1.03%	0.13%	0.03%	0.01%	0.01%	0.01%	0.00%

Source: HR Wallingford, SWAN wave transformation and Met Office WW3 offshore data, 1980-2015

Table C.74: Summer wave climate at Point 4, part-built, 2023 “present day”, significant wave height (Hs) against mean wave period (Tm-10)

			Mean Wave Period (Tm-10) in Seconds												
			0	1	2	3	4	5	6	7	8	9	10	11	12
			1	2	3	4	5	6	7	8	9	10	11	12	13
H_{s1} (m)	H_{s2} (m)	$P(H_s>H_{s1})$													
0	0.5	100.00%	46	6403	28923	30154	10206	1721	268	49	12	8	11	5	1
0.5	1	22.19%	-	11	879	7170	7391	1387	282	35	3	-	-	-	-
1	1.5	5.03%	-	-	1	157	1964	1832	162	6	6	2	-	-	-
1.5	2	0.90%	-	-	-	1	56	394	213	16	-	-	-	-	-
2	2.5	0.22%	-	-	-	-	1	49	112	12	-	-	-	-	-
2.5	3	0.05%	-	-	-	-	-	-	21	11	3	-	-	-	-
3	3.5	0.01%	-	-	-	-	-	-	-	12	2	-	-	-	-
3.5	4	0.00%	-	-	-	-	-	-	-	-	1	-	-	-	-
4	4.5	0.00%	-	-	-	-	-	-	-	-	-	-	-	-	-
4.5	5	0.00%	-	-	-	-	-	-	-	-	-	-	-	-	-
	Percentage Occurrence		0.05%	6.41%	29.80%	37.48%	19.62%	5.38%	1.06%	0.14%	0.03%	0.01%	0.01%	0.01%	0.00%

Source: HR Wallingford, SWAN wave transformation and Met Office WW3 offshore data, 1980-2015

Table C.75: Summer wave climate at Point 6, baseline, 2023 “present day”, significant wave height (Hs) against mean wave direction

			Wave direction											
			-15	15	45	75	105	135	165	195	225	255	285	315
			15	45	75	105	135	165	195	225	255	285	315	345
H_{s1} (m)	H_{s2} (m)	$P(H_s>H_{s1})$												
0	0.5	100.00%	12649	40328	15762	5542	4693	4102	2089	904	735	487	565	1234
0.5	1	10.91%	175	6753	2647	4	-	-	-	-	-	-	-	-
1	1.5	1.33%	2	968	168	-	-	-	-	-	-	-	-	-
1.5	2	0.19%	-	117	21	-	-	-	-	-	-	-	-	-
2	2.5	0.06%	-	41	3	-	-	-	-	-	-	-	-	-
2.5	3	0.01%	-	12	-	-	-	-	-	-	-	-	-	-
	Percentage Occurrence		12.83%	48.22%	18.60%	5.55%	4.69%	4.10%	2.09%	0.90%	0.73%	0.49%	0.56%	1.23%

Source: HR Wallingford, SWAN wave transformation and Met Office WW3 offshore data, 1980-2015

Table C.76: Summer wave climate at Point 6, fully-built, 2023 “present day”, significant wave height (Hs) against mean wave direction

			Wave direction											
			-15	15	45	75	105	135	165	195	225	255	285	315
			15	45	75	105	135	165	195	225	255	285	315	345
H_{s1} (m)	H_{s2} (m)	$P(H_s>H_{s1})$												
0	0.5	100.00%	6976	42470	17329	7701	6584	4341	1298	561	475	280	234	712
0.5	1	11.04%	28	7137	2534	4	-	-	-	-	-	-	-	-
1	1.5	1.34%	-	990	153	-	-	-	-	-	-	-	-	-
1.5	2	0.20%	-	128	12	-	-	-	-	-	-	-	-	-
2	2.5	0.06%	-	43	2	-	-	-	-	-	-	-	-	-
2.5	3	0.01%	-	12	-	-	-	-	-	-	-	-	-	-
	Percentage Occurrence		7.00%	50.78%	20.03%	7.70%	6.58%	4.34%	1.30%	0.56%	0.48%	0.28%	0.23%	0.71%

Source: HR Wallingford, SWAN wave transformation and Met Office WW3 offshore data, 1980-2015

Table C.77: Summer wave climate at Point 6, part-built, 2023 “present day”, significant wave height (Hs) against mean wave direction

			Wave direction											
			-15	15	45	75	105	135	165	195	225	255	285	315
			15	45	75	105	135	165	195	225	255	285	315	345
H_{s1} (m)	H_{s2} (m)	$P(H_s>H_{s1})$												
0	0.5	100.00%	10205	41822	16335	6182	4982	4117	1961	837	669	413	448	1014
0.5	1	11.01%	62	7052	2554	4	-	-	-	-	-	-	-	-
1	1.5	1.34%	-	992	153	-	-	-	-	-	-	-	-	-
1.5	2	0.20%	-	122	17	-	-	-	-	-	-	-	-	-
2	2.5	0.06%	-	43	3	-	-	-	-	-	-	-	-	-
2.5	3	0.01%	-	12	-	-	-	-	-	-	-	-	-	-
	Percentage Occurrence		10.27%	50.04%	19.06%	6.19%	4.98%	4.12%	1.96%	0.84%	0.67%	0.41%	0.45%	1.01%

Source: HR Wallingford, SWAN wave transformation and Met Office WW3 offshore data, 1980-2015

Table C.78: Summer wave climate at Point 6, baseline, 2023 “present day”, significant wave height (Hs) against mean wave period (Tm-10)

			Mean Wave Period (Tm-10) in Seconds													
			0	1	2	3	4	5	6	7	8	9	10	11	12	13
			1	2	3	4	5	6	7	8	9	10	11	12	13	14
H_{s1} (m)	H_{s2} (m)	$P(H_s>H_{s1})$														
0	0.5	100.00%	261	9396	27595	31212	16461	3502	520	93	26	10	9	2	2	1
0.5	1	10.91%	1	3	437	3223	3616	1985	276	28	10	-	-	-	-	-
1	1.5	1.33%	-	-	-	32	362	454	266	24	-	-	-	-	-	-
1.5	2	0.19%	-	-	-	-	9	52	63	14	1	-	-	-	-	-
2	2.5	0.06%	-	-	-	-	-	9	24	7	4	-	-	-	-	-
2.5	3	0.01%	-	-	-	-	-	-	-	12	-	-	-	-	-	-
3	3.5	0.00%	-	-	-	-	-	-	-	-	-	-	-	-	-	-
3.5	4	0.00%	-	-	-	-	-	-	-	-	-	-	-	-	-	-
4	4.5	0.00%	-	-	-	-	-	-	-	-	-	-	-	-	-	-
4.5	5	0.00%	-	-	-	-	-	-	-	-	-	-	-	-	-	-
	Percentage Occurrence		0.26%	9.40%	28.03%	34.47%	20.45%	6.00%	1.15%	0.18%	0.04%	0.01%	0.01%	0.00%	0.00%	0.00%

Source: HR Wallingford, SWAN wave transformation and Met Office WW3 offshore data, 1980-2015

Table C.79: Summer wave climate at Point 6, fully-built, 2023 “present day”, significant wave height (Hs) against mean wave period (Tm-10)

			Mean Wave Period (Tm-10) in Seconds													
			0	1	2	3	4	5	6	7	8	9	10	11	12	13
			1	2	3	4	5	6	7	8	9	10	11	12	13	14
H_{s1} (m)	H_{s2} (m)	$P(H_s>H_{s1})$														
0	0.5	100.00%	217	8958	27613	31700	16456	3372	508	84	26	12	6	3	2	1
0.5	1	11.04%	1	2	406	3204	3712	2056	282	29	11	-	-	-	-	-
1	1.5	1.34%	-	-	-	30	356	466	267	24	-	-	-	-	-	-
1.5	2	0.20%	-	-	-	-	7	53	64	14	1	-	-	-	-	-
2	2.5	0.06%	-	-	-	-	-	10	23	7	4	-	-	-	-	-
2.5	3	0.01%	-	-	-	-	-	-	-	12	-	-	-	-	-	-
3	3.5	0.00%	-	-	-	-	-	-	-	-	-	-	-	-	-	-
3.5	4	0.00%	-	-	-	-	-	-	-	-	-	-	-	-	-	-
4	4.5	0.00%	-	-	-	-	-	-	-	-	-	-	-	-	-	-
4.5	5	0.00%	-	-	-	-	-	-	-	-	-	-	-	-	-	-
	Percentage Occurrence		0.22%	8.96%	28.02%	34.93%	20.53%	5.96%	1.14%	0.17%	0.04%	0.01%	0.01%	0.00%	0.00%	0.00%

Source: HR Wallingford, SWAN wave transformation and Met Office WW3 offshore data, 1980-2015

Table C.80: Summer wave climate at Point 6, part-built, 2023 “present day”, significant wave height (Hs) against mean wave period (Tm-10)

			Mean Wave Period (Tm-10) in Seconds													
			0	1	2	3	4	5	6	7	8	9	10	11	12	13
			1	2	3	4	5	6	7	8	9	10	11	12	13	14
H_{s1} (m)	H_{s2} (m)	$P(H_s>H_{s1})$														
0	0.5	100.00%	212	8783	27226	31421	16952	3675	569	98	27	9	10	2	2	1
0.5	1	11.01%	1	4	460	3213	3606	2032	316	28	12	1	-	-	-	-
1	1.5	1.34%	-	-	-	32	369	449	269	27	-	-	-	-	-	-
1.5	2	0.20%	-	-	-	-	10	53	62	14	1	-	-	-	-	-
2	2.5	0.06%	-	-	-	-	-	9	26	7	4	-	-	-	-	-
2.5	3	0.01%	-	-	-	-	-	-	-	12	-	-	-	-	-	-
3	3.5	0.00%	-	-	-	-	-	-	-	-	-	-	-	-	-	-
3.5	4	0.00%	-	-	-	-	-	-	-	-	-	-	-	-	-	-
4	4.5	0.00%	-	-	-	-	-	-	-	-	-	-	-	-	-	-
4.5	5	0.00%	-	-	-	-	-	-	-	-	-	-	-	-	-	-
	Percentage Occurrence		0.21%	8.79%	27.69%	34.67%	20.94%	6.22%	1.24%	0.19%	0.04%	0.01%	0.01%	0.00%	0.00%	0.00%

Source: HR Wallingford, SWAN wave transformation and Met Office WW3 offshore data, 1980-2015

C.3. Winter (Oct-Mar) conditions

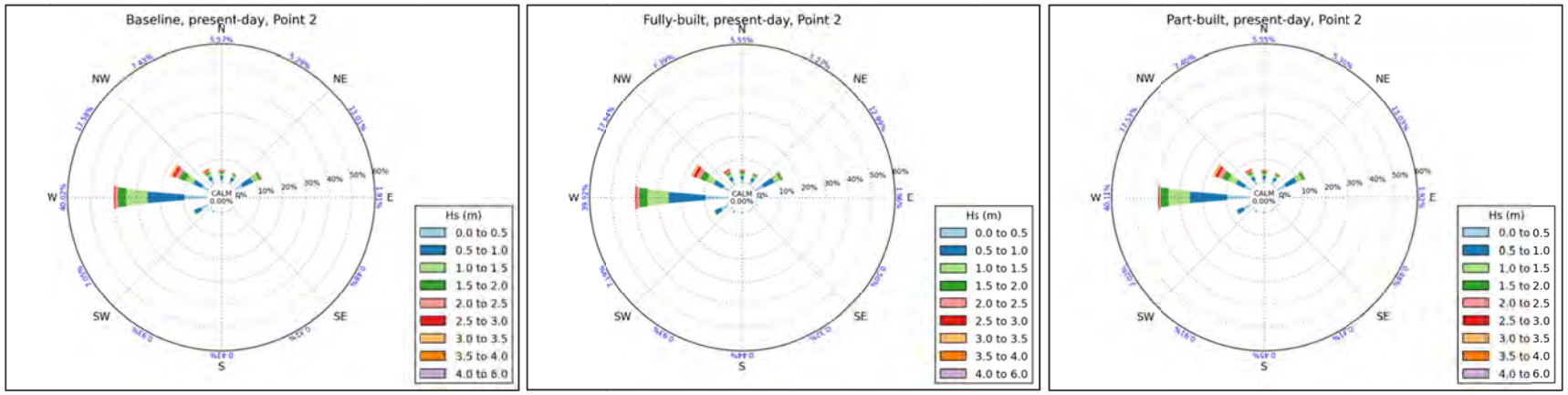

Figure C.14: Winter wave roses for nearshore prediction Point 2, present-day, baseline, part-built and fully-built layouts

Source: HR Wallingford, SWAN wave transformation and Met Office WW3 offshore data, 1980-2015

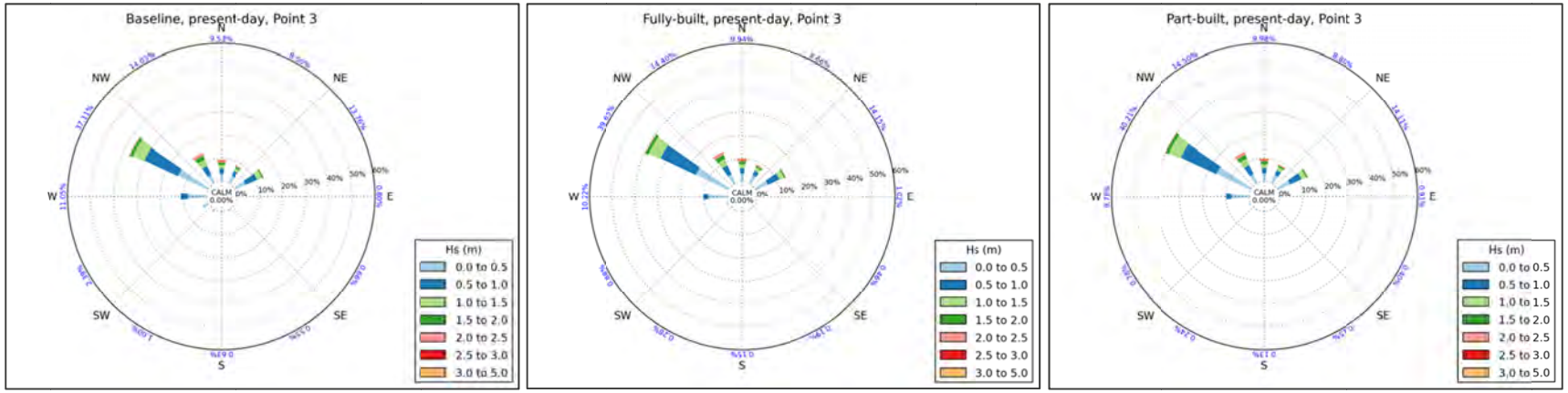

Figure C.15: Winter wave roses for nearshore prediction Point 3, present-day, baseline, part-built and fully-built layouts

Source: HR Wallingford, SWAN wave transformation and Met Office WW3 offshore data, 1980-2015

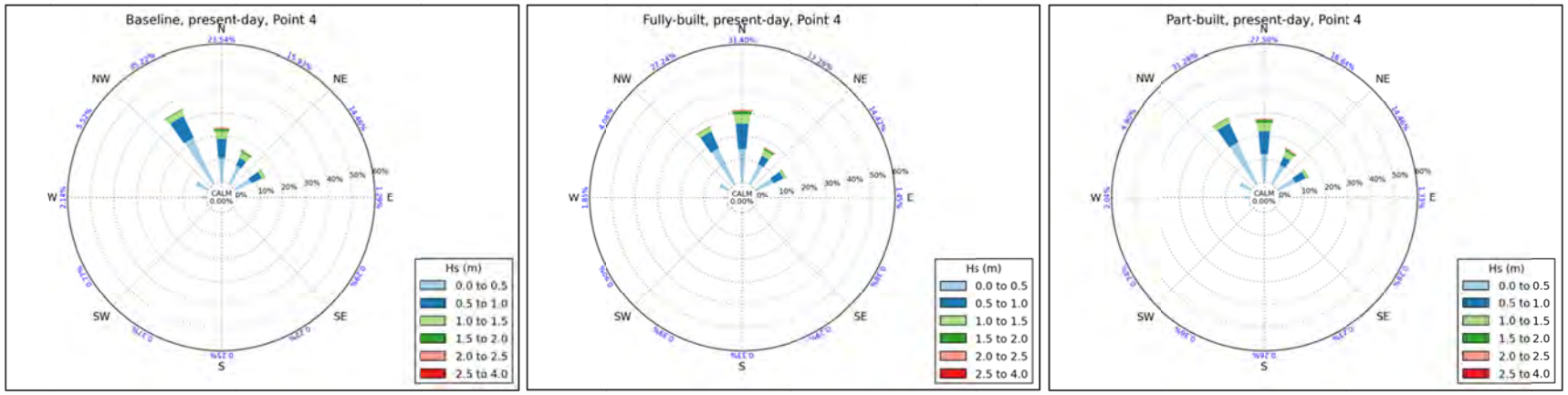

Figure C.16: Winter wave roses for nearshore prediction Point 4, present-day, baseline, part-built and fully-built layouts

Source: HR Wallingford, SWAN wave transformation and Met Office WW3 offshore data, 1980-2015

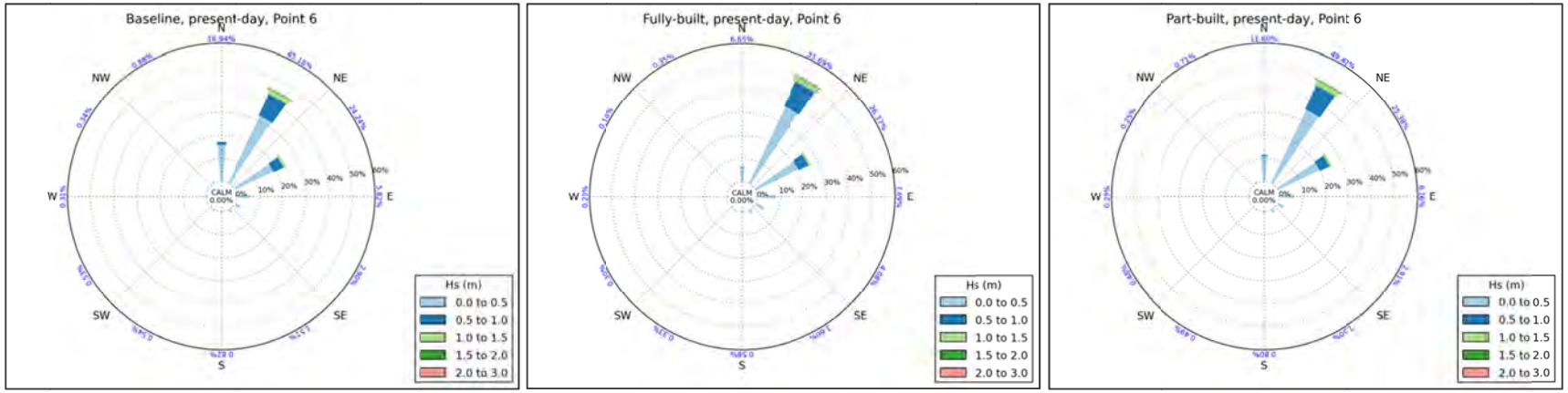

Figure C.17: Winter wave roses for nearshore prediction Point 6, present-day, baseline, part-built and fully-built layouts

Source: HR Wallingford, SWAN wave transformation and Met Office WW3 offshore data, 1980-2015

Table C.81: Winter wave climate at Point 2, baseline, 2023 “present day”, significant wave height (Hs) against mean wave direction

			Wave direction											
			-15	15	45	75	105	135	165	195	225	255	285	315
			15	45	75	105	135	165	195	225	255	285	315	345
H_{s1} (m)	H_{s2} (m)	$P(H_s>H_{s1})$												
0	0.5	100.00%	1494	1542	3803	1174	335	205	296	678	3522	9417	2901	1868
0.5	1	72.76%	1368	1524	5080	682	134	95	124	223	2967	16038	4099	1685
1	1.5	38.74%	1055	1062	2653	48	6	7	10	33	544	9265	3685	1346
1.5	2	19.03%	791	593	944	1	-	-	-	-	13	3523	2688	913
2	2.5	9.57%	351	350	405	-	-	-	-	-	-	1205	1912	631
2.5	3	4.71%	201	120	113	-	-	-	-	-	-	440	1214	467
3	3.5	2.16%	162	50	10	-	-	-	-	-	-	90	735	216
3.5	4	0.89%	84	27	3	-	-	-	-	-	-	28	276	148
4	4.5	0.33%	36	16	-	-	-	-	-	-	-	14	60	87
4.5	5	0.12%	17	2	-	-	-	-	-	-	-	2	11	47
5	5.5	0.04%	11	1	-	-	-	-	-	-	-	-	2	15
5.5	6	0.01%	3	-	-	-	-	-	-	-	-	-	-	6
	Percentage Occurrence		5.57%	5.29%	13.01%	1.91%	0.48%	0.31%	0.43%	0.93%	7.05%	40.02%	17.58%	7.43%

Source: HR Wallingford, SWAN wave transformation and Met Office WW3 offshore data, 1980-2015

Table C.82: Winter wave climate at Point 2, fully-built, 2023 “present day”, significant wave height (Hs) against mean wave direction

			Wave direction											
			-15	15	45	75	105	135	165	195	225	255	285	315
			15	45	75	105	135	165	195	225	255	285	315	345
H_{s1} (m)	H_{s2} (m)	$P(H_s>H_{s1})$												
0	0.5	100.00%	1461	1519	3811	1201	350	208	305	657	3611	9323	2879	1847
0.5	1	72.83%	1364	1525	5054	703	141	103	128	235	2968	16036	4101	1678
1	1.5	38.79%	1064	1062	2656	51	7	7	10	37	594	9212	3675	1338
1.5	2	19.08%	794	593	938	1	-	-	-	-	14	3568	2685	913
2	2.5	9.57%	353	349	410	-	-	-	-	-	-	1203	1908	629
2.5	3	4.72%	202	122	112	-	-	-	-	-	-	443	1208	468
3	3.5	2.17%	164	51	10	-	-	-	-	-	-	88	738	218
3.5	4	0.90%	86	27	3	-	-	-	-	-	-	27	277	148
4	4.5	0.33%	36	16	-	-	-	-	-	-	-	14	61	88
4.5	5	0.12%	17	2	-	-	-	-	-	-	-	2	11	45
5	5.5	0.04%	11	1	-	-	-	-	-	-	-	-	2	16
5.5	6	0.01%	4	-	-	-	-	-	-	-	-	-	-	5
	Percentage Occurrence		5.55%	5.27%	12.99%	1.96%	0.50%	0.32%	0.44%	0.93%	7.19%	39.92%	17.54%	7.39%

Source: HR Wallingford, SWAN wave transformation and Met Office WW3 offshore data, 1980-2015

Table C.83: Winter wave climate at Point 2, part-built, 2023 “present day”, significant wave height (Hs) against mean wave direction

			Wave direction											
			-15	15	45	75	105	135	165	195	225	255	285	315
			15	45	75	105	135	165	195	225	255	285	315	345
H_{s1} (m)	H_{s2} (m)	$P(H_s>H_{s1})$												
0	0.5	100.00%	1469	1554	3830	1177	336	204	307	650	3495	9408	2880	1855
0.5	1	72.84%	1357	1523	5069	695	141	95	130	223	2963	16124	4089	1676
1	1.5	38.75%	1065	1061	2654	50	6	9	9	34	552	9262	3681	1342
1.5	2	19.03%	794	591	942	1	-	-	-	-	13	3537	2676	913
2	2.5	9.56%	347	350	411	-	-	-	-	-	-	1202	1903	630
2.5	3	4.72%	201	119	112	-	-	-	-	-	-	443	1215	464
3	3.5	2.16%	163	51	10	-	-	-	-	-	-	88	736	219
3.5	4	0.90%	86	27	3	-	-	-	-	-	-	27	276	147
4	4.5	0.33%	36	16	-	-	-	-	-	-	-	15	60	88
4.5	5	0.12%	17	2	-	-	-	-	-	-	-	2	11	46
5	5.5	0.04%	11	1	-	-	-	-	-	-	-	-	2	15
5.5	6	0.01%	4	-	-	-	-	-	-	-	-	-	-	5
	Percentage Occurrence		5.55%	5.30%	13.03%	1.92%	0.48%	0.31%	0.45%	0.91%	7.02%	40.11%	17.53%	7.40%

Source: HR Wallingford, SWAN wave transformation and Met Office WW3 offshore data, 1980-2015

Table C.84: Winter wave climate at Point 2, baseline, 2023 "present day", significant wave height (H_s) against mean wave period (T_{m-10})

			Mean Wave Period (Tm-10) in Seconds										
			1	2	3	4	5	6	7	8	9	10	11
			2	3	4	5	6	7	8	9	10	11	12
H_{s1} (m)	H_{s2} (m)	$P(H_s>H_{s1})$											
0	0.5	100.00%	235	6836	12782	5677	1389	264	39	9	1	2	1
0.5	1	72.76%	-	518	13530	16480	3139	313	39	1	-	-	-
1	1.5	38.74%	-	4	879	11844	5244	1589	148	5	-	-	-
1.5	2	19.03%	-	-	11	2389	5802	861	356	47	-	-	-
2	2.5	9.57%	-	-	-	68	3824	820	100	38	3	-	-
2.5	3	4.71%	-	-	-	-	604	1816	121	13	1	-	-
3	3.5	2.16%	-	-	-	-	9	963	270	14	7	-	-
3.5	4	0.89%	-	-	-	-	1	102	445	16	1	-	-
4	4.5	0.33%	-	-	-	-	-	2	180	27	4	-	-
4.5	5	0.12%	-	-	-	-	-	1	32	40	4	1	-
5	#NUM!	0.04%	-	-	-	-	-	-	2	34	2	-	-
	Percentage Occurrence		0.24%	7.36%	27.20%	36.46%	20.01%	6.73%	1.73%	0.24%	0.02%	0.00%	0.00%

Source: HR Wallingford, SWAN wave transformation and Met Office WW3 offshore data, 1980-2015

Table C.85: Winter wave climate at Point 2, fully-built, 2023 "present day", significant wave height (H_s) against mean wave period (T_{m-10})

			Mean Wave Period (Tm-10) in Seconds										
			1	2	3	4	5	6	7	8	9	10	11
			2	3	4	5	6	7	8	9	10	11	12
H_{s1} (m)	H_{s2} (m)	$P(H_s>H_{s1})$											
0	0.5	100.00%	245	6929	12717	5588	1380	263	37	10	1	2	1
0.5	1	72.83%	-	534	13589	16467	3103	303	38	1	-	-	-
1	1.5	38.79%	-	4	885	11867	5282	1539	131	5	-	-	-
1.5	2	19.08%	-	-	11	2351	5835	905	357	46	-	-	-
2	2.5	9.57%	-	-	-	66	3814	828	105	36	3	-	-
2.5	3	4.72%	-	-	-	-	598	1823	118	15	1	-	-
3	3.5	2.17%	-	-	-	-	9	969	270	14	7	-	-
3.5	4	0.90%	-	-	-	-	1	101	449	15	1	-	-
4	4.5	0.33%	-	-	-	-	-	2	182	27	4	-	-
4.5	5	0.12%	-	-	-	-	-	1	30	40	4	1	-
5	#NUM!	0.04%	-	-	-	-	-	-	3	34	2	-	-
	Percentage Occurrence		0.24%	7.47%	27.20%	36.34%	20.02%	6.73%	1.72%	0.24%	0.02%	0.00%	0.00%

Source: HR Wallingford, SWAN wave transformation and Met Office WW3 offshore data, 1980-2015

Table C.86: Winter wave climate at Point 2, part-built, 2023 "present day", significant wave height (H_s) against mean wave period (T_{m-10})

			Mean Wave Period (Tm-10) in Seconds										
			1	2	3	4	5	6	7	8	9	10	11
			2	3	4	5	6	7	8	9	10	11	12
H_{s1} (m)	H_{s2} (m)	$P(H_s>H_{s1})$											
0	0.5	100.00%	248	6962	12665	5561	1396	274	44	11	1	2	1
0.5	1	72.84%	-	500	13512	16584	3137	313	39	1	-	-	-
1	1.5	38.75%	-	4	832	11832	5327	1578	146	5	-	-	-
1.5	2	19.03%	-	-	11	2282	5898	877	355	45	-	-	-
2	2.5	9.56%	-	-	-	67	3795	839	100	37	3	-	-
2.5	3	4.72%	-	-	-	-	562	1856	120	14	1	-	-
3	3.5	2.16%	-	-	-	-	9	967	271	13	7	-	-
3.5	4	0.90%	-	-	-	-	1	100	448	15	1	-	-
4	4.5	0.33%	-	-	-	-	-	2	182	27	4	-	-
4.5	5	0.12%	-	-	-	-	-	1	31	40	4	1	-
5	#NUM!	0.04%	-	-	-	-	-	-	2	34	2	-	-
	Percentage Occurrence		0.25%	7.47%	27.02%	36.33%	20.13%	6.81%	1.74%	0.24%	0.02%	0.00%	0.00%

Source: HR Wallingford, SWAN wave transformation and Met Office WW3 offshore data, 1980-2015

Table C.87: Winter wave climate at Point 3, baseline, 2023 “present day”, significant wave height (Hs) against mean wave direction

			Wave direction											
			-15	15	45	75	105	135	165	195	225	255	285	315
			15	45	75	105	135	165	195	225	255	285	315	345
H_{s1} (m)	H_{s2} (m)	$P(H_s>H_{s1})$												
0	0.5	100.00%	3312	3595	5273	774	652	543	628	990	2224	7871	14307	3788
0.5	1	56.04%	2215	2217	5519	22	5	6	5	7	165	3181	15971	4386
1	1.5	22.34%	1761	1482	2171	1	-	-	-	-	-	3	5319	2901
1.5	2	8.71%	1082	744	604	-	-	-	-	-	-	-	1238	1845
2	2.5	3.19%	549	306	150	-	-	-	-	-	-	-	247	836
2.5	3	1.10%	307	84	38	-	-	-	-	-	-	-	23	220
3	3.5	0.43%	209	48	2	-	-	-	-	-	-	-	4	52
3.5	4	0.12%	71	14	-	-	-	-	-	-	-	-	-	3
4	4.5	0.03%	17	3	-	-	-	-	-	-	-	-	-	-
4.5	5	0.01%	4	3	-	-	-	-	-	-	-	-	-	-
	Percentage Occurrence		9.53%	8.50%	13.76%	0.80%	0.66%	0.55%	0.63%	1.00%	2.39%	11.05%	37.11%	14.03%

Source: HR Wallingford, SWAN wave transformation and Met Office WW3 offshore data, 1980-2015

Table C.88: Winter wave climate at Point 3, fully-built, 2023 “present day”, significant wave height (Hs) against mean wave direction

			Wave direction											
			-15	15	45	75	105	135	165	195	225	255	285	315
			15	45	75	105	135	165	195	225	255	285	315	345
H_{s1} (m)	H_{s2} (m)	$P(H_s>H_{s1})$												
0	0.5	100.00%	3471	3784	5759	993	453	185	150	277	868	7985	15689	4086
0.5	1	56.30%	2300	2195	5495	29	4	5	3	2	14	2229	16924	4410
1	1.5	22.69%	1836	1472	2133	-	-	-	-	-	-	4	5489	2903
1.5	2	8.85%	1135	749	583	-	-	-	-	-	-	-	1281	1891
2	2.5	3.21%	578	313	144	-	-	-	-	-	-	-	241	834
2.5	3	1.10%	314	85	34	-	-	-	-	-	-	-	20	215
3	3.5	0.44%	216	46	2	-	-	-	-	-	-	-	4	54
3.5	4	0.11%	68	14	-	-	-	-	-	-	-	-	-	3
4	4.5	0.03%	17	3	-	-	-	-	-	-	-	-	-	-
4.5	5	0.01%	4	3	-	-	-	-	-	-	-	-	-	-
	Percentage Occurrence		9.94%	8.66%	14.15%	1.02%	0.46%	0.19%	0.15%	0.28%	0.88%	10.22%	39.65%	14.40%

Source: HR Wallingford, SWAN wave transformation and Met Office WW3 offshore data, 1980-2015

Table C.89: Winter wave climate at Point 3, part-built, 2023 “present day”, significant wave height (Hs) against mean wave direction

			Wave direction											
			-15	15	45	75	105	135	165	195	225	255	285	315
			15	45	75	105	135	165	195	225	255	285	315	345
H_{s1} (m)	H_{s2} (m)	$P(H_s>H_{s1})$												
0	0.5	100.00%	3520	3884	5772	887	399	145	131	243	766	7556	16273	4196
0.5	1	56.23%	2314	2205	5458	20	2	6	3	1	10	2218	16962	4401
1	1.5	22.63%	1830	1483	2114	-	-	-	-	-	-	3	5414	2930
1.5	2	8.86%	1134	760	585	-	-	-	-	-	-	-	1291	1873
2	2.5	3.21%	572	313	144	-	-	-	-	-	-	-	247	832
2.5	3	1.10%	314	88	33	-	-	-	-	-	-	-	21	216
3	3.5	0.43%	211	48	2	-	-	-	-	-	-	-	4	53
3.5	4	0.11%	69	14	-	-	-	-	-	-	-	-	-	3
4	4.5	0.03%	17	3	-	-	-	-	-	-	-	-	-	-
4.5	5	0.01%	4	3	-	-	-	-	-	-	-	-	-	-
	Percentage Occurrence		9.98%	8.80%	14.11%	0.91%	0.40%	0.15%	0.13%	0.24%	0.78%	9.78%	40.21%	14.50%

Source: HR Wallingford, SWAN wave transformation and Met Office WW3 offshore data, 1980-2015

Table C.90: Winter wave climate at Point 3, baseline, 2023 "present day", significant wave height (Hs) against mean wave period (Tm-10)

			Mean Wave Period (Tm-10) in Seconds												
			0	1	2	3	4	5	6	7	8	9	10	11	12
			1	2	3	4	5	6	7	8	9	10	11	12	13
H_{s1} (m)	H_{s2} (m)	$P(H_s>H_{s1})$													
0	0.5	100.00%	1	880	11498	19365	9543	2095	452	97	21	1	1	2	1
0.5	1	56.04%	-	-	399	10845	15438	5098	1684	221	14	1	-	-	-
1	1.5	22.34%	-	-	5	284	7325	4685	920	341	73	3	-	-	-
1.5	2	8.71%	-	-	-	6	468	3800	1037	154	41	5	-	-	-
2	2.5	3.19%	-	-	-	-	4	664	1190	195	24	11	-	-	-
2.5	3	1.10%	-	-	-	-	-	14	435	200	20	4	-	-	-
3	3.5	0.43%	-	-	-	-	-	-	56	244	7	6	1	-	-
3.5	4	0.12%	-	-	-	-	-	-	1	44	44	-	-	-	-
4	4.5	0.03%	-	-	-	-	-	-	-	3	15	2	-	-	-
4.5	5	0.01%	-	-	-	-	-	-	-	-	7	-	-	-	-
	Percentage Occurrence		0.00%	0.88%	11.90%	30.50%	32.78%	16.35%	5.78%	1.50%	0.27%	0.03%	0.00%	0.00%	0.00%

Source: HR Wallingford, SWAN wave transformation and Met Office WW3 offshore data, 1980-2015

Table C.91: Winter wave climate at Point 3, fully-built, 2023 “present day”, significant wave height (Hs) against mean wave period (Tm-10)

			Mean Wave Period (Tm-10) in Seconds											
			1	2	3	4	5	6	7	8	9	10	11	12
			2	3	4	5	6	7	8	9	10	11	12	13
H_{s1} (m)	H_{s2} (m)	$P(H_s>H_{s1})$												
0	0.5	100.00%	866	11547	19373	9418	1963	420	88	20	1	1	2	1
0.5	1	56.30%	-	377	11178	15319	4988	1539	197	11	1	-	-	-
1	1.5	22.69%	-	5	260	7662	4620	896	329	64	3	-	-	-
1.5	2	8.85%	-	-	6	479	3938	1027	149	36	4	-	-	-
2	2.5	3.21%	-	-	-	5	673	1212	184	27	9	-	-	-
2.5	3	1.10%	-	-	-	-	12	444	191	18	3	-	-	-
3	3.5	0.44%	-	-	-	-	-	59	250	6	6	1	-	-
3.5	4	0.11%	-	-	-	-	-	1	43	41	-	-	-	-
4	4.5	0.03%	-	-	-	-	-	-	3	17	-	-	-	-
4.5	5	0.01%	-	-	-	-	-	-	-	7	-	-	-	-
	Percentage Occurrence		0.87%	11.93%	30.82%	32.88%	16.19%	5.60%	1.43%	0.25%	0.03%	0.00%	0.00%	0.00%

Source: HR Wallingford, SWAN wave transformation and Met Office WW3 offshore data, 1980-2015

Table C.92: Winter wave climate at Point 3, part-built, 2023 "present day", significant wave height (Hs) against mean wave period (Tm-10)

			Mean Wave Period (Tm-10) in Seconds											
			1	2	3	4	5	6	7	8	9	10	11	12
			2	3	4	5	6	7	8	9	10	11	12	13
H_{s1} (m)	H_{s2} (m)	$P(H_s>H_{s1})$												
0	0.5	100.00%	853	11515	19308	9487	2048	441	93	21	1	1	2	1
0.5	1	56.23%	-	365	11055	15291	5039	1623	215	12	1	-	-	-
1	1.5	22.63%	-	5	255	7601	4609	895	335	69	3	-	-	-
1.5	2	8.86%	-	-	6	476	3938	1030	151	38	4	-	-	-
2	2.5	3.21%	-	-	-	4	668	1214	186	26	10	-	-	-
2.5	3	1.10%	-	-	-	-	12	448	190	19	3	-	-	-
3	3.5	0.43%	-	-	-	-	-	56	247	7	6	1	-	-
3.5	4	0.11%	-	-	-	-	-	1	41	44	-	-	-	-
4	4.5	0.03%	-	-	-	-	-	-	3	17	-	-	-	-
4.5	5	0.01%	-	-	-	-	-	-	-	7	-	-	-	-
	Percentage Occurrence		0.85%	11.88%	30.62%	32.86%	16.31%	5.71%	1.46%	0.26%	0.03%	0.00%	0.00%	0.00%

Source: HR Wallingford, SWAN wave transformation and Met Office WW3 offshore data, 1980-2015

Table C.93: Winter wave climate at Point 4, baseline, 2023 “present day”, significant wave height (Hs) against mean wave direction

			Wave direction											
			-15	15	45	75	105	135	165	195	225	255	285	315
			15	45	75	105	135	165	195	225	255	285	315	345
H_{s1} (m)	H_{s2} (m)	$P(H_s>H_{s1})$												
0	0.5	100.00%	10768	8883	7991	1281	294	223	246	373	767	2136	5248	21735
0.5	1	40.06%	7918	3617	5003	4	1	-	-	-	-	4	270	10473
1	1.5	12.76%	3206	2381	1089	-	-	-	-	-	-	-	-	2632
1.5	2	3.46%	1182	710	280	-	-	-	-	-	-	-	-	357
2	2.5	0.93%	382	250	89	-	-	-	-	-	-	-	-	21
2.5	3	0.19%	76	76	5	-	-	-	-	-	-	-	-	4
3	3.5	0.02%	7	13	-	-	-	-	-	-	-	-	-	-
3.5	4	0.00%	-	4	-	-	-	-	-	-	-	-	-	-
	Percentage Occurrence		23.54%	15.93%	14.46%	1.29%	0.29%	0.22%	0.25%	0.37%	0.77%	2.14%	5.52%	35.22%

Source: HR Wallingford, SWAN wave transformation and Met Office WW3 offshore data, 1980-2015

Table C.94: Winter wave climate at Point 4, fully-built, 2023 “present day”, significant wave height (Hs) against mean wave direction

			Wave direction											
			-15	15	45	75	105	135	165	195	225	255	285	315
			15	45	75	105	135	165	195	225	255	285	315	345
H_{s1} (m)	H_{s2} (m)	$P(H_s>H_{s1})$												
0	0.5	100.00%	14531	9579	8354	1444	382	288	328	395	902	1843	3857	17113
0.5	1	40.99%	10953	3933	4799	7	1	1	1	-	-	10	222	7954
1	1.5	13.10%	4076	2613	952	-	-	-	-	-	-	-	-	1912
1.5	2	3.55%	1363	768	240	-	-	-	-	-	-	-	-	247
2	2.5	0.93%	385	274	74	-	-	-	-	-	-	-	-	13
2.5	3	0.19%	81	72	4	-	-	-	-	-	-	-	-	1
3	3.5	0.03%	10	14	-	-	-	-	-	-	-	-	-	-
3.5	4	0.00%	-	4	-	-	-	-	-	-	-	-	-	-
	Percentage Occurrence		31.40%	17.26%	14.42%	1.45%	0.38%	0.29%	0.33%	0.39%	0.90%	1.85%	4.08%	27.24%

Source: HR Wallingford, SWAN wave transformation and Met Office WW3 offshore data, 1980-2015

Table C.95: Winter wave climate at Point 4, part-built, 2023 “present day”, significant wave height (Hs) against mean wave direction

			Wave direction											
			-15	15	45	75	105	135	165	195	225	255	285	315
			15	45	75	105	135	165	195	225	255	285	315	345
H_{s1} (m)	H_{s2} (m)	$P(H_s>H_{s1})$												
0	0.5	100.00%	12520	9150	8269	1323	281	226	257	356	736	2035	4645	19687
0.5	1	40.51%	9491	3829	4862	3	2	-	-	-	-	6	254	9101
1	1.5	12.97%	3707	2535	995	-	-	-	-	-	-	-	-	2197
1.5	2	3.53%	1315	760	253	-	-	-	-	-	-	-	-	274
2	2.5	0.93%	381	274	79	-	-	-	-	-	-	-	-	15
2.5	3	0.18%	74	72	5	-	-	-	-	-	-	-	-	2
3	3.5	0.03%	7	14	-	-	-	-	-	-	-	-	-	-
3.5	4	0.00%	-	4	-	-	-	-	-	-	-	-	-	-
	Percentage Occurrence		27.50%	16.64%	14.46%	1.33%	0.28%	0.23%	0.26%	0.36%	0.74%	2.04%	4.90%	31.28%

Source: HR Wallingford, SWAN wave transformation and Met Office WW3 offshore data, 1980-2015

Table C.96: Winter wave climate at Point 4, baseline, 2023 “present day”, significant wave height (Hs) against mean wave period (Tm-10)

			Mean Wave Period (Tm-10) in Seconds												
			0	1	2	3	4	5	6	7	8	9	10	11	12
			1	2	3	4	5	6	7	8	9	10	11	12	13
H_{s1} (m)	H_{s2} (m)	$P(H_s>H_{s1})$													
0	0.5	100.00%	35	2097	14246	23175	14719	4420	1014	197	32	4	4	-	1
0.5	1	40.06%	-	7	654	6061	11025	6054	2542	803	134	11	-	-	-
1	1.5	12.76%	-	-	1	151	2970	4151	1524	381	99	29	2	-	-
1.5	2	3.46%	-	-	-	-	106	1096	930	355	27	14	1	-	-
2	2.5	0.93%	-	-	-	-	1	79	322	288	37	10	5	-	-
2.5	3	0.19%	-	-	-	-	-	-	34	72	48	3	3	-	-
3	3.5	0.02%	-	-	-	-	-	-	-	12	7	1	-	-	-
3.5	4	0.00%	-	-	-	-	-	-	-	1	3	-	-	-	-
4	4.5	0.00%	-	-	-	-	-	-	-	-	-	-	-	-	-
4.5	5	0.00%	-	-	-	-	-	-	-	-	-	-	-	-	-
	Percentage Occurrence		0.04%	2.10%	14.90%	29.39%	28.82%	15.80%	6.37%	2.11%	0.39%	0.07%	0.02%	0.00%	0.00%

Source: HR Wallingford, SWAN wave transformation and Met Office WW3 offshore data, 1980-2015

Table C.97: Winter wave climate at Point 4, fully-built, 2023 “present day”, significant wave height (Hs) against mean wave period (Tm-10)

			Mean Wave Period (Tm-10) in Seconds												
			0	1	2	3	4	5	6	7	8	9	10	11	12
			1	2	3	4	5	6	7	8	9	10	11	12	13
H_{s1} (m)	H_{s2} (m)	$P(H_s>H_{s1})$													
0	0.5	100.00%	26	1976	14374	23100	14337	4070	916	178	30	3	4	-	1
0.5	1	40.99%	-	7	557	6239	11541	6099	2543	764	121	10	-	-	-
1	1.5	13.10%	-	-	1	133	3080	4344	1502	363	100	30	-	-	-
1.5	2	3.55%	-	-	-	-	97	1140	995	348	23	14	1	-	-
2	2.5	0.93%	-	-	-	-	1	72	340	283	38	7	4	-	-
2.5	3	0.19%	-	-	-	-	-	-	30	79	43	4	3	-	-
3	3.5	0.03%	-	-	-	-	-	-	-	12	10	1	1	-	-
3.5	4	0.00%	-	-	-	-	-	-	-	1	3	-	-	-	-
4	4.5	0.00%	-	-	-	-	-	-	-	-	-	-	-	-	-
4.5	5	0.00%	-	-	-	-	-	-	-	-	-	-	-	-	-
	Percentage Occurrence		0.03%	1.98%	14.93%	29.47%	29.06%	15.73%	6.33%	2.03%	0.37%	0.07%	0.01%	0.00%	0.00%

Source: HR Wallingford, SWAN wave transformation and Met Office WW3 offshore data, 1980-2015

Table C.98: Winter wave climate at Point 4, part-built, 2023 "present day", significant wave height (Hs) against mean wave period (Tm-10)

			Mean Wave Period (Tm-10) in Seconds												
			0	1	2	3	4	5	6	7	8	9	10	11	12
			1	2	3	4	5	6	7	8	9	10	11	12	13
H_{s1} (m)	H_{s2} (m)	$P(H_s>H_{s1})$													
0	0.5	100.00%	31	1986	14117	23065	14690	4386	983	190	29	4	4	-	1
0.5	1	40.51%	-	6	603	6117	11186	6083	2582	813	147	11	-	-	-
1	1.5	12.97%	-	-	1	141	3030	4234	1519	383	94	30	2	-	-
1.5	2	3.53%	-	-	-	-	104	1138	954	365	24	15	1	-	-
2	2.5	0.93%	-	-	-	-	1	81	333	280	40	9	5	-	-
2.5	3	0.18%	-	-	-	-	-	-	31	72	45	4	2	-	-
3	3.5	0.03%	-	-	-	-	-	-	-	11	9	1	1	-	-
3.5	4	0.00%	-	-	-	-	-	-	-	1	3	-	-	-	-
4	4.5	0.00%	-	-	-	-	-	-	-	-	-	-	-	-	-
4.5	5	0.00%	-	-	-	-	-	-	-	-	-	-	-	-	-
	Percentage Occurrence		0.03%	1.99%	14.72%	29.32%	29.01%	15.92%	6.40%	2.11%	0.39%	0.07%	0.02%	0.00%	0.00%

Source: HR Wallingford, SWAN wave transformation and Met Office WW3 offshore data, 1980-2015

Table C.99: Winter wave climate at Point 6, baseline, 2023 “present day”, significant wave height (Hs) against mean wave direction

			Wave direction											
			-15	15	45	75	105	135	165	195	225	255	285	315
			15	45	75	105	135	165	195	225	255	285	315	345
H_{s1} (m)	H_{s2} (m)	$P(H_s>H_{s1})$												
0	0.5	100.00%	15707	32157	18568	5783	2899	1511	815	535	529	313	344	884
0.5	1	19.96%	1219	10298	4705	34	2	1	-	-	-	-	-	-
1	1.5	3.70%	11	2199	770	-	-	-	-	-	-	-	-	-
1.5	2	0.72%	-	424	171	-	-	-	-	-	-	-	-	-
2	2.5	0.12%	-	89	20	-	-	-	-	-	-	-	-	-
2.5	3	0.01%	-	10	2	-	-	-	-	-	-	-	-	-
	Percentage Occurrence		16.94%	45.18%	24.24%	5.82%	2.90%	1.51%	0.82%	0.54%	0.53%	0.31%	0.34%	0.88%

Source: HR Wallingford, SWAN wave transformation and Met Office WW3 offshore data, 1980-2015

Table C.100: Winter wave climate at Point 6, fully-built, 2023 “present day”, significant wave height (Hs) against mean wave direction

			Wave direction											
			-15	15	45	75	105	135	165	195	225	255	285	315
			15	45	75	105	135	165	195	225	255	285	315	345
H_{s1} (m)	H_{s2} (m)	$P(H_s>H_{s1})$												
0	0.5	100.00%	6556	36825	20845	7649	4081	1597	579	332	300	199	164	346
0.5	1	20.53%	95	12012	4641	42	3	1	-	-	-	-	-	-
1	1.5	3.73%	-	2297	726	-	-	-	-	-	-	-	-	-
1.5	2	0.71%	-	454	140	-	-	-	-	-	-	-	-	-
2	2.5	0.12%	-	89	15	-	-	-	-	-	-	-	-	-
2.5	3	0.01%	-	11	1	-	-	-	-	-	-	-	-	-
	Percentage Occurrence		6.65%	51.69%	26.37%	7.69%	4.08%	1.60%	0.58%	0.33%	0.30%	0.20%	0.16%	0.35%

Source: HR Wallingford, SWAN wave transformation and Met Office WW3 offshore data, 1980-2015

Table C.101: Winter wave climate at Point 6, part-built, 2023 “present day”, significant wave height (Hs) against mean wave direction

			Wave direction											
			-15	15	45	75	105	135	165	195	225	255	285	315
			15	45	75	105	135	165	195	225	255	285	315	345
H_{s1} (m)	H_{s2} (m)	$P(H_s>H_{s1})$												
0	0.5	100.00%	11199	35173	19869	6134	2910	1494	803	491	477	288	252	713
0.5	1	20.20%	404	11435	4587	31	3	1	-	-	-	-	-	-
1	1.5	3.73%	-	2278	740	-	-	-	-	-	-	-	-	-
1.5	2	0.72%	-	442	159	-	-	-	-	-	-	-	-	-
2	2.5	0.12%	-	84	21	-	-	-	-	-	-	-	-	-
2.5	3	0.01%	-	10	2	-	-	-	-	-	-	-	-	-
	Percentage Occurrence		11.60%	49.42%	25.38%	6.16%	2.91%	1.50%	0.80%	0.49%	0.48%	0.29%	0.25%	0.71%

Source: HR Wallingford, SWAN wave transformation and Met Office WW3 offshore data, 1980-2015

Table C.102: Winter wave climate at Point 6, baseline, 2023 “present day”, significant wave height (Hs) against mean wave period (Tm-10)

			Mean Wave Period (Tm-10) in Seconds												
			0	1	2	3	4	5	6	7	8	9	10	11	12
			1	2	3	4	5	6	7	8	9	10	11	12	13
H_{s1} (m)	H_{s2} (m)	$P(H_s>H_{s1})$													
0	0.5	100.00%	118	3356	15180	25023	22474	10020	3048	694	115	15	-	1	1
0.5	1	19.96%	1	11	343	3353	5031	4275	2194	798	197	52	4	-	-
1	1.5	3.70%	-	-	1	45	750	1152	626	344	49	10	3	-	-
1.5	2	0.72%	-	-	-	-	17	198	196	136	47	1	-	-	-
2	2.5	0.12%	-	-	-	-	-	16	36	32	26	-	-	-	-
2.5	3	0.01%	-	-	-	-	-	-	-	9	3	-	-	-	-
3	3.5	0.00%	-	-	-	-	-	-	-	-	-	-	-	-	-
3.5	4	0.00%	-	-	-	-	-	-	-	-	-	-	-	-	-
4	4.5	0.00%	-	-	-	-	-	-	-	-	-	-	-	-	-
4.5	5	0.00%	-	-	-	-	-	-	-	-	-	-	-	-	-
	Percentage Occurrence		0.12%	3.37%	15.52%	28.42%	28.27%	15.66%	6.10%	2.01%	0.44%	0.08%	0.01%	0.00%	0.00%

Source: HR Wallingford, SWAN wave transformation and Met Office WW3 offshore data, 1980-2015

Table C.103: Winter wave climate at Point 6, fully-built, 2023 “present day”, significant wave height (Hs) against mean wave period (Tm-10)

			Mean Wave Period (Tm-10) in Seconds												
			0	1	2	3	4	5	6	7	8	9	10	11	12
			1	2	3	4	5	6	7	8	9	10	11	12	13
H_{s1} (m)	H_{s2} (m)	$P(H_s>H_{s1})$													
0	0.5	100.00%	99	3158	14860	25102	22508	9987	2957	683	101	15	1	1	1
0.5	1	20.53%	-	11	310	3328	5173	4574	2285	857	202	52	2	-	-
1	1.5	3.73%	-	-	1	47	732	1174	651	350	50	12	5	-	-
1.5	2	0.71%	-	-	-	-	15	194	200	135	50	1	-	-	-
2	2.5	0.12%	-	-	-	-	-	14	34	33	23	-	-	-	-
2.5	3	0.01%	-	-	-	-	-	-	-	9	3	-	-	-	-
3	3.5	0.00%	-	-	-	-	-	-	-	-	-	-	-	-	-
3.5	4	0.00%	-	-	-	-	-	-	-	-	-	-	-	-	-
4	4.5	0.00%	-	-	-	-	-	-	-	-	-	-	-	-	-
4.5	5	0.00%	-	-	-	-	-	-	-	-	-	-	-	-	-
	Percentage Occurrence		0.10%	3.17%	15.17%	28.48%	28.43%	15.94%	6.13%	2.07%	0.43%	0.08%	0.01%	0.00%	0.00%

Source: HR Wallingford, SWAN wave transformation and Met Office WW3 offshore data, 1980-2015

Table C.104: Winter wave climate at Point 6, part-built, 2023 “present day”, significant wave height (Hs) against mean wave period (Tm-10)

			Mean Wave Period (Tm-10) in Seconds												
			0	1	2	3	4	5	6	7	8	9	10	11	12
			1	2	3	4	5	6	7	8	9	10	11	12	13
H_{s1} (m)	H_{s2} (m)	$P(H_s>H_{s1})$													
0	0.5	100.00%	102	3148	14644	24727	22477	10492	3280	779	135	16	-	1	1
0.5	1	20.20%	1	12	353	3387	4941	4364	2255	887	205	53	4	-	-
1	1.5	3.73%	-	-	1	47	761	1149	631	352	59	10	7	-	-
1.5	2	0.72%	-	-	-	-	16	199	195	138	51	1	-	-	-
2	2.5	0.12%	-	-	-	-	-	15	35	32	23	-	-	-	-
2.5	3	0.01%	-	-	-	-	-	-	-	9	3	-	-	-	-
3	3.5	0.00%	-	-	-	-	-	-	-	-	-	-	-	-	-
3.5	4	0.00%	-	-	-	-	-	-	-	-	-	-	-	-	-
4	4.5	0.00%	-	-	-	-	-	-	-	-	-	-	-	-	-
4.5	5	0.00%	-	-	-	-	-	-	-	-	-	-	-	-	-
	Percentage Occurrence		0.10%	3.16%	15.00%	28.16%	28.19%	16.22%	6.40%	2.20%	0.48%	0.08%	0.01%	0.00%	0.00%

Source: HR Wallingford, SWAN wave transformation and Met Office WW3 offshore data, 1980-2015

D. The ARTEMIS wave disturbance model

The ARTEMIS Wave Disturbance Model

The ARTEMIS wave disturbance model was developed to predict wave conditions in ports and harbours. ARTEMIS employs state-of-the-art finite element techniques to compute wave heights throughout the area being modelled for each set of incident wave conditions. Hence wave disturbance at a variety of mooring positions can be calculated for particular incident wave conditions in a single run of the model. The model includes: wave diffraction by surface piercing structures as well as diffraction due to features of the sea bed; refraction and shoaling effects due to varying depths; and partial or complete reflection from harbour or coastal boundaries. In addition ARTEMIS includes the effects of sea bed friction and wave breaking.

The equation solved is based on the Mild Slope Equation or Berkhoff Equation given by:

$$\nabla\left[CC_g\nabla\emptyset\right] + \omega^2\frac{C_g}{C}\emptyset = 0$$

where C and C_g are the phase and group velocities respectively defined by:

$$C = \frac{\omega}{k} \quad \text{and} \quad C_g = \frac{1}{2}\left[1 + \frac{2kh}{sinh(2kh)}\right]C$$

where ω is the angular frequency, h is the still water depth, and k is the wave number defined by $2\pi/L$ where $L\ (=CT)$ is the wavelength.

Finite element discretisation of the mild slope equation results in a boundary valued problem which requires boundary conditions to be specified along the entire length of the boundary. ARTEMIS includes several different boundary conditions which can be selected including: incident wave boundary conditions, which also absorb reflected waves and are specified in terms of an incident wave height, period and direction; general absorbing boundary conditions, specified in terms of an assumed wave direction; and partial or fully reflecting boundary conditions, specified in terms of a reflection coefficient, phase change and assumed wave direction. The specification of reflection coefficients along partially reflecting boundaries enables different types of construction, e.g. rubble slopes or vertical walls, to be investigated.

ARTEMIS requires a linear triangular finite element mesh. To obtain accurate results it is important to sufficiently resolve the wave lengths in all water depths. Approximately 7 to 8 points per wavelength is the minimum requirement, although the optimum lies somewhere between 10 and 20 points per wavelength. The advantage of using a finite element mesh is that the resolution of the mesh can be tailored to a particular range of wave periods and water depths so that the amount of computation required, which is dependent on the number of nodes, can be minimised.

ARTEMIS can be used in either mono-frequency or random mode and either mono-directional or multi-directional. In the mono-frequency case a single period and direction component is used in the model. For some situations this will provide a reasonable description of the wave field. Due to constructive and destructive interference patterns caused by the interaction of waves of the same period, a more representative description of the wave field is sometimes achieved by using random incident waves. In this case many period and possibly direction components are run within the model and combined automatically according to the incident wave spectrum. ARTEMIS can also be used in period scanning mode to provide wave height fields for a sequence of wave periods.

ARTEMIS outputs wave heights and these are normally viewed in the form of colour contour plots using visualisation packages such as HRVIS or RUBENS. The results are also typically presented in the form of tables giving wave heights at specific analysis positions in the area of interest. Other physical terms can also be output, such as the still water depths and in the case of single period and direction runs. ARTEMIS can also output the free surface elevation and the wave phase as well as several other physical properties. Using the wave height and wave phase terms the free surface elevation at time steps within a single wave period can be computed later which can then be animated.

Typical results

1. Tables of wave height at proposed mooring positions for different harbour layouts. The model can be used, for example, to examine the effects of changing the length or orientation of a breakwater in providing shelter to existing berths.
2. Graphs of wave height against wave period at different positions within a harbour. These graphs can be used to identify wave periods for which the harbour is particularly responsive to.
3. Tables of wave height at locations in the harbour for extreme wave conditions for different directions and return periods. Such results would allow ‘downtime’ estimates to be made.

ARTEMIS can be used in conjunction with a physical model. This is done by calibrating the model against early physical model runs. Different options for harbour layout can be examined in the computational model, allowing the “best” scheme to be selected for more detailed evaluation in the physical model. The calibrated computational model can also be used to examine wave conditions other than those tested in the physical model.

E. Extreme wave conditions and joint exceedence extremes with sea levels at Point P1

This appendix describes the derivation of extreme wave conditions and joint exceedence wave and high water levels extremes at Point P1, in order to provide boundary conditions to the ARTEMIS wave disturbance model. Extreme conditions introduced here have been estimated during earlier work for Wylfa Newydd.

It is understood from Horizon NP, that this type of result should be prepared with inclusion of plausible conservatism, for example in the form of allowance for uncertainties. Hence: the wave modelling was undertaken at a constant high sea level; further refinement of the incident wave spectra of the highest ten percent of wave conditions was applied; and the joint probability assessment was undertaken using a conservative joint exceedence definition that more closely matches response function approaches typically used in coastal engineering studies.

The climate-changed scenario represented here is the 2087 reasonably foreseeable case.

E.1. Wave height extremes analysis

Wave and sea level conditions with joint exceedence return periods of 5, 25, 75, 200 and 1000 years on the ARTEMIS model boundary would be needed for selection of appropriate test conditions to be run in the ARTEMIS model. For this purpose it was necessary to derive extreme nearshore waves, and to generate joint exceedence results for a SWAN model nearshore wave prediction point on the ARTEMIS model boundary (Point P1, see Figure 5.3).

The full 3-hourly time series of waves at Point P1 was generated at MHWS sea level with the model emulation approach described in Section 4.4.1. The highest ten percent of wave heights at any or all of the five offshore locations, as used in Phase 1 (see Figure 4.1) were subsequently also re-run applying partitioned offshore wave spectra to the boundary of the SWAN model. These were re-created using two-dimensional boundary wave spectra derived from the partitioned integrated parameters output from the UK Met Office WaveWatchIII hindcast model (Bunney et al., 2013), and replaced in the emulated nearshore time series.

The resulting full 3-hourly nearshore time series, including the more accurate storm data, were used for the assessment and derivation of extremes.

A list of independent peak significant wave height values over a threshold were extracted from the full nearshore time series, with a minimum separation time between neighbouring peaks of 48 hours. Omni-directional significant wave height extremes were estimated by fitting a Generalised Pareto Distribution, using Bayesian techniques with an uninformative prior distribution attached to a Poisson process. The fitted distribution for P1 is shown in Figure E.1.

The derived extreme nearshore significant wave heights and associated wave periods for return periods of 5, 25, 75, 200 and 1000 years are listed in Table E.1. The mean wave periods listed are T_{m-10} (in seconds) and are assigned based on the average wave steepness of the highest wave records at each nearshore point.

Table E.1: Nearshore extreme wave conditions at the ARTEMIS model northern boundary (Point P1) for the "2087 reasonably foreseeable" climate changed scenario

Return period (years)	H_s (m)	T_{m-10} (s)
5	5.3	8.7
25	6.0	9.2
75	6.3	9.5
200	6.5	9.6
1000	6.8	9.8

Source: HR Wallingford analysis, SWAN wave transformation and Met Office WW3 offshore data, 1979-2015

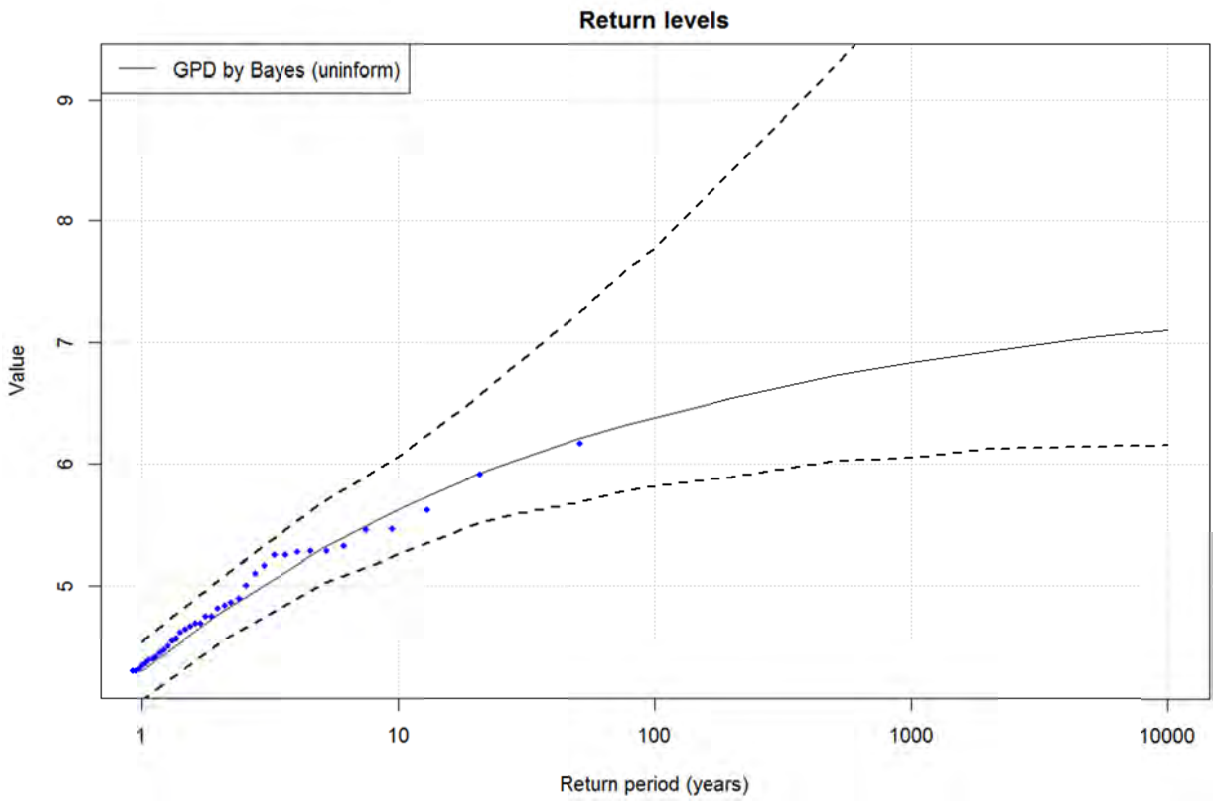

Figure E.1: Marginal extreme wave height distribution fit at P1, "2087 reasonably foreseeable" scenario

Source: HR Wallingford analysis, SWAN wave transformation and Met Office WW3 offshore data, 1979-2015

E.2. Joint probability of large waves and high sea levels

One might expect some degree of correlation between the occurrences of large waves and high sea levels, since both tend to occur during stormy conditions. However, because of the irregular shape of the coastline close to the site, the highest sea levels might be associated with a different wind direction to that producing the largest nearshore waves; also, there may be a time lag, relative to the passage of the storm, between the peak surge and the peak wave height. Hence, the joint probability assessment is undertaken nearshore,

rather than offshore as is more often done. The method used for estimation of joint exceedence extremes is similar to that used for Points A-D during the earlier flood hazard assessment (HR Wallingford, 2013; Amec, 2015).

The JOIN-SEA joint probability analysis programs (HR Wallingford, 2000; Hawkes et al, 2002) are used for analysis of time series data. Information on wave climate and extremes, sea level and extremes, and dependence, is combined in a Monte Carlo simulation of a very large sample (50,000 years) of nearshore sea conditions, retaining the distributions of wave height, sea level and wave period, and the extrapolated extreme values of these variables; also the derived level of dependence between wave height and sea level. This very large sample is then thought of as a best estimate of what would be observed over that period of time.

E.2.1. Correlation between large waves and high sea levels

The degree of dependence between large waves and high sea levels is best determined from site-specific data, as was done here. Dependence is analysed and quantified for the long period of wave predictions, 1979-2015, against available periods of Holyhead tide gauge measurements transformed to equivalent sea levels at Wylfa. The results derived during earlier work for Wylfa Newydd are shown in Figure E.2, in terms of the scatter of significant wave height against high-tide sea level for Points A-D near to the coast.

The dependence analysis is based on estimation of the correlation coefficient ($-1.0 < \rho < 1.0$) associated with a BiVariate Normal (BVN) distribution fitted to the pairings of significant wave height and high-tide sea level extracted from the nearshore time series results. However, the fitting is not based on the actual values of wave height and sea level but rather on their relative rankings within the data sample. A number of different thresholds were tried, with the BVN fitted to data above the threshold. As with any long-term simulation coupled with extremes analysis, in a later simulation of a large sample of data, below the threshold the dependence would be taken directly from the source data, and above the threshold the dependence would be smoothed out (but in this case not extrapolated) using the fitted distribution. (More detail and illustration of the method is given in HR Wallingford, 2000).

A correlation coefficient of $\rho = 1.0$ would indicate complete dependence; conversely, $\rho = 0.0$ would indicate independence, and a negative ρ-value would indicate negative dependence. As can be seen in Figure E.2 , correlation between wave height and sea level is near-zero for Point A, and slightly negative for Points B-D. This is consistent with the fact that the largest nearshore waves originate mainly from the north, but the surges tend to be associated with westerly and south-westerly conditions, the nearshore locations west of the site being a slight exception, being more exposed to westerly waves than the other three points.

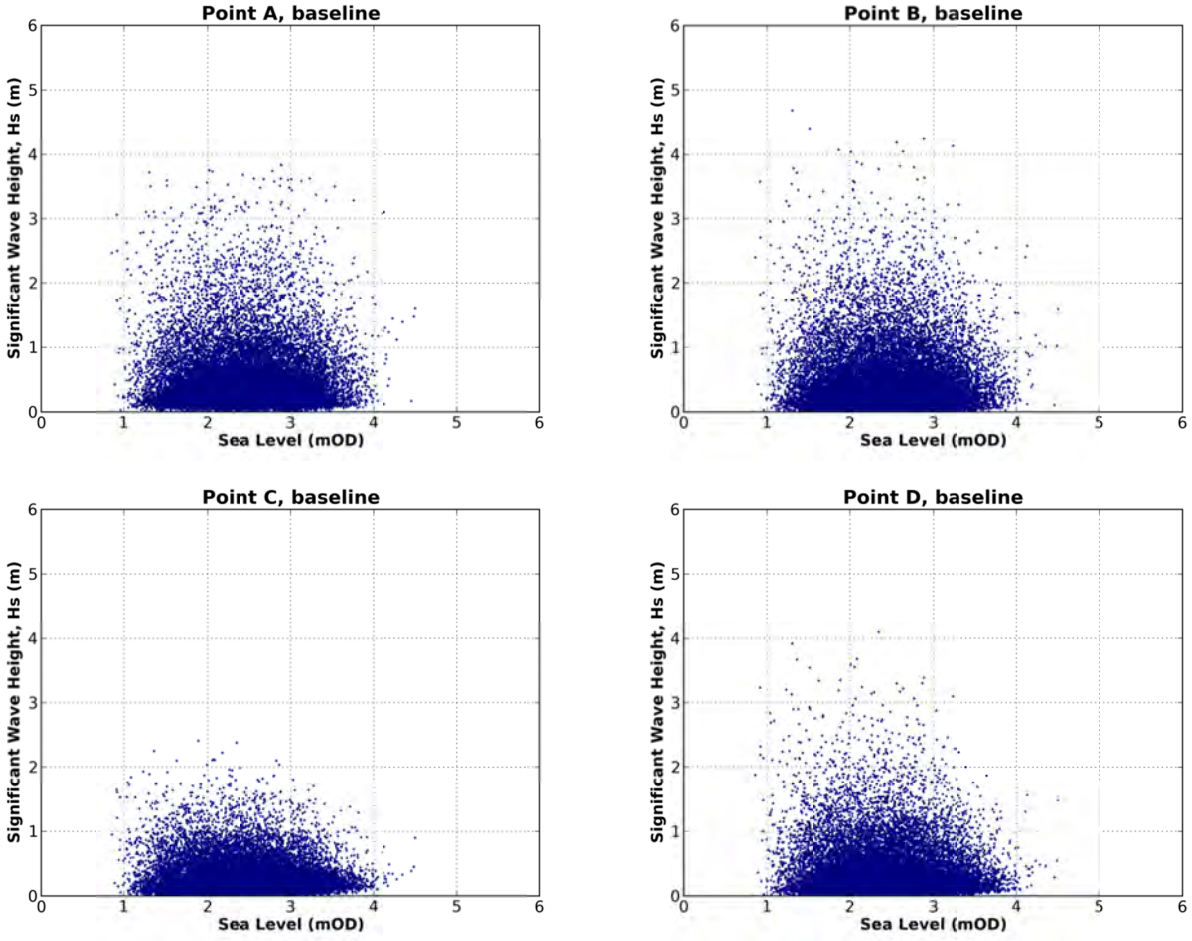

Figure E.2: Scatter plots of significant wave height vs. high tide sea level, for nearshore Points A-D, baseline, "2023 present-day" conditions

Source: HR Wallingford analysis, SWAN wave transformation and Met Office WW3 offshore data, coupled with Holyhead tide gauge data transformed to Wylfa, 1980-1985, 1987-1991, 1995-2015

E.2.2. Simulation of large samples of wave and sea level conditions

The information on dependence was combined with the extreme sea levels and extreme wave heights for each point, after which a large (50,000 year) sample of high-tide data was synthesised for each point, with the appropriate distributions and extremes of wave height, wave period and sea level (including the future sea level rise allowance). In this instance, aiming for plausible conservatism, the extreme wave conditions in the large sample simulation were re-scaled to the overall extreme values at the same positions, effectively "promoting" all of the high and extreme wave conditions in the source data to be as though they had occurred at high tide.

E.2.3. Estimation of joint exceedence extremes

Joint probability results are often summarised in terms of joint exceedence extremes. A joint exceedence probability refers to the frequency with which a specified value of a first variable (in this case wave height) is

equalled or exceeded at the same time as a specified value of a second variable (in this case sea level). For convenience, these probabilities are usually expressed in terms of joint exceedence return period, referring to the average period of time between such occurrences.

In this instance, as the results would subsequently be used in overtopping rate predictions, the joint exceedence curve for a given probability or return period is defined by the property that wave height / water level combinations exceeding the tangent to the curve at any point have the required probability of exceedence (Huseby et al., 2013). The maximum of a response sampled along a tangent joint exceedence curve gives an estimate of the extreme response at that probability level, corresponding to a linear approximation to the response (the tangent at that point).

Tangent joint exceedence extremes, with return periods up to 1000 years can be extracted directly from the 50,000 year sample. Results are expressed in terms of combinations of sea level, wave height and wave period with given frequencies of tangent joint exceedence corresponding to joint return periods of 5, 25, 75, 200 and 1000 years.

The same information is given in tabulated form for use in calculations in Table E.2, as lists of wave (significant wave height and mean wave period) and sea level conditions for 5, 25, 75, 200 and 1000 year joint exceedence return period. The intention is that all combinations in any one table will be tested in any one structure calculation (e.g. overtopping rate) in order to find the worst case for that point and calculation.

The joint exceedence curves for return periods of 5, 25, 75, 200 and 1000 years are presented in Figure E.3. The information is also tabulated in Table E.2 (the first row of each block of data representing the marginal extreme wave condition for that return period).

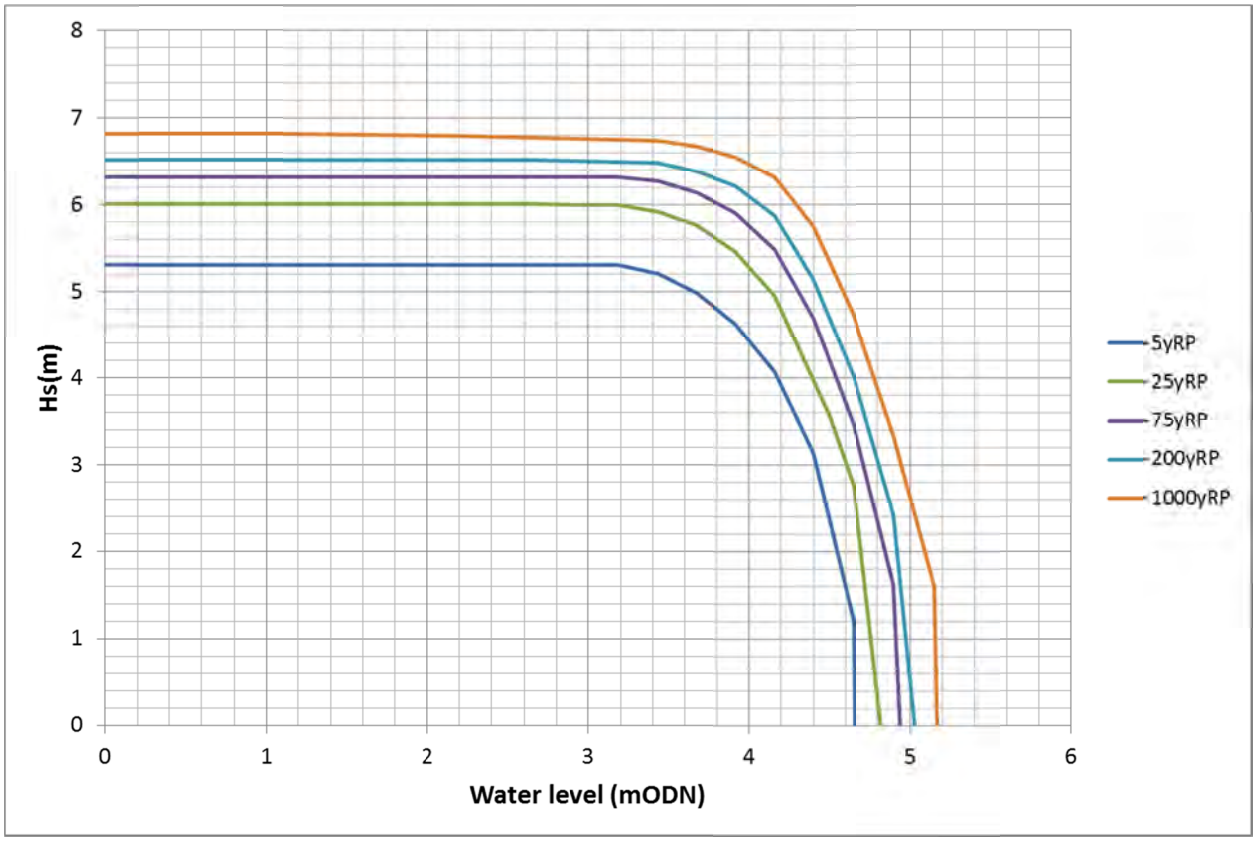

Figure E.3: High water joint probability, Point P1, fully-built "2087 reasonably foreseeable" conditions

Source: SWAN modelling

Table E.2: Sea conditions, Point P1, fully-built, "2087 reasonably foreseeable" scenario

Return period (years)	H_s(s)	T_{m-10} (s) mean	Sea level (mOD)
5	5.3	8.7	3.19
5	5.2	8.6	3.43
5	5.0	8.4	3.67
5	4.6	8.1	3.92
5	4.1	7.6	4.16
5	3.1	6.7	4.40
5	1.2	4.1	4.65
5	0.0	-	4.66
25	6.0	9.2	3.19
25	5.9	9.2	3.43
25	5.8	9.1	3.67
25	5.5	8.8	3.92
25	5.0	8.4	4.16
25	3.6	7.1	4.50

Return period (years)	H_s(s)	T_{m-10} (s) mean	Sea level (mOD)
25	2.8	6.3	4.65
25	0.0	-	4.82
75	6.3	9.5	3.19
75	6.3	9.4	3.43
75	6.1	9.3	3.67
75	5.9	9.2	3.92
75	5.5	8.8	4.16
75	4.7	8.2	4.40
75	3.9	7.5	4.56
75	3.5	7.0	4.65
75	1.6	4.8	4.90
75	0.0	-	4.94
200	6.5	9.6	3.19
200	6.5	9.6	3.43
200	6.4	9.5	3.67
200	6.2	9.4	3.92
200	5.9	9.1	4.16
200	5.1	8.5	4.40
200	4.2	7.7	4.61
200	4.0	7.6	4.65
200	2.4	5.9	4.90
200	0.0	-	5.03
1000	6.8	9.8	3.19
1000	6.7	9.8	3.43
1000	6.7	9.7	3.67
1000	6.5	9.7	3.92
1000	6.3	9.5	4.16
1000	5.8	9.0	4.40
1000	4.7	8.2	4.65
1000	4.5	8.0	4.69
1000	3.3	6.9	4.90
1000	1.6	4.8	5.15
1000	0.0	-	5.17

Source: HR Wallingford joint probability analysis

E.3. References

Amec Foster Wheeler Environment & Infrastructure UK Ltd (Amec, 2015). Wylfa Newydd: Nuclear safety, meteorological and hydrological hazards assessment (NSMHHA). Amec Foster Wheeler Environment & Infrastructure report 200383-000-000-RPT-0003 to Horizon Nuclear Power, dated 31 July 2015.

Bunney, B., Saulter, A., and Palmer, T. (2013). Reconstruction of complex 2D wave spectra for rapid deployment of nearshore wave models. Coasts, Marine Structures and Breakwaters, 2013.

Hawkes, P.J., Gouldby B.P., Tawn, J.A. and Owen, M.W. (2002). The joint probability of waves and water levels in coastal defence design. Journal of Hydraulic Research, Vol 40, No 3, pp241-251.

HR Wallingford (2000) with Lancaster University. The joint probability of waves and water levels: JOIN-SEA: A rigorous but practical new approach. HR Report SR 537, originally dated November 1998, re-issued with minor amendments in final form in May 2000, copy available on request.

HR Wallingford (2013). Wylfa, Anglesey: Proposed new nuclear power plant: Marine study report. HR Wallingford report EBR5141-RT003-R03-00 to Amec, dated 13 December 2013.

Huseby et al (2013). A new approach to environmental contours for ocean engineering applications based on direct Monte Carlo simulations. Ocean Engineering 60:124–135, March 2013.

F. Nearshore joint exceedence wave and high water levels results inside the harbour

Table F.1: Sea conditions, MOLF Berth 1 (A1), part-built, “2023 present-day” scenario

Return Period (years)	H_s (m)	T_{m-10} (s) mean	Sea level (mOD)
5	3.4	8.6	2.57
5	3.4	8.5	2.81
5	3.2	8.3	3.05
5	3.0	8.0	3.30
5	2.7	7.5	3.54
5	2.0	6.6	3.78
5	0.8	4.1	4.03
5	0.0	-	4.04
25	3.8	9.1	2.57
25	3.8	9.1	2.81
25	3.7	9.0	3.05
25	3.5	8.7	3.30
25	3.2	8.3	3.54
25	2.3	7.1	3.88
25	1.8	6.2	4.03
25	0.0	-	4.20
75	4.0	9.4	2.57
75	4.0	9.3	2.81
75	3.9	9.2	3.05
75	3.8	9.1	3.30
75	3.6	8.8	3.54
75	3.1	8.1	3.78
75	2.3	6.9	4.03
75	1.1	4.7	4.28
75	0.0	-	4.32
200	4.1	9.5	2.57
200	4.1	9.5	2.81
200	4.0	9.4	3.05
200	4.0	9.3	3.30
200	3.8	9.0	3.54
200	3.3	8.4	3.78

Return Period (years)	H_s (m)	T_{m-10} (s) mean	Sea level (mOD)
200	2.6	7.4	4.03
200	1.6	5.8	4.28
200	0.0	-	4.41
1000	4.2	9.7	2.57
1000	4.2	9.7	2.81
1000	4.2	9.7	3.05
1000	4.1	9.6	3.30
1000	4.0	9.4	3.54
1000	3.7	8.7	3.78
1000	3.1	7.7	4.03
1000	2.2	6.8	4.28
1000	1.0	4.7	4.53
1000	0.0	-	4.55

Source: ARTEMIS modelling and HR Wallingford analysis

Table F.2: Sea conditions, MOLF Berth 2 (A2), part-built, “2023 present-day” scenario

Return Period (years)	H_s (m)	T_{m-10} (s) mean	Sea level (mOD)
5	3.5	8.6	2.57
5	3.4	8.5	2.81
5	3.3	8.2	3.05
5	3.1	8.0	3.30
5	2.7	7.6	3.54
5	2.1	6.7	3.78
5	0.8	4.1	4.03
5	0.0	-	4.04
25	3.7	9.0	2.57
25	3.7	8.9	2.81
25	3.6	8.8	3.05
25	3.5	8.6	3.30
25	3.3	8.2	3.54
25	2.4	7.1	3.88
25	1.8	6.3	4.03
25	0.0	-	4.20
75	3.8	9.2	2.57
75	3.8	9.1	2.81
75	3.8	9.0	3.05
75	3.7	8.9	3.30
75	3.5	8.6	3.54
75	3.1	8.1	3.78
75	2.3	7.0	4.03
75	1.1	4.8	4.28
75	0.0	-	4.32
200	3.9	9.3	2.57
200	3.9	9.3	2.81
200	3.8	9.2	3.05
200	3.8	9.1	3.30
200	3.7	8.8	3.54
200	3.3	8.4	3.78
200	2.7	7.5	4.03
200	1.6	5.8	4.28
200	0.0	-	4.41

Return Period (years)	H_s (m)	T_{m-10} (s) mean	Sea level (mOD)
1000	4.0	9.5	2.57
1000	4.0	9.5	2.81
1000	3.9	9.4	3.05
1000	3.9	9.4	3.30
1000	3.8	9.2	3.54
1000	3.6	8.6	3.78
1000	3.1	7.6	4.03
1000	2.2	6.8	4.28
1000	1.1	4.7	4.53
1000	0.0	-	4.55

Source: ARTEMIS modelling and HR Wallingford analysis

Table F.3: Sea conditions, cofferdam (A3a), part-built, “2023 present-day” scenario

Return Period (years)	H_s (m)	T_{m-10} (s) mean	Sea level (mOD)
5	2.1	8.4	2.57
5	2.1	8.3	2.81
5	2.1	8.1	3.05
5	2.0	7.8	3.30
5	1.8	7.3	3.54
5	1.5	6.5	3.78
5	0.6	4.0	4.03
5	0.0	-	4.04
25	2.3	8.8	2.57
25	2.3	8.7	2.81
25	2.3	8.6	3.05
25	2.3	8.5	3.30
25	2.1	8.1	3.54
25	1.6	6.9	3.88
25	1.2	6.1	4.03
25	0.0	-	4.20
75	2.5	9.2	2.57
75	2.5	9.1	2.81
75	2.5	9.0	3.05
75	2.4	8.8	3.30
75	2.2	8.4	3.54
75	2.0	7.8	3.78
75	1.5	6.7	4.03
75	0.7	4.6	4.28
75	0.0	-	4.32
200	2.6	9.3	2.57
200	2.6	9.3	2.81
200	2.6	9.2	3.05
200	2.5	9.1	3.30
200	2.4	8.8	3.54
200	2.2	8.2	3.78
200	1.7	7.3	4.03
200	1.1	5.6	4.28
200	0.0	-	4.41

Return Period (years)	H_s (m)	T_{m-10} (s) mean	Sea level (mOD)
1000	2.7	9.6	2.57
1000	2.7	9.6	2.81
1000	2.7	9.6	3.05
1000	2.7	9.5	3.30
1000	2.6	9.3	3.54
1000	2.4	8.5	3.78
1000	2.1	7.4	4.03
1000	1.5	6.7	4.28
1000	0.7	4.6	4.53
1000	0.0	-	4.55

Source: ARTEMIS modelling and HR Wallingford analysis

Table F.4: Sea conditions, cofferdam (A3b), part-built, “2023 present-day” scenario

Return Period (years)	H_s (m)	T_{m-10} (s) mean	Sea level (mOD)
5	2.9	8.4	2.57
5	2.8	8.4	2.81
5	2.7	8.2	3.05
5	2.6	7.9	3.30
5	2.3	7.5	3.54
5	1.9	6.5	3.78
5	0.7	4.0	4.03
5	0.0	-	4.04
25	3.3	9.1	2.57
25	3.3	9.0	2.81
25	3.2	8.9	3.05
25	3.0	8.6	3.30
25	2.7	8.1	3.54
25	2.0	7.0	3.88
25	1.6	6.2	4.03
25	0.0	-	4.20
75	3.5	9.5	2.57
75	3.5	9.4	2.81
75	3.4	9.2	3.05
75	3.3	9.0	3.30
75	3.1	8.6	3.54
75	2.7	8.0	3.78
75	2.0	6.9	4.03
75	0.9	4.7	4.28
75	0.0	-	4.32
200	3.6	9.6	2.57
200	3.5	9.6	2.81
200	3.5	9.5	3.05
200	3.5	9.3	3.30
200	3.3	9.0	3.54
200	2.9	8.4	3.78
200	2.3	7.4	4.03
200	1.4	5.7	4.28
200	0.0	-	4.41

Return Period (years)	H_s (m)	T_{m-10} (s) mean	Sea level (mOD)
1000	3.7	9.7	2.57
1000	3.6	9.7	2.81
1000	3.7	9.7	3.05
1000	3.6	9.6	3.30
1000	3.5	9.4	3.54
1000	3.2	8.7	3.78
1000	2.7	7.6	4.03
1000	1.9	6.7	4.28
1000	0.9	4.7	4.53
1000	0.0	-	4.55

Source: ARTEMIS modelling and HR Wallingford analysis

Table F.5: Sea conditions, MOLF Berth 1 (A1), fully-built, “2087 reasonably foreseeable” scenario

Return Period (years)	H_s (m)	T_{m-10} (s) mean	Sea level (mOD)
5	3.4	8.9	3.19
5	3.4	8.9	3.43
5	3.2	8.7	3.67
5	3.0	8.3	3.92
5	2.7	7.8	4.16
5	2.0	7.0	4.40
5	0.8	4.3	4.65
5	0.0	-	4.66
25	3.9	9.6	3.19
25	3.8	9.5	3.43
25	3.7	9.4	3.67
25	3.5	9.1	3.92
25	3.2	8.6	4.16
25	2.3	7.3	4.50
25	1.8	6.4	4.65
25	0.0	-	4.82
75	4.1	9.8	3.19
75	4.0	9.8	3.43
75	4.0	9.7	3.67
75	3.8	9.4	3.92
75	3.5	9.0	4.16
75	3.1	8.3	4.40
75	2.3	7.2	4.65
75	1.1	4.9	4.90
75	0.0	-	4.94
200	4.2	10.0	3.19
200	4.2	10.0	3.43
200	4.1	9.9	3.67
200	4.0	9.8	3.92
200	3.8	9.5	4.16
200	3.4	8.8	4.40
200	2.7	7.8	4.65
200	1.6	6.0	4.90
200	0.0	-	5.03

Return Period (years)	H_s (m)	T_{m-10} (s) mean	Sea level (mOD)
1000	4.4	10.2	3.19
1000	4.3	10.1	3.43
1000	4.3	10.1	3.67
1000	4.2	10.0	3.92
1000	4.1	9.8	4.16
1000	3.8	9.2	4.40
1000	3.1	8.2	4.65
1000	2.2	7.1	4.90
1000	1.1	4.9	5.15
1000	0.0	-	5.17

Source: ARTEMIS modelling and HR Wallingford analysis

Table F.6: Sea conditions, MOLF Berth 2 (A2), fully-built, “2087 reasonably foreseeable” scenario

Return Period (years)	H_s (m)	T_{m-10} (s) mean	Sea level (mOD)
5	3.3	8.9	3.19
5	3.2	8.8	3.43
5	3.1	8.7	3.67
5	2.8	8.2	3.92
5	2.5	7.7	4.16
5	2.0	6.9	4.40
5	0.8	4.3	4.65
5	0.0	-	4.66
25	3.6	9.5	3.19
25	3.6	9.4	3.43
25	3.5	9.2	3.67
25	3.3	9.0	3.92
25	3.0	8.6	4.16
25	2.2	7.2	4.50
25	1.7	6.4	4.65
25	0.0	-	4.82
75	3.8	9.7	3.19
75	3.8	9.7	3.43
75	3.8	9.6	3.67
75	3.6	9.3	3.92
75	3.3	8.9	4.16
75	2.8	8.2	4.40
75	2.1	7.0	4.65
75	1.0	4.8	4.90
75	0.0	-	4.94
200	4.0	10.0	3.19
200	4.0	10.0	3.43
200	3.9	9.9	3.67
200	3.8	9.7	3.92
200	3.6	9.4	4.16
200	3.1	8.7	4.40
200	2.4	7.6	4.65
200	1.5	5.9	4.90
200	0.0	-	5.03

Return Period (years)	H_s (m)	T_{m-10} (s) mean	Sea level (mOD)
1000	4.1	10.2	3.19
1000	4.1	10.2	3.43
1000	4.1	10.1	3.67
1000	4.0	10.0	3.92
1000	3.9	9.8	4.16
1000	3.5	9.1	4.40
1000	2.9	8.1	4.65
1000	2.1	7.0	4.90
1000	1.0	4.9	5.15
1000	0.0	-	5.17

Source: ARTEMIS modelling and HR Wallingford analysis

Table F.7: Sea conditions, MOLF Berth 1 (A1), fully-built, “2187 reasonably foreseeable” scenario

Return Period (years)	H_s (m)	T_{m-10} (s) mean	Sea level (mOD)
5	3.5	8.9	4.64
5	3.4	8.8	4.88
5	3.2	8.6	5.12
5	3.0	8.3	5.37
5	2.7	7.9	5.61
5	2.1	7.0	5.85
5	0.8	4.3	6.10
5	0.0	-	6.11
25	3.9	9.6	4.64
25	3.9	9.6	4.88
25	3.8	9.4	5.12
25	3.6	9.1	5.37
25	3.2	8.6	5.61
25	2.3	7.3	5.95
25	1.8	6.5	6.10
25	0.0	-	6.27
75	4.2	9.9	4.64
75	4.1	9.9	4.88
75	4.1	9.8	5.12
75	3.9	9.6	5.37
75	3.6	9.2	5.61
75	3.1	8.5	5.85
75	2.3	7.3	6.10
75	1.1	5.0	6.35
75	0.0	-	6.39
200	4.3	10.0	4.64
200	4.3	10.0	4.88
200	4.2	9.9	5.12
200	4.1	9.8	5.37
200	3.8	9.5	5.61
200	3.4	8.9	5.85
200	2.7	7.9	6.10
200	1.6	6.1	6.35
200	0.0	-	6.48

Return Period (years)	H_s (m)	T_{m-10} (s) mean	Sea level (mOD)
1000	4.4	10.1	4.64
1000	4.4	10.1	4.88
1000	4.3	10.1	5.12
1000	4.3	10.0	5.37
1000	4.1	9.8	5.61
1000	3.8	9.3	5.85
1000	3.1	8.4	6.10
1000	2.2	7.1	6.35
1000	1.0	4.9	6.60
1000	0.0	-	6.62

Source: ARTEMIS modelling and HR Wallingford analysis

Table F.8: Sea conditions, MOLF Berth 2 (A2), fully-built, “2187 reasonably foreseeable” scenario

Return Period (years)	H_s (m)	T_{m-10} (s) mean	Sea level (mOD)
5	3.3	8.8	4.64
5	3.2	8.7	4.88
5	3.1	8.6	5.12
5	2.8	8.2	5.37
5	2.5	7.7	5.61
5	2.0	6.8	5.85
5	0.8	4.2	6.10
5	0.0	-	6.11
25	3.7	9.6	4.64
25	3.7	9.5	4.88
25	3.6	9.4	5.12
25	3.4	9.0	5.37
25	3.0	8.5	5.61
25	2.2	7.2	5.95
25	1.7	6.3	6.10
25	0.0	-	6.27
75	4.0	9.9	4.64
75	3.9	9.9	4.88
75	3.9	9.8	5.12
75	3.7	9.6	5.37
75	3.4	9.1	5.61
75	2.9	8.4	5.85
75	2.1	7.1	6.10
75	1.0	4.9	6.35
75	0.0	-	6.39
200	4.1	10.0	4.64
200	4.1	10.0	4.88
200	4.0	9.9	5.12
200	4.0	9.8	5.37
200	3.8	9.5	5.61
200	3.3	8.9	5.85
200	2.6	7.8	6.10
200	1.5	6.0	6.35
200	0.0	-	6.48

Return Period (years)	H_s (m)	T_{m-10} (s) mean	Sea level (mOD)
1000	4.2	10.2	4.64
1000	4.2	10.1	4.88
1000	4.1	10.1	5.12
1000	4.1	10.0	5.37
1000	3.9	9.8	5.61
1000	3.6	9.3	5.85
1000	2.9	8.4	6.10
1000	2.1	7.1	6.35
1000	1.0	4.9	6.60
1000	0.0	-	6.62

Source: ARTEMIS modelling and HR Wallingford analysis

Table F.9: Sea conditions, MOLF Berth 1 (A1), fully-built, “2087 credible maximum” scenario

Return Period (years)	H_s (m)	T_{m-10} (s) mean	Sea level (mOD)
5	3.4	8.9	4.02
5	3.4	8.8	4.42
5	3.2	8.6	4.83
5	3.0	8.3	5.23
5	2.7	7.9	5.64
5	2.1	7.0	6.03
5	0.8	4.3	6.28
5	0.0	-	6.29
25	3.9	9.6	4.02
25	3.9	9.5	4.42
25	3.8	9.4	4.83
25	3.5	9.1	5.23
25	3.2	8.6	5.64
25	2.3	7.3	6.13
25	1.8	6.5	6.28
25	0.0	-	6.45
75	4.1	9.9	4.02
75	4.1	9.8	4.42
75	4.0	9.7	4.83
75	3.9	9.5	5.23
75	3.6	9.2	5.64
75	3.1	8.4	6.03
75	2.3	7.2	6.28
75	1.1	4.9	6.53
75	0.0	-	6.57
200	4.2	10.0	4.02
200	4.2	10.0	4.42
200	4.2	9.9	4.83
200	4.1	9.8	5.23
200	3.8	9.5	5.64
200	3.4	8.8	6.03
200	2.7	7.8	6.28
200	1.6	6.1	6.53
200	0.0	-	6.66

Return Period (years)	H_s (m)	T_{m-10} (s) mean	Sea level (mOD)
1000	4.4	10.1	4.02
1000	4.4	10.1	4.42
1000	4.3	10.1	4.83
1000	4.3	10.0	5.23
1000	4.1	9.8	5.64
1000	3.7	9.1	6.03
1000	3.1	8.1	6.28
1000	2.2	7.0	6.53
1000	1.0	4.9	6.78
1000	0.0	-	6.80

Source: ARTEMIS modelling and HR Wallingford analysis

Table F.10: Sea conditions, MOLF Berth 2 (A2), fully-built, “2087 credible maximum” scenario

Return Period (years)	H_s (m)	T_{m-10} (s) mean	Sea level (mOD)
5	3.3	8.8	4.02
5	3.2	8.7	4.42
5	3.1	8.6	4.83
5	2.8	8.2	5.23
5	2.4	7.7	5.64
5	2.0	6.8	6.03
5	0.8	4.2	6.28
5	0.0	-	6.29
25	3.7	9.5	4.02
25	3.6	9.5	4.42
25	3.5	9.3	4.83
25	3.3	9.0	5.23
25	3.0	8.5	5.64
25	2.1	7.1	6.13
25	1.7	6.3	6.28
25	0.0	-	6.45
75	3.9	9.9	4.02
75	3.9	9.8	4.42
75	3.8	9.7	4.83
75	3.7	9.5	5.23
75	3.4	9.1	5.64
75	2.9	8.3	6.03
75	2.1	7.1	6.28
75	1.0	4.8	6.53
75	0.0	-	6.57
200	4.1	10.0	4.02
200	4.1	10.0	4.42
200	4.0	9.9	4.83
200	3.9	9.8	5.23
200	3.8	9.5	5.64
200	3.2	8.8	6.03
200	2.5	7.7	6.28
200	1.5	6.0	6.53
200	0.0	-	6.66

Return Period (years)	H_s (m)	T_{m-10} (s) mean	Sea level (mOD)
1000	4.2	10.2	4.02
1000	4.2	10.1	4.42
1000	4.2	10.1	4.83
1000	4.1	10.0	5.23
1000	3.9	9.8	5.64
1000	3.6	9.1	6.03
1000	2.9	8.1	6.28
1000	2.1	7.0	6.53
1000	1.0	4.9	6.78
1000	0.0	-	6.80

Source: ARTEMIS modelling and HR Wallingford analysis

HR Wallingford
Working with water

HR Wallingford is an independent engineering and environmental hydraulics organisation. We deliver practical solutions to the complex water-related challenges faced by our international clients. A dynamic research programme underpins all that we do and keeps us at the leading edge. Our unique mix of know-how, assets and facilities includes state of the art physical modelling laboratories, a full range of numerical modelling tools and, above all, enthusiastic people with world-renowned skills and expertise.

HR Wallingford, Howbery Park, Wallingford, Oxfordshire OX10 8BA, United Kingdom
tel +44 (0)1491 835381 fax +44 (0)1491 832233 email info@hrwallingford.com
www.hrwallingford.com

FS 516431
EMS 558310
OHS 595357